Biochemical and Structural Characterization

Of Three Thermostable and Metagenome-Derived

Lipolytic Enzymes

Dissertation

for obtaining the degree Doctor rerum naturalium (Dr. rer. nat.)

at the Department of Biology

Subdivision of the Faculty of Mathematics, Informatics and Natural Sciences

of the University of Hamburg

by

Jennifer Von-Huey Chow

from Tübingen

Hamburg 2012

Genehmigt vom Fachbereich Biologie
der Fakultät für Mathematik, Informatik und Naturwissenschaften
an der Universität Hamburg
auf Antrag von Professor Dr. W. STREIT
Weiterer Gutachter der Dissertation:
Professor Dr. W. SCHÄFER
Tag der Disputation: 21. September 2012

Hamburg, den 06. September 2012

Professor Dr. J. Fromm
Vorsitzender des Promotionsausschusses
Biologie

Universität Hamburg
DER FORSCHUNG | DER LEHRE | DER BILDUNG

Fakultät für
Mathematik, Informatik
und Naturwissenschaften

Jun. Prof. Dr. Mirjam Perner
Molecular Biology of Microbial Consortia
Microbiology and Biotechnology
Department of Biology
Ohnhorststr. 18
D-22609 Hamburg

Tel. +49 (0)40 42816 -444
Fax +49 (0)40 42816 -459
mirjam.perner@uni-hamburg.de

16.07.2012

English language declaration

As a native English speaker, I hereby declare that I have checked the thesis "Biochemical and Structural Characterization of Three Thermostable and Metagenome-Derived Lipolytic Enzymes" by Jennifer Chow for grammatically correct English and the scientific accuracy of the language.

Sincerely,

Jun. Prof. Dr. Mirjam Perner
Universität Hamburg
Biozentrum Klein Flottbek • Mikrobiologie
Ohnhorststraße 18 • D-22609 Hamburg
Tel: ++49-40-428 16 444
Fax: ++49-40-428 16 459

Mirjam Perner

Table of Contents

List of figures

List of tables

Abbreviations

Å	Ångström (1×10^{-10} m)
aa(s)	Amino acid(s)
Acc. no	Accession number
AIX	Ampicillin-IPTG-X-Gal
Amp^R	Ampicillin resistance
approx.	Approximately
bidest	Bidistilled water
bp	Base pair(s)
BCIP	5-Bromo-4-chloro-3-indolyl phosphate
BSA	Bovine serum albumin
c	Conversion
°C	Degree Celsius
ca.	Circa
Cm^R	Chloramphenicol resistance
conc.	Concentrated
DNA	Deoxyribonucleic acid
DNTP(s)	Deoxyribonucleotide triphosphate
DMF	Dimethylene formamide
DMSO	Dimethyl sulfoxide
DTT	Dithiothreitol
E	Enantiomeric ratio
E	Estimated enantiomeric ratio
E.	*Escherichia*
E-cup	Eppendorf cups (reaction tubes)
ee	Enantiomeric excess
et al.	*et alii*
EtOH	Ethanol
EDTA	Ethylene diamine tetraacetic acid
g	Gram
Gm^R	Gentamicin resistance
h	Hour
IgG	Immunoglobulin G
IPTG	Isopropyl β-D-1-thiogalactopyranoside

g	Radial centrifugal force
k	Kilo
Kan^R	Kanamycin resistance
kb	Kilobase(s)
kD	Kilodalton
l	Liter
λ	Lambda
LB	Luria Bertani or lysogeny broth
m	Milli (1×10^{-3})
M	Molar
max.	Maximum
Mb	Mega base pair(s)
MCS	Multiple cloning site
min	Minutes
MSM	Mineral salt medium
MW	Molecular weight
MWCO	Molecular weight cut off
µ	Micro (1×10^{-6})
n	Nano (1×10^{-9})
NBT	Nitro blue tetrazolium chloride
NCBI	National Center for Biotechnology Information
NTA	Nitrilotriacetic acid
OD	Optical density
ORF	Open reading frame
p	Pico- (1×10^{-12})
P.	*Pseudomonas*
Pfu	*Pyrococcus furiosus* (polymerase)
PB	Phosphate buffer
PCR	Polymerase chain reaction
PMSF	Phenylmethylsulfonyl fluoride
*p*NP(s)	*Para*-nitrophenyl ester(s) [=4-nitrophenyl ester(s)]
rRNA	Ribosomal ribonucleic acid
RNA	Ribonucleic acid
Rnase	Ribonuclease A
rpm	Rotation per minute

RhB	Rhodamine B
RT	Room temperature
s	Seconds
S	Svedberg unit
SDS	Sodium dodecyl sulfate
sol.	Solution
sp.	Species
TAE	Tris-acetate EDTA
Taq	*Thermus aquaticus* (polymerase)
TBT	Tributyrin, glycerol tributyrate
Tc^R	Tetracycline resistance
TE	Tris-HCl EDTA
TEMED	N, N, N´, N´ tetramethyl-ethane-1,2-diamine
TEV	Tobacco etch virus (protease)
T_m	Melting temperature
t_R	Retention time
U	Unit (enzyme activity)
UV	Ultra violet
V	Volt
vol.	Volume
v/v	Volume per volume
w/v	Weight per volume
X-Gal	5-Bromo-4-chloro-3-indolyl-β-D-galactopyranoside

Abbreviations of nucleic acids

A	Adenine	C	Cytosine
G	Guanine	T	Thymine

Abbreviations of amino acids

A	Ala	Alanine	N	Asn	Asparagine
C	Cys	Cysteine	P	Pro	Proline
D	Asp	Aspartate	Q	Gln	Glutamine
E	Glu	Glutamate	R	Arg	Arginine
F	Phe	Phenylalanine	S	Ser	Serine
G	Gly	Glycine	T	Thr	Threonine
H	His	Histdine	U	Sec	Selenocysteine
I	Ile	Isoleucine	V	Val	Valine
K	Lys	Lysine	W	Trp	Tryptophan
L	Leu	Leucine	Y	Tyr	Tyrosine
M	Met	Methionine			

Data submission to public databases

The sequences of the genes *lipT* and *lipS* were deposited at GenBank under the accession numbers JQ028671 and JQ028672. The crystallographic data can be accessed from the PDB-database under code 4FBL and 4FBM.

1 Introduction

1.1 Carboxylesterases and lipases

Carboxylesterases (BRENDA category EC 3.1.1.1) and lipases (EC 3.1.1.3), also known as triacylglycerol acylhydrolases, belong to the enzyme class of hydrolases (EC 3) that cleave organic bonds reversibly under consumption of water. These lipolytic enzymes catalyze the cleavage of ester bonds by the addition of water into fatty acids and glycerol or another alcoholic residue in an equilibrium (Figure 1). In organic solvents, when no or only a low amount of water is present, they are able to catalyze the reverse esterification reaction or a transesterification, where a carbonyl residue of an ester is exchanged against another carbonyl group of an alcohol. Generally, the two groups of lipolytic enzymes can be distinguished by the difference that esterases act preferably on short-chain acylglycerols (≤ 10 C-atoms) and "true" lipases act on long-chain acylglycerols (≥ 10 C-atoms) that are less water-soluble. Besides, most lipases show increased activity at interfaces between water and lipids, i. e. on emulsions, which is due to their molecular structure (Sarda and Desnuelle 1958; Verger 1997).

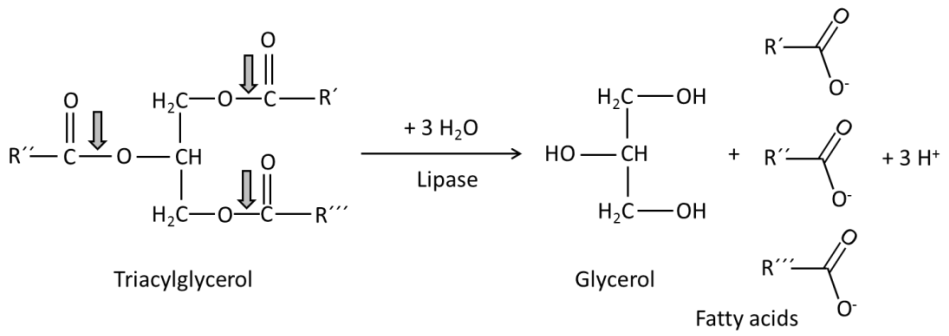

Figure 1. Hydrolysis reaction of lipases exemplary shown on triacylglycerols. The arrows indicate the ester bonds that are being cleaved.

1.1.1 Structure, catalytic mechanisms and secretion of lipolytic enzymes

All hydrolases share a common α/β hydrolase fold pattern in their enzyme structure (Ollis *et al.* 1992). It consists of a central β sheet composed of usually eight strands (Figure 2). Although many variations among lipases occur, the second β strand (β2) is usually antiparallel to the other strands and β3 to β8 are connected with each other by five α-helices (Jaeger *et al.* 1999). The active site of serine α/β hydrolases consists of a catalytic triad which is constituted by a nucleophilic serine residue, an acidic residue (aspartic acid or glutamic acid) and a histidine (Figure 2).

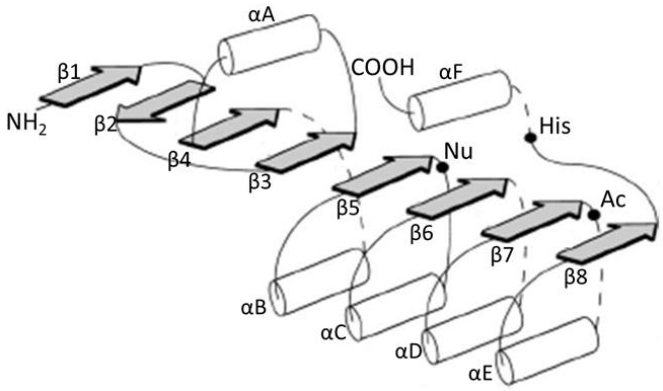

Figure 2. The canonical fold of α/β-hydrolases usually consists of six α helices (αA-αF) and eight β-sheets (β1-β8). The active site residues are indicated as black dots. Nu: nucleophile residue (serine), Ac: acidic residue (aspartic acid or glutamic acid) and His: histidine (Jaeger *et al.* 1999).

Within lipases, the serine residue usually is embedded in a highly conserved Gly-X-Ser-X-Gly (G-X-S-X-G) motif (Ollis *et al.* 1992). It is located at the so-called nucleophilic elbow where the catalytic mechanism of ester hydrolysis is initiated by a "nucleophilic attack". The oxygen atom of the serine hydroxyl group interacts with the activated carbonyl group of the lipid´s ester bond (Jaeger *et al.* 1999). A transient tetrahedral intermediate with this carbonyl carbon in its center is formed. It is stabilized, amongst others, by hydrogen bonds to amide groups that belong to the enzyme's negatively charged carbonyl oxygen atom and NH groups that form the so called "oxyanion hole". The lipase´s histidine residue acts catalytic because a proton from the catalytic serine is transferred to it. This process is supported by the catalytic acid-residue of the enzyme. After protons have been translocated, a covalent intermediate is formed and the acidic residue of the substrate is esterified to the nucleophilic serine. The alcohol component then is released and subsequently, a deacylation step follows, in which a water molecule, activated by the catalytic histidine to a hydroxide ion, is used to hydrolyze the serine-acyl complex. Through this hydrolysis reaction, the enzyme and a free fatty acid are released (Jaeger *et al.* 1999). In organic solvents, the reverse esterification reaction is favored and the acyl-enzyme complex reacts with an alcoholic residue resulting in the formation of an ester bond (Laumen *et al.* 1988). As mentioned above, many lipases (in contrast to carboxylesterases) show increased activity at interfaces between water and lipid. This effect is presumably linked to a structural feature of many, though not all, lipases, the so-called "lid" which is formed by a loop or one or two helices that cover the active site in the presence of hydrophilic substances (Jaeger *et al.* 1999). In presence of hydrophobic substrates, the lid opens up and by this conformational change access to the hydrophobic surface of the active site is provided (Nardini *et*

al. 2000). The shape of the active site´s groove is related to the kinds of substrates that the lipolytic enzymes are able to convert (Pleiss *et al.* 1998).

As most lipases are extracellular enzymes, they have to be secreted through the cell membrane. Many lipases of Gram-negative and Gram-positive bacteria possess a secretional signal sequence at the N-terminus that mediates transportation through the inner membrane with the Sec-translocase system (Jaeger *et al.* 1999; Rosenau and Jaeger 2000). In the periplasm of Gram-negative bacteria, lipases are processed to an enzymatically active form before they are translocated by the type II secretion pathway. Lipases that do not contain a secretion signal sequence can be transported with the type I secretion system (ABC-transporters).

1.1.2 Classification of bacterial and archaeal carboxylesterases and lipases

Esterases and lipases have been classified by Arpigny and Jaeger into eight families according to amino acid sequence homologies and physiological functions (Arpigny and Jaeger 1999). Recently, the classification of the "true" lipases of family I was extended with family I.7 and I.8 by Hausmann and Jäger (Hausmann and Jaeger 2010). Table 1 presents the key-features of the different groups. The vast number of bacterial but only few archaeal lipolytic enzymes can be accessed with online databases like BRENDA (http://www.brenda-enzymes.info/), the Lipase Engineering Database (LED, http://www.led.uni-stuttgart.de), the Microbial Esterase and Lipase Database (MELDB, http://www.gem.re.kr/meldb) and the ESTHER database (http://bioweb.ensam.inra.fr/esther). They provide information about lipase classifications and recent functional and biochemical studies. Nevertheless, the number and structural diversity of lipolytic enzymes is so high, that some cannot be grouped in any of these existing families.

Table 1. Classification of lipases and carboxylesterases into eight major families based on sequence similarities and physiological functions (Arpigny and Jaeger 1999; Hausmann and Jaeger 2010).

Fam.	Characteristics	~Size (kDa)	Example (NCBI acc. no.)
I.1[1)]	Mostly from Gram-negative bacteria. Secreted by type II pathway. N-terminal secretion signal. "Lif" proteins. Two catalytic Asp residues. Cys residues for disulfide bridges. Ca^{2+} dependent.	30-32	*P. aeruginosa* lipase (P26876)
I.2[1)]	Mostly from Gram-negative bacteria. Secreted by type II pathway. N-terminal secretion signal. "Lif" proteins. Two catalytic Asp residues. Cys residues for disulfide bridges. Two additional antiparallel beta-strands. Ca^{2+} dependent.	32-37	*B. glumae* lipase (Q05489)
I.3	Secreted by type I pathway. Ca^{2+} dependent. C-terminal secretion signal and glycine-rich repeats that mediate Ca^{2+}.	50-65	*P. fluorescens* PfO1 lipase (Q3KCS9)

Fam.	Characteristics	~Size (kDa)	Example (NCBI acc. no.)
I.4	Mostly from Gram-positive *Bacilli*. Conserved penta peptide sequence modified to Ala-X-Ser-X-Gly. Optimal pH between 10.0 and 11.5. Ca^{2+} independent.	20	*B. subtilis* lipase (P37957)
I.5	Mostly from Gram-positive bacteria. Optimal pH between 7.5 and 9.5. Some have zinc-binding site.	46	*B. thermocatenulatus* lipase (Q59260)
I.6	Mostly from *Staphylococcus* spp. N-terminal secretion signal (approx. 200 aa). Some are Ca^{2+} independent. Often virulence factor.	Preprot. 75; mature 46	*Staphylococcus hyicus* lipase (P04635)
I.7	Significant similarity of aa 50-150 to members of family I.2. Acting on short (C_2) and long (C_{16}) fatty acid residues. Supposed to act as virulence factors.	29-37	*Streptomyces cinnamoneus* lipase (O33969)
I.8	No lid structure, Ca^{2+} independent. Consensus motif Leu-Gly-Gly-(Phe/Leu/Tyr)-Ser-Thr-Gly surrounding catalytic serine.	51	*Pseudoalteromonas haloplanktis* lipase (Q3IF07)
II	GDSL: Gly-Asp-Ser-(Leu) motif near the N-terminus. Sometimes C-terminal domain that acts as autotransporter through outer membrane.	21-70	*B. thuringensis* lipase (Q3EV80)
III	Typical catalytic triad. Extracellular enzymes. Similarity to intracellular and plasma monomeric isoforms of human platelet activating-factor acetylhydrolase (PAF-AH).	29-35	*Streptomyces exfoliatus* lipase (Q56008)
IV	High similarity to mammalian hormone-sensitive lipases (HSL). Three conserved motif blocks, block III with His-Gly-Gly-Gly consensus sequence.	33-40	*Archaeoglobus fulgidus* lipase (O28558)
V	Typical catalytic triad. Significant aa similarity to various bacterial non-lipolytic α/β hydrolases. Originate from different bacterial genera. Three conserved motif blocks. Ser in block II, Asp and His in block III.	27-35	*Psychrobacter immobilis* lipase (Q02104)
VI	Typical catalytic triad. Mostly act on small substrates. Approx. 40% sequence similarity to eukaryotic lysophospholipases. Three conserved blocks.	23-26	*Xanthomonas campestris* esterase (Q3BXV6)
VII	Aa similarity to eukaryotic acetylcholine esterase and intestine/liver carboxylases. Four conserved motif blocks. Mostly active on short fatty acid chains.	55	*Arthrobacter oxydans* esterase (Q01470)
VIII	Class C β-lactamase-like fold. Ser-X-X-Lys motif at the N-terminus.	39-43	*Arthrobacter globiformis* esterase (Q44050)

[1)] Members of family I.1 and I.2 are processed into an active form by special chaperones, the so called "Lif" proteins (lipase-specific foldases). Normally, genes encoding these proteins are located in an operon together with the respective lipase (Rosenau *et al.* 2004).

1.1.3 Physiological functions of bacterial lipases and esterases

As intracellular or secreted enzymes, lipases and esterases appear in all organisms. Generally, the enzymes contribute to the growth of the host cell by hydrolyzing acyl glycerols. In this way, lipases provide the host metabolism with carbon sources and modify these in various ways. But there are also a lot of other functions that these enzymes fulfill and some are given in Figure 3. Spreading of bacterial populations can be supported, because new ecological niches can be colonized when lipases and esterases pave the way. As an example, many pathogenic bacteria produce lipases that act as virulence factors because they affect the host tissue like for example the plant pathogen *Xanthomonas campestris* (Tamir-Ariel *et al.* 2011) similar to pathogenic fungi that produce lipases for lipid turnover within the host cell and for plant infection (Nguyen *et al.* 2011). Lipase production is sometimes regulated by quorum-sensing like e. g. in the pathogens *Pseudomonas aeruginosa, Burkholderia cepacia* and *Burkholderia glumae* (McKenney *et al.* 1995; Devescovi *et al.* 2007).

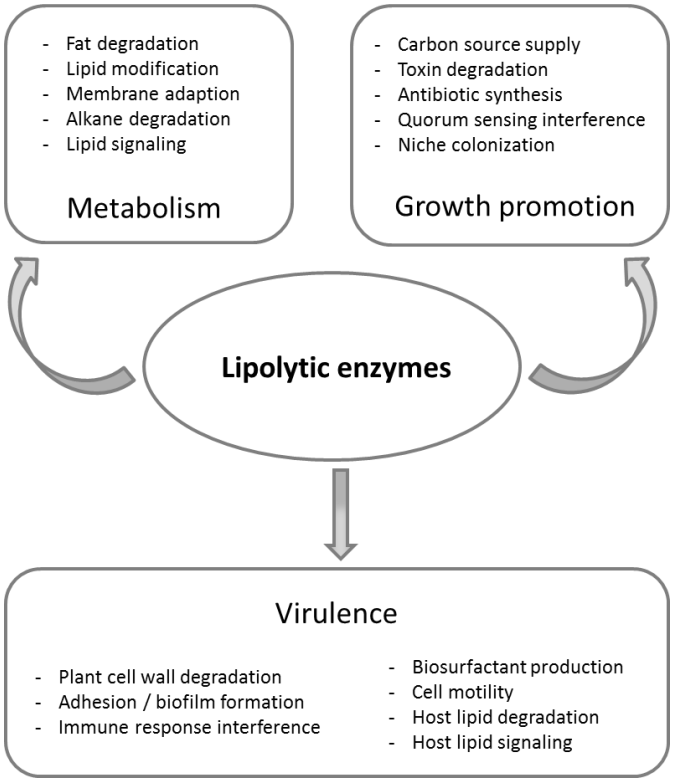

Figure 3. Possible physiological functions of carboxylesterases and lipases (Hausmann and Jaeger 2010).

1.2 Industrial biotechnology

The field of biotechnology can be divided into three different branches. While the term “green biotechnology” refers to agricultural applications and “red biotechnology” to medical tasks, “white” or industrial biotechnology is distinguished by the use of living organisms or parts of them and especially their enzymatic products for industrial processes (Frazzetto 2003). In today´s industrial biotechnology, enzymes of microorganisms are used in a lot of different fields of industry, for example for the production of pharmaceuticals and cosmetics or in textile and food manufacturing (Kirk *et al.* 2002). The advantages biotechnological methods bring are enormous. Costs can be reduced by saving energy, resources and investments and production processes can be created simpler and environmentally friendly by avoiding hazardous substances (i. e. “green chemistry”). Furthermore, independency from fossil fuels could be achieved through sustainable chemistry in which renewable resources from plants (sugars, vegetable oils) can be converted into fine and bulk chemicals as well as biofuels (bioethanol and biodiesel). Additionally, biocatalysts are becoming more and more important for the production of biodegradable plastic materials for example by “metabolic engineering” methods (Soetaert and Vandamme 2006).

1.2.1 Biotechnological relevance of carboxylesterases and lipases

Next to proteases, cellulases and amylases, lipases and esterases from microbes belong to the most important biocatalysts. Lipases and esterases are applied in food, beverage and dairy industry e. g. for flavor development or improvement in cheese, changes in fatty acid compositions by transesterification (polyunsaturated fatty acids) to provide health benefits or for improving bread dough stability, volume and consistence (Kirk *et al.* 2002; Gupta *et al.* 2004; Panda and Gowrishankar 2005). Furthermore, lipases are added to cleaning agents in order to remove oil stains and as surfactants. This is possible, because these enzymes are often extraordinary stable against detergents. Most esterases and lipases also show high stability against organic solvents, which is an important advantage for many reaction conditions. As lipases usually display high solvent and salt tolerance, these enzymes can even be applied in pure organic solvents (Klibanov 2001) or in ionic liquids (Kragl *et al.* 2002). The wide majority of carboxylesterases and lipases act cofactor-independently which makes their industrial application easier and cost-effective.

Lipases and esterases are used for the production of esters as flavors or odorous substances for perfumes (Divakar and Manohar 2007) and they are able to process hydrophobic waste

products (waxes, triglycerides) that accumulate during the production of textiles and paper (Jaeger and Reetz 1998). During the production of biodiesel from vegetable oils and methanol, lipases perform esterification and transesterification reactions that result in the desired methyl esters (H_3C-COO-R´; Robles-Medina *et al.* 2009; Fan *et al.* 2012).

As some lipases are able to react highly chemo-, regio- and stereoselectively, they offer many possibilities in organic synthesis (Koeller and Wong 2001; Reetz 2002). For instance, they can be applied for the resolution of chiral secondary and tertiary alcohols that serve as enantiopure building blocks (Mitsuda *et al.* 1988; Kourist and Bornscheuer 2011). In pharmaceutical industry, they can be used to produce enantiopure nonsteroidal anti-inflammatory drugs like naproxen, keto- and ibuprofen (Tsai *et al.* 1997). Concerning ibuprofen, the (*S*)-enantiomer is about 160 times more physiologically active than the (*R*)-enantiomer (Henke *et al.* 2000) which, moreover, can even cause intolerance (Fazlena *et al.* 2006). Lipases are employed for polycondensation reactions resulting in the synthesis of polyesters (Kobayashi 2010) that can for example be applied as medical devices because of their biodegradability (Jiang 2008) and because they are non-toxic. Sugar-esters that are often used as emulsifiers in food industry can be synthesized by lipases, too (Kobayashi 2011). Natural polyphenols and phenolic antioxidants provide benefits for health and are supposed to be stabilized by lipase-mediated acylation (Torres *et al.* 2012).

Finally, fatty acid esters are important components of cosmetic products for example as pure oils for skin care (so called emollients, i. e. “softeners”), emulsifiers, thickening and re-fatting agents or solubilizers (Hills 2003). Emollient esters like for example decyl oleate, decyl cocoate, myristyl myristate and polyglycerol-3 laurate can be produced lipase-catalyzed with high purity and under profitable conditions (Hills 2003; Hilterhaus *et al.* 2008; Thum and Oxenbell 2008). One problem, however, is that these esters are highly viscous and the production process demands working temperatures above 70°C to facilitate handling with these substances. Most of the carboxylesterases and lipases used in today´s biotechnology originate from mesophilic organisms and are thus susceptible to heat denaturation (Levisson *et al.* 2009). The thermal instability of many biocatalysts is therefore a limiting and restricting factor (Hills 2003; Brummund *et al.* 2011). There is a high demand for novel thermostable lipolytic enzymes with elevated temperature optima so biotechnological processes taking place above 70°C can be created more efficiently for ecological and economic reasons.

1.2.2 Thermostability

According to their optimal growth temperature, organisms are classified as generally thermophiles (>55°C) or as moderate thermophiles (>65°C), extreme thermophiles (>75°C) and hyperthermophiles (>90°C; Imanaka 2011). Of course, the stability of these organisms´ cell components and the enzymes they produce has to be adapted to high temperatures and against thermal denaturation in appropriate ways. Some factors beneficial for thermostability of enzymes are a relatively small hydrophobic surface exposed, N- and C-termini as well as loops that are fixated near the center of the enzyme, strong ion-pairs, e. g. with arginine residues, hydrogen and disulfide bonds, interactions between aromatic pairs and hydrophobic interactions, e. g. by methyl groups (Vieille and Zeikus 2001). Generally, an increase in internal hydrophobicity and stabilization of the secondary structure together with compactness and rigidity of the overall structure enhance protein thermostability (Feller 2010; Imanaka 2011). Nevertheless, only by structural observations the actual thermostability of an enzyme can hardly be predicted and functional tests offer the best conclusions. The number of lipases and esterases with temperature optima of around 70°C that are as well stable at this temperature for long time periods is still limited. In the following part, a promising way to find novel thermostable enzymes is described.

1.3 Metagenomics

The “great plate count anomaly” describes the phenomenon that much more bacterial cells from an environmental sample can be counted under the microscope than are growing under laboratory conditions as colonies on agar-plates (Staley and Konopka 1985). It is estimated that less than 1% of all microbes are cultivable (Amann *et al.* 1995). In order to avoid the diversity-decreasing cultivation step, metagenomics was invented. It denotes a culture-independent approach of direct cloning that provides access to the large diversity of uncultivable bacteria and was first proposed almost 30 years ago (Lane *et al.* 1985). Therefore, the entire bacterial DNA of an environmental sample is isolated, cloned into vectors and transferred into a well-cultivable host organism, most often *Escherichia coli* (Handelsman *et al.* 1998). Subsequently, the metagenomic libraries constructed this way can be explored and analyzed for certain genes (e. g. 16S rRNA genes or genes encoding key-enzymes of certain pathways) by using a sequence-based approach which is often used to answer ecological questions. The clones of the libraries can also be screened for biochemical properties by using a function-based approach. This reveals a large reservoir of novel biocatalysts, drugs or other biotechnologically useful molecules from uncultivated bacteria (Streit and Schmitz 2004; Schmeisser *et al.* 2007;

Steele *et al.* 2009). Within the last decade, methods and instruments were developed and established that enable shotgun sequencing of whole-genomes of environmental samples. Thereby, enormous sequence data is produced and the often underestimated diversity of non-cultivable microbes can be explored (Venter *et al.* 2004; Simon and Daniel 2011).

1.3.1 Metagenome-derived carboxylesterases and lipases and their biochemical properties

Over ten years ago, the first lipolytic enzymes were discovered from metagenomes (Henne *et al.* 2000). Since then, many esterases and lipases have been discovered in metagenomic libraries that were most often constructed with DNA from soil bacteria (Lee *et al.* 2004; Elend *et al.* 2007; Hong *et al.* 2007; Lee *et al.* 2010; Nacke *et al.* 2011; Yu *et al.* 2011), from bacteria of marine sediment (Lee *et al.* 2006; Hardeman and Sjoling 2007; Jeon *et al.* 2009; Jeon *et al.* 2009; Peng *et al.* 2011) or from animal gut (Liu *et al.* 2009; Bayer *et al.* 2010), because the microbial diversity is very high in these environments in particular. In order to find esterases and lipases that are especially thermostable due to habitat related properties, metagenomic libraries were constructed with DNA isolated from samples of thermal environments like hot springs (Rhee *et al.* 2005; Tirawongsaroj *et al.* 2008; Sharma *et al.* 2012). Unfortunately, the access for taking samples from most of these thermal habitats is often difficult or restricted. Ways to overcome this problem are sampling of man-made thermal habitats that contain thermophilic microbes as well and laboratory enrichment cultures of environmental samples incubated at higher temperatures. Although the microbial diversity is being reduced within the enrichments, this strategy has led to an increase in the detection frequency of positive clones in previous studies (Entcheva *et al.* 2001; Knietsch *et al.* 2003; Elend *et al.* 2006).

So far, more than 80 metagenomic esterase and lipase genes have been reported (Steele *et al.* 2009). One reason for the relatively high number of novel carboxylesterases and lipases obtained from metagenomic libraries is the broad repertoire of function-based screening techniques (Beisson *et al.* 2000; Reyes-Duarte *et al.* 2012). Most esterases and lipases were identified by using tributyrin or other triglycerols as substrates in indicator plates. Nevertheless, recombinant overexpression and purification was by far not possible with every metagenomic esterase and lipase discovered (Steele *et al.* 2009), not only because of time-concerning constraints but also because of expression problems that made a higher yield of recombinant protein difficult to achieve.

1.3.2 Heterologous expression of lipases

By means of metagenomics combined with function-based screening techniques, a certain level of expression is provided, as otherwise no activity could be detected for the recombinant enzyme produced by its heterologous host. Next to many different problems that impede the expression of recombinant proteins, enzymes can be misfolded because of missing chaperones, truncated or even not produced at all because of different codon usages. These enzymes can hardly be detected in function-based screenings.

The difficulty often lies in reaching high yields of pure and soluble enzyme out of an acceptable volume of cell culture. As lipases have the potential to interfere with the host metabolism and cell membranes, some hosts, especially *E. coli*, repress the high-level production of these enzymes or they store them inactivated in inclusion bodies (Chung *et al.* 1991; Ogino *et al.* 2008). In order to avoid the time-consumptive refolding procedure, fungal hosts like *Pichia pastoris* (Quyen *et al.* 2003; Jiang *et al.* 2006), *Saccharomyces cerevisiae* (Lopez-Lopez *et al.* 2010), *Kluyveromyces* species (Rocha *et al.* 2011) and *Candida rugosa* (Ferrer *et al.* 2001), but also the actinomycete *Streptomyces lividans* (Cote and Shareck 2010) were used as expression strains for bacterial lipases. Nevertheless, *E. coli* remains the most often used expression host for bacterial lipases because of its uncomplicated and inexpensive culture conditions and the many different strains and expression systems available. In some cases, lowering of the temperature during the time of expression was leading to an increased production of the recombinant proteins in *E. coli* (Terpe 2006). Particularly thermophilic lipases that are barely active at temperatures beneath 20 to 30°C are less innocuous when expressed at low temperatures. In order to find a bacterial strain that grows optimally at lower temperatures than *E. coli* with 37°C, *Pseudomonas antarctica* was investigated in this study concerning its properties for serving as a novel heterologous expression host.

1.4 Intention of this work

The aim of this study was to discover novel thermostable lipolytic enzymes. In order to find enzymes with the desired environment-related thermostability, metagenomic libraries should be constructed in *E. coli* with bacterial genomic DNA of thermophilic enrichment cultures and these should be screened for lipolytic activity. Positive clones should be examined for the respective genes conferring lipolytic activity. The lipase or carboxylesterase genes should be overexpressed in *E. coli* or *P. antarctica* and the enzymes characterized for their biochemical properties in a detailed way in order to elucidate their applicability as biocatalysts. If possible, the crystal structure of the enzymes should be solved.

2 Materials and methods

2.1 Environmental samples

Ten samples were collected from different sites at the Botanical Garden in Klein Flottbek (Hamburg, Germany). The sample sites included six different topsoils consisting predominantly of sand as well as humus-rich soils. Four water samples were taken from sweet water brooks and ponds.

Water samples from a heating system in the Biocenter Klein Flottbek (Hamburg, Germany) were taken. The temperature of the water at the time of sampling was above 50°C.

2.2 Bacterial strains, vectors and constructs

Table 2. Bacterial strains used in this study.

Strain	Characteristics[1)]	Reference/source
E. coli DH5α	*supE*44 Δ*lacU*169 (Φ80 lac*Z* ΔM15) *hsdR*17 *recA*1 *endA*1 *gyrA*96 *thi*-1 *relA*1	Invitrogen (Karlsruhe, Germany; Hanahan 1983)
E. coli Epi100	F^- *mcrA* Δ(*mrr-hsdRMS-mcrBC*) Φ80*dlacZ*ΔM15 Δ*lacX*74 *recA1 endA1 ar-aD139* Δ(*ara, leu*) 7697 *galU galK* λ-*rpsL nupG*	Epicentre (Madison, WI, USA)
E. coli BL21 (DE3)	F^-, *ompT*, *hsdS* B (r_B^- m_B^-) *gal*, *dcm*, λDE3	Novagen/Merck (Darmstadt, Germany)
P. antarctica (DSM-no. 15318)	Wild-type strain	DSMZ (German Collection of Microorganisms and Cell Cultures, Braunschweig, Germany; Reddy *et al.* 2004)

[1)] Geno- and phenotypes according to (Bachmann 1983).

Table 3. Vectors used in this study.

Vector	Characteristics[1)]	Size (kb)	Reference/source
pDrive	TA-cloning vector, *oriEc*, P_{lac}*lacZ*, Amp^R, Kan^R, T7-promotor	3.85	QIAGEN (Hilden, Germany)
SuperCos	Cosmid-vector, Amp^R, Neo^R, *cos*, T3- and T7-promotor	7.94	Stratagene/Agilent Technologies (Santa Clara, CA, USA)

Vector	Characteristics[1)]	Size (kb)	Reference/source
pWE15	Cosmid-vector, Amp^R, Kan^R, *cos*, T3- and T7-promotor	8.16	Stratagene /Agilent Technologies (Santa Clara, CA, USA)
pTZ19R::Cm^R	Cloning vector, *lacZ*, Cm^R, T7-promotor	3.14	Fermentas (St. Leon-Rot, Germany)
pET-21a	Expression vector, *lacI*, Amp^R, T7-promotor, C-terminal His_6-tag coding sequence	5.44	Novagen/Merck (Darmstadt, Germany)
pETM11	Crystallization vector, N- and C-terminal His_6-tag coding sequences, TEV site	6.03	EMBL c/o DESY (Hamburg, Germany)
pBR22b	Broad host range expression vector, *rep, mob, lacI*^{q} (MCS: pET-22b), Cm^R, C-terminal His_6-tag coding sequence	6.42	Rosenau and Jaeger 2004
pML5-T_7	T_7-polymerase vector, Tc^R, *lacI*^{q}, P_{lacUV5}	20	Drepper *et al.* 2005
pBBR1MCS-5	Broad host range expression vector, *rep*, *mob*, *lacZ*, Gm^R	4.77	Kovach *et al.* 1995

[1)] Geno- and phenotypes according to (Taylor and Trotter 1972)

Table 4. Constructs created in this study.

Construct	Vector	Insert size (kb)	Characteristics
pCos6B1	SuperCos	27.0	Possible esterase- or lipase-gene containing insert sequence from heating water enrichment
pCos9D12	SuperCos	26.5	Possible esterase- or lipase-gene containing insert sequence from soil- and water samples enrichment
pCos5E5	pWE15	36.6	Possible esterase- or lipase-gene containing insert sequence from fresh water pipeline biofilm (Schmeisser 2004).
lipT::pET-21a	pET-21a	0.990	*lipT*, derived from pCos6B1, with C-terminal His_6-tag coding sequence. Inserted at *Nde*I and *Hind*III restriction sites
lipS::pET-21a	pET-21a	0.843	*lipS*, derived from pCos9D12, with C-terminal His_6-tag coding sequence. Inserted at *Nde*I and *Hind*III restriction sites
lipS::pETM11+26	pETM11	0.918	*lipS*, derived from pCos9D12, with C-terminal His_6-tag coding sequence. Inserted at *Nco*I and *Hind*III restriction sites

Construct	Vector	Insert size (kb)	Characteristics
lipS::pETM11-26	pETM11	0.843	See *lipS*::pETM11+26, only with a truncated region encoding the N-terminal 26 aa
est5E5::pET-21a	pET-21a	1.386	*est5E5*, derived from pCos5E5, with C-terminal His_6-tag coding sequence. Inserted at *Nde*I and *Hind*III restriction sites
lipT::pBR22b	pBR22b	1.025	*lipT*, derived from pCos6B1, with C-terminal His_6-tag coding sequence. Inserted at *Nde*I and *Hind*III restriction sites
lipT::pBBR1MCS-5	pBBR1MCS-5	1.150	*lipT*, derived from pCos6B1 together with C-terminal His_6-tag coding sequence. Inserted at *Apa*I and *Pst*I restriction sites

2.3 Primers

Table 5. Primers used in this study. Restriction sites are underlined.

Primer	Sequence[1)]	T_m (°C)	Reference
616V	`5-AGA GTT TGA TYM TGG CTC AG-3´	55	*E. coli* 16S rDNA positions 8 to 27 (Brosius *et al.* 1981)
1492R	`5-CGG YTA CCT TGT TAC GAC-3´	55	Kane *et al.* 1993
Arch21f	`5-TTC CGG TTG ATC CYG CCG GA-3´	57	DeLong 1992
927R	`5- CCS TTG TGG TGC TCC C-3´	57	Dees and Ghiorse 2001
M13-20 for	`5-GTA AAA CGA CGG CCA GT-3´	59	Eurofins MWG Operon (Ebersberg, Germany)
M13 rev	`5-CAG GAA ACA GCT ATG ACC-3´	56	Eurofins MWG Operon (Ebersberg, Germany)
T_7-promotor	`5-TAA TAC GAC TCA CTA TAG GG-3´	54	Eurofins MWG Operon (Ebersberg, Germany)
T_3-promotor	`5-ATT AAC CCT CAC TAA AG-3´	48	Eurofins MWG Operon (Ebersberg, Germany)
KAN-2 FP-1	`5-ACC TAC AAC AAA GCT CTC ATC AAC C-3´	72	Epicentre (Madison, WI, USA)
KAN-2 RP-1	`5-GCA ATG TAA CAT CAG AGA TTT TGA G-3´	68	Epicentre (Madison, WI, USA)
lipT for	`5-<u>CAT ATG</u> CGG CGG TTA CTA GCC TTG C-3´	69	This study
lipT rev	`5-<u>AAG CTT</u> CCG CAC CCT AGG CGC CGC CTT C-3´	79	This study
lipS for	`5-<u>CAT ATG</u> AGC CCG AAA AGC AGG-3´	63	This study

Primer	Sequence[1)]	T_m(°C)	Reference
lipS rev	`5-AAG CTT GCT GTG CTT CCG GAT GAA C-3´	69	This study
lipS::pETM11 + 26 for	´5- TACACATGTGCCGGAAAAGCAGGAACTG-3´	71	This study
lipS::pETM11 - 26 for	`5- AACATGTCCGGTATGTCGACGACGCCCCTTC -3´	53	This study
lipS::pETM11 rev	`5-GTGCGGCCGCAAGCTTTCAGTGCTTCCG-3´	68	This study
est1 for	`5-CAT ATG GTC GCT AGG GCG CAG GTG-3´	71	This study
est1 rev	`5-AAG CTT CTT CAC GAT GAT GTC GAA GG-3´	67	This study
*lipT_Apa*I for	`5-GGG CCC TTA TGC GAC TCC TGC ATT AG-3´	70	This study
*lipT_Pst*I rev	`5-CTG CAG AGC CAA CTC AGC TTC CTT TC-3´	69	This study

[1)] R: purine base A or G, Y: pyrimidine base C or T, S: strong binding base C or G. Restriction sites are underlined.

2.4 Culture media and supplements

All media and vessels were autoclaved at 121°C and 2 bar for 20 min. Antibiotics and heat sensitive supplements (Table 6) were sterilized by sterile filtration and added after the media cooled down to ca. 56°C. Media with supplements were stored at 4°C.

2.4.1 LB-medium (Sambrook 2001)

Tryptone	10 g
Sodium chloride	5 g
Yeast extract	5 g
(Agar	12 g)
H_2O	*ad* 1000 ml

2.4.2 Mineral salt medium (MSM)

One liter of MSM contained 100 ml of buffer stock solution and mineral salt stock solution. The pH was adjusted to 7.2. After autoclaving, 1 ml of sterile filtered trace element stock solution and vitamin stock solution were added.

Buffer stock solution (10x):

Na_2HPO_4	70 g	K_2HPO_4	20 g
H_2O_{bidest}	*ad* 1000 ml		

Mineral salt stock solution (10x):

$(NH_4)_2SO_4$	10 g	$MgCl_2 \cdot 6\ H_2O$	2 g
$Ca(NO_3)_2 \cdot 4\ H_2O$	1 g	H_2O_{bidest}	*ad* 1000 ml

Trace element stock solution (1000x; Pfennig and Lippert 1966):

EDTA	500 mg	$NaMoO_4 \cdot 2\ H_2O$	3 mg
$FeSO_4 \cdot 7\ H_2O$	300 mg	$NiCl_2 \cdot 6\ H_2O$	2 mg
$CoCl_2 \cdot 6\ H_2O$	5 mg	H_3BO_3	2 mg
$ZnSO_4 \cdot 7\ H_2O$	5 mg	$CuCl_2 \cdot 2\ H_2O$	1 mg
$MnCl_2 \cdot 4\ H_2O$	3 mg	H_2O_{bidest}	*ad* 200 ml

Vitamin stock solution (1000x):

Ca-pantothenate	10 mg	Cyanocobalamine (B_{12})	10mg
Nicotinic acid	10 mg	Pyridoxal-HCl (B_6)	10 mg
Riboflavin	10 mg	Thiamin-HCl (B_1)	10 mg
Biotin	1 mg	Folic acid	1 mg
p-amino benzoic acid	1 mg	H_2O_{bidest}	*ad* 100 ml

2.4.3 *Thermus* medium (medium D, mod. according to Castenholz 1969)

Solution A:

Nitrilotriacetic acid	1 g	$CaSO_4 \cdot 2\ H_2O$	0.6 g
$MgSO_4 \cdot 7\ H_2O$	1 g	NaCl	80 mg
KNO_3	1 g	$NaNO_3$	6.9 g
Na_2HPO_4	1.1 g	H_2O_{bidest}	*ad* 1000 ml

Solution B:

$FeCl_3$	28 mg	H_2O_{bidest}	*ad* 1000 ml

Solution C:

H_2SO_4 (conc.)	0.5 ml	$MnSO_4 \cdot H_2O$	220 mg
$ZnSO_4 \cdot 7$ H2O	50 mg	H_3BO_3	50 mg
$CuSO_4$	1.6 mg	$Na_2MoO_4 \cdot H_2O$	2.5 mg
H_2O_{bidest}	*ad* 1000 ml		

Medium D:

Tryptone	1 g	Yeast extract	1 g
Solution A	100 ml	Solution B	10 ml
Solution C	10ml	H_2O_{bidest}	*ad* 1000 ml

The pH was adjusted to 8.2 before autoclaving.

2.4.4 Supplements

Table 6. Antibiotics and other supplements.

Antibiotic/supplement	Solvent	Stock solution	Working concentration
Ampicillin	H_2O	100 mg/ml	100 µg/ml
Chloramphenicol	EtOH	50 mg/ml	50 µg/ml or 150 µg/ml
Kanamycin	H_2O	25 mg/ml	25 µg/ml
Gentamicin	H_2O	50 mg/ml	50 µg/ml
Tetracycline	EtOH	7 mg/ml	7 µg/ml
IPTG	H_2O	100 mg/ml	100 µg/ml
X-Gal	DMF	50 mg/ml	50 µg/ml
Tributyrin (TBT)	Medium	-	1% (v/v)
Olive oil	Medium	-	1% (v/v)
Pyruvate	Medium	-	0.1% (w/v)

2.5 Culture conditions

2.5.1 Enrichment cultures

2.5.1.1 MSM enrichment

A spatula of each soil sample (0.5 g) and 0.5 ml of each water sample were combined in a 100 ml Erlenmeyer-flask which contained 50 ml of MSM (2.4.2) supplemented with olive oil and pyruvate (Table 6). The suspension was incubated on a shaker with 150 rpm at RT for one day in order to disassociate bacteria from inorganic and organic particles. The particles were sedimented and the supernatant was used for inoculating 1 l of MSM with olive oil, pyruvate (Table 1), vitamins and trace elements (2.4.2) in a 2 l glass bottle. The enrichment was held at 65°C under moderate aeration for several weeks.

2.5.1.2 *Thermus* enrichment

One liter of medium D (2.4.3) was inoculated in a 2 l glass bottle with 20% sample (v/v) from the water of a heating system without pre-incubation. The enrichment culture was incubated at 75°C at 200 rpm aerobically for several weeks.

2.5.2 Cultivation of bacteria

Bacterial strains were grown in test tubes (5 ml) or Erlenmeyer flasks (25 ml to 1 l) on a shaker (Infors HT minitron, Infors AG, Switzerland) at 150 to 250 rpm. Cultures harboring a plasmid were supplemented with antibiotics in order to keep selection pressure. Cultures were inoculated either with a small amount of colony material from an agar plate, 0.001% of a glycerol stock or with max. 3% of a liquid pre-culture.

For the preparation of metagenomic libraries, colonies were transferred to a 96 well microtiter plate containing 150 µl of liquid LB with 100 µg/ml of ampicillin in each well. The plates were incubated at 37°C for 18 to 24 h without shaking.

2.5.2.1 *E. coli* culture conditions

E. coli strains were grown overnight at 37°C on complex LB medium (2.4.1) supplemented with appropriate antibiotics (Table 6).

2.5.3 *P. antarctica* culture conditions

P. antarctica was grown aerobically on LB medium (2.4.1) supplemented with the appropriate antibiotics (Table 6) at 17 to 22°C.

2.5.4 Strain maintenance

Bacterial colonies were kept for up to 4 weeks on agar plates at 4°C. For long-time storage, glycerol stocks were prepared. Two parts of a fresh overnight culture were mixed with one part of glycerol (87%) in a screw-cap tube and stored at -70°C.

Cosmid libraries (2.5.2) were mixed with 50 µl of glycerol (87%) per well and stored at -70°C.

2.5.5 Measurement of optical density (OD)

Optical densities of bacterial cultures were measured in a cuvette (Sarstedt, Nümbrecht, Germany) with 1 cm thickness using a photometer (SmartSpec™ Plus Spectrophotometer, BIO RAD, Hercules, CA, USA) at a wave length of 600 nm (OD_{600}) against sterile medium. If the OD

exceeded 0.8, samples were diluted with sterile medium in order to avoid errors in measurement. A value of 0.1 (OD_{600}) corresponds to a cell density of approximately $1x10^8$ cells/ml for *E.coli* cells.

2.5.6 Cell harvesting

Liquid cell cultures were harvested by centrifugation. Up to 5 ml were transferred to E-cups and sedimented in a tabletop microcentrifuge (minispin Plus, Eppendorf, Hamburg, Germany) or a refrigerated centrifuge 5417R (Eppendorf, Hamburg, Germany) at 9,000 rpm and 4°C for 1 min. Larger volumes were harvested either using a Falcon centrifuge 5804R (up to 45 ml, rotor A-4-44, Eppendorf, Hamburg, Germany) or a Sorvall RC6+ centrifuge (up to 50 ml: rotor SS-34; up to 400 ml: rotor F10S-6x500y; Thermo scientific, Braunschweig, Germany) at 5,000 to 8,000 rpm and 4 °C for 20 min.

2.6 Standard techniques for working with DNA

Thermostable solutions, glass vessels and other instruments were autoclaved at 121°C for 20 min for sterilization and also in order to inactivate nucleases. Solutions sensitive to heat were sterilized by filtration. Materials that could not be autoclaved were washed with 70% EtOH and flamed.

2.6.1 Isolation of genomic DNA

After three weeks of incubation, a volume of 15 to 50 ml was taken from the enrichment cultures and cells were harvested by centrifugation (2.5.6). The supernatant was discarded before the cell pellet was resuspended in 1 ml of washing solution and the suspension was transferred in a 2 ml E-cup. The sample was incubated on ice for 1 h. The cells were sedimented in a minispin tabletop centrifuge for 2 min at 9,000 rpm and the supernatant was discarded. The cell pellet was resuspended in 250 µl of TE-sucrose solution before 250 µl of lysis buffer were added. The sample was mixed carefully and incubated at 37°C for 1 h. Subsequently, the sample was mixed with 150 µl of proteinase K solution and incubated for another hour at 37°C. The cell lysate was then mixed thoroughly with 250 µl of phenol/chloroform (1:1). Phases were segregated in a refrigerated centrifuge 5417R (Eppendorf, Hamburg, Germany) at 13,000 rpm and 4°C for 20 min. The aqueous supernatant was transferred to a sterile E-cup und supplemented again with 250 µl of phenol/chloroform and centrifuged. This step was repeated three times in order to remove proteins. Afterwards, the sample was mixed well with 250 µl of chloroform and centrifuged for 5 min at 13,000 rpm and 4°C. After a repeating step, DNA was pre-

cipitated with 2.5 vol of 99% EtOH and 0.1 vol. of sodium acetate solution after incubation at -20°C for 30 min and centrifugation (13,000 rpm, 4°C, 20 min). The supernatant was discarded carefully and the DNA pellet was washed twice with 1 ml of 70% EtOH by centrifugation (13,000 rpm, 4°C, 5 min). Finally, the DNA pellet was dried at room temperature and resuspended in sterile H_2O_{bidest} at 8°C overnight.

Washing solution:	NaCl	0.8 M	EDTA	0.1 M
TE-buffer with sucrose:	Tris-HCl	10 mM	EDTA	1 mM
	sucrose	20% (w/v)		
Lysis buffer:	Tris-HCl	10 mM	EDTA	1 mM
	lysoszyme	10 mg/ml		
Proteinase K solution:	Proteinase K	1 mg/ml	SDS	20% (w/v)
	RNase	1 mg/ml		
Sodium acetate solution:	Na-acetate	3M		
	pH was adjusted to 5.5.			

All solutions were dissolved in H_2O_{bidest}. The pH values of the TE-buffer with sucrose and the lysis buffer were adjusted to pH 8.0. All solutions were sterilized by filtration before use.

The lysis buffer and the proteinase K solution were stored as aliquots of 1 ml at -20°C until needed.

2.6.2 Plasmid isolation by alkaline cell lysis (Birnboim and Doly 1979)

The alkaline cell lysis method was applied in order to analyze the recombinant plasmids or cosmids of clones and to separate it from genomic DNA.

One to five ml of an overnight culture were centrifuged in an E-cup for 30 sec and the supernatant was removed. The cell pellet was resuspended thoroughly in 100 µL of buffer P1. Then, 200 µL of buffer P2 were added and the E-cup was inverted five times. After incubation at RT for 1 min, 200 µL of chloroform were added and mixed well. In order to precipitate proteins, 150 µL of buffer P3 were added and the E-cup was inverted five times. After 1 min of incubation at RT, the sample was centrifuged for 2 min. The upper phase (approx. 400 µL) was transferred into a sterile 1.5 ml E-cup and 1 ml of ice cold 96% EtOH was added to precipitate plasmid DNA. After inverting the E-cup, the sample was incubated for 30 min at -20°C or for 10 min at -70°C. The plasmid DNA was sedimented by centrifugation at 13,000 rpm and 4°C for 20 min in a centrifuge 5417R (Eppendorf, Hamburg, Germany). The supernatant was discarded and

the pellet washed with 0.5 ml of ice cold 70% EtOH. The sample was centrifuged for 2 min (13,000 rpm, 4°C). This washing step was repeated once and the supernatant was removed. The DNA pellet was dried at 50°C and resuspended in 20 to 50 µl H_2O_{bidest}. The plasmid or cosmid DNA was analyzed by agarose gel electrophoresis (2.6.6).

Buffer P1:	Tris-HCl	50 mM	EDTA	10 mM
	RNase A	1 mg/ml	H_2O_{bidest}	*ad* 100 ml
	The pH was adjusted to pH 8.0.			
Buffer P2:	NaOH	200 mM	SDS	1% (w/v)
	H_2O_{bidest}	*ad* 200 ml		
Buffer P3:	K-acetate	3 M	H_2O_{bidest}	*ad* 200 ml
	The pH was adjusted to 5.5 with acetic acid.			

All solutions were sterilized by filtration before use. Buffer P1 was stored at 4°C.

2.6.3 Plasmid isolation with a plasmid mini kit

In order to obtain pure plasmid and cosmid DNA that can be used for sequencing, a "High-Speed Plasmid mini kit" was used according to the manufacturer´s instructions (Avegene life science, Taipei, Taiwan, China). DNA was isolated from 2-5 ml of an overnight culture and the DNA was eluted with 20 to 50 µl of H_2O_{bidest}.

2.6.4 Purification and concentration of DNA

When purification of DNA was required, the "Gel/PCR DNA Fragments Extraction kit" (Avegene life science, Taipei, Taiwan, China) was used and the protocol for PCR cleanup was followed according to the manual. DNA was eluted with 20 to 40 µl of H_2O_{bidest}. The concentration of small volumes of DNA solutions was carried out in a vacuum concentrator (Concentrator 5301, Eppendorf, Hamburg, Germany) at 45°C for up to 5 min.

2.6.5 Analysis of DNA concentration and purity

The quantity and purity of DNA was measured using a photometer (SmartSpecTM Plus Spectrophotometer, BIO RAD, Hercules, CA, USA). DNA concentration was measured in a disposable micro UV cuvette (Plastibrand®, Brand, Wertheim, Germany) at 260 nm against H_2O_{bidest}. An OD_{260} of 1.0 corresponds to 50 µg/ml of double-stranded DNA. The purity was determined by calculating the ratio of the extinction values at 260 and 280 nm. Pure DNA solutions have a ratio OD_{260}:OD_{280} of 1.8 to 2.0 (Sambrook 2001).

2.6.6 Agarose gel electrophoresis

The size, quality and quantity of DNA were analyzed by agarose gel electrophoresis. The DNA is negatively charged and moves through a 0.8% (w/v) agarose gel. The run time of the DNA fragments is dependent on their size. Smaller fragments move faster through the matrix and thus, fragments are separated according to their size. The electrophoresis was performed at 100 V for at least 35 min with a power supply PowerPac™ Basic (BioRad, Munich, Germany) in an electrophoresis gel chamber (HE-33 mini horizontal submarine unit, Hoefer™, Holliston, MA, USA) filled with TAE buffer. Samples (1-5 µl) were mixed with 1 µl of loading dye before they were applied on the gel. After performing the electrophoresis, the DNA was stained in an ethidium bromide solution (10 µg/ml) for 5 to 15 min and visualized under UV light of 254 nm in a Molecular Imager® (GelDoc™ XR+ Imaging System, BioRad, Munich, Germany). The gel was documented with a Quantity One 1-D analysis software (version 4.6.9, BioRad, Munich, Germany). The size of the DNA fragments was estimated by comparison with marker bands between 100 bp and 10 kb of a GeneRuler™ 1 kb DNA Ladder (Fermentas, St. Leon-Rot, Germany) that was also loaded on the gel.

TAE buffer (50x):	Tris-Ac	2 M	EDTA	100 mM
	Dissolved in H_2O_{bidest}			
	The pH was adjusted to 8.0 with acetic acid.			
Loading dye:	Glycerol (30%)	60 ml	EDTA	50 mM
	Bromphenol blue (0.25%)	0.5 g		
	Xylencyanol (0.25%)	0.5 g		
	H_2O_{bidest} *ad* 200 ml			

2.6.7 Gel extraction of DNA

Extraction of DNA fragments from an agarose gel was performed after PCR or digestion and subsequent electrophoresis (2.6.6) by using the "Gel/PCR DNA Fragments Extraction kit" (Avegene life science, Taipei, Taiwan, China) according to the manufacturer´s instructions. The DNA fragments were eluted with up to 30 µl H_2O_{bidest}.

2.6.8 Enzymatic modification of DNA

2.6.8.1 Digestion of DNA

All type II restriction endonucleases and their appropriate buffers were purchased from Fermentas (St. Leon-Rot, Germany). These enzymes cleave double-stranded DNA at specific

recognition sites that usually consist of a palindromic sequence of 4 to 8 nucleotides. DNA fragments with cohesive or blunt ends are being produced that can be used for analysis or further cloning.

2.6.8.1.1 Partial digestion of genomic DNA

For the construction of cosmid libraries, the insert size of DNA fragments has to be about 30 to 40 kb. Genomic DNA was partially digested in order to obtain this fragment size and to create complementary sticky ends for the ligation into the *Bam*HI restriction site of the cosmid vector SuperCos. The enzymes *Bam*HI and *Bsp*143I produce compatible ends. Different dilutions of the restriction enzyme *Bsp*143I between 1:1,000 and 1:64,000 (final concentration) were tested on genomic DNA in order to obtain the best result. Therefore, a master mix was prepared.

Master mix:	DNA solution (depending on conc.)	
	*Bsp*143I buffer (10x)	8 µL
	H_2O_{bidest}	*ad* 80 µL

The master mix was divided into aliquots of 7 µL in sterile E-cups. 1 µL of stepwise increasing enzyme dilution of *Bsp*143I was added to each E-cup and mixed. One aliquot of 7 µL remained as enzyme-free control. The reaction was incubated at 37°C for 20 min and stopped immediately afterwards by heat inactivation of the restriction enzyme at 65°C for 20 min. The digestion progress due to different enzyme concentrations was determined and compared with the undigested control by agarose gel electrophoresis (2.6.6). The enzyme dilution that produced only high molecular weight DNA fragments with a desired size between 30 and 40 kb was applied for a preparative partial digestion.

Preparative partial digestion:	Genomic DNA	ca. 15 µg
	*Bsp*143I (diluted with H_2O_{bidest})	1 µl
	*Bsp*143I buffer (10x)	20 µl
	H_2O_{bidest}	*ad* 200 µl

After 20 min of incubation at 37°C, the enzyme was inactivated for 20 min at 65°C. The DNA was purified (2.6.4) and analyzed by agarose-gel electrophoresis (2.6.6).

2.6.8.1.2 Complete digestion of plasmid DNA

For a complete digestion, two different scales were used depending on the further purpose of the DNA (Table 7). The reaction mixtures were incubated for 2 h to overnight at the optimal temperature of the enzymes (usually 37°C). If necessary, the enzymes were heat inactivated at

65 or 80°C for 20 min. Vector preparations were dephosphorylated immediately afterwards (2.6.8.2).

Table 7. Digestion of DNA.

	Analytical scale	**Preparative scale**
DNA	0.4 - 1 µg	4 - 10 µg
Restriction enzyme (10 U/µl)	0.5 µl	2 µl
Restriction buffer (10x)	1 µl	10 µl
H_2O_{bidest}	*ad* 10 µl	*ad* 100 µl

2.6.8.2 Dephosphorylation of complementary ends

In order to avoid re- or self-ligation, the 5´-end phosphate groups of digested DNA were cleaved enzymatically with Antarctic phosphatase (New England Biolabs, Frankfurt am Main, Germany).

Preparative digestion	95 µl
Antarctic phosphatase buffer (10x)	11 µl
Antarctic phosphatase	4 µl

After 20 min of incubation at 37°C, the enzyme was inactivated at 60°C for 5 min. Finally, the DNA was purified (2.6.4).

2.6.8.3 Ligation of DNA

2.6.8.3.1 Ligation of PCR products

Genes or other DNA fragments that were amplified by PCR were ligated into pDrive cloning vector (Table 3, “PCR cloning kit”, QIAGEN, Hilden, Germany) according to the manufacturer´s instructions after being purified (2.6.4). The pDrive vector is provided in linearized form with U-overlaps on each side. The A-overlaps of the PCR-product that are produced by the *Taq* polymerase ligate with the vector ends.

Purified insert	2 µl
pDrive	0.5 µl
Ligation master mix	2.5 µl

The ligation was incubated for at least 2 h at 16°C. Subsequently, the plasmids were transformed in competent *E. coli* DH5α cells by heat shock (2.6.9.1).

2.6.8.3.2 Ligation of genomic DNA fragments

Genomic DNA fragments with a size of 30-40 kb obtained after partial *Bsp*143I digestion were ligated into the *Bam*HI restriction site of the cosmid vector SuperCos (Table 3). The ligation was accomplished with the ATP-dependent T4-ligase (Fermentas, St. Leon-Rot, Germany). A molar ratio of 1:5 was chosen, which is dependent on size and concentration of the DNAs. The ligation mixture had a total volume of 20 µl.

Insert DNA (ca. 30 kb, ca. 1800 ng/µl)	4 µl
SuperCos DNA (7.9 kb, ca. 100 ng/µl)	6 µl
T4-ligase	1 µl
T4-ligase buffer (10x)	2 µl
ATP (10 mM)	2 µl
H_2O_{bidest}	5 µl

The ligation was incubated at 8°C overnight. The result was compared with non-ligated DNA and vector by agarose gel electrophoresis (2.6.6).

2.6.8.3.3 Ligation of other DNA fragments

Other DNA fragments with a size of up to 10 kb, for example digested cosmid fragments for subcloning, were inserted into the MCS of the *lacZ*-gene of the dephosphorylated vector pTZ19R::Cm^R (2.6.8.2, Table 3). For recombinant gene expression in *E. coli* at higher levels by induction, genes were ligated into the MCS of pET-21a (Table 3). The genes were cloned directional with restriction sites into the vector. For the expression of genes in *P. antarctica*, the vectors pBBR1MCS-5 and pBR22b were used (Table 3). Usually, a molar vector-insert ratio of 1:2 was used and T4-ligase (Fermentas, St. Leon-Rot, Germany) was applied like described in 2.6.8.3.2. The reactions were incubated for 2 h to overnight at 8 or 16°C. The ligation was compared with a non-ligated control by agarose gel electrophoresis (2.6.6).

2.6.9 Cloning of DNA

2.6.9.1 Heat shock transformation of *E. coli*

Competent *E. coli* DH5α and BL21 (DE3) cells (2.6.9.1.1) were transformed by heat shock with recombinant plasmids. One aliquot of competent cells in an E-cup was thawed on ice for 5 min. After adding 5 µl of ligation reaction mixture (ca. 0.1 µg of DNA) and gentle stirring with a pipette, the cells were incubated on ice for 20 min. The heat shock was carried out by incubating the cells at 42°C for 90 sec. The cells were put on ice immediately and incubated for another 5 min. 500 µl of liquid LB medium were added to the cells before they incubated at 37°C for 30

to 45 min. Finally, the transformed cells were plated out on LB agar plates containing selective antibiotics. The plates were incubated overnight at 37°C.

2.6.9.1.1 Preparation of competent *E. coli* cells

An overnight culture of the desired *E. coli* strain (2.5 ml) was used to inoculate 250 ml of pre-heated liquid LB medium (37°C) in a 1 l Erlenmeyer flask. The culture was incubated at 37°C on a rotary shaker (200 rpm) for 90 to 120 min until an OD_{600} of 0.5 was reached. The culture was cooled on ice for 5 min and then the cells were sedimented by centrifugation (4,000 g, 4°C, 5 min, Sorvall RC6+ centrifuge, rotor F10S-6x500y, Thermo scientific, Braunschweig, Germany). The supernatant was removed while the cell pellet was kept on ice. The cells were resuspended in 75 ml of cooled buffer TFB1. The suspension was divided into two 50 ml Falcon tubes and incubated on ice for 90 min. Then, the cells were sedimented again by centrifugation (5,000 rpm, 4°C, 5 min, centriuge 5804R, Eppendorf, Hamburg, Germany), the supernatant was discarded and the cell pellet resuspended in 5 ml of cold buffer TFB2. The cell suspension was divided into aliquots of 100 µl in cooled E-cups, frozen in liquid nitrogen and stored immediately at -70°C.

Buffer TFB1:	RbCl	100 mM	$MnCl_2$	50 mM
	K-acetate	30 mM	$CaCl_2$	10 mM
	Glycerol	15%	H_20_{bidest} *ad* 100 ml	

The pH was adjusted to 5.8 with acetic acid and the solution was sterilized by filtration.

Buffer TFB2:	MOPS	10 mM	RbCl	10 mM
	$CaCl_2$	75 mM	Glycerol	15%
	H_20_{bidest}	*ad* 20 ml		

The pH was adjusted to 6.8 with KOH_{aq} and the solution was sterilized by filtration.

2.6.9.2 Heat shock transformation of competent *P. antarctica* cells

In an E-cup, 100 µl of competent *P. antarctica* cells (2.6.9.2.1) were gently mixed with 5 µl (ca. 0.2 µg) of recombinant plasmid pBBR1MCS-5 or pBR22b. The latter had to be transformed together with 3 µl (ca. 0.2 µg) of the vector pML5-T_7. The cells were incubated on ice for 60 min. The heat shock was performed by incubating the cells at 42°C for 2 min. Incubation on ice for 10 min followed immediately, before 900 µl of LB medium were added and the cells were incubated at 22°C for 1 to 2 h. Then, the cells were sedimented (5,000 g, RT, 60 s, minispin Plus, Eppendorf, Hamburg, Germany) and the supernatant was removed except 50 to 100 µl of it remaining in the tube. The cells were resuspended carefully and plated out on LB agar plates

supplemented with appropriate antibiotics. The plates were incubated at 22°C for 2 to 4 days before colonies were visible.

2.6.9.2.1 Preparation of competent *P. antarctica* cells

A preculture (0.5 ml) of *P. antarctica* was used to inoculate 50 ml of LB medium in a 300 ml Erlenmeyer flask. The culture was incubated at 22°C on a rotary shaker (200 rpm) until an OD_{600} of 0.5 was reached. The flask was cooled on ice for 10 min. The cell suspension was transferred to a 50 ml Falcon tube and centrifuged (4,000 g, 10 min, 4°C, Centriuge 5804R, Eppendorf, Hamburg, Germany). The supernatant was removed and the cells resuspended in 25 ml of a cooled 10 mM NaCl-solution. The cells were again sedimented (4,000 g, 10 min, 4°C) and the supernatant was discarded. The cell pellet was then resuspended in 25 ml of a 100 mM $CaCl_2$-solution. The cells were incubated on ice for 20 min and subsequently sedimented (4,000 g, 10 min, 4°C). Finally, the pellet was resuspended in 500 µl of a 100 mM $CaCl_2$ solution, divided into aliquots of 100 µl which were ready for transformation (2.6.9.2).

2.6.9.3 Blue-white-screening

The strain *E. coli* DH5α has a deletion in its *lacZ* gene so that it cannot produce an active β-galactosidase, only the C-terminal ω-subunit. Vectors like pDrive and pTZ19R::Cm^R encode the N-terminal α-subunit of the β-galactosidase which has an additional MCS within. Together with both subunits, the β-galactosidase is being complemented to its functional form. Transformations of *E. coli* with recombinant pDrive and pTZ19R::Cm^R were plated out on agar plates containing the inductor IPTG and the glucose-analog X-Gal as well as appropriate antibiotics. Colonies of clones with active β-galactosidase can be screened, as the β-galactosidase cleaves the X-Gal molecule and by oxidation with aerial oxygen, a blue color develops. By the insertion of a DNA fragment into the MCS of the α-subunit-coding gene of the vector, no active β-galactosidase can be produced and so, the colonies of clones with an insert appear white.

2.6.9.4 Library construction

Libraries were constructed by using the cosmid vector SuperCos (Stratagene/Agilent Technologies, Santa Clara, CA, USA) which carries ampicillin and neomycin resistance genes and λ phages that were used to introduce recombinant DNA into the host cell *E. coli* Epi100. Both vector and phage particles were supplied within the "Gigapack® III Gold Packaging Extract" kit (Stratagene/Agilent Technologies, Santa Clara, CA, USA) and used according to protocols provided by the manufacturer.

2.6.9.4.1 Packaging of DNA into λ phage particles

Phage packaging mixes from the "Gigapack® III Gold Packaging Extract" kit were used according to the manufacturer's protocol. An E-cup containing the packaging extract was thawed before it was mixed with 3 µl of the ligation mixture of SuperCos (2.6.8.3.2). The reaction was incubated for 2 h at 22°C and then 500 µl of buffer SM and 50 µl of chloroform were added and mixed carefully. The suspension was centrifuged briefly and the supernatant containing the λ phages with the recombinant cosmid was transferred to a new E-cup. The phages were stored at 4°C until used for transduction.

Buffer SM:	NaCl	0.58 g	$MgSO_4$	200 mg
	Tris-HCl (pH 7.5)	50 mM	Gelatine	0.01% (w/v)
	H_2O_{bidest}	*ad* 100 ml		

2.6.9.4.2 Preparation of phage competent cells

E. coli Epi100 was used as a host strain. In a test tube, 5 ml of liquid LB medium supplemented with 10 mM $MgSO_4$ and 0.2% (w/v) maltose were inoculated with a single colony of freshly grown *E. coli* Epi100. The culture was incubated on a rotary shaker at 200 rpm and 37°C for 4 to 6 h until the OD_{600} reached 0.8 to 1.0. Cells were transferred to E-cups and harvested at 2,000 rpm and 4°C for 10 min in a centrifuge 5417R (Eppendorf, Hamburg, Germany). The supernatant was discarded and the cell pellet was resuspended in few ml of 10 mM $MgSO_4$ in order to set the OD_{600} to 0.5. The phage competent cells were stored on ice until used for transduction.

2.6.9.4.3 Transduction with λ phage particles

Different dilutions of the λ phages were tested in order to find the most efficient titer for the transduction of the competent cells. The phages were diluted 1:2, 1:10 and 1:50 with buffer SM. In E-cups, 25 µl of each dilution was mixed with 25 µl of the competent *E. coli* Epi100 cells (2.6.9.4.2) and the transduction took place for 30 min at 22°C. To each E-cup, 200 µl of liquid LB were added and the cells were incubated at 37°C for 45 min, being inverted every 15 min. Cosmid clones were grown overnight at 37°C on LB agar plates supplemented with 100 µg/ml ampicillin.

2.6.9.5 Subcloning

For the identification of ORFs encoding lipolytic activity, the lipase- or esterase-positive cosmid clones were subcloned with restriction enzymes like *Eco*RI, *Hind*III and *Sac*I (2.6.8.1.2) so that a clear number of fragments with approximately 1 to max. 10 kb resulted from the digestion.

The fragments were ligated into dephosphorylated pTZ19R::Cm^R (2.6.8.2; 2.6.8.3.3), which carries a chloramphenicol resistance gene, and cloned into *E. coli* DH5α by heat shock (2.6.9.1). Colonies containing clones with insert were selected (2.6.9.3), their insert size was analyzed by digestion (2.6.8.1.2) and the clones were tested on lipolytic activity (2.8). The ORF encoding the lipase or esterase of the positive subclone was then identified by transposon mutagenesis (2.6.9.6), sequencing (2.6.11.1) and, if necessary, "primer walking".

2.6.9.6 Transposon mutagenesis

On positive subclones, *in vitro* transposon mutagenesis using the EZ::TN^{TM} <KAN-2> transposon kit (Epicentre, Madison, WI, USA) was carried out following the manufacturer's instructions. Clones harboring a transposon grew on LB agar plates containing kanamycin. If the transposon inserted in the gene responsible for lipolytic activity, the clone was screened negative on LB agar plates supplemented with TBT (2.8.1). With the inserted priming sites of the transposon, the corresponding gene was sequenced using specific KAN-2 primers (Table 5) and automated sequencing ABI377 technology (2.6.11.1).

2.6.10 Polymerase chain reaction (PCR)

2.6.10.1 Primers

Depending on the melting temperature (T_m) of the primer, annealing is taking place at varying temperatures. The melting temperature T_m is depending on the length and the GC-content of the primer (Equation 1; Chester and Marshak 1993):

$$T_m = 69.3°C + 0.41°C \times [GC\%] - (650 / \text{no. of bp}) \quad (1)$$

The melting temperatures of the primers used in this study are given in Table 5.

The annealing temperature T_{ann} is calculated as follows (Equation 2):

$$T_{ann} = T_m - 5°C \quad (2)$$

When the T_{ann} of two primers used in one PCR reaction significantly differs, the lower T_{ann} is being used.

Some primers were designed to introduce a 5'-*Nde*I and a 3'-*Hind*III restriction site into the PCR products (Table 5) so that directional cloning in an expression vector was possible.

2.6.10.2 Standard reaction conditions

PCR reaction mixtures were prepared on ice to avoid false annealing. Usually, a *Taq* DNA-polymerase was applied, only in sensitive cases a *Pfu* polymerase was used because of its

proof-reading function. In case of amplification problems, DMSO was added for better results. Mostly, a total volume of 50 µl reaction mixture was prepared in a 100 µl PCR-tube.

DNA template	1-2 µL
Taq polymerase buffer (10x)	5 µL
dNTPs (2 mM)	2 µL
Forward primer (10 µM)	1 µL
Reverse Primer (10 µM)	1 µL
(DMSO	2 µL)
Taq polymerase (ca. 2.5 U/µl)	0.5 µL
H_2O_{bidest}	*ad* 50 µL

The PCR reaction was carried out in a thermocycler (Mastercycler® personal, Eppendorf, Hamburg, Germany) and the conditions were used as indicated in Table 8. Usually, 35 cycles were performed. An elongation time of 1 kb per min was estimated for the *Taq* polymerase.

Table 8. Standard PCR reaction conditions.

Initial denaturation		95°C	2 min
Denaturation	35 x	95°C	30 sec
Annealing		$T_{ann} = T_m$-5°C	30 sec
Elongation		72°C	1 min/kb
Final elongation		72°C	5 min

2.6.10.3 Direct colony PCR

Direct colony PCR was used to check clones for their correct insert size. A small amount of colony material was suspended in 20 µL of H_2O_{bidest}. 2 µL of cell suspension were used as a template.

Template	2 µL
Taq polymerase buffer (10x)	2.5 µL
dNTPs (2 mM)	1 µL
Forward primer (5 µM)	1 µL
Reverse primer (5 µM)	1 µL
Taq polymerase	0.25 µL
H_2O_{bidest}	*ad* 25 µL

The PCR reaction conditions were as indicated in Table 8.

2.6.10.4 Purification of PCR products

The size of PCR products was analyzed by agarose gel electrophoresis (2.6.6). Subsequently, the “Gel/PCR DNA Fragments Extraction kit” (Avegene life science, Taipei, Taiwan, China) was used for purification of the PCR products as described in the manufacturer´s protocol. The samples were eluted with up to 30 µl H_2O_{bidest}.

2.6.11 Sequencing of DNA

2.6.11.1 ABI sequencing

Sequencing was carried out in the group of Prof. S. Schreiber at the “Institut für klinische Molekularbiologie” (IKMB, Christian Albrechts University, Kiel, Germany). Samples were purified (2.6.4) and adjusted to a DNA concentration of 100 ng/µL (plasmids) or 120 ng/µl (cosmids) in H_2O_{bidest}. Then, 3 µl of DNA were mixed with 1 µl of primer (4.8 µM). According to the manufacturer´s instructions, a reaction mixture was added. An ABI 3730XL DNA analyzer (Applied Biosytems/Life technologies, Darmstadt, Germany) was used based on the Sanger technique (Sanger *et al.* 1977).

2.6.11.2 454 sequencing

Sequencing of entire cosmids was accomplished by M. Schilhabel in the group of Prof. S. Schreiber at the IKMB (2.6.11.1) with a 454 FLX sequencer system (Roche 454, Branford, USA). The pyrosequencing technique is based on *de novo* sequencing by a whole shotgun approach (Ronaghi *et al.* 1998). Isolated DNA with a minimum concentration of 300 ng/µL and an optical purity of $E_{260/280}$ of 1.8-2.0 in H_2O_{bidest} was required. Fosmids were pooled in equimolar amounts and afterwards sequenced with the Roche FLX.

Whole-genome sequencing was performed in the Göttingen Genomics Laboratory (G2L) in the working group of Prof. Rolf Daniel (Genomic and Applied Microbiology, University of Göttingen) using the 454 FLX pyrosequencing system (Roche 454, Branford, USA). The isolated DNA provided for sequencing was used to create 454-shotgun and paired end libraries following the GS FLX general library protocol (Roche 454, Branford, USA).

2.7 Standard techniques for working with proteins

2.7.1 Induction

Cultures were inoculated with 1-3% of an overnight culture and grown on a rotary shaker (200 rpm). In order to find the optimal temperature for expression, different incubation temperatures were tried out. Cultures were incubated at 37°C for 2-3 h, at 28°C for 3-4 h and at 17°C for 6- 8 h until an OD_{600} of 0.8 was reached. The production of the recombinant proteins by *E. coli* BL21 (DE3) was then induced by the addition of 0.1 to 1 mM isopropyl-beta-D-thiogalactopyranoside (IPTG). The induced cells were then further incubated until a high cell density was reached (up to 4 h at 37°C and up to 18 h at 17°C). The temperature and concentration of IPTG that brought the best yield of recombinant enzyme were applied in further expression studies.

2.7.2 Preparation of crude cell extracts

After incubation, the induced cultures were harvested by centrifugation (2.5.6). The pellets were resuspended in phosphate (PB) or lysis buffer (2 to 5 ml per g wet weight). Cells of pellets resulting from a culture volume bigger than 100 ml were disrupted in a French pressure cell (American Instrument Company, Silver Spring, MD, USA) with at least one repeating step in order to obtain a clear lysate. The cells burst through the high pressure within the pressure cell. High viscosity of the lysate due to genomic DNA was lowered by ultrasonication for 5 to 15 min. This method was also applied for cell pellets resulting from culture volumes of less than 100 ml with a sonotrode (ultrasonication processor UP 200S, 24 kHz, 200 W, Dr. Hielscher GmbH, Teltow, Germany). The cell suspension was sonicated on ice in an E-cup for 5 to 30 min (amplitude 50%, cycle 0.5) until the lysate visibly started to clear. Cellular debris was sedimented by centrifugation at 13,000 rpm and 4°C for 20 min (centrifuge 5417R, Eppendorf, Hamburg, Germany). Larger volumes were harvested in a Sorvall RC6+ centrifuge (rotor SS-34; Thermo scientific, Braunschweig, Germany) at 13,000 rpm and 4°C for 20 min. The supernatant containing the proteins was transferred to a new E-cup or Falcon tube and stored at 4°C for up to two weeks and the cell pellet was discarded if not used for denaturing purification.

0.1 M Phosphate buffer (PB) pH 7.0:	$KH_2PO_{4\ aq}$ (0.2 M)	39 ml
	$K_2HPO_{4\ aq}$ (0.2 M)	61 ml
	H_2O_{bidest}	*ad* 200 ml

0.1 M Phosphate buffer (PB) pH 8.0:	$KH_2PO_{4\ aq}$ (0.2 M)	5.3 ml
	$K_2HPO_{4\ aq}$ (0.2 M)	94.7 ml
	H_2O_{bidest}	*ad* 200 ml

The pH was measured and if necessary adjusted with $KH_2PO_{4\ aq}$ (0.2 M) or K_2HPO_{4aq} (0.2 M).

Lysis buffer:	NaH_2PO_4	50 mM	NaCl	300 mM
	Imidazole	10 mM		

The substances were solved in H_2O_{bidest} and pH was adjusted to 8.0 with NaOH.

2.7.3 His_6-tagged protein purification under native conditions by immobilized metal ion affinity chromatography (IMAC)

Cell extracts of cultures containing six fold histidine (His_6)-tagged proteins in the soluble fraction were prepared in lysis buffer (2.7.2) and were incubated with 1 ml of Ni-NTA agarose (Ni-NTA coupled to sepharose, QIAGEN, Hilden, Germany) per 4 ml of lysate. The His_6-tagged proteins bound to the matrix at 4°C on a rotary shaker (200 rpm) for 2 h to overnight. The sample was loaded on a column and the flow through was collected for analysis. Two washing steps with 4 ml of wash buffer followed before the His_6-tagged proteins were eluted with 8 x 0.5 ml of elution buffer.

Wash buffer:	NaH_2PO_4	50 mM	NaCl	300 mM
	Imidazole	20 mM		
Elution buffer:	NaH_2PO_4	50 mM	NaCl	300 mM
	Imidazole	250 mM		

Both solutions were solved in H_2O_{bidest} and pH was adjusted to 8.0 using NaOH.

2.7.4 His_6-tagged protein purification under denaturing conditions

Some overexpressed proteins are deposited in inclusion bodies within the *E. coli* cells. In order to purify proteins from this insoluble fraction, cell lysates were made by resuspending the cell pellet in 5 ml of denaturing lysis buffer per gram wet weight. The cells were stirred for up to 60 min at RT until the lysate turned clear. The lysate was centrifuged for 30 min at RT (13,000 rpm, centrifuge 5417R, Eppendorf, Hamburg, Germany). The supernatant was incubated with Ni-NTA Agarose as described in 2.7.3 at RT and loaded on a column. The Ni-NTA agarose was washed twice with 4 ml of wash buffer. Elution of the recombinant protein was carried out 4-times with 0.5 ml buffer E1 and 4-times with 0.5 ml buffer E2. All fractions were collected and analyzed by SDS-PAGE (2.7.7).

Lysis, wash and elution buffers E1 and E2 were all composed of

NaH_2PO_4	100 mM	Tris	10 mM
Urea	8 M	solved in H_2O_{bidest}.	

The pH of the lysis buffer was adjusted to 8.0 using NaOH. With HCl, the wash buffer was adjusted to pH 6.3, the elution buffer E1 to pH 5.9 and E2 to pH 4.5 before usage.

2.7.5 Dialysis

Dialysis was performed in order to change the buffer and thus to remove salts from the enzyme solution that may have a negative influence on further assays or stability. Protein containing elution fractions (2.7.3) were combined and dialyzed against 0.1 M PB (pH 8.0) in a dialysis membrane (Membra-Cel™, MWCO 7,000, 22 mm diameter, Serva Electrophoresis GmbH, Heidelberg, Germany). Therefore, the membrane was prepared according to the manufacturer´s instructions and filled with the elution fractions. It was put in 1 l of PB and stirred slowly overnight on a magnetic stirrer at 4°C. The buffer was exchanged against fresh 0.1 M PB the next day and the proteins were dialyzed for another 2 h. Alternatively, the fractions were combined in a concentrator (Vivaspin20, MWCO 10,000, Sartorius Stedim Biotech GmbH, Göttingen, Germany) and centrifuged with 5,000 rpm at 4°C in a Falcon centrifuge 5804R (rotor A-4-44, Eppendorf, Hamburg, Germany). When only concentrated protein solution was remaining above the filter membrane, the enzyme solution was washed twice with 2-4 ml of 0.1 M PB (pH 8.0) and finally diluted in PB to approximately 10 mg/ml of protein.

2.7.6 Protein quantification (Bradford 1976)

For the quantitative measurement of a protein concentration, the Roti®-Quant solution was applied (Carl Roth GmbH, Karlsruhe, Germany) according to the manufacturer´s protocol. The anionic dye Coomassie Brilliant Blue G250 within the solution binds to positively charged amino acids of the proteins and thus a color change reaction takes place. By this, the protein concentration was measured after an incubation of 5 min in the dark in a photometer (SmartSpec™ Plus, BIO RAD, Hercules, CA, USA) at 595 nm against a protein free blank with buffer. The extinctions were compared with a standard curve made with concentrations of BSA between 0.2 and 1 mg/ml as a reference protein, so the concentrations could be calculated.

2.7.7 SDS-polyacrylamide gel electrophoresis (SDS-PAGE; Laemmli 1970)

The protein solutions were analyzed by SDS-PAGE. SDS is an anionic amphipathic substance that binds to polypeptides. It acts denaturing and confers an almost evenly distributed charge. The denatured proteins can migrate in the electromagnetic field through the matrix. The electrophoretic mobility is dependent on a function of the length of a polypeptide chain and its charge. Smaller polypeptides move faster through the matrix than bigger ones. The Mini-Protean equipment (BioRad, Munich, Germany) was used for preparing the gels and for carrying out the electrophoresis.

2.7.7.1 Preparation of denaturing SDS-polyacrylamide gels

Usually, discontinuous gels with a 7% stacking gel and a 12 or 15% separating gel were prepared. After cleaning both with 70% EtOH, a spacer plate was put together with a short plate and arrested in a casting frame. The glass plate sandwich was clamped in a casting stand and loaded with approximately 5 ml of separating gel (Table 9). The gel was overlaid with a thin wall of water in order to get a smooth gel surface and to ensure almost anoxic polymerization. After ca. 30 min, the water was removed with a tissue and the stacking gel (Table 9) was applied on the separating gel. A comb with 10 molds was set in the stacking gel before its polymerization. After ca. 20 min, the comb was removed and the gel ready for electrophoresis.

Separating gel stock solution:	Tris	1.5 M	SDS	0.4% (w/v)
	H_2O_{bidest}	*ad* 250 ml	pH 8.8	
Stacking gel stock solution:	Tris	0.5 M	SDS	0.4% (w/v)
	H_2O_{bidest}	*ad* 100 ml	pH 6.8	
Acrylamide stock solution:	Rotiphorese® Gel 40 with bisacrylamide (19:1; Carl Roth GmbH, Karlsruhe, Germany)			
Ammonium persulfate (APS):	10% (w/v) in H_2O_{bidest}			

Table 9. Pipetting scheme for SDS polyacrylamide gels.

	Separating gel		**Stacking gel**
	12%	**15%**	**7%**
Acrylamide stock solution	3.0 ml	3.75 ml	0.7 ml
Separating gel stock solution	2.5 ml	2.5 ml	/
Stacking gel stock solution	/	/	0.96 ml
H_2O_{bidest}	4.5 ml	3.75 ml	2.34 ml
TEMED	9 µl	11 µl	6 µl
APS	45 µl	55 µl	20 µl
Total volume	10.054 ml	10.066 ml	4.026 ml

After the glass plates with the SDS-gel were put into a Mini-Protean (BioRad, Munich, Germany) inner chamber they were put horizontally into an electrophoresis tank which was filled with running buffer.

Running buffer (10 x):	Tris	30.3 g	Glycine	144.1 g
	SDS	10 g	H_2O_{bidest}	*ad* 1l

2.7.7.2 Sample preparation for SDS-PAGE and electrophoresis conditions

Samples were mixed 4:1 with denaturing loading dye and incubated at 95 °C for 5 min. After centrifugation at 13,000 rpm for 2 min in a minispin centrifuge (Eppendorf, Hamburg, Germany), samples were applied in the molds of the SDS-gel.

Loading dye:	Glycerol	50% (v/v)	Dithiothreitol (DTT)	100 mM
	SDS	4% (w/v)	Bromphenol blue	0.02% (w/v)
	Tris-HCl (pH 6.8)	150 mM	EDTA	1 mM
	NaCl	30 mM	H_2O_{bidest}	*ad* 10 ml

The loading dye was stored as aliquots of 1 ml at -20°C.

When two gels were running in parallel, amperage of 40 mA was set until the dye front passed the stacking gel. The power was supplied by a PowerPac™ Basic (BioRad, Munich, Germany). The samples passed through the separating gel with 60 mA. For only one gel, the amperage was lowered to 20 mA and 30 mA, respectively, until the dye front reached the end of the gel.

2.7.7.3 Coomassie staining of proteins and estimation of molecular weight

After electrophoresis, the SDS-gels were stained overnight with Coomassie Brilliant Blue R250 (Gerbu Biotechnik GmbH, Gaiberg, Germany) that binds non-specifically to proteins.

Staining solution (1 l):	Coomassie Brilliant Blue R-250 (10% solution)	4 ml
	Methanol	0.4 l
	Acetic acid	0.1 l
	H_2O_{bidest}	0.5 l

The gel was discolored for a few hours with 20% acetic acid so separate blue protein bands were visible. The protein bands were compared with the bands of a protein molecular weight marker (#SM0431, #SM0661, #SM0671, Fermentas, St.Leon-Rot, Germany) that was also applied on each SDS-gel.

2.7.8 Transfer of proteins on nitrocellulose membranes (Western Blot; Towbin *et al.* 1979)

Western immunoblotting was accomplished in order to detect His_6-tag purified proteins with penta-His- (His_5-) specific antibodies. After SDS-PAGE (2.7.7), proteins and a prestained molecular weight marker (# SM0671, Fermentas, St. Leon-Rot, Germany) were transferred on a nitrocellulose membrane by semi-dry transfer electrophoresis. Therefore, the SDS-gel was covered carefully with a nitrocellulose membrane and laid in between 6 wet sheets of Whatman-paper. The gel and membrane sandwich was laid between two sponges and arrested horizontally in a blotting cassette (Trans-Blot SD cell, BioRad, Munich, Germany) and put into an electrophoresis tank. The SDS-gel on the side of the cathode and the nitrocellulose membrane on the anode side, the tank was filled half-full with transfer buffer.

Transfer buffer:	Tris	125 mM	Glycine	192 mM
	Methanol (100%)	20% (v/v)	H_2O_{bidest}	*ad* 1 l

The pH was adjusted to 8.6 and the buffer stored at 4°C.

With a power supply (PowerPac^{TM} Basic, BioRad, Munich, Germany), the proteins were transferred on the membrane with 5 mA/cm^2 (ca. 300 mA) for 90 min.

2.7.8.1 Immunodetection of six fold histidines

After blotting, the membrane was washed twice with TBS buffer (100 mM Tris, 0.9% (w/v) NaCl, pH 7.5) for 10 min. In order to block unspecific binding-sites, the membrane was incubated overnight at RT in 5% milk powder solution made with TBST buffer (100 mM Tris, 0.9%

(w/v) NaCl, 0.1% (v/v) Tween-20, pH 7.5). The next day, the membrane was washed three times with TBST for 5 to 10 min. Then, the membrane was incubated with the primary His_5-antibodies (dissolved 1:5,000 in TBST; polyclonal from rabbit, MoBiTec, Göttingen, Germany) for at least 1 h to overnight at 4°C. Afterwards, the membrane was washed three times with TBST for 10 min each. The secondary anti-rabbit IgG antibodies were supplied as a conjugate with alkaline phosphatase (dissolved 1:10,000 in 5% milk powder solution, derived from goat, Sigma, Munich, Germany) and incubated together with the membrane for 1 h at RT so that they could bind to the primary antibodies. The membrane was washed again three times with TBST for 10 min. Finally, the detection of the His-tagged proteins was possible by the reaction of the alkaline phosphatase bound to them. The membrane was equilibrated against detection buffer (100 mM Tris-HCl, 100 mM NaCl, pH 9.5) for 3 min. In 10 ml of BCIP/NBT-staining solution, the membrane was incubated without light until signals were visible as dark-brown precipitated substrate. The reaction was stopped by washing the membrane with water.

BCIP/NBT-staining solution:	NBT-solution (75 mg/ml NBT in 70% DMF)	66 µl
	BCIP-solution (50 mg/ml BCIP in 100% DMF)	33 µl
	Detection buffer	*ad* 10 ml

2.7.9 Lyophilization

In order to store enzyme for longer periods (> 3 weeks) at 4°C, the dialyzed solution was frozen and subsequently dried overnight in a freeze-drying machine (Alpha 1-4 Loc-1M, Martin Christ GmbH, Osterode am Harz, Germany).

2.8 Enzyme assays

2.8.1 Tributyrin (TBT) agar plate assay

E. coli clones were tested for lipolytic activity by transferring them on LB agar plates containing 1% tributyrin (TBT) as indicator substrate. For the preparation of the medium, LB agar was prepared and heated in a microwave. Then, the TBT was added and the medium was homogenized for 3 min with an ULTRA TURRAX® T18 basic homogenizer (IKA WORKS Inc., Wilmington, NC, USA). The agar was autoclaved immediately and the plates were prepared as soon as possible to avoid TBT drops. Active clones hydrolyze TBT, butyric acid is being released and the colonies show the formation of clear halos surrounding them after growth for one night at 37°C and a following incubation of 1-3 days at 56°C. Cosmid DNA was isolated from the positive clones obtained in the initial screening, retransformed in *E. coli* DH5α and the resulting

clones were examined on the same type of indicator plates for esterase/lipase activity in order to avoid false positive clones due to contamination. Subclones and transposon mutant clones were also streaked onto LB-TBT agar plates and tested for hydrolytic activity.

2.8.2 *Para*-nitrophenol (*p*NP) ester assay

*P*NP esters are substrates that release chromogenic *para*-nitrophenol (=4-nitrophenol or *p*NP) when the ester bond to a fatty acid is being hydrolyzed by an esterase or lipase. Activity tests were performed by incubating the enzymes with 0.1 to 1 mM *p*NP substrate in 0.1 M potassium phosphate buffer (PB, pH 8.0) at assay temperatures between 50 and 75°C, unless otherwise indicated. Substrates with different acyl chain lengths were purchased at Sigma Aldrich (Munich, Germany): butyrate (C_4), hexanoate (C_6), octanoate (C_8), decanoate (C_{10}), dodecanoate (C_{12}), myristate (C_{14}), palmitate (C_{16}) and stearate (C_{18}). Stock solutions with each substrate were prepared with a 10 mM concentration in isopropanol and stored at 4°C for not more than 4 weeks.

The reaction was measured by quantification of the released yellow *para*-nitrophenol at 405 nm in disposable cuvettes (Sarstedt, Nümbrecht, Germany) with 1 cm thickness using a spectrophotometer (SmartSpec™ Plus Spectrophotometer, BIO RAD, Hercules, CA, USA). The extinction was measured against an enzyme-free blank with the respective *p*NP ester.

In order to determine the extinction coefficients (ε), calibration curves were made with *para*-nitrophenol concentrations ranging from 0.05 mM to 2 mM in PB with a pH of 7.0 and 8.0. At pH 7.0, an ε of 10,400 $M^{-1}cm^{-1}$ and at pH 8.0, an ε of 19,454 $M^{-1}cm^{-1}$ was assumed for all following calculations.

2.8.2.1 *P*NP ester assay with crude cell extracts of single clones

Of single *E. coli* clones, crude cell extracts were prepared in PB pH 7.0 or 8.0 (2.7.2). In E-cups, 20 to 40 µl of crude cell extract were mixed with a *p*NP substrate which was diluted to a final concentration of 0.5 to 1 mM in 0.1 M PB (pH 7.0 or 8.0). The total volume of 500 µl was incubated at the desired temperature for up to 20 min. In order to avoid false-positive clones, an *E. coli* clone with an empty vector was tested in parallel. After incubation, the samples were centrifuged at 13,000 rpm and 2°C for 5 min in a centrifuge 5804R (Eppendorf, Hamburg, Germany). The extinction of the supernatant was measured at 405 nm in one way cuvettes (1 cm thickness, Sarstedt, Nümbrecht, Germany), if necessary diluted with ice-cold PB against enzyme free blank.

2.8.2.2 *P*NP ester assay in a microtiter plate scale

In a microtiter plate scale, clones were grown in a 96 deep-well plate containing 1.2 ml of LB with ampicillin per well. After incubation for 16 to 24 h at 37°C and 250 rpm, cells were harvested by centrifugation (centrifuge 5804R, Eppendorf, Hamburg, Germany) and the supernatant was discarded. Cells were lysed during 1 h incubation at 37°C with 125 µL/ well of lysozyme (10 mg/ml) containing phosphate buffer pH 8.0. Cell debris was collected by a centrifugation step (5,000 rpm, 20 min, 4°C; centrifuge 5804R, Eppendorf, Hamburg, Germany). From the deep-well plate, 10 µl of crude cell extract were transferred to a 96 well microtiter plate and incubated with 190 µL of phosphate buffer (pH 8.0) that contained either 1 mM *p*NP butyrate or dodecanoate in order to screen enzymes that are active on long- or short-chain esters. The samples were incubated for 30 min at 56°C and subsequently, the extinction of the cleaved *para*-nitrophenol was measured in a microtiter plate spectrophotometer (Benchmark, Bio-Rad, Hercules, CA, USA) at 405 nm against enzyme free blank.

2.8.2.3 Activity assays with purified enzymes using *p*NP substrates

With purified and dialyzed enzymes it was possible to calculate specific activities based on the Lambert-Beer law expressed in units. One unit is defined as the amount of enzyme that catalyzes the appearance of 1 µmol *para*-nitrophenol per min at conditions described below.

Usually, up to 1 µg of enzyme was applied per reaction in order to get a clear result. After incubation, the reaction was stopped by adding 0.2 M (final concentration) Na_2CO_3. The reaction mixture was centrifuged (centrifuge 5804R, Eppendorf, Hamburg, Germany) at 13.000 rpm and 2°C for 5 min, in order to sediment turbid particles that interfere in the measurement of the extinction that was carried out in one-way cuvettes (Sarstedt, Nümbrecht, Germany) with 1 cm thickness using a spectrophotometer (SmartSpec™ Plus Spectrophotometer, BIO RAD, Hercules, CA, USA) against an enzyme-free blank.

2.8.2.3.1 Substrate specificity

In order to find out if the enzymes are active on short or long-chain fatty acid esters, they were incubated with *p*NP butyrate (C_4), hexanoate (C_6), octanoate (C_8), decanoate (C_{10}), dodecanoate (C_{12}), myristate (C_{14}), palmitate (C_{16}) and stearate (C_{18}). The substrates had a final concentration of 1 mM and the incubation took place at the optimal temperature (2.8.2.3.2) depending on the enzyme for exactly 10 min. The reaction was stopped with Na_2CO_3, the samples were centrifuged and subsequently measured against an enzyme free blank with the respective substrate. The *p*NP-reaction that showed the highest E_{405} value was the optimal substrate for the enzyme.

2.8.2.3.2 Temperature optimum

Temperature optima of the enzymes were determined with *p*NP decanoate or dodecanoate as substrates at temperatures ranging from 10°C to 90°C, as these substrates are not showing auto-hydrolysis at elevated temperatures. In E-cups, the enzymes were preincubated in PB (pH 8.0) at the given temperatures for 2 min. The enzyme reaction was started by the addition of the substrate to a final concentration of 1 mM. The reaction was stopped after exactly 10 min with Na_2CO_3. The highest E_{405} value could be measured at the optimal temperature for the enzyme.

2.8.2.3.3 Temperature stability

To study the stability against thermal denaturation, the enzymes were incubated in aliquots at 50, 60, 70 or 90°C for up to 72 hours. When the incubation time was over, the enzyme solutions were stored at 4°C until their residual activity was measured with *p*NP dodecanoate or decanoate. Therefore, PB (0.1 M, pH 8.0) containing substrate solution (1 mM final concentration) was added to the enzyme solutions to final volumes of 500 µl. The reaction mixtures were incubated at the optimal temperature of the enzyme for 20 min. The resulting E_{405} values were compared and set in relation to the initial enzyme activity.

2.8.2.3.4 pH-optimum and -stability

The pH optimum was investigated by incubation of the enzymes in buffers at different pH adjustments [pH 5-5.6, citrate buffer (0.05 M); pH 5.6-8, PB (0.1 M); pH 8-9, Tris-HCl (0.1 M); pH 9-10.6, glycine/NaOH (0.1 M)]. Enzyme activity was assayed using *p*NP octanoate or decanoate as substrate for 5 min at the optimal temperature of each enzyme. The reaction was measured spectrophotometrically at 405 nm against an enzyme free blank for each pH value containing the respective substrate.

2.8.2.3.5 Effect of metal ions, inhibitors, detergents and solvents

The enzymes were tested for their stability and activity in the presence of metal ions, inhibitors, detergents and solvents. After 1 h incubation with these substances at RT, their residual activity was determined by using *p*NP octanoate or dodecanoate as substrates and incubation for 10 min at each enzyme´s optimal temperature. Extinction of *p*NP was measured in a photometer at 405 nm against enzyme-free blanks that also contained the respective additives. The activities were compared with metal-, inhibitor-, detergent- and solvent-free controls.

As metal ions, Ca^{2+}, Co^{2+}, Cu^{2+}, Fe^{3+}, Mg^{2+}, Mn^{2+}, Rb^{2+} and Zn^{2+} were tested with a concentration of 1 and 10 mM in 0.1 M PB pH 7.0.

EDTA, DTT and PMSF were used as enzyme activity inhibiting substances with 1 and 10 mM concentration in 0.1 M PB pH 8.0.

In order to measure the stability against detergents, SDS, Triton X-100 and Tween 80 were applied with 1 and 5% concentration (w/v, v/v) in 0.1 M PB pH 8.0.

The stability of the enzymes was tested in the presence of the following solvents: DMSO, isopropanol, methanol, DMF, acetone, acetonitrile and ethanol with a final concentration of 10% and 30% (v/v) in 0.1 M PB pH 8.0.

2.8.2.3.6 Kinetic studies

In order to characterize the kinetic behavior of the enzymes, *p*NP substrate concentrations between 0.1 and 1 mM were tested by incubation at the optimal reaction temperature of the enzyme for 10 min. The three substrate concentrations where the best results could be measured were used for further studies. In a total volume of 1.2 ml, 0.1 M PB (pH 8.0) and *p*NP substrate were mixed and preincubated for 5 min at the optimal temperature of the enzyme. The reaction started when 5 µl of enzyme solution (approximately 1 µg) was added to the reaction mixture and the E-cup was vortexed. Immediately after the enzyme was added as well as 1, 2, 4, 6 and 10 min later, 200 µl samples were taken and stopped in an E-cup containing 50 µl of 1 M Na_2CO_3. The samples were incubated on ice until centrifugation (13,000 rpm, 2°C, 2 min). The reaction was measured at 405 nm against enzyme-free blank. With the E_{405} values, it was possible to calculate the specific activity (Units/mg of protein) as well as v_{max}, K_m and k_{cat} after Lineweaver-Burk, Eadie-Hofsteen or Hanes. The catalytic efficiency of an enzyme is expressed as k_{cat}/K_m.

2.8.2.3.7 Activity on other *p*NP and methylumbelliferyl (MU) esters

In addition to the "simple" acyl chains of the *p*NP esters mentioned in 2.8.2.3.1, the substrate range of the enzymes was also tested with the following *p*NP esters in a final concentration of 0.5 mM in PB (0.1 M, pH 8.0): 2-phenylpropanoate [racemic mixture (rac)], 3-phenylbutanoate (rac), cyclohexanoate, 2-(3-benzoylphenyl) propanoate (=ketoprofen), 2-naphthoate, 1-naphthoate, adamantanoate and 2-(4-isobutylphenyl)-N-(4-nitrophenol) propanamide. Activity was measured at 405 nm after 10, 20 and 30 min incubation at 50 or 70°C.

Table 10. Chemically and pharmaceutically relevant *p*NP substrates used in this study. The *p*NP residue is represented by R^1.

R^1 = ***para*-nitrophenol** - 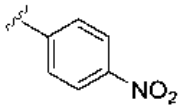 ***p*NP**	
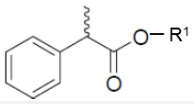	2-phenylpropanoate (rac)
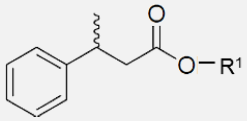	3-phenylbutanoate (rac)
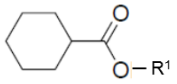	cyclohexanoate
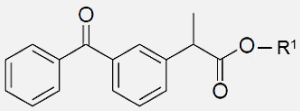	2-(3-benzoylphenyl) propanoate (=ketoprofen)
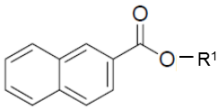	2-naphthoate
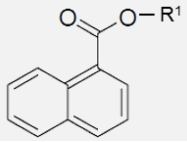	1-naphthoate
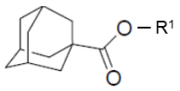	adamantanoate
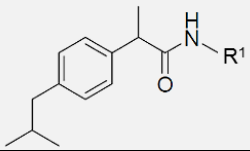	2-(4-isobutylphenyl)-N-(4-nitrophenol) propanamide (=ibuprofenmide)

In order to assay (*R*)- or (*S*)- selectivity of the enzymes, activity on chiral *p*NP and MU esters was tested with (*S*)-/(*R*)-2-methyldecanoic acid ester, (*S*)-/rac-/(*R*)-2,3-dihydro-1*H*-indene-1-carboxylate (indancarboxylic acid ester), (*S*)-/rac-ibuprofen-ester and (*S*)-/rac-/(*R*)-naproxen-ester (Table 11). Enzyme activity on *p*NP esters (0.33 mM final concentration, ε = 7,392 M^{-1} cm^{-1}) was measured at 410 nm after incubation at 60 and 65°C, while activity on MU esters (0.03 mM final concentration) was measured after excitation at 360 nm by detection of fluorescence

at 465 nm. One unit is defined as the amount of enzyme that catalyzes the appearance of either 1 µmol *para*-nitrophenol or methylumbelliferone per min.

Table 11. Chiral substrates used in this study. The residue R^1 of the compounds can either be *p*NP or MU. The asterisk indicates the stereogenic center.

R^1 = *para*-nitrophenol - 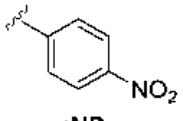 **pNP**	**R^1 = methylumbelliferyl -** 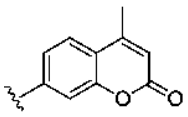 **MU**
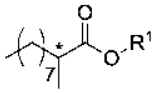	2-methyldecanoic acid ester
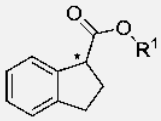	2,3-dihydro-1H-indene-1-carboxylate (= indancarboxylic acid ester)
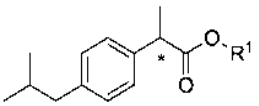	ibuprofen ester
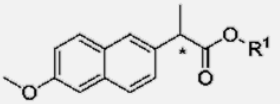	naproxen ester

2.8.3 HPLC-analysis of LipS

HPLC (high performance liquid chromatography) analysis was carried out in cooperation with the IBOC (Institute for Bioorganic Chemistry, Heinrich Heine University Düsseldorf, Research Center Jülich, Germany) within the group of Prof. Jörg Pietruszka. To determine enantioselectivity referring to the *p*NP ester and the phenyl ester, kinetic resolution has been carried out in an analytical scale: 17.32 ml of PB (0.1 M, pH 8.0) were mixed with 2 ml DMSO and 0.66 ml of a substrate stock solution (10 mM in DMSO). 652 µg freeze-dried LipS (2.7.9) were added and the reaction was mixed at 60°C for 30 min. The reaction was stopped by adding 8 ml 2 M HCl and uninterrupted extracting with 2-times 20 ml of methyl *tert*-butyl ether followed. The solvent was removed by reduced pressure. The extracted ibuprofen was converted to the corresponding methyl ester by addition of a 0.5 M diazomethane solution in diethyl ether. The solvent was removed by reduced pressure. The *ee* was determined by HPLC (Dionex) using a chiral stationary phase: Chiralpak IA (Daicel), 99.8:0.2 (*n*-heptane:isopropanol), 0.5 ml/min, 225 nm, t_R(*S*)=10.23 min, t_R(*R*)=11.17 min. The *ee* of the phenyl ester was determined using the same conditions as the methyl ester [t_R(*S*)=16.32 min, t_R(*R*)=18.07 min]. Because the enantiomers of the *p*NP ester could not be separated by chiral HPLC, the *ee* was determined by measuring the g factor (dissymmetry factor) with achiral HPLC with circular dichroism (CD) detector

(Salvadori *et al.* 1991; Reetz *et al.* 2000; Hamzic *et al.* 2011): Column: Hyperclone ODS C18, conditions: 90:10, $CH_3CN:H_2O$, 0.5 ml/min, 220 nm, t_R(ibuprofen)=2.7 min, t_R(*p*NP ester)=4.5 min. Calculation of the enantioselectivity (*E*) value and the conversion (c) was performed by the method of Faber *et al.* (Kroutil et al. 1997).

2.8.4 Titration assays

Tributyrin, triolein and polyglycerol-3-laurate were chosen as substrates to study activity on triglycerides using a titrator (Titrando, Metrohm, Filderstadt, Germany) and the pH-stat method. The substrate concentrations of the triglycerides ranged from 5 to 50 mM and of polyglycerol-3-laurate from 0.5 to 7.5% (w/v) in 2 mM Tris-HCl buffer pH 7.0. In order to compensate the pH of the solution that is decreasing during the hydrolysis reaction because of the liberated free fatty-acids, 20 mM KOH solution was added in order to keep the pH at 7.0. The reaction was performed at 60°C in order to avoid autohydrolysis of the substrates that occurs at higher temperatures. It was carried out for at least 5 min before the enzyme was added in order to have a control rate. The amount of 20 mM KOH solution that had to be added was used to calculate the specific activity expressed as units per milligram of enzyme (U/mg). One unit was the amount that produces 1 µmol of fatty acid per minute under the specified assay conditions.

2.8.5 Propyl laurate esterification assay

The propyl laurate assay was applied with 1-propanol and lauric acid as well as 1-tetradecanol and myristic acid as substrates for LipS. Both reactants were incubated in equimolar conditions (20 mmol) at 70°C together with 15 mg of lyophilized enzyme in a bottle under slow rotation. After 0, 24 and 48 h, samples of 0.5 g were taken and the acid value of the reaction mixture was determined by titration. Therefore, the samples were solved in 20 ml of toluol and phenolphthalein as pH indicator was added. Then, titration was carried out with 0.5 M $KOH_{ethanol}$ until the pH indicator changed its color. As a control, the acid values of a control without enzyme were also tested. The acid values (AV) were calculated and used for the determination of propyl laurate/tetradecyl myristate units (PLU/MMU) per mg of enzyme (Equation 3-5). One unit was defined as 1 µmol of propyl laurate or tetradecyl myristate formed per minute by the enzyme under above mentioned assay conditions.

$$\text{Acid value} = \frac{\text{M [KOH]x N [KOH]x V [KOH]}}{\text{W [sample]}} \qquad (3)$$

(M, molecular weight [g/mol]; N, molarity; V, volume [ml], W, weight [g])

$$\text{Ester [\%]} = \frac{\text{AV t0} - \text{AV t1}}{\text{AVt0}} \text{ x } 100 = \text{C x } 100 \qquad (4)$$

(AV t0, acid value after 0h; AV t1, acid value after 24 or 48 h; C, conversion)

$$\text{Activity [U/mg]} = \frac{\text{M [educts] x C}}{\text{W x t}} \qquad (5)$$

(M, molecular weight [mmol]; C, conversion; W, weight of enzyme [mg]; t, time [min])

2.8.6 Enzyme-catalyzed kinetic resolution of four acetates of secondary alcohols

The research on the resolution of the acetates of secondary alcohols was accomplished in the working group of Prof. Uwe Bornscheuer (Institute of Biochemistry, Dept. of Biotechnology & Enzyme Catalysis, Greifswald University, Germany). Three racemic acetates, i. e. 1-phenyl-1-propyl acetate, 1-phenyl-2-butyl acetate and 1-phenyl-2-pentyl acetate, were synthesized from the corresponding racemic alcohols (Musidlowska *et al.* 2001; Musidlowska-Persson and Bornscheuer 2002) except for 1-phenyl-1-ethylacetate, which was commercially available (**Fehler! Ungültiger Eigenverweis auf Textmarke.**). For the kinetic resolution, 10 mM acetate were added to a 1 ml solution containing 0.25 mg pure enzyme dissolved in PB (0.1 M, pH 7) and were mixed in a thermoshaker (Eppendorf, Hamburg, Germany) at 13,000 rpm and 70°C. Samples of 100 µl were taken at different time intervals and extracted twice with (100 µl) dichloromethane. The combined organic layers were dried over anhydrous sodium sulfate and the organic solvent was removed in a nitrogen stream. The *ee* of substrate and product were determined by gas chromatography [GC, Shimadzu GC-14A gas chromatograph, column: heptakis(2,6-O-methyl-3-O-pentyl)-beta-cyclodextrin (Machery-Nagel, Düren, Germany); carrier gas: H_2; flame ionization detector] as described earlier (Musidlowska *et al.* 2001). The retention times were as follows: 1-phenyl-1-propyl acetate $t_R(S)$= 5.7 min, $t_R(R)$= 6.9 min; 1-phenyl-1-propanol $t_R(S)$= 11.8 min, $t_R(R)$= 12.7 min; 1-phenyl-1-ethyl acetate $t_R(S)$= 3.9 min, $t_R(R)$= 5.3 min; 1-phenyl-1-ethanol $t_R(S)$= 6.2 min, $t_R(R)$= 6.8 min; 1-phenyl-2-butyl acetate $t_R(S)$= 17.5 min, $t_R(R)$= 19.3 min; 1-phenyl-2-butanol $t_R(S)$= 21.9 min, $t_R(R)$= 23.6 min; 1-phenyl-2-pentyl acetate $t_R(S)$= 31.5 min, $t_R(R)$= 31.9 min; 1-phenyl-2-pentanol $t_R(S)$= 37.5 min, $t_R(R)$= 37.5 min. Enantioselectivity and conversion were calculated from the *ee* of substrate and product according to Chen *et al*. (Chen *et al.* 1982).

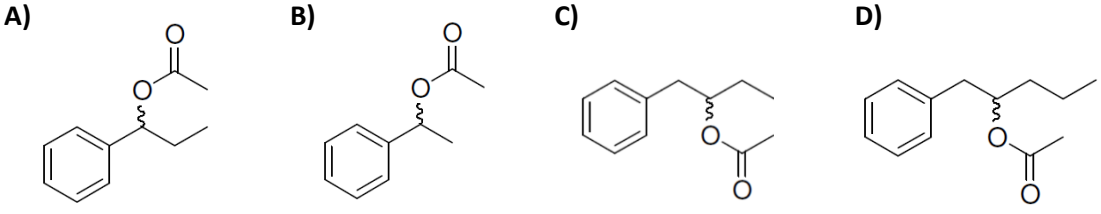

Figure 4. Acetates of secondary alcohols for kinetic resolution. A) 1-phenyl-1-propyl acetate; B) 1-phenyl-1-ethyl acetate; C) 1-phenyl-2-butyl acetate; D) 1-phenyl-2-pentyl acetate.

2.9 Crystallization

Crystallization, resolution and analysis of the crystal structure of LipS were accomplished in the X-ray Crystallography laboratory of Dr. Jochen Müller-Dieckmann (EMBL Hamburg Outstation, c/o DESY, Hamburg, Germany).

In order to follow different approaches, three constructs of *lipS* were overexpressed (2.7.1) in *E. coli* BL21 (Fersini *et al.* 2012). LipS-His_6 was expressed from *lipS*::pET-21a (Table 4) including C-terminal His_6-tag, purified (2.7.3) and applied for crystallization experiments. Additionally, *lipS* was cloned into pETM11 in its full length (amplification with the primers *lipS*::pETM11+26 for and *lipS*::pETM11 rev) and lacking 26 N-terminal amino acids (amplification with the primers *lipS*::pETM11-26 for and *lipS*::pETM11 rev). As this vector provides an N-terminal His_6-tag coding region and a TEV-protease cleavage site (Table 3), the His_6-tag can be removed by digestion from the overexpressed LipS-WT. Further details concerning any conditions are described in Fersini *et al.* 2012.

LipS was crystallized and crystallographic data sets were collected (Fersini *et al.* 2012; Chow *et al.* 2012). The structure of LipS-WT in space group (SG) P_4 was solved by molecular replacement (MR) using the structure of the carboxylesterase Est30 from *Geobacillus stearothermophilus* (PDB code 1TQH, 27% sequence identity) as a model. The search was carried out with Molrep (Vagin and Teplyakov 1997), which identified 4 molecules per asymmetric unit (a.u.), as expected from a Matthews parameter of 2.6 (Matthews 1968). Iterative cycles of manual rebuilding in COOT (Emsley *et al.* 2010) with crystallographic refinement in Refmac5 (Murshudov *et al.* 1997) converged at a final model at 1.99 Å resolution of good quality. The last rounds of refinement were done without non-crystallographic symmetry (NCS) restraints and with individual, isotropic B-factors.

LipS-His_6 with His_6-tag at the C-terminus crystallized in SG $P4_22_12$ and diffracted X-ray radiation to 2.08 Å resolution. Those data were phased by MR using the refined structure of LipS solved in SG P4. Crystals in this SG contained only 2 molecules per a.u..

The PyMOL software was used for structural alignment, analysis and visualization of protein structures (DeLano 2002).

2.10 Classification of LipS and LipT

The classification of LipS and LipT into one of the existing lipase/esterase families was accomplished by Dr. Ulrich Krauss (IMET; Institute of Molecular Enzyme Technology, Heinrich Heine University Düsseldorf, Research Center Jülich, Germany).

Amino acid sequences of the eight major lipase/esterase families (Arpigny and Jaeger 1999) were obtained from the NCBI GenBank database (Chow *et al.* 2012). Independent alignments for all families were constructed using T-coffee (Notredame *et al.* 2000). All metagenome derived lipase/esterase sequences were sorted into the eight families based on alignment scores and visual inspection of the respective alignments. Sequences homologous to LipS and LipT were retrieved from the NCBI GenBank database. Due to low sequence conservation between the different lipase/esterase sequence families, alignments were constructed independently using ClustalW2 multiple alignment (http://www.ebi.ac.uk/Tools/msa /clustalw2/) and were subsequently visualized with the software Mega 5.1 (http://www.megasoftware.net/).

2.11 Computational analysis

Nucleotide and amino acid sequences were analyzed and processed with programs and databases listed below.

2.11.1 Programs

- BioEdit (http://www.mbio.ncsu.edu/bioedit/bioedit.html)
- Clone Manager Suite 7 (SciCentral Software, licenced)
- Mega 5.1 (http://www.megasoftware.net/)
- Quality One (Bio-Rad Laboratories, Munich, Germany)
- Staden Package containing Pregap and Gap4 (http://staden.sourceforge.net/)

2.11.2 Databases

- BRENDA Enzyme database (http://www.brenda-enzymes.info/)
- ClustalW2 multiple alignment (http://www.ebi.ac.uk/Tools/msa/clustalw2/)
- IMG (integrated microbial genomes; https://img.jgi.doe.gov/cgi-bin/er/main.cgi)
- Needle EMBOSS pairwise alignment (http://www.ebi.ac.uk/Tools/psa/)
- NCBI Database (http://www.ncbi.nlm.nih.gov/)
    - BLAST Alignment tools (http://blast.ncbi.nlm.nih.gov/Blast.cgi)
    - GenBank® Sequence database (http://www.ncbi.nlm.nih.gov/genbank/)
- Pfam (http://pfam.sanger.ac.uk/)
- RCSB PDB (Protein Data Base; http://www.rcsb.org/pdb/explore.do)
- Signal IP signal peptide prediction (http://www.cbs.dtu.dk/services/SignalP/)
- UniProt (Swiss-Prot and TrEMBL, http://www.uniprot.org/)

3 Results

3.1 Enrichment cultures, construction of metagenomic libraries and screening for clones with lipolytic activity

The two enrichment cultures described in this section were analyzed and used for the construction of metagenomic libraries within the Diploma thesis of Jennifer Chow (Chow 2008). The results are summarized briefly below together with the lipolytic clones that were found by screening the libraries (Chow 2008).

3.1.1 Enrichment of soil and water samples on MSM supplemented with olive oil and pyruvate

Soil and water samples were taken from ten different sites at the Botanical Garden in Klein-Flottbek (Hamburg, Germany, 53°33´44.56´´N, 9°51´40.11´´E; Chow 2008). Six sites differed concerning the quality of the soil, the content of sand, humus and humidity. Water samples were taken from four different ponds. These environmental samples were pooled and the thermophilic bacteria they contained were successfully enriched under aerobic conditions at 65°C on MSM (2.5.1) that was supplemented with vitamins as well as pyruvate and olive oil (2.4.4) as carbon sources for heterotrophic organisms. After three weeks of incubation, genomic DNA was isolated from the enrichment culture (2.6.1) and served as a template for PCR with primers that bind specifically to the 16S rRNA genes of bacteria or archaea (Table 5, 2.6.10). In this way, the microbial community was characterized on a phylogenetic level by amplification of 16S rRNA genes with the primers 616V/1492R for bacteria and Arch20f/927R for archaea. No PCR product could be received by using the archaea-specific 16S rRNA gene primers. The PCR products obtained with the bacterial 16S rRNA primers were cloned into pDrive cloning vector (QIAGEN, 2.6.8.3.1) and sequenced (2.6.11.1) with the primers M13 for and rev (Table 5). The 20 sequences were processed (Gap4, 2.11.1) and analyzed by comparison with 16S rRNA gene sequences deposited in the NCBI database using BLAST (2.11.2; Altschul and Koonin 1998; Chow 2008). All of the sequences originated from members of *Firmicutes*. The majority, i. e. 16 of the 16S rRNA genes that were amplified, could be assigned to *Symbiobacterium thermophilum* strain IAM 14863 (NCBI acc. no. NC_006177, max. identity 95-99%, E-values 0.0, see Figure 5). Two sequences were highly similar to a *Geobacillus debilis* 16S rRNA gene (NCBI acc. no. NR_029016.1, max. identity 93-97%, E-value 0.0), one to a 16S rRNA

gene from an uncultivated compost member of *Clostridia* (NCBI acc. no. FN667168, max. identity 92%, E-value 0.0) and one sequence was assigned to an uncultured member of *Enterobacteriaceae* (NCBI acc. no., JF733455.1, max. identity 92%, E-value 0.0).

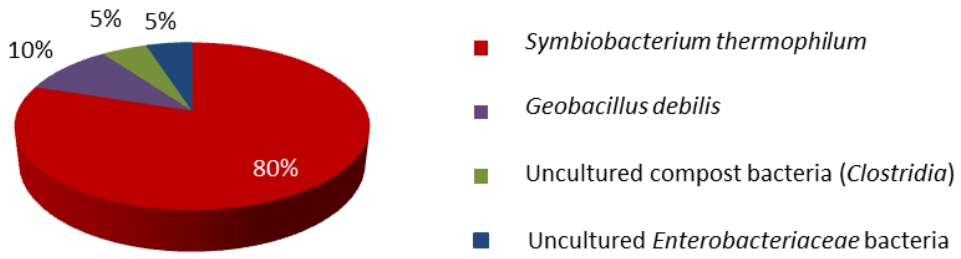

Figure 5. Phylogenetic composition of the soil and water enrichment culture based on comparison of amplified 16S rRNA gene sequences with sequences deposited in the NCBI database.

3.1.2 Enrichment of *Thermus* sp.

Another enrichment culture was prepared with water samples from a heating water system of the Biocenter Klein Flottbek (Hamburg, Germany). The enrichment was incubated at 75°C on *Thermus* medium (medium D; 2.5.1.2, 2.4.3; Chow 2008) under moderate aeration. After three weeks of incubation, cells were harvested and genomic DNA was isolated (2.6.1).

Amplification of bacterial and archaeal 16S rRNA genes was carried out with the primer pairs 616V/1492R and Arch20f/927R (Table 5). No product could be received with the primer pair that binds specifically to archaeal 16S rRNA genes. The amplified bacterial 16S rRNA genes were ligated into pDrive and sequenced (2.6.8.3.1, 2.6.11.1). Five sequences were processed and aligned with nucleotide sequences deposited in the NCBI database via BLAST-search (2.11.2; Altschul and Koonin 1998; Chow 2008). With high similarities, all sequences could be assigned to a *Thermus scotoductus* 16S rRNA gene (NCBI acc. no. EU330195.1, max. identity 97%, E-value 0.0).

3.2 Construction of metagenomic libraries

The extracted DNA of both enrichment cultures was subsequently used for the construction of two large insert metagenomic libraries by using the vector SuperCos and *E. coli* Epi100 as heterologous host (2.6.9.4, 2.2). The library of the MSM-enrichment consisted of 6,500 clones. 87 cosmids were analyzed after digestion with *Bam*HI (2.6.8.1.2) and the insert rate was 96% (Chow 2008). The library of the *Thermus*-enrichment culture comprised 576 clones, of which 28 analyzed cosmids had an average insert rate of 70%. The cosmids of both libraries had an

average insert size of 27.5 kb. With the equation of Seed *et al.* (Seed *et al.* 1982), the genome coverage of both libraries was calculated. Considering a mean genome size of 4 Mb for the MSM-enrichment (*Symbiobacterium thermophilum*: 3.57 Mb, *Geobacillus* sp. approx. 3.6 mb, *Enterobacteriaceae* bacterium approx. 4.70 Mb, *Clostridia* bacterium approx. 4.00 Mb), the library with a total of 38.38 Mb covers all four different genomes with 99.9% probability (Chow 2008). The *Thermus*-library is large enough to cover 3.45 Mb and hence the genome of *Thermus scotoductus* (2.35 Mb) with a probability of 99.9%, when assumed that it is the only occurring species in the metagenomic library.

3.3 Screening for clones with lipolytic activity

Screening of both libraries on TBT agar plates (2.8.1) only resulted in the identification of weakly positive clones that could not be verified. With the microtiter plate assay (2.8.2.2) performed between 50 and 75°C and 4-nitrophenol (*p*NP) dodecanoate as substrate, four clones of the *Thermus*-enrichment library and six clones of the MSM-enrichment library showed verifiable activity (Table 12; Chow 2008). These cosmid clones were further investigated and two of them described and characterized within this dissertation in detail in the following sections. One of these positive clones derived from the heating water enrichment library was designated pCos6B1 and the other clone from the soil and water samples enrichment library was called pCos9D12.

3.4 Screening of other metagenomic libraries on TBT agar plates

Six other metagenomic libraries constructed within the working group were also screened for clones with lipolytic activity. Most of the esterase- or lipase-positive clones were identified by using the TBT assay (2.8.1) as they showed clear halos surrounding the colonies on the turbid agar plate. The activity of some other clones was detected by using *p*NP esters of different C-chain lengths (2.8.2.2). Table 12 gives an overview of the screening results.

Table 12. Lipolytic clones from different metagenomes.

Metagenomic library	Lipolytic clones	Vector/ resistance/ *E. coli* strain	Insert size (kb)	Screened positive on	ORFs cloned in pET-vector	Active in *E. coli* BL21
***Thermus*-enrichment**	pCos6B1, 4/D1, 9/B4, 4/H7	pWE15/ Amp^R/ Epi100	15-25	*p*NP C_{10}-C_{14}	*lipT* of pCos6B1	yes
MSM enrichment	pCos9D12, Cos3D7, Cos4F8, Cos3E2, Cos5G6, Cos6G11	SuperCos/ Amp^R/ Epi100	20-30	*p*NP C_{10}-C_{14}	*lipS* of pCos9D12	yes
Elefant feces enrichment	20/D3, 11/A7, 11/B11, 19/C11, 30/B5, 34/E7, 41/D9, 45/E2, 45/G2, 45/G5, 45/B6	pWE15/ Amp^R/ Epi100	10-22.5	TBT	-	-
Biofilm on water pipeline	pcos5E5 (=BioIII5/E5), BioIII3/B1, BioIII2/A3, BioIII1/C5, BioIII1/F8, BioIII7a/B9, BioIII3/G1	pWE15/ Amp^R/ Epi100	15-40	TBT	*est5E5* of pCos5E5	yes
***Thermococcales* consortium**	61/B6, 62/E8, 69/D4, 70/F8, 71/G8, 73/E12, 74/C11, 79/C1	pWE15/ Amp^R/ VCS257	29	TBT, *p*NP C_{12}	see table 13	no
Elbe sediment "Glückstadt"	114/D1, 126/E11, 139/G2, 143/F5, 149/H12	pCC1FOS/ Cm^R/ Epi300	24-39	TBT	*est143/F5*	yes
Elbe sediment "Teufelsbrück"	TB 49 E9, TB 60 F10, TB 65 C10, TB 66 C2, TB 67 F2, TB 98 D3, TB 99 B4, TB 1 C10	pCC1FOS/ Cm^R/ Epi300	30-35	TBT	-	-
Elefant feces	18/1G, 23/10D, 39/3A, 66/5B, 69/5A, 71/9C, 77/10G, 84/2G, 124/6H, 137/8G, 148/3G, 167/8E and 51 other	pCC1FOS/ Cm^R/ Epi300	37.5	TBT	-	-

As far as possible, the clones were subcloned into the vector pTZ19R::Cm^R (2.6.9.5) or sequenced by 454- or Illumina-sequencing (2.6.11). Putative ORFs were searched (Clone Manager, 2.11.1) and genes encoding α/β-hydrolases, esterases or lipases were found by a BLAST-comparison (2.11.2; Altschul and Koonin 1998) to sequences deposited in the NCBI database. The most promising genes with high similarity to putative esterases or lipases were amplified with specific primers (appendix) and cloned into pET-21a for protein expression in *E. coli* BL21 (DE3) with subsequent His-tag purification (2.6.9, 2.7.3). Some of the purified enzymes, however, did not show verifiable lipolytic activity when tested on *p*NP substrates or TBT agar plates (see 3.5.3).

3.5 Cloning and heterologous expression of lipolytic enzymes

3.5.1 Subcloning of *lipS* and *in vitro* transposon mutagenesis of *lipT*

The cosmids were isolated from the lipolytic clones pCos6B1 and pCos9D12 (2.6.2) and cut in a preparative digestion (2.6.8.1.2). The insert of pCos6B1 was cut into 5 fragments (9.0, 8.0, 4.0, 3.5 and 2.5 kb) with *Eco*RI that altogether had a size of 27 kb. The 26.5 kb insert of pCos9D12 was cut into 6 fragments with *Sac*I (9.0, 8.0, 4.2, 2.3, 1.7, 1.3 kb). These DNA fragments were subcloned by ligation into pTZ19R::Cm^R (2.6.9.5). The plasmids were transformed into *E. coli* DH5α (2.6.9.1) and the resulting subclones were tested for lipolytic activity on LB-TBT agar plates (2.8.1). One subclone of pCos6B1 designated AF7 showed activity on TBT after incubation at 37°C overnight and at 56°C for one day. Subsequently, a transposon mutagenesis was carried out with the isolated plasmid DNA of AF7 (2.6.9.6). Transposon mutant clones were selected on LB agar plates supplemented with kanamycin (2.4.4) and streaked out on TBT agar plates. In case the transposon inserted into the gene conferring lipolytic activity, the mutant clone did not show lipolytic activity on TBT agar, because the gene sequence could not be translated correctly. One mutant clone was tested negative on TBT and consequently, the insert of this clone was partially sequenced by using transposon-specific primers (2.3, 2.6.11.1). The sequences were analyzed (2.11) and revealed an open reading frame (ORF) that was designated *lipT*. The subclones of pCos9D12 did not show lipolytic activity on TBT so that the inserts of the pTZ19R::Cm^R subclones had to be sequenced with vector specific primers (2.6.10.1). One sequence contained a part of a gene sequence that was designated *lipS.* As it was cut by the restriction endonuclease during subcloning, the ORF was completed by sequencing with gene specific primers using the cosmid clone as template.

3.5.2 Cloning of *lipS* and *lipT* into expression vectors

The genes upstream and downstream of the putative hydrolases were analyzed by a NCBI BLASTX-search (2.11.2).

Figure 6 illustrates the genes *lipS* and *lipT* in their genetic context. As the surrounding genes did not seem to have an influence on the enzymes, e.g. as maturation proteins, they were not considered as necessary for expression or activity and were not cloned.

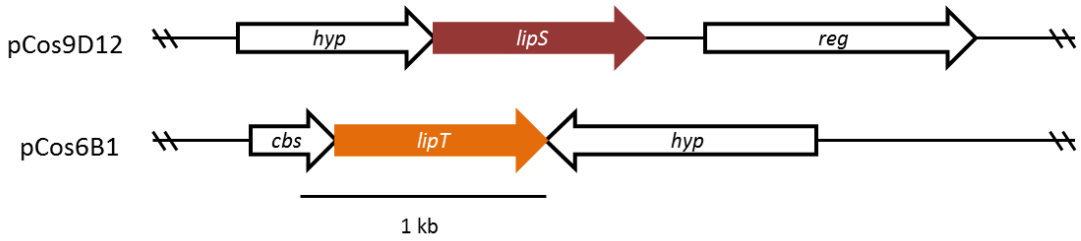

Figure 6. The genes *lipS* and *lipT* with their surrounding genes on the insert of the respective cosmids pCos9D12 and pCos6B1. **pCos9D12:** *hyp*, hypothetical protein, similarity to *Symbiobacterium thermophilum* IAM14863 (GenBank acc. no. YP_075873, max. identity 98%, E-value 0.0); *reg*, two-component response regulator variant, similarity to *Symbiobacterium thermophilum* IAM14863 (GenBank acc. no. YP_075875, max. identity 99%, E-value $1e^{-81}$). **pCos6B1:** *cbs*; CBS (cystathionine β synthase) domain-containing protein, similarity to *Thermus* sp. CCB_US3_UF1 (GenBank acc. no. AEV15940.1, max. identity 93%, E-value $2e^{-66}$); *hyp*, hypothetical protein, similarity to *Thermus scotoductus* SA-01 (GenBank acc. no. YP_004201973.1, max. identity 87%, E-value $4e^{-139}$).

The genes were amplified with specific primers (2.6.10.1) that contained *Nde*I restriction sites in the forward primers and *Hind*III sites in the reverse primers for directional cloning into the expression vector pET-21a. After PCR, the products were purified with a PCR clean-up kit (2.6.10.4) and ligated into pDrive (2.6.8.3.1). The plasmids were transformed into *E. coli* DH5α (2.6.9.1) and selected on LB agar plates containing ampicillin, IPTG and X-Gal (2.4.4). White colonies that were supposed to carry the genes were grown in 5 ml LB medium supplemented with ampicillin. The plasmids were isolated (2.6.3), digested with *Nde*I and *Hind*III (2.6.8.1.2), the resulting fragments gel-extracted (2.6.7), ligated into pET-21a (2.6.8.3.3) and transformed into *E. coli* BL21 (DE3) (2.6.9.1). The *E. coli* cells containing pET-21a and the respective genes were selected on LB agar plates with ampicillin, the plasmids were isolated (2.6.2) and their inserts were verified by direct colony PCR with gene specific primers (2.6.10.3). Additionally, the inserts were sequenced (2.6.11.1).

3.5.3 Cloning of esterase genes from active cosmid clones belonging to the *Thermococcales* consortium-library and expression and activity of the respective enzymes

The *Thermococcales* library was constructed, analyzed and screened for lipolytic activity in the Diploma thesis of Thomas Meier (Meier 2009).

In 2960 to 3060 m depth, samples were taken from low temperature diffuse emissions of a hydrothermal vent in the Logatchev Hydrothermal Field (Mid-Atlantic Ridge; 14°45'N, 44°58'W). They were used as inoculum for a thermophilic enrichment culture that was grown anaerobically at 70°C and 200 rpm on MJ-medium (Sako *et al.* 1996) and consisted predominantly of species belonging to *Thermococcales* (Meier 2009). DNA was isolated from the enrichment culture and a large-insert metagenomic library was constructed that comprised 8,500 cosmid clones (Meier 2009). Screening on TBT agar plates did not result in reproducibly active clones (Meier 2009). In a microtiter plate screening with *p*NP dodecanoate as substrate (2.8.2.2), eight cosmid clones showed significant activity. These cosmid clones were subcloned, but the subclones derived from 61/B6, 62/E8, 69/D4, 70/F8 and 74/C11 showed low activity compared to an enzyme-free negative control when tested on long and short C-chain *p*NP ester substrates at 50 to 90°C (data not shown). Nevertheless, the inserts of the subclones were sequenced while the sequences of the cosmids 71/G8, 73/E12 and 79/C1 were obtained entirely by 454 sequencing (2.6.11.2; appendix). Subsequently, all sequences were analyzed by a BLAST search (BLASTX, 2.11.2) in comparison with sequences deposited at the NCBI database. Four of eight clones (70/F8, 71/G8, 73/E12 and 61/B6) contained genes with high similarities (E-values $6e^{-63}$ to $1e^{-113}$, max. identities 69 to 98%) to four different metallophosphoesterase-genes of *Thermococcus onnurineus* NA1 (GenBank acc. no. ACJ16475.1 and AEK74001.1) and *Thermococcus* sp. 4557 (GenBank acc. no. AEK72907.1 and AEK72511.1). One clone (79/C1) showed similarity to a lysophospholipase-gene from *Thermococcus* sp. AM4 (GenBank acc. no. EEB74685.1, E-value $5e^{-150}$, max. identity 88%). For three clones (62/E8, 69/D4 and 74/C11), no significant homologies to a hydrolase-coding gene could be found. As far as an intact ORF with similarity to an esterase or lipase gene was maintained, the gene sequences (appendix) were amplified by PCR (2.6.10.2) and cloned into pET-21a for overexpression in *E. coli* BL21 (DE3; 2.6.8.3, 2.7.1). The proteins were purified by Ni-ion chromatography (2.7.3) and the sizes of the protein bands compared to their estimated molecular weight after SDS-PAGE (2.7.7; data not shown). Expression of the respective genes of Est71/G8_1 (55.4 kDa), Est71/G8_2 (22.2 kDa), Est73/E12 (18.7 kDa) and Est79/C1 (29.2 kDa) yielded the highest amounts of recombinant protein when carried out at 17°C and 200 rpm after induction with 1 mM IPTG (2.7.1).

The enzymes were tested for activity in *p*NP tests (2.8.2.1) with *p*NP octanoate, decanoate and dodecanoate as substrates at 56 to 100°C. No significant activity could be measured for the crude cell extract of the subclones or for Est71/G8_1, Est71/G8_2, Est73/E12 and Est79/C1 that were overexpressed in *E. coli* BL21 (DE3; data not shown). The results of the investigations are summarized in Table 13.

Table 13. Putative positive clones from the *Thermococcus* library with their corresponding subclones and putative genes.

Cosmid clone	Insert (kb)	Investigation type	Subclone (insert kb) in pTZ19R::Cm^R	Gene (kb) in pET-21a	Activity
61/B6	24.5	Subcloning (*Eco*RI)	Est61B6 (3.5)	/	low, *p*NP C_{12} at 70-100°C
62/E8	36	Subcloning (*Bam*HI)	Est62E8 (4.3)	/	low, *p*NP C_4 at 56°C
69/D4	18	Subcloning (*Hind*III)	Est69D4 (5.0)	/	low, *p*NP C_{12} at 70-100°C
70/F8	19	Subcloning (*Hind*III)	Est70F8 (2.4)	/	low, *p*NP C_4 at 56°C
71/G8	>15	454 sequencing	/	*est71G8_1* (1.5); *est71G8_2* (0.6)	no activity
73/E12	>15	454 sequencing	/	*est73E12* (0.5)	no activity
74/C11	40	Subcloning (*Hind*III)	Est74C11 (3.5)	/	low, *p*NP C_{12} at 70-100°C
79/C1	22.4	454 sequencing	/	*est79C1* (0.8)	low activity

As esterases and lipases from other libraries showed better activity, further investigation of these clones was postponed.

3.5.4 Cloning, expression and activity of a lipolytically active fosmid clone from the river Elbe sediment library "Glückstadt"

The "Glückstadt" library was constructed within the Diploma thesis of Stefanie Böhnke (Böhnke 2010) with DNA that was isolated directly from marshland and sediment samples collected from the river Elbe estuary near Glückstadt (43° 46'46.11"N, 9°24'50.69"E; Böhnke

2010). 5,000 fosmid clones were screened for esterase activity on LB-TBT agar plates (2.8.2.2; Böhnke 2010). For four out of five fosmid clones (Table 12) that showed activity, sequences could be obtained by 454 sequencing. One of these fosmid clones was designated 143/F5 and carried an ORF that showed low similarity to a putative hydrolase from *Pelagibacterium halotolerans* B2 (GenBank acc. no. AEQ51793.1, E-value $9e^{-60}$, max. identity 46%) in a BLASTX search (2.11.2, appendix). The putative gene sequence was amplified by PCR with specific primers (appendix) and cloned into pET-21a (2.6.8.3.3). For optimal expression in *E. coli* BL21 (DE3), the culture was incubated at 28°C after induction with 0.5 mM IPTG (2.7.1). The respective protein Est143/F5 was purified by Ni-ion affinity chromatography (2.7.3) and dialyzed (2.7.5). The protein concentration was determined using the Bradford protein assay (2.7.6) and its estimated size of 37.3 kDa was checked by SDS-PAGE (2.7.7, data not shown). After initial qualitative activity tests on *p*NP decanoate in 0.1 M PB (pH 8.0), the enzyme had the highest activity of 0.06 Units/mg (U/mg) after 15 min incubation at 45°C (2.8.2.1). As the enzyme Est143/F5 only showed relatively low activity, was not active above 45°C and probably worked better on short-chained fatty acid esters, it was not further investigated.

3.5.5 Analysis of the cosmid pCos5E5 derived from a biofilm library and cloning of its lipase/esterase genes

A metagenomic library was constructed with DNA that was isolated from biofilm on rubber-coated valves of a drinking water pipeline in a previous study (Schmeisser *et al.* 2003; Schmeisser 2004). Six out of 1,600 *E. coli* clones showed lipolytic activity when screened on LB-TBT agar plates (Schmeisser 2004). The insert of one positive cosmid clone designated pCos5E5 (=BioIII5/E5) had a size of approx. 36.58 kb and was sequenced by 454 pyrosequencing (2.6.11.2, appendix). A BLAST-analysis (BLASTX, 2.11.2) of the protein coding ORFs against sequences in the NCBI database revealed three putative genes that could be responsible for hydrolytic activity (Table 14).

Table 14. Three different putative esterase ORFs located on the insert of pCos5E5.

Putative ORF	Start on contig	End on contig	Length (bp)
***est1* (=*est5E5*)**	30,569	31,954	1,386
***est2* (complementary strand)**	31,915	30,566	1,350
est3	33,475	34,680	1,206

The putative genes designated *est1* and the complementary located *est2* were similar to an esterase of *Acidovorax radicis* N35 (GenBank acc. no. ZP_08949193.1, both E-values 0.0, max. identities 83%). The third putative gene *est3* possessed high similarity to an annotated GDSL-family lipolytic protein from *Acidovorax ebreus* TPSY (GenBank acc. no. YP_002554716.1, E-value $8e^{-160}$, max. identity 79%).

Figure 7. The gene *est5E5* (=*est1*) with its surrounding genes on the insert of the cosmid pCos5E5. *pep*, D-alanyl-D-alanine carboxypeptidase/D-alanyl-D-alanine-endopeptidase, similarity to *Acidovorax* sp. NO-1 (GenBank acc. no. ZP_09327363.1, max. identity 82%, E-value 0.0); *trp*, transposase, similarity to *Asticcacaulis excentricus* CB 48 (GenBank acc. no. YP_004087758.1, max. identity 72%, E-value 0.0); *est3*, GDSL family lipolytic protein, similarity to *Acidovorax ebreus* TPSY (GenBank acc. no. ACM34716.1, max. identity 79%, E-value $8e^{-16}$). The gene *est2* is complementary to *est5E5*.

As the genes surrounding the putative esterase ORFs did not seem to have an influence on expression or activity of the respective enzymes, they were not considered for cloning.

The three putative esterase genes were amplified with the primers *est1* for/rev (2.6.10, Table 5), *est2* for/rev and *est3* for/rev (appendix) that contained *Nde*I and *Hind*III restriction sites within their sequences. The PCR products were ligated into pDrive (2.6.8.3.1) and subsequently, the gene sequences were cloned (2.6.8.3.2) into pET-21a (Table 3). The constructs were transformed into *E. coli* BL21 (DE3; 2.6.9.1) and for optimal expression of the genes, the cultures were grown at 28°C and induced by the addition of 0.5 mM IPTG (2.7.1). The respective enzymes were purified by immobilized metal ion affinity chromatography (2.7.3), dialyzed (2.7.5) and the protein concentrations were determined using Bradford assay (2.7.6). Initial activity tests were performed with 1 mM *p*NP decanoate in PB (pH 8.0) at 45°C for 15 min (2.8.2.1). Est2 did not show significant activity in contrast to Est1 and Est3 (Figure 8). As the activity of Est1 (1.54 U/mg) was almost three times as high as the activity of Est3 (0.54 U/mg, see Figure 8), only Est1 was further on investigated and designated Est5E5.

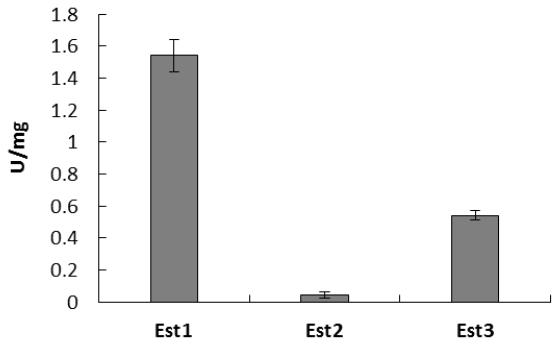

Figure 8. Specific activity of Est5E5 (=Est1), Est2 and Est3 derived from the cosmid pCos5E5 and tested on 1 mM *p*NP decanoate at 45°C.

3.6 Characterization of Est5E5, LipT and LipS

Biochemical characterization was focused on these three enzymes, because they showed the highest activity at elevated temperatures (>50°C) and were sufficiently expressed by *E. coli* compared to the other esterases and lipases examined in this study.

3.6.1 Sequence analysis of *est5E5, lipT* and *lipS*

The genes *est5E5 lipT* and *lipS* were sequenced (2.6.11.1) and the resulting sequences processed (Gap4, 2.11.1). Furthermore, they were analyzed by using Clone Manager (2.11.1) and the estimated protein size was calculated. The nucleotide sequences were compared with sequences deposited in the NCBI database with BLASTX (2.11.2; Altschul and Koonin 1998). Table 15 provides information about these results.

Table 15. Gene sizes and molecular weights of the respective proteins encoded by *est5E5*, *lipT* and *lipS* with the closest relative according to a BLASTX-search.

ORF	*est5E5*	*lipT*	*lipS*
Size of gene (bp) of native protein (aa/kDa)	1,386 461/48.4	990 329/35.8	843 280/30.2
Metagenomic origin	Biofilm on fresh water pipeline	*Thermus* enrichment culture	Enrichment of soil and water samples
Annotation as (GenBank acc. no.)	Conserved hypothetical protein (ZP_04764880) of *Acidovorax radicis* N35	Putative esterase (YP_004201971.1) of *Thermus scotoductus* SA-01	Esterase (YP_075874) of *Symbiobacterium thermophilum* IAM14863
Expect (E)-value	0.0	0.0	0.0
% Identity (no. of identical aa/total aa considered)	84 (359/432)	96 (317/329)	100 (280/280)

Both *lipT* and *lipS* showed high identities to genes annotated as putative esterase genes from the thermophilic bacteria *Thermus scotoductus* (Gram-negative, optimal growth at 70°C; Tenreiro *et al.* 1995) and *Symbiobacterium thermophilum* (Gram-positive, optimal growth at 60°C; Ohno *et al.* 2000). The esterase gene *est5E5* showed highest similarity to an annotated conserved hypothetical protein of *Acidovorax radicis* N35, a Gram-negative wheat-root-colonizing bacterium with an optimal growth temperature around 30°C (Li *et al.* 2011).

3.6.2 Analyses of the amino acids sequences of Est5E5, LipS and LipT

Sequence analyses with SignalP. 4.0 (http://www.cbs.dtu.dk/services/SignalP/; Nielsen *et al.* 1997) were carried out in order to calculate the probability for the occurrence of cleavage sites. These sites indicate that signal sequences are present at the N-termini of the enzymes which are necessary for secretion. For Est5E5 and LipS, no significant signs for a secretion signal could be observed as the C-scores (cleavage site score) are low with a value of approx. 0.1. This means that the amino acids at the N-termini are part of the mature protein. Only LipT presumably contains a secretion signal sequence with a possible cleavage site between Ala21 and Val22, as the C-score reaches a comparably high value of 0.366.

The amino acid sequences of the three enzymes were compared with four to six sequences sharing high similarities with them according to a BLASTX-search (2.11.2; Altschul and Koonin 1998). The sequences were aligned with ClustalW algorithm using the software Bioedit (2.11.1). Multiple alignments were then visualized with Espript software (Gouet *et al.* 1999). Conserved regions within LipS, LipT, Est5E5 and their alignment partners are marked in black in Figure 9 to Figure 11. A catalytic triad common in all hydrolases was found for the three enzymes. It is composed of a serine, an aspartate and a histidine residue. In all cases, the nucleophilic serine is embedded in a G-X-S-X-G motif that occurs in carboxylesterases and lipases. In LipS, the catalytic serine is embedded in a G-L-S-M-G motif (aa 124-128, Figure 9), while LipT contains a G-C-S-A-G motif (aa 157-161, Figure 10). The catalytic serine of Est5E5 is embedded in a G-Y-S-Q-G pentapeptide (aa 221-225, Figure 11). The catalytic aspartate of LipS is located at position 227, the catalytic histidine at position 257. For the other two enzymes, the exact position can only be speculated (LipT: Asp170, 186 or 242 and His293; Est5E5: Asp239, 292, 335, 362, 380, 395, 408, 410, 426 and His251, 388, 440 or 449).

Interestingly, LipS only shared relatively low sequence homologies with the five next similar α/β hydrolases and carboxylesterases from *Rhodopseudomonas palustris* DX-1 (E-value 9e-77, max. identity 49%), *Rhodopseudomonas palustris* CGA009 (E-value 1e-77, max. identity 49%), *Bacillus* sp. 2_A_57_CT2 (E-value 2e-74, max. identity 52%), *Bacillus* sp. NRRL B-14911 (E-value

1e-74, max. identity 54%) and *Geobacillus thermodenitrificans* esterase EstGtA (E-value 3e-76, max. identity 51%, Figure 9).

LipT showed high sequence similarities to esterases from other members of the genus *Thermus* sp. The highest similarities were observed for *Thermus scotodutctus* SA-01 (E-value 0.0, max. identity 96%), *Thermus aquaticus* Y51MC23 (E-value 0.0, max. identity 88%), *Thermus* sp. CCB_US3_UF1CCB (E-value 0.0, max. identity 85%) and *Thermus thermophilus* HB27 (E-value 0.0, max. identity 84%, Figure 10). The largest parts of the sequences seem to be highly conserved.

Concerning Est5E5, amino acid sequence homologies were found to carboxylesterases from *Acidovorax delafieldii* 2AN (E-value 0.0, max. identity 79%), *Acidovorax radicis* N35 (E-value 0.0, max. identity 83%), *Acidovorax* sp. NO-1 (E-value 0.0, max. identity 84%) and *Ramlibacter tataouinensis* TTB310 (E-value 0.0, max. identity 68%, Figure 11). Especially the N-terminus of Est5E5 differs from the other putative esterases.

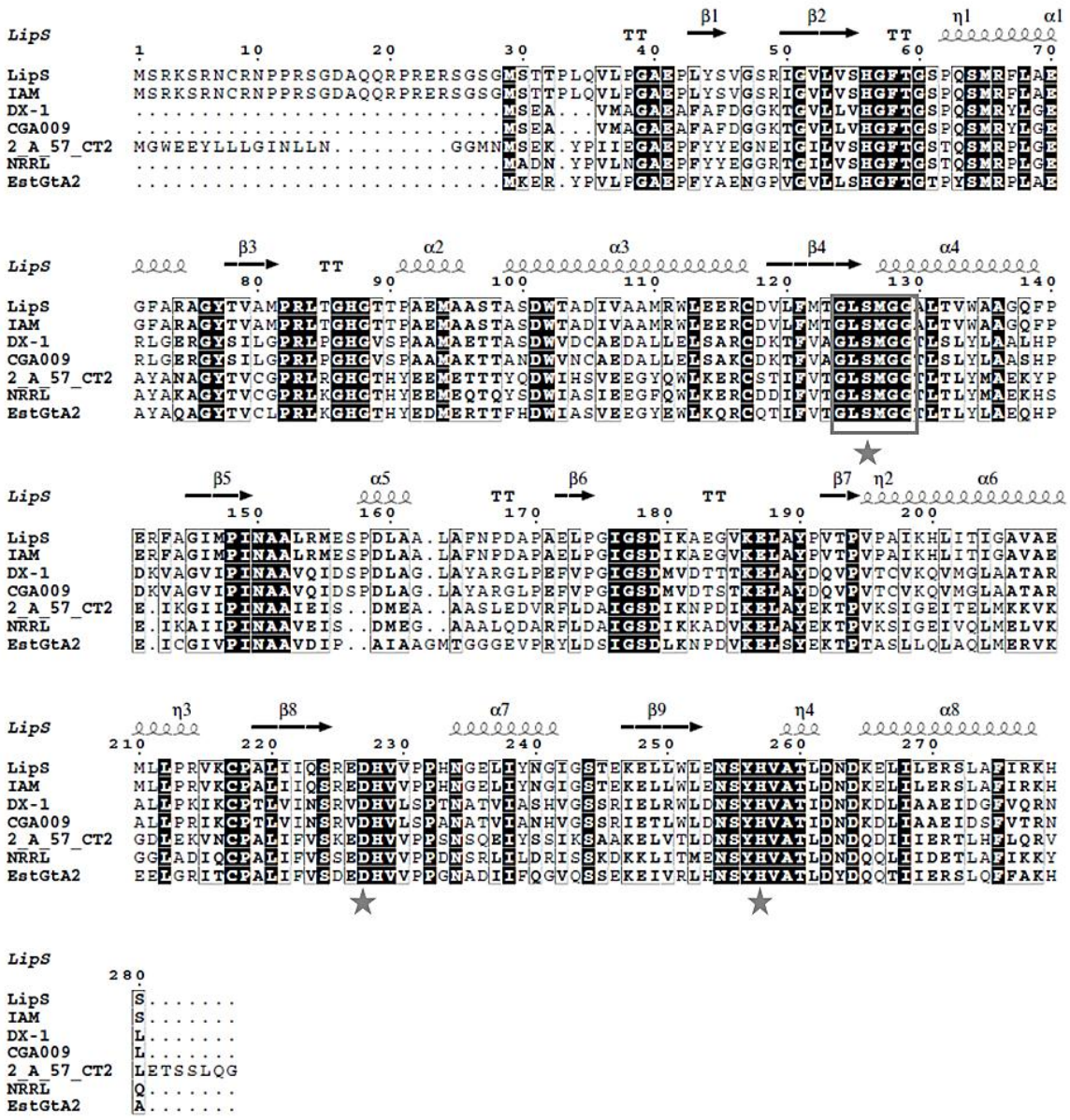

Figure 9. Amino acid alignment of LipS against similar sequences. IAM, *Symbiobacterium thermophilum* IAM 14863 esterase (BAD41030.1); DX-1, *Rhodopseudomonas palustris* DX-1 acylglycerol lipase (ADU46368.1); CGA009, *Rhodopseudomonas palustris* CGA009 putative carboxylesterase (CAE30086.1); 2_A_57_CT2, *Bacillus* sp. 2_A_57_CT2 esterase (EFV74766.1); NRRL, *Bacillus* sp. NRRL B-14911 esterase (EAR67363.1); EstGtA2, *Geobacillus thermodenitrificans* esterase EstGtA (AEN92268.1). Positions of α helices and β sheets as well as the catalytic triad are known, because the crystal structure of LipS was solved (3.7). The stars indicate the catalytic serine, aspartate and histidine residues. Strictly conserved residues are highlighted with black boxes. Numbering refers to the amino acids of LipS.

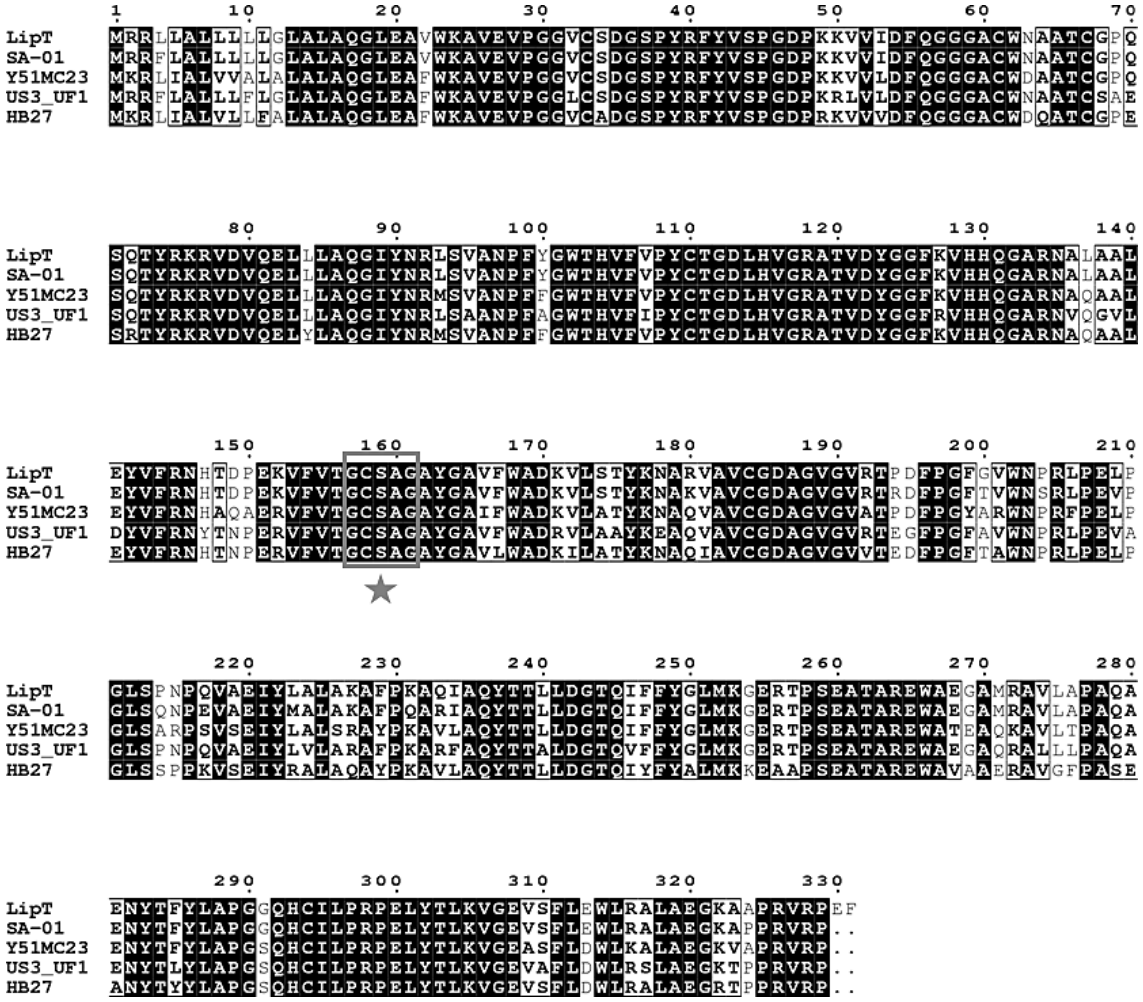

Figure 10. Amino acid alignment of LipT with SA-01, *Thermus scotodutctus* SA-01 putative esterase (ADW21422.1); Y51MC23, *Thermus aquaticus* Y51MC23 putative esterase (EED09760.1); US3_UF1, *Thermus* sp. CCB_US3_UF1CCB US3 UF1 hypothetical protein TCCBUS3UF1_8960 (AEV15941.1); HB27, *Thermus thermophilus* HB27 putative esterase (AAS81248.1). The star points out the catalytic serine. Strictly conserved residues are highlighted with black boxes. Numbering refers to the amino acids of LipT.

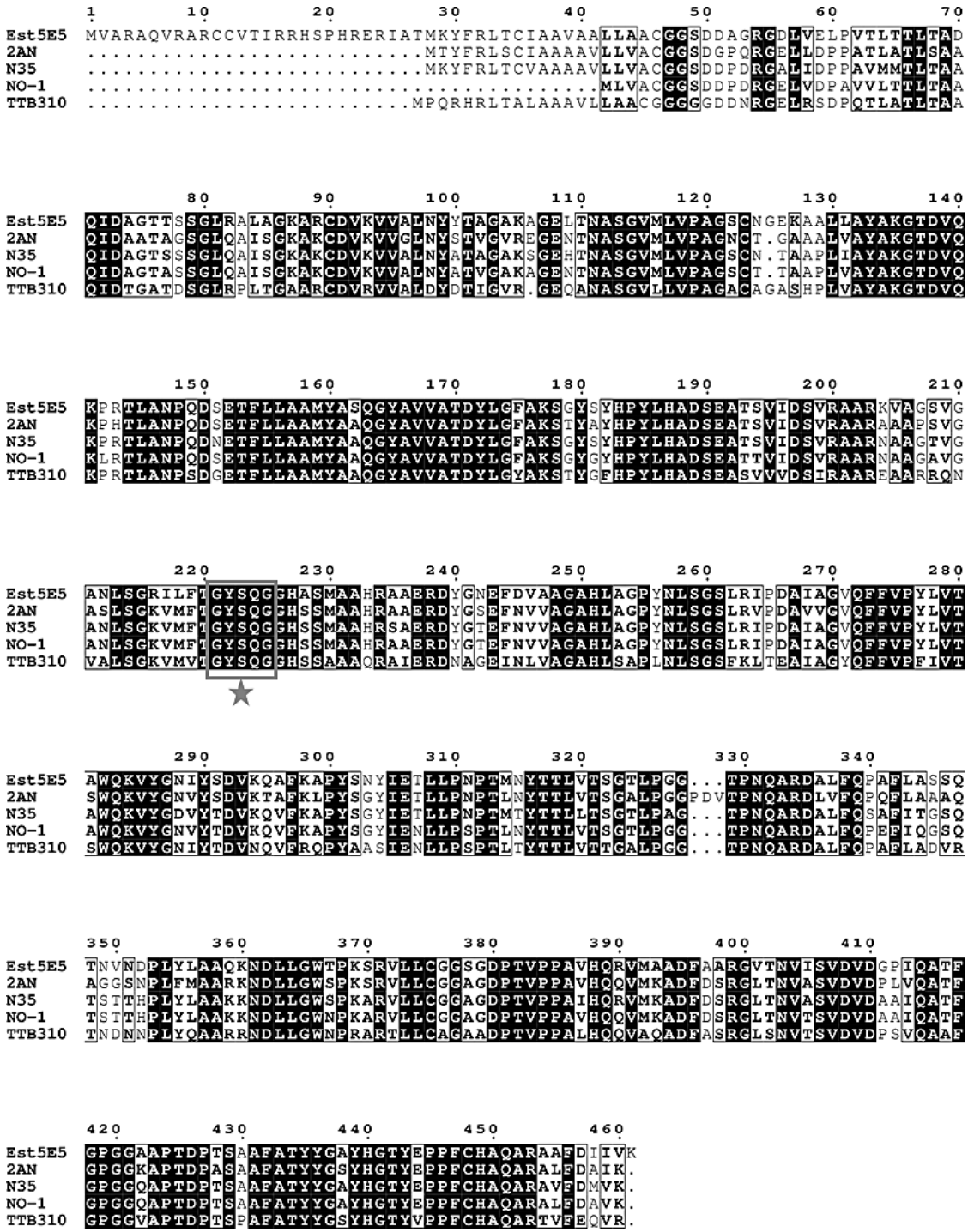

Figure 11. Amino acid alignment of Est5E5 with similar sequences from 2AN, *Acidovorax delafieldii* 2AN conserved hypothetical protein (ZP_04764880); N35, *Acidovorax radicis* N35 esterase (ZP_08949193.1); NO-1, *Acidovorax* sp. NO-1 esterase (ZP_09327365.1); TTB310, *Ramlibacter tataouinensis* TTB310 esterase (YP_004620806.1). The star points out the catalytic serine. Strictly conserved residues are highlighted with black boxes. Numbering refers to the amino acids of Est5E5.

3.6.3 Classification of LipS, LipT and Est5E5 into lipase/esterase families

With the amino acid sequences of LipS, LipT and Est5E5, independent alignments were made for all of the major lipase/esterase families I-VIII using the program T-Coffee (for LipS and LipT, U. Krauss, Research Center Jülich, Germany; 2.11.1) and ClustalW (for Est5E5, BioEdit; 2.11.1). Neither LipS nor LipT could be grouped into any of the existing families due to a lack of sequence homologies. Est5E5 showed slight similarity to members of family I.3, but according to a search with SignalP (2.11.2), the enzyme does not contain the essential C-terminal secretion signal that mediates translocation of family I.3´s members into extracellular space (Hausmann and Jaeger 2010). Subsequently, sequences with similarity to LipS, LipT and Est5E5 were found by a BLASTX-search (3.6.2) and aligned with each other using ClustalW (BioEdit; 2.11.1) in order to illustrate the LipS, LipT and Est5E5 groups of esterases and lipases (Figure 12).

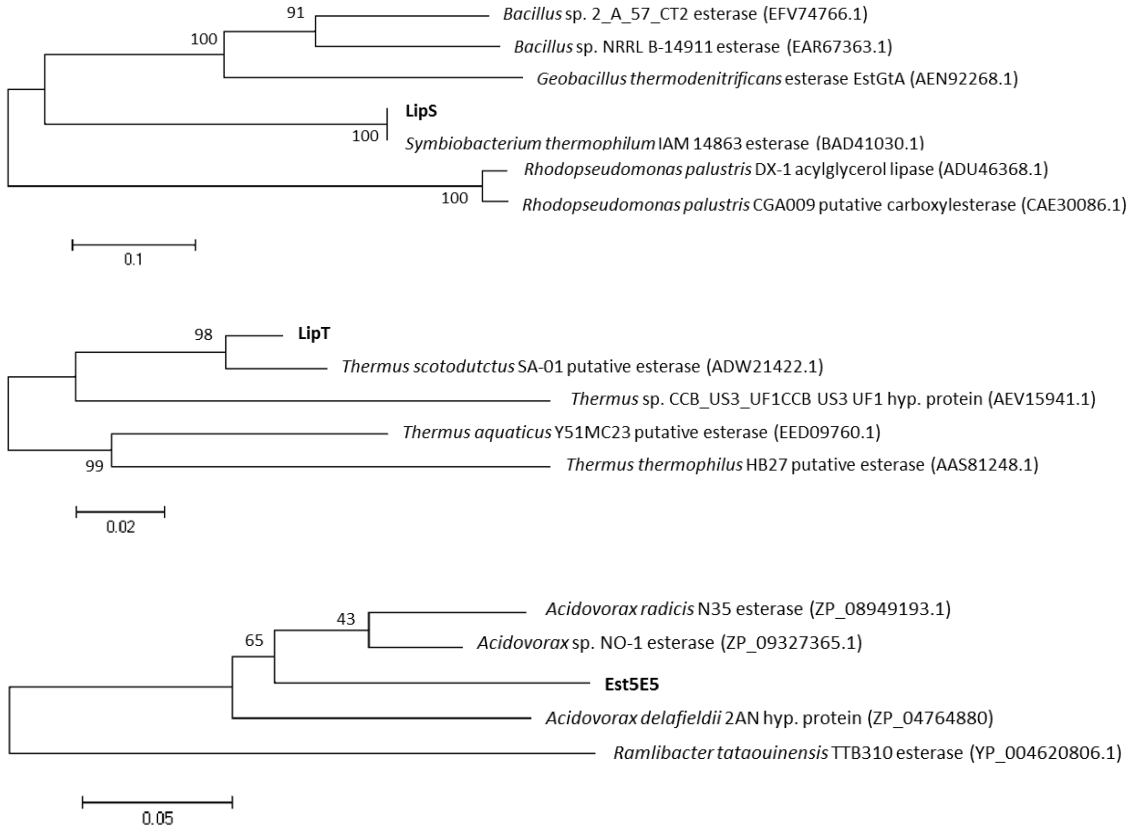

Figure 12. The amino acids of the three enzymes LipS, LipT and Est5E5 were aligned with similar sequences found by a BLASTX search (Altschul and Koonin 1998) by performing a ClustalW alignment (Bioedit, 2.11.1). The trees based on the protein sequences were constructed with the Maximum Likelyhood method using Mega5 (2.11.1). Bootstrap values are shown at the branches and the scale bars indicate the number of substitutions per amino acid.

3.6.4 Overexpression and purification of Est5E5, LipT and LipS

The genes *est5E5, lipS* and *lipT* were cloned and overexpressed in order to characterize the activity of the corresponding enzymes (2.6.8.3.3, 2.6.9.1, 2.7.1). Overnight cultures of *E. coli* BL21 (DE3) strains containing *lipS*::pET-21a, *lipT*::pET-21a or *est5E5*::pET-21a were grown at 37°C and 200 rpm. In order to find the optimal expression conditions, cultures of 250 ml were inoculated with 1% of the overnight culture and incubated at 17, 22, 28 and 37°C for 4 to 9 hours until an optical cell density of OD_{600} 0.6 to 0.8 was reached (2.5.5). Protein expression was induced by supplementation of 0.5 mM IPTG to the culture. After 16 hours (17 C), 8 hours (22 and 28 C) and 4 hours (37 C) of further incubation, the cells were harvested (2.5.6) and the pellets stored at -20°C before cell extracts were prepared by French press and subsequent ultrasonication (2.7.2). The recombinant His_6-tagged proteins were purified from the soluble fraction by immobilized Ni-ion affinity chromatography (2.7.3). The protein concentrations were measured by Bradford (2.7.6) and the molecular weight of the proteins was examined by SDS-PAGE under denaturing conditions (2.7.7) together with a sample of the crude cell extract. The incubation temperature, at which the highest yield of the desired protein was obtained, was chosen to try different concentrations of IPTG. One control culture was incubated without adding IPTG, while protein expression in the other cultures was induced with 0.1, 0.5 or 1 mM IPTG. To yield the highest quantities of the enzymes LipS, LipT and Est5E5, overexpression had to be carried out by induction with 1 mM IPTG. Best results concerning the quantity of LipS and LipT were achieved at an incubation temperature of 17°C. At 37°C, significantly less protein was expressed. The expression of Est5E5 was equally possible at 17 and 22°C. LipS could be purified with up to 15.0 mg/g of cell pellet (wet weight). The average maximum yield of LipT was around 1.6 mg/g and of Est5E5 approx. 3.4 mg/g.

Efforts to purify LipT and Est5E5 from the insoluble fractions (inclusion bodies) of the cell pellets with urea (2.7.4) did not yield any of the two enzymes according to visual inspection of the protein bands on a SDS-PAGE gel (2.7.7) and to measurement of protein concentrations by Bradford (2.7.6).

The elution fractions that contained the desired proteins were combined, dialyzed against 0.1 M PB pH 8.0 (2.7.5) and, if necessary, concentrated. After Coomassie Brilliant Blue staining of the 15% acrylamide gels after SDS-PAGE (2.7.7), LipS was visible as one single band at a size of approx. 31.7 kDa including His_6-tag of 1.65 kDa (Figure 13). In contrast, LipT and Est5E5 had to be concentrated and could not be purified as single proteins as they showed several bands. In case of LipT, protein bands were observed with the size of the enzyme expressed as a monomeric protein (38 kDa estimated size including C-terminal His_6-tag), a dimer (76 kDa) or a tri-

mer (114 kDa) although the SDS-PAGE was carried out under denaturing conditions (sample buffer contained DTT, incubation at 95°C for 5-10 min; Figure 13). Est5E5 also showed several bands, but also a distinctive band at approx. 50 kDa which corresponds to its estimated size including His_6-tag (Figure 13).

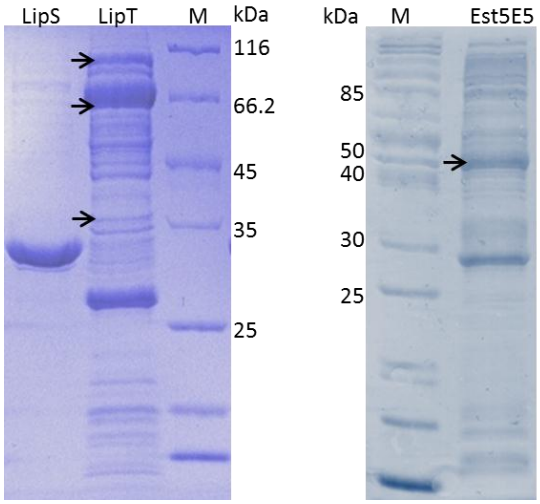

Figure 13. The purified proteins LipS, LipT and Est5E5 on 15% acrylamide gels after SDS-PAGE. Gels were stained with Coomassie Brilliant Blue solution. Arrows are indicating the possible protein bands of LipT and Est5E5. M: marker (Fermentas unstained protein molecular weight marker, left #SM0431, right #SM0661). Approx. 15 µg of protein were applied per sample.

A Western Blot immunoassay was carried out after separation of the proteins by denaturing SDS-PAGE to detect the His_6-tag of the three enzymes with His_5-specific antibodies (2.7.8). The assay showed that LipS was detectable with a strong signal at approx. 32 kDa that is consistent with the calculated molecular size. A thinner band was also detected that could correspond to a dimer with a size of about 72 kDa (Figure 14 A). The western blot analysis of LipT revealed that it occurs as approx. 38 kDa protein (Figure 14 B) and concerning Est5E5, its molecular weight could be verified with about 50 kDa (Figure 14 C). A strong signal at approx. 95 kDa was also observed in both cases. Yet, Western Blot analysis of a negative control of crude cell extract from *E. coli* BL21 (DE3) that contained the empty vector pET-21a also showed a band at approximately 95 kDa, when the amount of protein that was loaded on the gel was rather high. Presumably, this protein belongs to *E. coli* and has a histidine rich part in its amino acid sequence so that it also binds to the Ni-NTA and can be detected with His_5-specific antibodies.

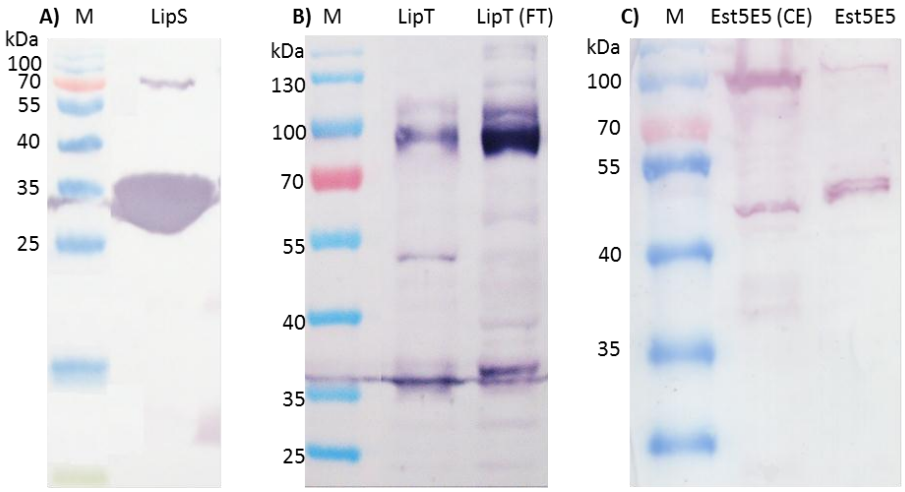

Figure 14. Western Blot immunoassay for detection of His_6-tagged proteins with penta-His-specific antibodies. M: marker (Fermentas prestained protein molecular weight marker #SM0671). A) Purified LipS; B) purified LipT; LipT (FT, Flow through); C) Est5E5 (CE, crude cell extract); purified Est5E5. Approx. 20-25 µg of protein was applied per sample.

3.6.5 Activity of Est5E5, LipS and LipT on ester compounds

3.6.5.1 Substrate specificity

Usually, lipases prefer to act on long-chain fatty acids with more than ten C-atoms, while esterases act on shorter C-chains (Jaeger *et al.* 1999). Therefore, a substrate spectrum was recorded with *p*NP esters which had a carbon chain length of 4 to 18 C-atoms (2.8.2.3.1). The best results were observed with *p*NP octanoate (C_8) in case of LipS and Est5E5. LipT showed highest activity on *p*NP decanoate (C_{10}; Figure 15). LipS and LipT were most active between acyl-chain lengths of 6 to 14 C-atoms (25-58% of the maximum activity) and only weak activities were measured with shorter (C_4) and longer (C_{16} and C_{18}) acyl chain lengths. In contrast, Est5E5 showed a broader substrate range between *p*NP butyrate (C_4) to *p*NP myristate (C_{14}) with at least 60% of the maximum activity. Interestingly, it was not active at all on *p*NP palmitate (C_{16}) and stearate (C_{18}).

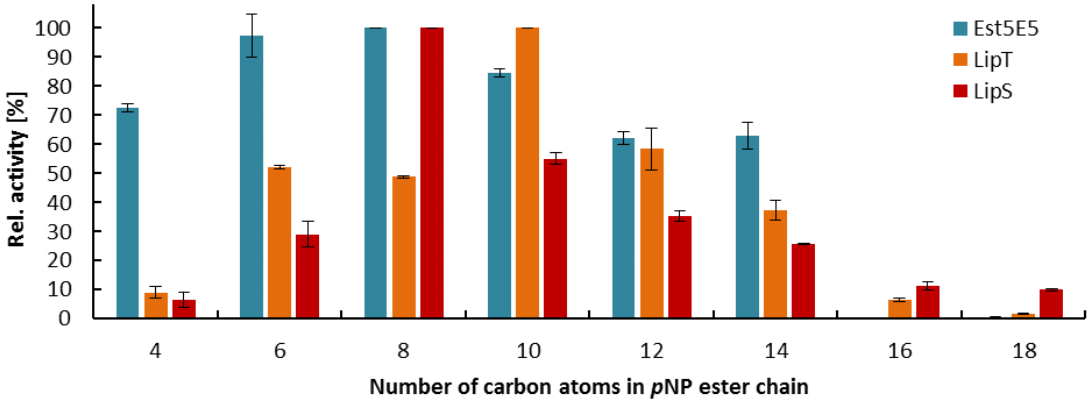

Figure 15. Substrate range of Est5E5, LipT and LipS tested on *p*NP esters with C-chain lengths between C_4 and C_{18}. Reactions were incubated at 50°C (Est5E5), 70°C (LipS) or 75°C (LipT) with final substrate concentrations of 1 mM in PB (0.1 M, pH 8.0). Extinction was measured at 405 nm against an enzyme-free blank. Data are mean values of at least three independent measurements and bars indicate the standard deviation.

3.6.5.2 Temperature range and thermostability of Est5E5, LipS and LipT

In a temperature assay, the activity of the recombinant enzymes was tested by incubation at temperatures between 10 and 90°C for 10 min (2.8.2.3.2). As substrate, 1 mM *p*NP decanoate or dodecanoate were used because of their low autohydrolysis reaction. The extinctions were measured at 405 nm in a photometer. LipS and LipT showed thermophilic properties as their temperature optimum lied at 70 and 75°C, respectively (Figure 16). With 11.5%, LipS had low activity at temperatures beneath 40°C, whereas LipT showed 50% activity at 40°C. At 90°C, LipT still had 91% activity, LipS only 23.5%. The temperature optimum of Est5E5 laid at 50°C, above this temperature, the enzyme activity declined to 65% at 60°C and 23% at 90°C. Est5E5 showed 23% activity at 10°C to 34% activity at 40°C. Figure 16 shows the temperature ranges of Est5E5, LipT and LipS.

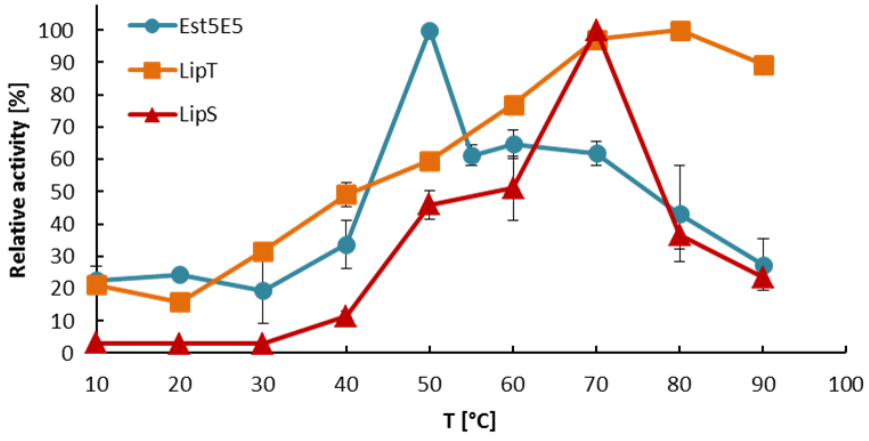

Figure 16. Temperature range of Est5E5, LipT and LipS measured with 1 mM *p*NP dodecanoate.

The enzymes were tested for their thermal stability by incubation at 70 and 90°C for different time periods (2.8.2.3.3). Afterwards, the residual activity was measured by incubation at the optimal temperature of each enzyme with 1 mM *p*NP dodecanoate (LipS, LipT) or *p*NP decanoate (Est5E5) as substrate (2.8.2.1).

As no residual activity was measureable with Est5E5 after 10 min at 70 and 90°C, the test was repeated at 50 and 60°C. At 50 °C, Est5E5 was stable up to 30 min (89 % residual activity), before activity decreased rapidly to 2% after 1 h incubation (Figure 17 A). Est5E5 was almost inactive (2% residual activity) after 30 min incubation at 60°C. A residual activity of 50% for Est5E5 is estimated with about 7 min at 60°C and approx. 40 min at 50°C.

LipT and LipS showed a much higher stability against thermal denaturation. After 24 h incubation at 70°C, LipS still possessed 50% residual activity, while after 72 h, 13.6% of the maximum activity could be measured (Figure 17 B). Incubated at 90°C, LipS showed 52% residual activity after 4 h of incubation, while after 24 h, less than 1% of residual activity was measured. At 70°C, LipT showed 43% residual activity after 24 h and 23% after 52 h (Figure 17 C). Incubation at 90°C for 24 h resulted in a residual activity of 22%. Hence, both LipS and LipT were able to resist high thermal pressure for long time periods.

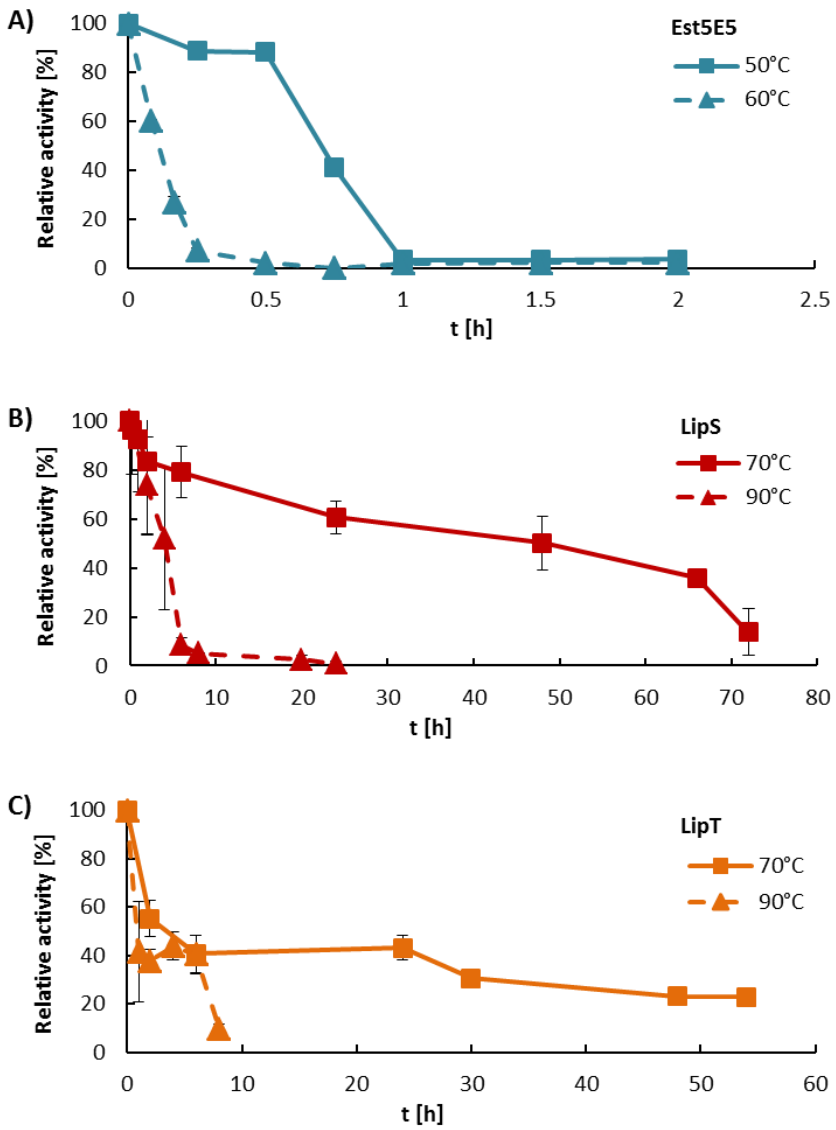

Figure 17. Thermal stability of Est5E5 (A), LipS (B) and LipT (C). The enzymes were incubated at 50 and 60°C (Est5E5) or 70 and 90°C (LipS, LipT). These temperatures were chosen because they lie around the optimal temperature of the enzymes and with 10 to 20°C significantly above. Residual activity was measured afterwards by incubation with *p*NP decanoate or dodecanoate at the enzymes´ optimal temperatures.

3.6.5.3 pH range of Est5E5, LipS and LipT

Three different kinds of buffers were used with pH values between 5.0 and 9.0 (2.8.2.3.4). Est5E5 was most active in Tris-HCl buffer pH 8.6 (Figure 18 A). At pH 7.0, the enzyme showed 28% activity and it was inactive below pH 6.0. LipS (Figure 18 B) as well as LipT (Figure 18 C) showed the highest activity at pH 8.0 when tested with 0.1 M phosphate buffer. Below pH 8.0, activity was rapidly decreasing and at pH 6.0, only 11.4% (LipS) and 6.8% (LipT) residual activity could be measured. In glycine-buffer above pH 9.0, no activity could be measured for any of the three enzymes.

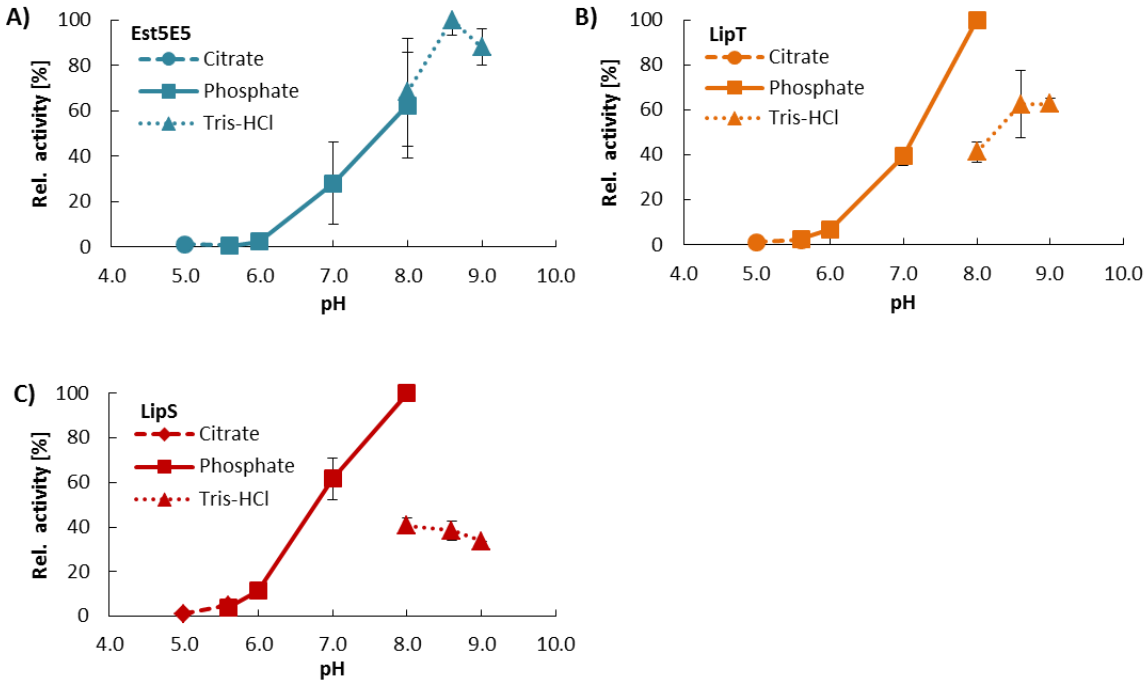

Figure 18. pH range of Est5E5 (A), LipT (B) and LipS (C) measured with citrate (pH 5-6), phosphate (pH 6-8) and Tris-HCl buffer (pH 8-9).

3.6.5.4 Activity of Est5E5, LipS and LipT in the presence of metal ions

Different metal ions like Ca^{2+}, Co^{2+}, Cu^{2+}, Fe^{3+}, Mg^{2+}, Mn^{2+}, Rb^{2+} and Zn^{2+} were tested in 1 and 10 mM concentration by incubation together with the enzymes for one hour at room temperature (2.8.2.3.5). Afterwards, remaining activity was measured for 10 min at the enzyme´s optimal temperature and quantified in a photometer at 405 nm against an enzyme free blank that also contained 1 mM or 10 mM of the respective metal ion. For this measurement, *p*NP octanoate (Est5E5) and dodecanoate (LipS, LipT) were chosen as substrate, because activity was well measureable and autohydrolysis rates are lower with long-chained acyl residues. The activities of the enzymes were then compared to metal ion-free controls. LipS as well as LipT showed activity in the presence of all ions and weak positive effects were measured with Rb^{+} (LipT) and 1 mM Mg^{2+} (LipS) that were not significant enough to consider the ions as cofactors (Figure 19 A, B). In the presence of most cations activity decreased, sometimes even significantly to a residual activity of 39.1% (LipT with 10 mM Fe^{3+}) and 16.9% (LipS with 10 mM Zn^{2+}).

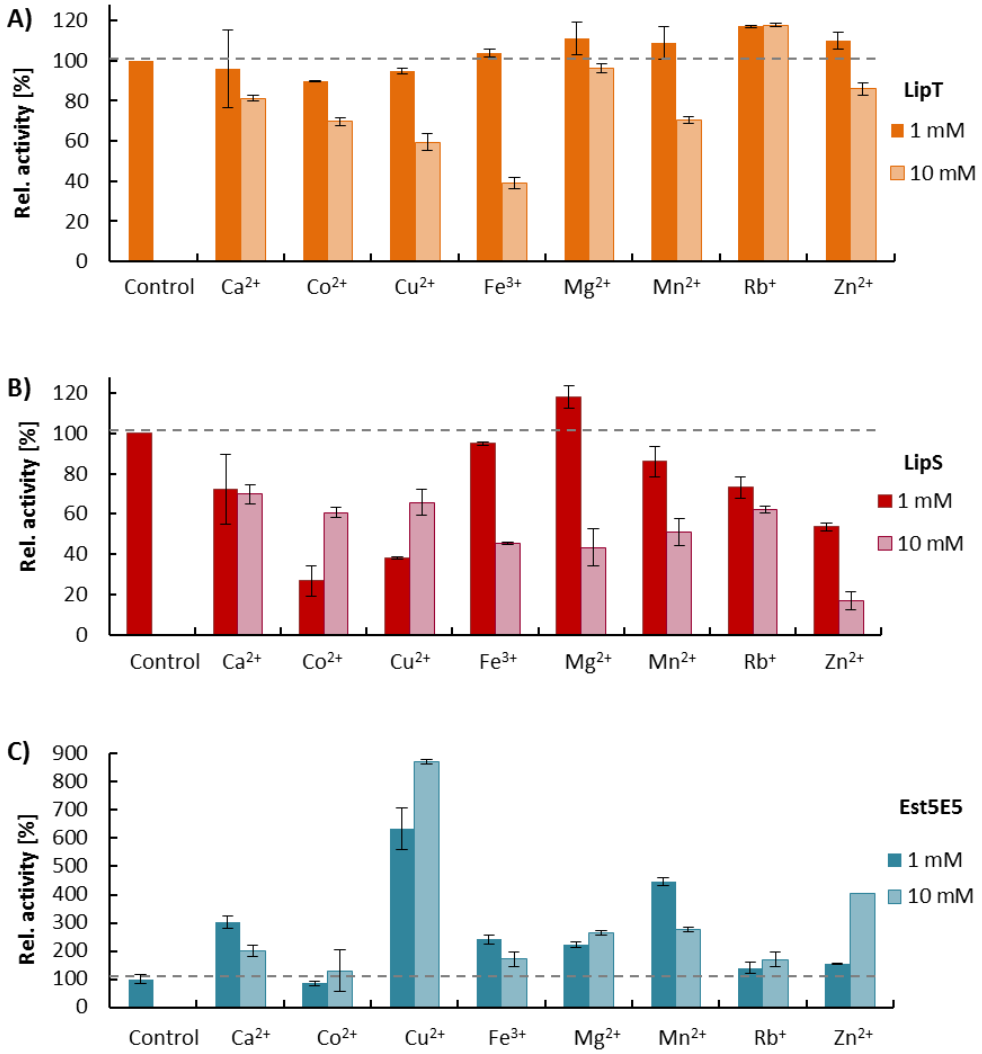

Figure 19. Influence of different metal ions on the activity of LipT (A), LipS (B) and Est5E5 (C) compared to a metal ion-free control.

In contrast to LipS and LipT, Est5E5 significantly showed an increased activity in the presence of Ca^{2+}, Fe^{3+}, Mg^{2+}, Mn^{2+}, Rb^{+}, Zn^{2+} and especially Cu^{2+} ions (Figure 19 C). In order to verify the stimulating effect of Cu^{2+}, different concentrations of the metal ion (0, 1, 5 and 10 mM) were tested in a defined reaction volume of 500 µl that contained 0.9 mM *p*NP octanoate as substrate. After 10 min incubation at 50°C, the reaction was stopped on ice and the amounts of *p*NP that were released during the reactions were quantified in a photometer at 405 nm against enzyme-free blanks that contained the respective amounts of Cu^{2+}. The results of the measurements show, that Est5E5 is more active in the presence of Cu^{2+} ions. Without Cu^{2+} as possible cofactor, the specific activity of Est5E5 lied at an average of 2.61 U/mg. It increased the more Cu^{2+} was added and with 1 mM of Cu^{2+}, 5.35 U/mg were measured. With 5 mM Cu^{2+} 8.73 U/mg were reached and with 10 mM Cu^{2+} 9.50 U/mg (Figure 20).

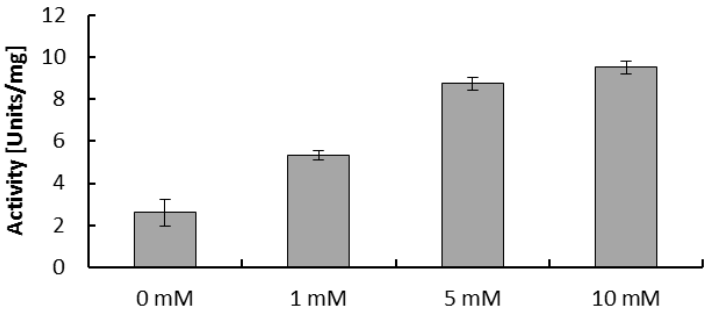

Figure 20. Impact of Cu^{2+} ions on the activity of Est5E5. The enzyme activity was tested in the presence of 0, 1, 5 and 10 mM Cu^{2+} with 0.9 mM *p*NP octanoate as substrate at 50°C. The concentration of *p*-nitrophenol released in the hydrolytic reaction was determined spectrophotometrically at 405 nm.

3.6.5.5 Stability of Est5E5, LipT and LipS against inhibitors and detergents

As activity inhibiting substances, the effect of EDTA, DTT and PMSF on the enzymes was tested in final concentrations of 1 and 10 mM (in 0.1 M PB pH 8.0) for an incubation time of 1 h (2.8.2.3.5). The residual activities of the enzymes were measured with *p*NP octanoate (Est5E5) and dodecanoate (LipS, LipT; 2.8.2) and compared to a control without additives. The results are listed in Table 16. Of all three enzymes, LipT was most stable against EDTA, DTT and PMSF as 1 mM concentrations of the inhibitors did not significantly lower its activity. It still possessed at least 49.0% residual activity when incubated with 10 mM concentration of the inhibitors. Est5E5 and LipS were most strongly impaired by 10 mM EDTA, where 43.5 and respectively 46.0% activity remained.

In 1 and 5% concentration (w/v or v/v) of the detergents, SDS, Triton X-100 and Tween 80 were incubated with the enzymes (2.8.2.3.5). Table 16 provides information about the residual activities of the enzymes after incubation with the detergents for 1 h. LipS showed the highest residual activity of all three enzymes. After incubation with 1% of the detergents in the solution, it kept 59.7% (SDS) to 73.3 % (Tween 80) of its initial activity. Activity strongly decreased with 5% of the detergents and only up to 12.0% activity remained with Tween 80. LipT, however, was completely inactivated by SDS in both concentrations and only possessed up to 18.4% of its initial activity when incubated with 1% Tween 80. Est5E5 was only tested on SDS, that decreased the activity to 50.7% (1% SDS) and 8.7% (5% SDS).

Table 16. Influence of different inhibitors and detergents on the relative enzyme activity of Est5E5, LipS and LipT. ± indicates the standard deviation; n. d., not determined.

Rel. activity of	Est5E5 (%)	LipS (%)	LipT (%)
Control	100.0 ± 7.9	100.0 ± 15.2	100.0 ± 4.6
Inhibitors			
EDTA 1 mM	82.7 ± 10.5	74.1 ± 3.4	98.0 ± 1.1
10 mM	43.5 ± 5.4	46.0 ± 6.6	65.7 ± 4.8
DTT 1 mM	98.6 ± 10.0	76.3 ± 8.1	107.1 ± 3.3
10 mM	64.3 ± 8.0	71.5 ± 9.3	85.4 ± 1.5
PMSF 1 mM	62.5 ± 12.4	80.1 ± 0.8	105.6 ± 7.9
10 mM	70.6 ± 8.5	59.5 ± 6.7	49.0 ± 9.4
Detergents			
SDS 1%	50.7 ± 2.8	59.7 ± 2.5	0.0 ± 0.0
5%	8.7 ± 1.6	0.0 ± 0.0	0.0 ± 0.0
Triton X-100 1%	n. d.	70.4 ± 9.1	13.0 ± 3.5
5%	n. d.	8.5 ± 0.4	3.3 ± 0.8
Tween 80 1%	n. d.	73.3 ± 3.3	18.4 ± 0.9
5%	n. d.	12.0 ± 0.1	0.4 ± 0.1

3.6.5.6 Stability of Est5E5, LipT and LipS against solvents

The activities of Est5E5, LipS and LipT under the influence of solvents were tested with DMSO, isopropanol, methanol, DMF, acetone, acetonitrile and ethanol which were applied in concentrations of 10 and 30% (v/v) in PB pH 8.0 (2.8.2.3.5). The enzymes were incubated at room temperature for 1 h together with the solvents. The residual activities were measured with 1 mM *p*NP dodecanoate at the optimal temperatures and quantified in a photometer at 405 nm against an enzyme-free blank that also contained the respective solvents. The results compared to a control without solvent are shown in Table 17. The presence of the solvents influenced the activities of Est5E5, LipS and LipT more or less negatively. The only exception is DMSO that increased the activity of Est5E5 (30% DMSO: 166.1%) and LipT (10% DMSO: 156.5%) and only marginally inhibited LipS (30% DMSO: 92.9%). In the presence of other solvents, LipS only kept 67.9% (30% methanol) to 8.5% (30% acetone) residual activity. With concentrations of 30% solvent, Est5E5 also lost activity to residual activities between 80.0% (isopropanol) and 3.6% (acetone). In contrast, LipT showed more stability against solvents and

possessed 108.5% (10% methanol) to 47.7% (30% DMF) residual activity. Only against 10 and 30% isopropanol, LipT showed a relatively low stability with 49.2% and 6.2% activity remaining.

Table 17. Relative activity of Est5E5, LipS and LipT in the presence of solvents. The activities were compared to a control without solvent. ± indicates the standard deviation; n. d., not determined.

Rel. activity of	Est5E5 (%)	LipS (%)	LipT (%)
Control	100.0 ± 6.1	100.0 ± 5.5	100.0 ± 4.9
DMSO 10%	120.4 ± 2.8	65.5 ± 3.6	156.5 ± 1.7
30%	166.1 ± 5.6	92.9 ± 8.5	100.1 ± 1.5
Isopropanol 10%	186.1 ± 0.6	64.9 ± 2.6	49.2 ± 4.9
30%	80.0 ± 0.6	45.9 ± 2.6	6.2 ± 1.5
Methanol 10%	35.8 ± 0.6	67.9 ± 2.0	108.5 ± 3.3
30%	n. d.	31.3 ± 0.6	57.5 ± 5.0
DMF 10%	n. d.	31.9 ± 9.7	98.8 ± 5.8
30%	n. d.	17.0 ± 9.3	47.7 ± 2.9
Acetone 10%	n. d.	39.8 ± 12.7	103.0 ± 14.1
30%	3.6 ± 5.1	8.5 ± 0.4	50.7 ± 1.1
Acetonitrile 10%	142.9 ± 0.9	67.3 ± 5.9	96.3 ± 3.6
30%	13.0 ± 3.4	15.4 ± 0.4	50.9 ± 2.1
Ethanol 10%	n. d.	27.7 ± 5.9	87.8 ± 15.3
30%	36.9 ± 13.3	8.9 ± 8.1	57.8 ± 3.1

3.6.5.7 Kinetic measurements of Est5E5, LipT and LipS

As the enzymes should be able to work cofactor independently in further biotechnological applications, kinetic measurements were carried out without addition of any metal ions (2.8.2.3, 2.8.2.3.6). The kinetic studies were performed with two different *p*NP substrates for each enzyme. In case of Est5E5 and LipS, kinetics were studied with *p*NP octanoate and decanoate and in case of LipT, *p*NP decanoate and dodecanoate were used. The substrate concentrations ranged from 0.1 to 0.7 mM. The assays were performed at the enzymes´ optimal reaction temperatures. The catalytic properties of LipS showed the highest specific activity with 12.03 U/mg (Table 18). LipS and Est5E5 showed a much higher specific activity and a better efficiency (k_{cat}/K_m) than LipT (Table 18). Est5E5 showed specific activities comparable to LipS and with *p*NP octanoate, it even had a better catalytic efficiency.

Table 18. Catalytic properties of Est5E5, LipS and LipT.

Enzyme and *p*NP substrate	Units/mg	v_{max} (mol/min)	K_m (mol/l)	k_{cat} (min^{-1})	k_{cat}/K_m ($M^{-1}sec^{-1}$)
Est5E5					
Octanoate	7.685	4.746×10^{-8}	5.852×10^{-4}	0.540	15.375
Decanoate	4.336	3.623×10^{-8}	8.369×10^{-4}	0.412	8.207
LipS					
Octanoate	12.029	2.016×10^{-7}	2.170×10^{-3}	1.336	10.260
Decanoate	6.039	2.903×10^{-8}	2.674×10^{-4}	0.192	12.009
LipT					
Decanoate	0.559	5.416×10^{-8}	1.148×10^{-3}	0.055	0.796
Dodecanoate	0.361	1.108×10^{-8}	1.477×10^{-4}	0.011	1.268

3.6.5.8 Further substrate range and enantioselectivity of Est5E5, LipS and LipT

Est5E5, LipS and LipT were tested on special *p*NP esters in a final concentration of 0.5 mM in PB (pH 8.0). With LipS and LipT, the assay was carried out at 70°C and with Est5E5 at 50°C (2.8.2.3.7). The reaction was measured at 405 nm against an enzyme-free blank and the specific activity calculated (2.8.2.3). The results are given in Table 19. Est5E5 was most active on cyclohexanoate (0.35 U/mg) and it was able to act on every other substrate, except 2-naphtoate. LipS hydrolyzed cyclohexanoate with the highest activity of 1.26 U/mg measured, but it did not show activity on 1-naphtoate and adamantanoate. The substrate range of LipT was narrower in comparison. It showed relatively low activity in comparison with Est5E5 and LipS and was unable to convert 2-phenylpropanoate, cyclohexanoate and adamantanoate. Its highest activity was observed on ibuprofen amide with 0.08 U/mg.

Table 19. Specific activity of Est5E5, LipS and LipT on selected *p*NP substrates.

4-nitrophenyl ester substrate (0.5 mM)	Specific activity (U/mg)		
	Est5E5	**LipS**	**LipT**
2-phenylpropanoate	0.25	0.42	0.00
3-phenylbutanoate	0.07	0.09	0.03
Cyclohexanoate	0.35	1.26	0.00
2-(3-benzoylphenyl) propanoate (ketoprofen)	0.18	0.62	0.06
2-naphtoate	0.00	0.06	0.02
1-naphtoate	0.19	0.00	0.01
Adamantanoate	0.03	0.00	0.00
Ibuprofen amide	0.25	0.07	0.08

The stereoselectivities of Est5E5, LipS and LipT were tested in comparison with the commercial lipases CalB (*Candida antarctica* lipase B, purchased from Sigma Aldrich, Buchs, Switzerland) and ROL (*Rhizopus oryzae* lipase, purchased from Fluka/Sigma Aldrich, Buchs, Switzerland) on chiral *p*NP and methylumbelliferyl (MU) esters namely (*S*)-/(*R*)-2-methyldecanoic acid ester, (*S*)-/rac-/(*R*)-2,3-dihydro-1*H*-indene-1-carboxylate (=indancarboxylic acid ester), (*S*)-/rac-ibuprofen ester and (*S*)-/rac-/(*R*)-naproxen ester (2.8.2.3.7, Table 11). As reference, the achiral *p*NP and MU octanoate was also tested.

Reactions with chiral *p*NP esters as substrates were measured in a photometer at 410 nm against enzyme-free blank after incubation at 60 and 65°C. The assay temperatures were lower than the optimal temperatures of LipS and LipT and higher than the optima of Est5E5, CalB and ROL in order to avoid autohydrolysis that easily occurs at higher temperatures or due to the experimental setup (2.8.2.3.7). All of the five enzymes were principally active on chiral *p*NP ester compounds and the specific activities are listed in Table 20. Est5E5 showed the highest activity of all enzymes on the achiral *p*NP octanoate (0.71 U/mg). It was also able to hydrolyze chiral substrates with activities comparable to LipS. Thereby, it acted preferably on the (*R*)-enantiomers of *p*NP methyldecanoate, ibuprofen and naproxen. In case of *p*NP indancarboxylic acid ester, the stereoselectivity was less distinctive. In comparison with Est5E5, LipS showed a much higher stereoselectivity as it clearly preferred the (*R*)-enantiomer and only had very low

activity on the (*S*)-enantiomers. It was even inactive on the (*S*)-enantiomer of *p*NP ibuprofen ester. On most (*R*)-enantiomers, LipS and Est5E5 showed comparable specific activities, but on (*R*)-*p*NP naproxen ester, LipS clearly had the highest specific activity (0.59 U/mg) of all five enzymes tested.

LipT preferred the achiral substrate *p*NP octanoate (0.26 U/mg) and it only showed low activity on the chiral substrates (max. 0.09 U/mg on *p*NP methyldecanoate). Stereoselective properties could not be observed for this enzyme. CalB also did not clearly exhibit stereoselective properties on any of the substrates. As the temperature optima of CalB and ROL usually lie between 30 and 45°C, the specific activities observed at 60 and 65°C were relatively low with a maximum of 0.09 U/mg on (*S*)- and (*R*)-*p*NP methyldecanoate in case of CalB and 0.13 U/mg in case of ROL on *p*NP octanoate. ROL showed a slight preference for the (*R*)-enantiomers.

Table 20. Specific activities of Est5E5, LipS and LipT on chiral *p*NP substrates in comparison with the commercial enzymes CalB and ROL. The activities of Est5E5 and CalB were measured at 60°C, while the activities of LipS, LipT and ROL were assayed at 65°C. The specific activity of CalB and ROL refers to the weight of the lyophilisate.

4-nitrophenyl ester substrate (0.33 mM)		**Specific activity (U/mg)**				
	Enantiomer	**Est5E5**	**LipS**	**LipT**	**CalB**	**ROL**
Octanoate	-	0.71	0.54	0.26	0.07	0.13
Methyldecanoate	(*S*)	0.28	0.20	0.06	0.09	0.03
	(*R*)	0.61	0.58	0.09	0.09	0.12
2,3-dihydro-1H-indene-1-carboxylate	(*S*)	0.32	0.06	0.07	0.06	0.00
(=indancarboxylic acid ester)	rac	0.38	0.26	0.07	0.06	0.02
	(*R*)	0.40	0.41	0.06	0.07	0.02
Ibuprofen ester	(*S*)	0.02	0.00	0.02	0.01	0.00
	rac	0.27	0.31	0.03	0.01	0.03
Naproxen ester	(*S*)	0.08	0.06	0.06	0.01	0.01
	rac	0.15	0.24	0.04	0.01	0.01
	(*R*)	0.26	0.59	0.02	0.01	0.03

In order to verify these stereoselective properties of the lipolytic enzymes, the same chiral compounds were tested as methylumbelliferyl (MU) esters. The substrates were applied with a final concentration of 0.03 mM and the assay was performed at 60°C. The reaction was measured by detection of fluorescence at 465 nm (2.8.2.3.7). The results are given in Table 21.

Table 21. Specific activity of the five different enzymes tested on chiral MU esters at 60°C. The specific activity of CalB and ROL refers to the weight of the lyophilisate.

MU ester substrate (0.03 mM)		Specific activity (U/mg)				
	Enantiomer	Est5E5	LipS	LipT	CalB	ROL
Octanoate	-	1413.99	1795.21	147.87	5.64	19.81
Methyldecanoate	(*S*)	243.37	727.02	53.64	2.96	2.65
	(*R*)	1750.54	1992.37	72.27	1.58	8.92
2,3-dihydro-1H-indene-1-carboxylate	(*S*)	105.229	332.56	4.63	5.01	-
(indancarboxylic acid ester)	rac	213.16	638.69	10.39	2.97	-
	(*R*)	271.865	793.28	11.39	1.34	-
Ibuprofen ester	(*S*)	234.90	224.53	10.42	0.12	0.10
	rac	772.46	541.02	9.24	0.16	0.15
Naproxen ester	(*S*)	434.35	874.12	0.56	0.07	-
	rac	522.95	1111.32	0.61	0.06	-
	(*R*)	660.18	1313.1	0.73	0.08	-

With the MU esters, the preference for (*R*)-enantiomers was verified concerning Est5E5 and LipS. The highest activity of all enzymes was observed with LipS and (*R*)-MU methyldecanoate as substrate (1992.37 U/mg). LipT, CalB and ROL showed comparably low activities between 147.87 and 5.64 U/mg and all three enzymes preferred MU-octanoate as substrate. Concerning MU methyldecanoate, indancarboxylic acid ester and naproxen, LipT acted preferably on the (*R*)-enantiomers. On ibuprofen ester, however, LipT showed a higher activity on the (*S*)-enantiomer. For CalB, a preference for the (*S*)-enantiomer was observed on MU methyldecanoate and indancarboxylic acid ester, but it acted undifferentiated on ibuprofen and naproxen ester. ROL was more active on the (*R*)-enantiomer of methyldecanoate, but it did not show a clear preference for one enantiomer of ibuprofen ester. Concerning indancarboxylic acid and naproxen ester, no activity could be measured.

The estimated *E*-values according to Kazlauskas (Kazlauskas 2006) provide qualitative conclusions about the enantioselectivity of an enzyme. They are calculated by the initial reaction rates (ΔE/min) of both enantiomers measured separately (Equation 8).

$$\text{Estimated } E = \frac{rate\ of\ fast\ enantiomer}{rate\ of\ slow\ enantiomer} \quad (8)$$

The estimated *E* values are listed in Table 22.

Table 22. The five different enzymes show different estimated *E*-values on *p*NP and MU esters. A higher *E*-value indicates a higher stereoselectivity

Estimated *E*	Est5E5	LipS	LipT	CalB	ROL
***p*NP methyldecanoate**	4.0 (*R*)	8.2 (*R*)	1.5 (*R*)	1.5 (*S*)	6.1 (*R*)
MU methyldecanoate	7.2 (*R*)	2.7 (*R*)	1.4 (*R*)	2.7 (*S*)	2.5 (*R*)
***p*NP indancarboxylic acid ester**	1.5 (*R*)	10.3 (*R*)	1.7 (*R*)	2.3 (*S*)	3.7 (*R*)
MU indancarboxylic acid ester	2.2 (*R*)	2.9 (*R*)	2.4 (*R*)	3.7 (*S*)	-
***p*NP naproxen ester**	2.9 (*R*)	7.1 (*R*)	2.5 (*S*)	2.8 (*S*)	2.0 (*R*)
MU naproxen ester	1.4 (*R*)	1.5 (*R*)	1.1 (*S*)	1.7 (*R*)	-

Est5E5, LipS and ROL show selectivity for the (*R*) enantiomers of each of the three kinds of compounds. LipT is (*R*)-selective on methyldecanoate and indancarboxylic acid ester and (*S*)-selective on naproxen ester. CalB acts mostly on the (*S*) enantiomers. LipS showed the highest stereoselectivity of all enzymes with estimated *E* values between 7.1 and 10.3 for the (*R*) enantiomers. The enzyme acted more selectively on *p*NP esters than on MU esters. Est5E5 is more selective on the MU ester of methyldecanoate, as the estimated *E* value of 7.2 indicates, while ROL is more selective on the *p*NP ester of methyldecanoate. LipT and CalB show a relatively low selectivity as the estimated *E* values only reach 2.5 (LipT on (*S*)-naproxen ester) or 3.7 (CalB on (*S*)-indancarboxylic acid ester).

3.6.5.9 HPLC-MS analysis of LipS on ibuprofen *p*NP and phenyl ester

The results measured by HPLC-MS analysis (2.8.3) were accomplished in the group of Prof. Jörg Pietruszka [Institute for Bioorganic Chemistry (IBOC), Heinrich Heine University Düsseldorf, Forschungszentrum Jülich, Germany]. LipS showed a preference for the (*R*)-enantiomer of ibuprofen *p*NP ester with an enantiomeric excess (*ee*) of more than 83% (Figure 21 A). The stereoselectivity of LipS was even higher on ibuprofen phenyl ester, where an *ee* of 99% was detected for the product and 77% for the substrate (Figure 21 B) which leads to an enantioselectivity of E = 200 (c = 45%) for the phenyl ester (Figure 21 C).

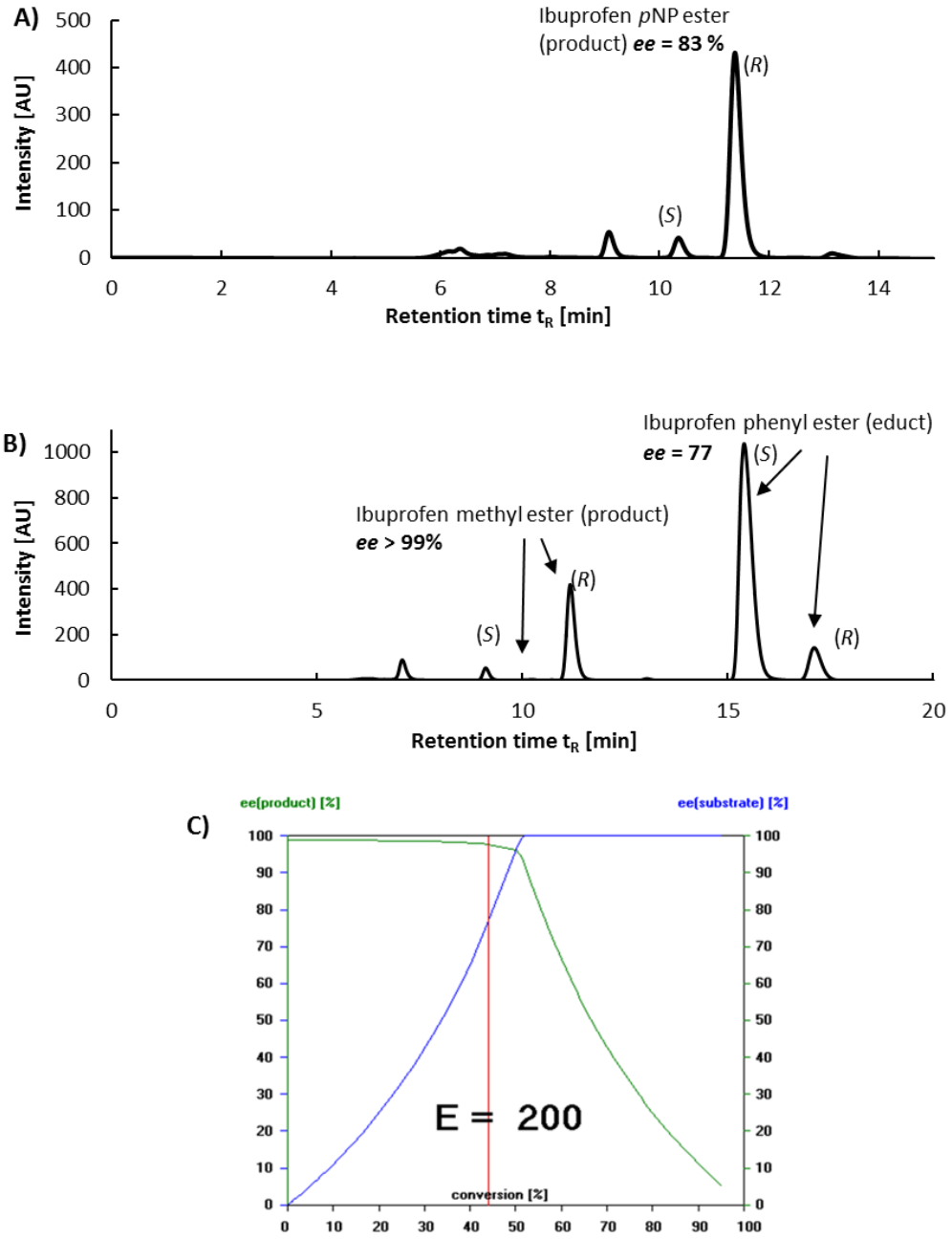

Figure 21. HPLC-MS analysis of LipS acting (*R*)-enantioselectively on racemic ibuprofen esters. A) *p*NP ester (99,8:0,2 n-heptan/isopropanol, 0,5ml/min, 220 nm, Chiralpak IA) and B) phenyl ester (225 nm). As ibuprofen could not be measured directly in acidic form on the HPLC column, it was converted to a methyl ester before measurement. The enantioselectivity value E was calculated for ibuprofen phenyl ester (C).

3.6.5.10 Activity on tri- and polyglycerides

The pH-stat method was applied in an automated titrator with tributyrin, triolein and polyglycerol-3-laurate as substrates (2.8.4). Through the hydrolysis of the tri- and polyglycerides, free fatty acids were released that decreased the pH of the emulsion. The consumption rate of 20 mM KOH which was used to keep the pH at 7.0 indicated enzyme activity. As LipT and Est5E5

did not show activity in the titration assay, the tests were only carried out with LipS. With 50 mM tributyrin as substrate in PB pH 8.0, an amount of 0.825 ml of 20 mM KOH solution had to be added during a reaction time of 16.7 min and consequently, LipS had a specific activity of 0.14 U/mg at 60°C (Figure 22 A). The activity was higher with 50 mM triolein as substrate and reached 0.20 U/mg (1.2 ml of 20 mM KOH solution added after 16.7 min, Figure 22 B). LipS showed its highest activity of 0.61 U/mg on a 7.5% emulsion of polyglycerol-3-laurate (3.7 ml of 20 mM KOH solution added after 16.7 min, Figure 22 C).

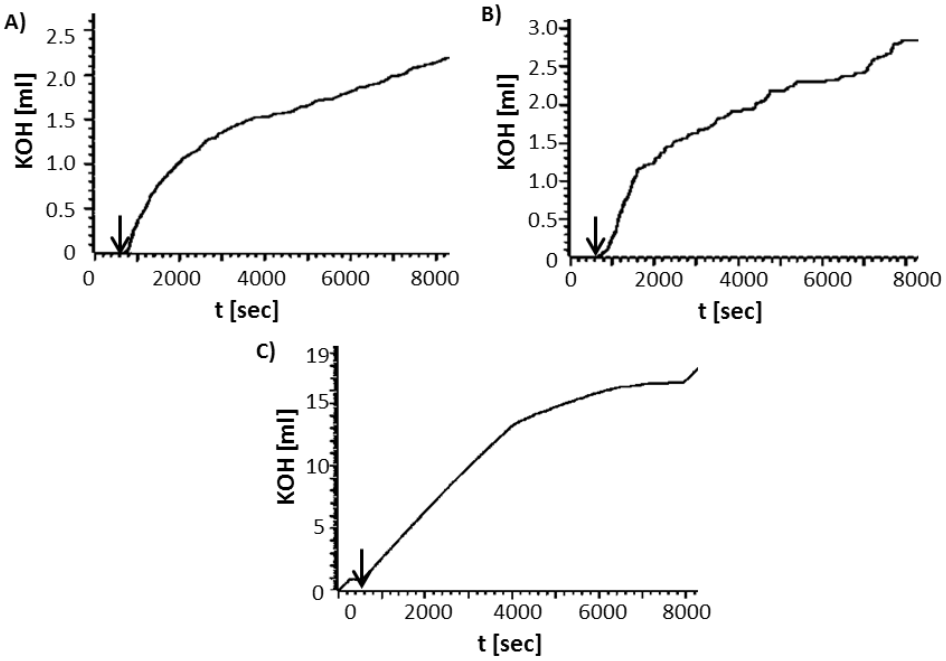

Figure 22. Titration curves of LipS acting on 50 mM tributyrin (A), 50 mM triolein (B) and 7.5% polyglycerol-3-laurate (C). Arrows indicate the time point (600 sec) when LipS was added into the reaction vessel.

3.6.5.11 Esterification by LipS

LipS was applied in esterification assays (2.8.5) and its activity was compared with CalB (purchased from c-lecta, Leipzig, Germany) as control. These assays require lyophilized enzyme (2.7.9) in order to avoid the hydrolysis reaction that occurs in the presence of water. At 70°C, the esterification reactions between 1-propanol and decanoic acid ("propyl laurate assay") as well as 1-tetradecanol and myristic acid were catalyzed by 15 mg of lyophilized LipS and CalB. By titration, the acid values of the control reaction mixtures and the products 1-propyl laurate and 1-tetradecyl myristate were determined after 0, 24 and 48 h. In the control flask without enzyme, no significant changes of the acid values that indicate enzyme activity could be determined for both reactions. During the synthesis reaction of 1-propyl laurate, the acid values of the reaction mixtures decreased from 294.58 to 70.14 in case of CalB and from 283.56 to 210.41 in case of LipS (Figure 23 A). CalB also showed better activity during the synthesis of 1-

tetradecyl myristate, as the acid value decreased from 204.80 to 42.08, while the acid value decreased from 190.77 to 143.08 with LipS as catalyst (Figure 23 B). After 48 h, the formation of 1-propyl laurate was catalyzed by LipS with 0.12 U/mg and by CalB with 0.35 U/mg (Figure 23 C). Activity of both enzymes was slightly lower during synthesis of 1-tetradecyl myristate (LipS 0.09 U/mg and CalB 0.28 U/mg).

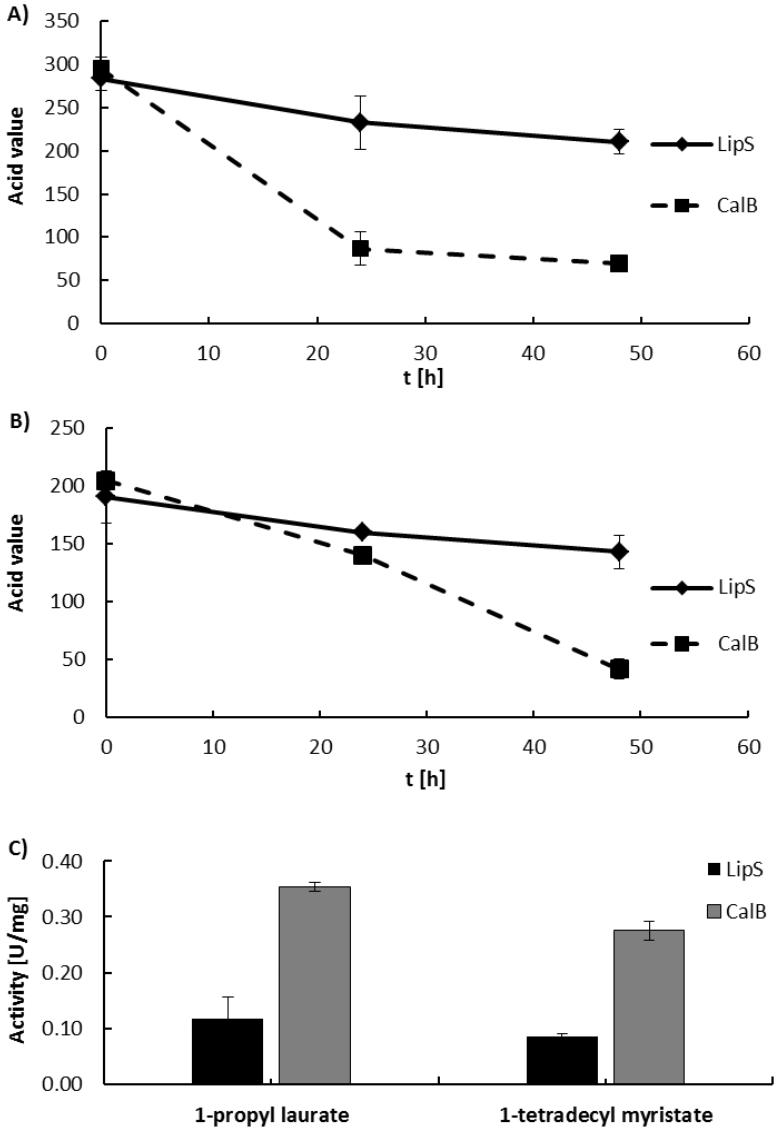

Figure 23. Acid values of the reaction mixtures decreased during the synthesis of 1-propyl laurate (A) and 1-tetradecyl myristate (B). The specific activities of LipS and CalB were higher during synthesis of 1-propyl laurate (C).

3.6.5.12 Kinetic resolution of secondary alcohols by LipS

The enantioselective hydrolysis of four acetates of secondary alcohols by LipS was investigated by gas chromatographic analyses in the working group of Prof. Uwe Bornscheuer (Institut of Biochemistry, Dept. of Biotechnology and Enzyme Catalysis, Ernst-Moritz-Arndt University Greifswald, Germany; 2.8.6). Whereas the hydrolysis of 1-phenyl-1-propylacetate and 1-

phenyl-1-ethylacetate proceeded with low enantioselectivity (E=3-4), high selectivity of LipS was observed for 1-phenyl-2-butylacetate and 1-phenyl-2-pentylacetate. In both cases, the corresponding chiral (*R*)-alcohols were obtained with at least 96% *ee* at approx. 50% conversion.

3.7 X-ray crystallographic analysis of LipS

The efforts leading to a crystal structure of LipS were made in the X-ray crystallography group of Dr. Jochen Müller-Dieckmann (EMBL c/o DESY, Hamburg, Germany). Crystallographic data sets were collected and reduced as described previously (Fersini *et al.* 2012). The structure model of LipS was solved with a resolution of 1.99 Å by using the protein LipS-WT derived from the construct *lipS::*pETM11+26 in *E. coli* BL21 (2.2; Chow *et al.* 2012). It crystallized in space group (SG) P4 and was solved by molecular replacement using the structure of the carboxylesterase Est30 from *Geobacillus stearothermophilus* (PDB code 1TQH, 27% sequence identity) as a model (2.9). The construct LipS-His_6 derived from expression of *lipS*::pET-21a in *E. coli* BL21 contained a His_6-tag at the C-terminus and crystallized in SG $P4_22_12$ (2.9; Chow *et al.* 2012, Figure 24 A). It diffracted X-ray radiation to 2.08 Å resolution.

During purification by size-exclusion chromatography (Fersini *et al.* 2012), LipS appeared as a dimer. Accordingly, the asymmetric units of LipS in SG P4 and $P4_22_12$ contained one and two identical dimers, respectively. The enzymes´ contact area contains 1245$Å^2$ of accessible surface per monomer with several hydrogen bonds, salt bridges and many hydrophobic contacts that probably stabilize the dimer interface (Chow *et al.* 2012).

LipS contains the fold of a classical α/β hydrolase family member (Ollis *et al.* 1992). It consists of a central β-sheet consisting of seven β-strands (β1, β2, β3, β4, β5, β8, β9) with β1 arranged antiparallel to the other strands (Figure 24 C). The sheet is sandwiched by helices αA and αG on one side and helices αB through αF on the opposite side. The catalytic triad consisting of Ser126, Asp227 and His257 composes the active site (Figure 24 B, C). The serine residue is located at the so called “nucleophilic elbow”. A 17 residues long loop between two short antiparallel β-strands β6 and β7 and $αD_{1'}$ forms an extension (Figure 24 B, C). It covers the active site like a lid and creates a closed cavity around the active site residues Ser126 and His257.

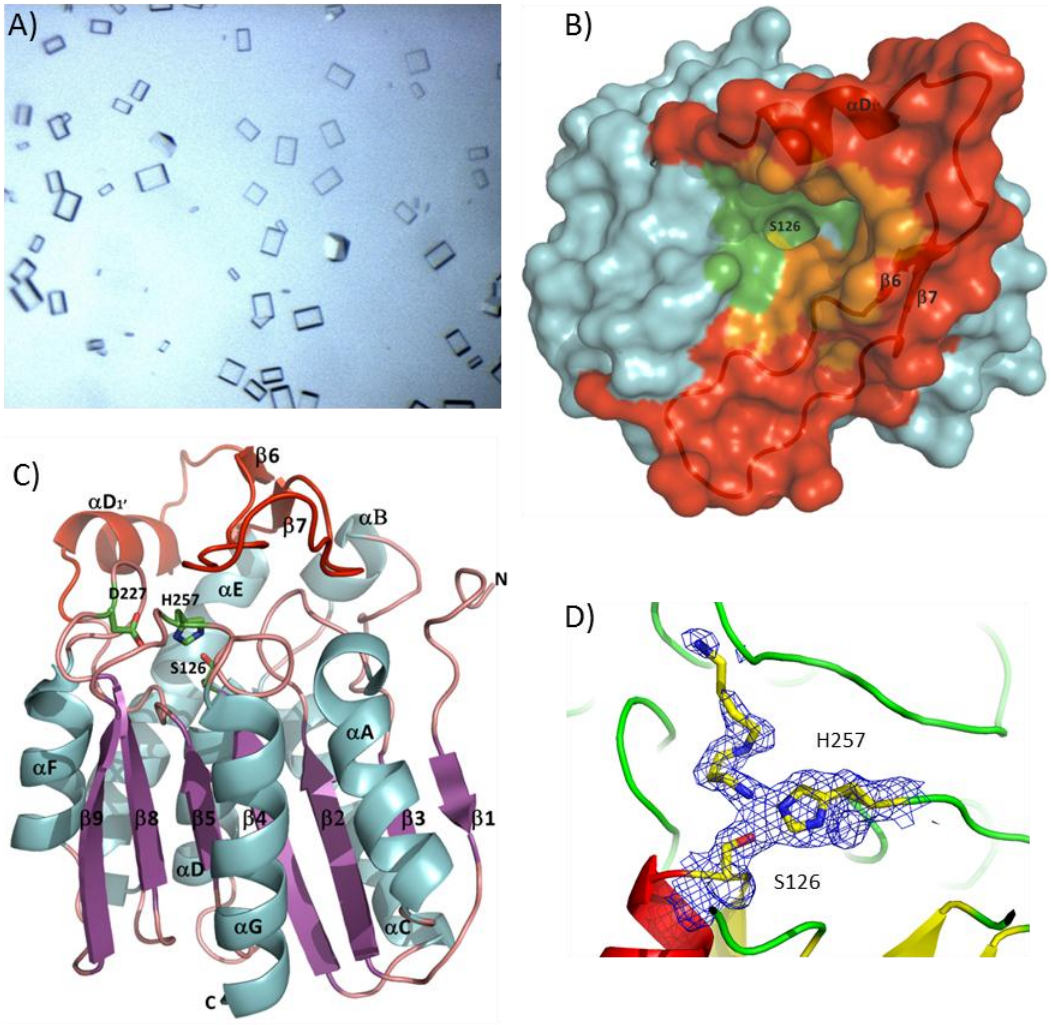

Figure 24. Crystal structure of LipS. A) Single rectangular crystals of LipS-WT (Fersini *et al.* 2012). B) Monomer of LipS displayed as surface representation. The lid-domain (β6, β7, $\alpha D_{1'}$) is colored in red and is shown as ribbon-representation (Chow *et al*. 2012). C) Ribbon representation of LipS (Chow *et al.* 2012). The enzyme contains an α/β hydrolase fold consisting of seven central β-sheets (β1, β2, β3, β4, β5, β8, β9; purple) in between α helices (αA, αG, αD-F, blue). The active site residues S126, D227 and His257 are shown as stick representation. The lid domain is colored in red. D) Electron density (blue) around the catalytic residues S126 and H257 that was interpreted as spermidine (Chow *et al.* 2012). Figures were prepared using secondary structure assignment obtained by PyMOL (DeLano 2002).

The active site of LipS-WT in SG P4 contained strong residual electron density around S126 and H257 (Chow *et al.* 2012; Figure 24 D). This density was interpreted with spermidine which was used as an additive for improving crystal quality of LipS-WT. For crystallization of LipS-His_6, spermidine was not added and the electron density thus could not be observed.

The enzyme was incubated with a final concentration of 3 and 5 mM spermidine for 5 min at room temperature before 0.5 mM *p*NP decanoate was added to the reaction mixture. Subsequently, the mixture was incubated at 70°C for 10 min and the reaction measured in a photometer at 405 nm. Interestingly, the activity test showed that LipS was inhibited by spermi-

dine depending on its concentration (Figure 25). With 65.6% and 43.4%, the residual activity of LipS was significantly lower when 3 and 5 mM spermidine, respectively, was present.

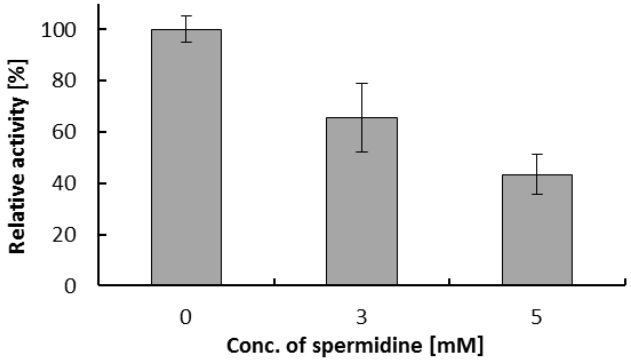

Figure 25. The activity of LipS was inhibited by spermidine. Activity was determined in a photometer after 5 min of preincubation with spermidine and subsequent incubation with 0.5 mM *p*NP decanoate at 70°C.

3.8 *Pseudomonas antarctica* Shivaji CMS 35 as novel expression platform for lipolytic enzymes

Different organisms were tested for their ability to express recombinant lipolytic enzymes and the best results were obtained with *P. antarctica* strain Shivaji CMS 35 (DSMZ, no. 15318). The strain was originally isolated from cyanobacterial mat samples found in pond L3 of Wright Valley, Adam's glacier stream 1 (Antarctica, 78°6'0"S, 163°45'0"E; Reddy *et al.* 2004). The Gram-negative member of the *Pseudomonadaceae* (Gammaproteobacteria) grows aerobic and has a rod-shaped body. *P. antarctica* is non-pathogenic, free living and motile as it possesses a polar flagellum. The psychrophilic bacterium is able to grow between 4 and 30°C with an optimum at 22°C and pH 7.0 (Reddy *et al.* 2004). Common Luria Bertani (LB) and CASO broth can be used as medium. It only has weak endogenic lipase activity and can utilize adonitol, *meso*-erythritol, D-galactose, D-glucose, glycerol, *meso*-inositol and D-mannitol as carbon sources in contrast to e.g. D-cellobiose, lactose, D-maltose and sucrose (Reddy *et al.* 2004). It is sensitive to antibiotics like ampicillin, chloramphenicol, kanamycin, gentamicin, penicillin, rifampicin and tetracycline for which most commonly used vectors carry resistance genes. *P. antarctica* is able to express genes carried on common broad-host-range vectors (pBBR1MCS-5, pBR22b; 2.2). With its ability to grow at low temperatures, its easy transformability and physiological properties, *P. antarctica* has the potential to be a promising heterologous expression host for thermophilic lipases difficult to express in *E. coli*.

Special interest lies in the genetic properties. The genome of *P. antarctica* was sequenced, assembled and annotated by Sonja Voget and coworkers in the Göttingen Genomics Laboratory (G2L, Georg-August University, Göttingen, Germany). The draft genome sequence is available in the IMG database (https://img.jgi.doe.gov/cgi-bin/er/main.cgi) and currently contains 93 contigs. Presently, more than 3,600 other bacterial genomes can be accessed at the IMG database, among them are 65 genomes of *Pseudomonas* species. Figure 26 provides an overview of the phylogenetic relationship between *P. antarctica* and some of these *Pseudomonas* species.

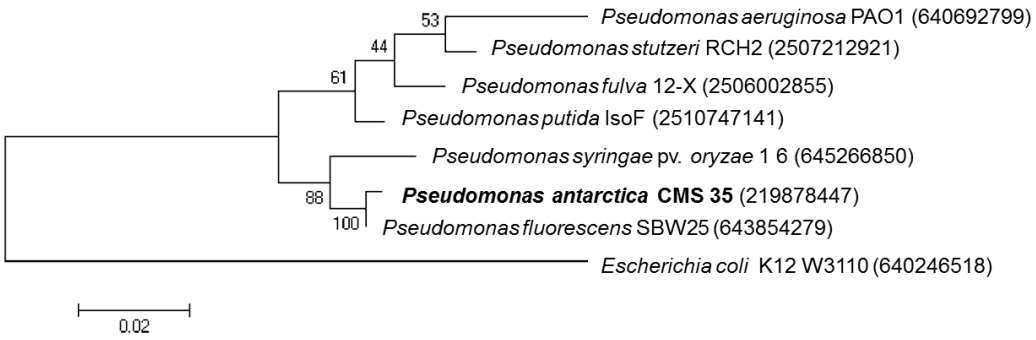

Figure 26. Phylogenetic relationship between 16S rRNA genes of *P. antarctica* and other Pseudomonads. Gene sequences were obtained from IMG (https://img.jgi.doe.gov/cgi-bin/er/main.cgi) and had a minimum size of 1,400 bp. IMG Gene Object IDs are given in brackets, except for *P. antarctica*, which carries a NCBI accession number. Sequences were aligned by using ClustalW (Bioedit; Hall 1999, 2.11.1) and the Neighborhood-Joining method. The tree was calculated using the software MEGA 5.05 and the Maximum-Likelihood method. The scale bar represents the expected base changes per nucleotide position. Bootstrap values are given at the branches.

P. antarctica has an overall genome size of approx. 6.27 Mb and a G+C content of 59.63%. The genome comprises 5,781 protein coding genes of which until now 5,590 have a predicted function. There are about 60 gaps of 2 to 3 kb in length left that have not been closed until now. Phylogenetically, 81.91% of the genes are closely related to genes from Gammaproteobacteria with at least 30% identity according to BLAST. Another 11.16% are unassigned, 3.56% are from Betaproteobacteria and 1.21% belongs to Alphaproteobacteria. Within the genes belonging to Gammaproteobacteria, 96.28% belong to Pseudomonadaceae (mostly *P. fluorescens*) and 1.96% to Enterobacteriaceae.

According to the COGs (Clusters of Orthologous Groups of proteins) database (Tatusov *et al.* 2003), a function could be predicted for 4,528 genes (78.33% of all genes; Figure 27).

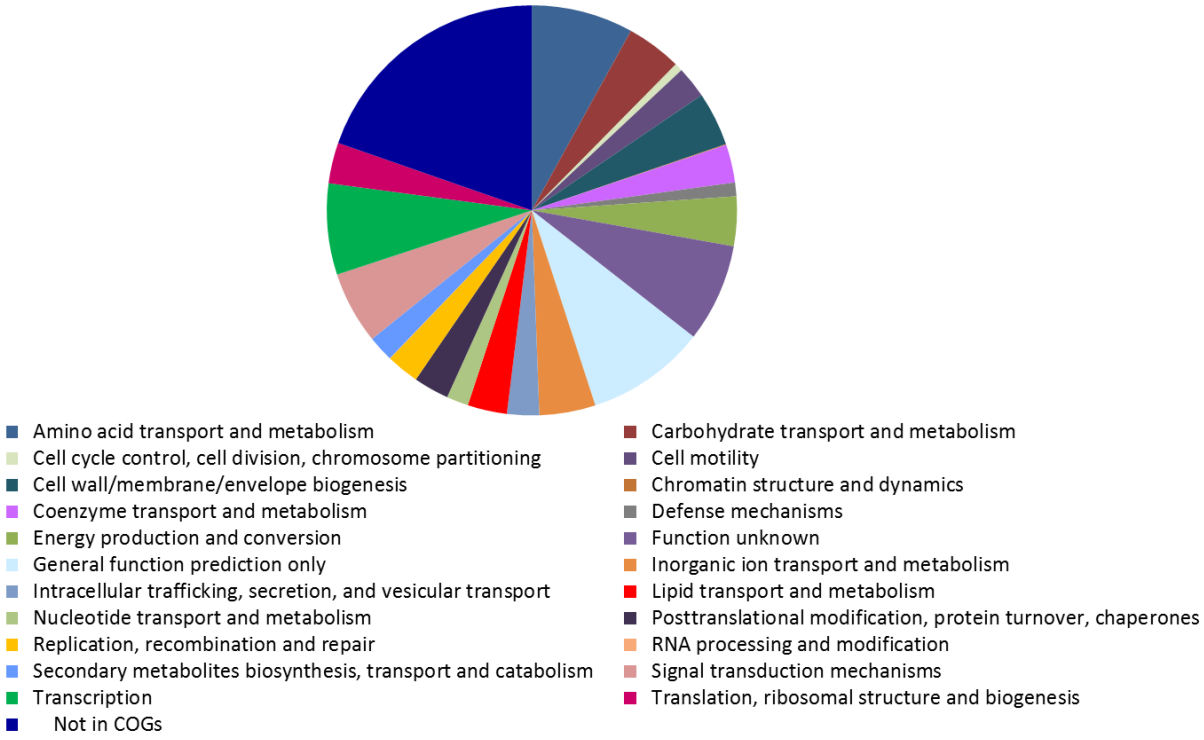

Figure 27. Proteins of *P. antarctica* and their predicted functions according to COGs. Until now, no particular function could be assigned to about one third of the proteins.

Concerning hydrolytic enzymes, 38 annotated α/β hydrolase family members, 10 putative β-lactamases, 27 putative esterases (including thio- and phosphodiesterases) and 7 putative lipases (including phosphor- and lysophospholipases) occur. *P. antarctica* possesses genes encoding proteins necessary for the Sec and Tat translocation systems as well as the Sec/Tat-dependent type II and Sec-dependent type Vb (autotransporter) secretion systems. For Sec-independent secretion, it contains the genes for type I, III and VI secretion systems. The genes *yscFOPX* that encode for proteins responsible for the assembly of a needle complex belonging to the type III secretion system are not present (Figure 28).

Assumedly, *P. antarctica* does not produce signal molecules for cell-cell communication. Within its genome, no genes were annotated as auto-inducer synthase genes. Searches for an auto-inducer synthase from *Pseudomonas fluorescens* (GenBank acc. no. AAC18898), two different putative acylhomoserine lactone synthases from *Pseudomonas fluorescens* (GenBank acc. no. AAF61720.1 and AAF61718.1) and an acyl homoserine lactone biosynthetic protein from *P. syringae* pv. *syringae* (GenBank: AAC24591.1) did not lead to any results when blasted against the *P. antarctica* genome. Searches for the PcoI/PcoR quorum sensing system in *P. fluorescens* (GenBank acc. no. AAT42217.1 and AAT42219.1) were also not successful. Interestingly, annotated genes in relationship with the auto-inducer receptor LuxR were found in genome. There

are three putative LuxR-type transcriptional regulators (IMG gene object ID 2510911850, 2510912117 and 2510913402) and five putative LuxR-family regulatory proteins (IMG gene object ID 2510913223, 2510910960, 2510912396, 2510913645 and 2510914061).

Concerning motility, genes encoding two proteins A (2510911775 and 2510915155) and one motility protein B (2510915154) as well as one gliding motility regulatory protein (2510914450) and two swarming motility regulation sensor proteins rssA (2510912802 and 2510914230) were found within the genome.

Figure 28 shows a comparison between secretion systems components of *P. antarctica* and *E. coli* BL21. *P. antarctica* could offer benefits for protein export especially concerning the type I and type V system, because enzymes can be transported through the inner and outer membrane (Henderson *et al.* 2004).

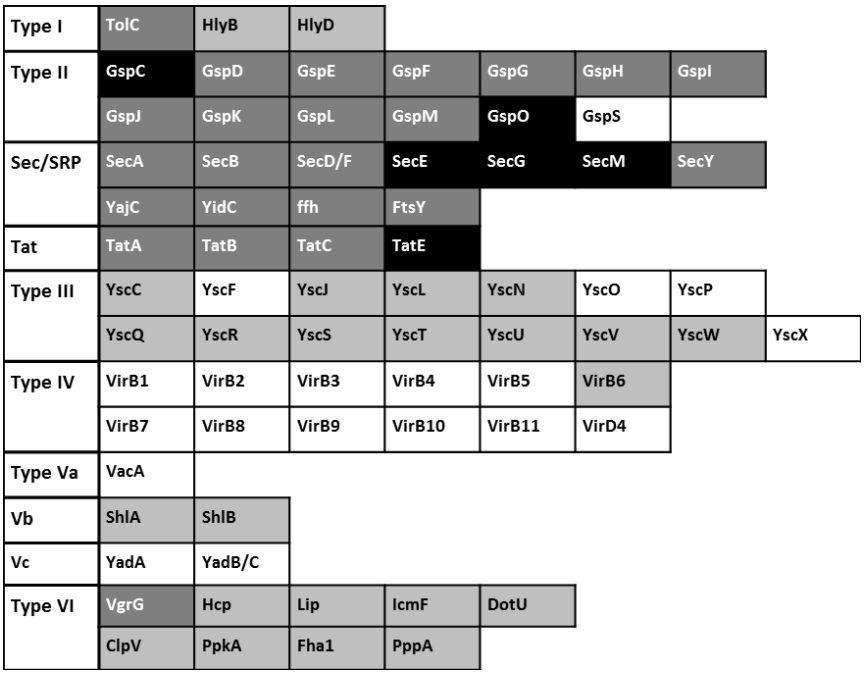

Figure 28. Components of protein secretion systems from *E. coli* BL21 and *P. antarctica* according to a KEGG pathway search (http://www.genome.jp/kegg/pathway/map/map03070.html). Light gray, proteins occurring in *P. antarctica* Shivaji CMS 35; black, proteins from *E. coli* BL21; dark gray, proteins from both organisms. Proteins that do not occur in both species are colorless. SRP, small recognition particles.

3.8.1 Overexpression of LipT in *Pseudomonas antarctica* Shivaji CMS 35

As the expression rates of LipT were low in *E. coli* (3.6.4), *P. antarctica* was chosen as a new expression host that has optimal growth at lower temperatures between 17 and 22°C. Beneath 25°C, LipT is supposed to have a lower lipolytic activity (3.6.5.2) that probably affects the host bacterium. The gene *lipT* was amplified by PCR from *lipT*::pET-21a with the primer pair *lipT_Apa*I for and *lip*T_*Pst*I rev (2.3). The product contained a His_6-coding sequence and was ligated into the broad host range vector pBBR1MCS-5 (2.2). As another expression vector, pBR22b was chosen, because it enables an induction of gene expression with IPTG when the vector is present together with the T_7-polymerase coding vector pML5-T_7 in *P. antarctica* (2.2). The gene was cut out of the plasmid *lipT*::pET-21a with *Nde*I and *Hind*III and ligated into the vector pBR22b (2.6.8.3) that encodes a C-terminal His_6-tag sequence. Competent *P. antarctica* cells (2.6.9.2.1) were transformed with the constructs by heat-shock (2.6.9.2). The transformants were selected on LB-agar supplemented with 50 µg/ml gentamicin (*lipT*::pBBR1MCS-5) or 150 µg/ml chloramphenicol and 7 µg/ml tetracycline (*lipT*::pBR22b and pML5-T_7; 2.4.4). Presumably because the constructs *lipT*::pBR22b and pML5-T_7 together had a size of more than 27 kb, *P. antarctica* cultures that contained both of them grew very slowly so that about three days were required until the cell density was high enough to use it as inoculum. For expression cultures, 300 ml of LB medium supplemented with the appropriate antibiotics were inoculated with up to 3% of freshly grown cultures of *P. antarctica* containing the respective plasmids. Protein expression in *P. antarctica* cultures with *lipT*::pBR22b and pML5-T_7 was induced with 1 mM IPTG at an OD_{600} of 0.8. The cultures were incubated up to three days until an OD_{600} of at least 10.0 was reached. The cultures were harvested by centrifugation (2.5.6) and crude cell extracts were prepared by French pressure cell and ultrasonication (2.7.2). The His_6-tagged LipT was purified from the soluble fraction by Ni-ion affinity chromatography (2.7.3). Protein concentrations were determined using Bradford (2.7.6). The elution fractions were concentrated if necessary (2.7.5) and analyzed by SDS-PAGE and Western Blot (2.7.7, 2.7.8, Figure 29).

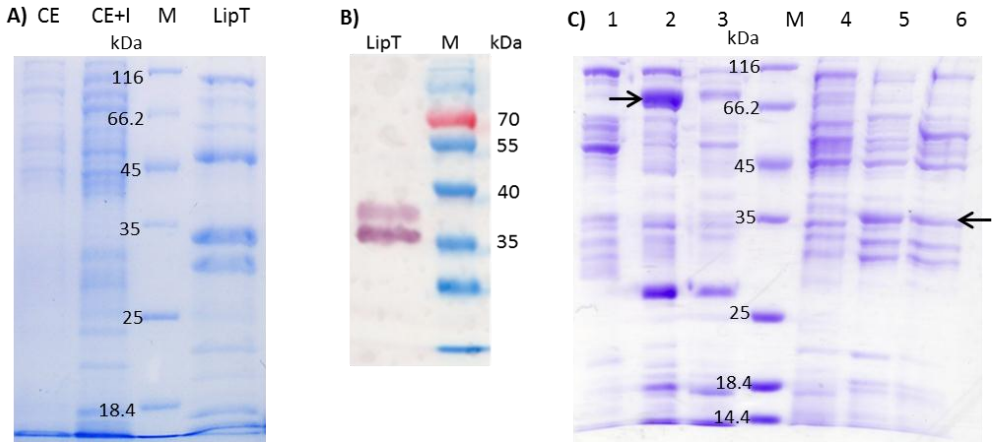

Figure 29. LipT expressed in *P. antarctica* and *E. coli*. A) SDS-PAGE of a 15% acrylamide gel stained with Coomassie solution. It shows recombinant proteins derived from *P. antarctica* containing *lipT*::pBR22b. CE, crude cell extract of non-induced culture; CE+I, crude cell extract of culture induced with 1 mM IPTG; M, marker Fermentas SM0431; LipT, concentrated elution fractions after His_6-tag purification. A visible band according to the size of LipT was only visible after Western Blot analysis. B) Western Blot after SDS-PAGE on a 15% acrylamide gel showing proteins derived from *P. antarctica* expressing *lipT*::pBR22b. LipT, concentrated elution fractions after His_6-tag purification; M, marker Fermentas SM0671. C) SDS-PAGE of a 15% acrylamide gel with proteins derived from *E. coli* BL21 (DE3) expressing *lipT*::pET-21a (lane 1 to 3: 1, elution fraction no. 1; 2, elution fraction no. 3; 3, elution fraction no. 5.) as well as proteins derived from *P. antarctica* expressing *lipT*::pBBR1MCS-5 including His_6-tag (lane 4 to 6: 4, elution fraction no. 1; 5, elution fraction no. 3; 6, elution fraction no. 5). M, marker Fermentas SM0431. The arrows indicate possible bands of LipT that correspond with the calculated sizes of 38 kDa for the monomer and 76 kDa for the dimer including His_6-tag. Between 10 and 20 µg of protein were applied of each sample.

An explicit band that could be assigned to LipT could not be observed in the crude cell extracts of *P. antarctica* with *lipT*::pBR22b that have been induced with 1 mM IPTG or served as non-induced control (Figure 29 A). The concentrated elution fractions after His_6-tag purification contained 10 protein fractions with sizes between approx. 16 and 100 kDa. However, none of the fractions corresponded with the estimated size of LipT as monomer (38 kDa incl. His_6-tag), although the sample was treated with denaturing sample buffer and 5 min incubation at 95°C. Only a Western Blot analysis with His_5-specific antibodies (Figure 29 B) showed two bands at approx. 38 and 38.5 kDa that correspond in their sizes with LipT including His_6-tag. In contrast, the SDS-PAGE of elution fractions containing LipT purified from *P. antarctica lipT*::pBBR1MCS-5 contained one protein fraction next to many others, that is consistent with the estimated protein size of LipT (Figure 29 C). The SDS-PAGE analysis of these elution fractions showed in comparison with elution fractions obtained from His_6-tag purified LipT expressed in *E. coli* BL21 (DE3; *lipT*::pET-21a), that the protein pattern strongly differs (Figure 29 C). An explicit band is only visible after expression in *E. coli* BL21 (DE3) in the elution fraction no. 3 at ca. 78 kDa. This size corresponds with the calculated size of the dimer.

Due to the relatively slow growth of the *P. antarctica* cultures that contained *lipT*::pBR22b and pML5-T_7, further tests were carried out with the plasmid *lipT*::pBBR1MCS-5. The protein yield after His_6-tag purification was determined by using the Bradford assay (2.7.6). The culture of *E. coli* BL21 (DE3) containing *lipT*::pET-21a that was grown at 17°C and induced with 1 mM IPTG produced the highest amounts of LipT (3.01 mg/g pellet after extended incubation time of 20 h, Figure 30). Expression in *P. antarctica* with *lipT*::pBBR1MCS-5 was also possible in significant amounts (1.15 mg/g pellet). The specific activity of LipT was calculated after measuring the enzyme activity at 75°C with 1 mM *p*NP decanoate in 0.1 M PB pH 8.0 for 6 min (2.8.2.3).

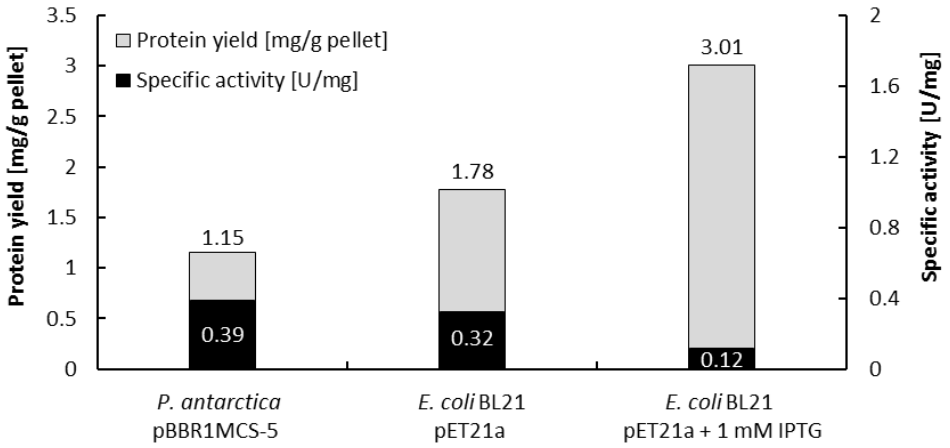

Figure 30. Comparison between protein yield and specific activity of LipT expressed in *P. antarctica* and *E. coli* BL21 (DE3). One culture of *E. coli* remained uninduced, one was induced with 1 mM IPTG. Activity was measured with 1 mM *p*NP decanoate at 75°C.

LipT was slightly more active when expressed in the psychrophilic host *P. antarctica*. (Figure 30). The activity reached 0.39 U/mg when expressed in *P. antarctica* (*lipT*::pBBR1MCS-5), 0.32 U/mg expressed in *E. coli* BL21 (DE3; *lipT*::pET-21a) and 0.12 U/mg when the respective *E. coli* culture was induced with 1 mM IPTG. Measurements with 1 mM *p*NP dodecanoate as substrate at 75°C for 10 min (2.8.2.3) resulted in a specific activity of LipT with 0.18 U/mg when expressed in *P. antarctica* and 0.17 U/mg when expressed in *E. coli* BL21 (DE3) both with and without IPTG induction. Because quantitatively more protein was produced and the culture growth was faster, further research was accomplished with LipT expressed in *E. coli* BL21 (DE3).

4 Discussion

Some biotechnological processes demand working temperatures above 70°C and thus biocatalysts that are able to resist high temperatures for longer time periods. Thermophilic bacteria are able to produce enzymes with high thermostability that can be applied in biotechnology. The aim of this study was to identify lipases with optimal activity above 70°C and resistance against thermal denaturation for an extended time period. Additionally, the lipases should be active on long-chained acyl esters with more than eight carbon atoms. In order to find these enzymes, metagenomics was applied. It is estimated that 99% of all microorganisms are not cultivable with standard techniques under laboratory conditions (Riesenfeld *et al.* 2004). By avoiding the cultivation step and enrichment of pure cultures, metagenomics provides access to the unexplored genes and proteins of these microorganisms.

Therefore, metagenomic libraries constructed from thermophilic enrichment cultures as well as other libraries available in the working group were screened for clones with lipolytic activity. Three of the clones that showed elevated temperature optima were further investigated. The lipases Est5E5, LipT and LipS were identified, purified and subsequently characterized in detail for their enzymatic properties and regarding their applicability in industry.

4.1 Thermophilic enrichment cultures

Two enrichment cultures, inoculated with samples from soil and water of the Botanical Garden in Klein Flottbek (Hamburg, Germany) or heating water from the Biocenter Klein Flottbek, were incubated at 65 and 75°C (2.5.1; 3.1). Although this kind of cultivation step decreases the overall bacterial diversity, it helps to preselect thermophilic bacteria and thus to find the desired enzymes with habitat-related properties (i. e. high temperature stability and high temperature optimum). Metagenomics using DNA of enrichment cultures was often applied and led to the discovery of the desired enzymes, especially when a carbon source or substrate was added to the medium that was selective for species containing the genes of interest (Voget *et al.* 2003; Daniel 2005; Meilleur *et al.* 2009; Beloqui *et al.* 2010; Schmidt *et al.* 2010). For example, the growth of biotin-producing microbes was favored in a previuos study by the addition of avidin to the culture medium which resulted in the identification of seven different cosmid clones carrying biotin biosynthesis operons (Entcheva *et al.* 2001). Another advantage is the often higher yield and better quality of DNA that can be extracted. Especially DNA isolation directly from soil is often related with difficulties because of humic acids and other complex polyphenols present in the sample (Tebbe and Vahjen 1993).

The enrichment culture inoculated with soil and water samples from the Botanical Garden was held at 65°C on mineral salt medium (MSM) supplemented with pyruvate and olive oil as sole carbon sources under moderate aeration (2.5.1.1). Although the sample sites were located in the moderate climate zone, they contained thermophilic bacteria or at least bacteria with high thermotolerance that were enriched at this temperature. This corresponds with other observations indicating that soil bacteria can also be thermophilic, e. g. like many *Geobacillus* species (Marchant *et al.* 2002). The phylogenetic diversity of bacteria within soil belongs to the highest known ranging from 2,000 to 18,000 different genomes and up to 10^9 cells per gram of soil (Torsvik *et al.* 1990; Daniel 2005). Of course, these numbers depend on the DNA extraction and investigation method applied (Delmont *et al.* 2011). Considering studies estimating that 10% of all cultivable soil bacteria have thermophilic properties (Marchant *et al.* 2008), this would lead to more than several hundreds of thermophilic species, cultivable and uncultivable, per gram of soil that could be accessed by metagenomics. Besides, many lipolytic enzymes were found in metagenomic libraries constructed with DNA from soil bacteria before (Henne *et al.* 2000), see introduction 1.3.1). Additionally, lipolytic bacteria within the enrichment were favored by supplementation of olive oil to the culture medium (3.1.1). Olive oil consists of triglycerides with acyl chain residues of 14 to 22 carbon atoms (Fedeli 1977) that can be utilized by lipase-producing bacteria.

Next to *Geobacillus debilis* and uncultured *Clostridia* and *Enterobacteriaceae*, the most abundant member of the enriched consortium was *Symbiobacterium thermophilum* (3.1.1). This symbiotic bacterium was first isolated in co-culture with a *Bacillus* strain from compost and has an optimal growth temperature of approx. 60°C (Ohno *et al.* 2000). The complete genome of the strain IAM14863 was sequenced (Ueda *et al.* 2004) and contains four putative esterase genes and two genes encoding putative lipases. As this bacterium´s growth depends on metabolites of a related *Bacillus* species, it is likely, that these species were also present in the enrichment culture. Perhaps their DNA could not be extracted or their 16S rRNA genes were not amplified by PCR with specific primers. It is also possible that their sequences were just not considered as only 20 sequences were evaluated (3.1.1). Probably this number did not represent all species occurring in the enrichment.

The second enrichment culture was inoculated with samples from a heating water system in the Biocenter Klein Flottbek (3.1). Decades ago, such kinds of water-systems were found to be man-made thermal habitats for bacteria (Brock and Boylen 1973). Compared with soil, the diversity within this habitat is estimated to be lower, but the abundance of thermophilic bacteria is probably higher. The phylogenetic analysis of the enrichment culture revealed that mostly species related to *Thermus scotoductus* were present in the enrichment (3.1.2). Again, the

quantity of analyzed clones should have been higher for a precise analysis. *Thermus* species are well-known producers of lipolytic enzymes (Sigurgisladottir *et al.* 1993; Fucinos *et al.* 2005), so the possibility to find a lipase-producing bacterium in this enrichment was assessed as relatively high.

4.2 Metagenomics and screening methods

The metagenomic library constructed from the soil and water enrichment culture (MSM-enrichment) comprised 38.38 Mb and the heating water enrichment culture (*Thermus*-enrichment) a total of 3.45 Mb (3.2). Both libraries assumedly contained enough heterologous DNA to represent most organisms present in the enrichments.

Functional screening should be preferred to sequence based screening methods, especially when the aim is to discover novel lipolytic enzymes, because the gene sequences of lipases and carboxylesterases are very diverse and contain different conserved amino acid motifs (Pleiss *et al.* 2000). Thereby, recombinant enzymes that are functionally expressed and active can be detected that probably contain unknown sequence motifs.

Screening of the metagenomic libraries was performed with the short-chained ester substrate tributyrin (C_4, TBT) and long-chained *p*NP esters. Interestingly, some clones further investigated in this study were often not clearly active on TBT and were finally screened positive at temperatures between 50 and 75°C on *p*NP dodecanoate (C_{12}; 3.3). The microtiter plate screening with *p*NP esters of different C-chain lengths is more laborious and expensive, but in this case, activity could be observed more clearly and thus, it showed better results. Statistically, one in 144 clones was screened active on *p*NP dodecanoate in the *Thermus*-enrichment library and one in 1083 clones from the MSM-enrichment showed activity on this substrate (3.3).

Although LipS and LipT were screened positive with *p*NP substrates, the esterase Est5E5 was detected with the common TBT test in the metagenomic library constructed with DNA from a biofilm growing on the valve of a drinking-water pipeline (3.4; Schmeisser 2004). Esterases and lipases are exoenzymes that commonly occur in biofilms and are for example produced by pathogenic bacteria. The biofilm forming *Staphylococcus epidermidis* secretes lipases as virulence factors that play an important role for host tissue colonization (Zhang *et al.* 2003). The esterase EstA produced by *P. aeruginosa* PAO1 is bound on the outer-membrane and is essential for rhamnolipid production. Rhamnolipids, however, play a key-role for cell motility and biofilm formation (Wilhelm *et al.* 2007).

Previously, the esterase EstA3 was discovered in the same metagenomic library like Est5E5

and was subsequently characterized (Schmeisser 2004; Elend *et al.* 2006). Unlike Est5E5, the amino acid sequence of this esterase shared 59% identity with a β-lactamase from *Sphingopyxis alaskensis* (ZP_00579205.1). EstA3 acted preferably on short-chained ester substrates like *p*NP butyrate (C_4) and had its optimal activity at 50°C. Environmental biofilms provide conditions that promote the accumulation of enzymes with unusual properties, for example EstA3 worked much better at an alkaline pH of 9.0.

From five other libraries that were screened, i. e. the metagenomic libraries of an elephant feces enrichment as well as directly of elephant feces, of enriched fluids from a hydrothermal vent (*Thermococcales* consortium-library) and of sediment from the river Elbe in Glückstadt and Teufelsbrück, altogether 95 clones were screened positive (see Table 12). The screening was performed mostly on TBT and at 37°C, except for the *Thermococcales* consortium-library which was screened with *p*NP dodecanoate at 60°C, too (2.8.2.2, 3.4). Disappointingly, the archaeal putative esterases and lipases from this cosmid library that were screened active on *p*NP dodecanoate only showed low yields after cloning and overexpression in *E. coli* BL21 (3.5.3) and activities in the standard *p*NP assay at 60-90°C that were not higher than measured for the cosmid clones. One of the genes had a significant similarity to a metallophosphoesterase gene from *Thermococcus onnurineus* NA1 (GenBank acc. no. ACJ16475.1) that was identified as a hyperthermostable enzyme after 2 h heat-treatment at 100°C in a proteome study, but it was not expressed in *E. coli* (Yun *et al.* 2011). In other studies, three enzymes from *Thermococcus hydrothermalis,* i.e. an α-amylase, a NADPH group III alcohol dehydrogenase and a type III pullulanase, were successfully overexpressed in *E. coli* (Antoine *et al.* 1999; Erra-Pujada *et al.* 1999; Leveque *et al.* 2000).

Nevertheless, there are only few archaeal esterases known that were recombinantly expressed in *E. coli*. One example is the thermostable and thermophilic esterase AFEST from *Archaeoglobus fulgidus* which has the best activity with *p*NP hexanoate (C_6; Manco *et al.* 2000). Another recombinant esterase from the hyperthermophilic archaeon *Pyrococcus furiosus* showed a temperature optimum of 100°C and a high thermostability with a half-life of 50 min at 126°C (Ikeda and Clark 1998). It was most active on the short-chained MU acetate (C_3) and analysis of the cloned fragment and expression studies revealed that the esterase coding gene was under control of its own promotor of which transcription in *E. coli* was initiated from. Perhaps better yields could be achieved for the esterases or lipases originating from the *Thermococcales*-enrichment library, if the cloned fragments also contained their native promotor sequence that seems to be recognized by *E. coli*. Another promising approach would be to express the enzymes in a modified *Thermococcus* strain. Santangelo and coworkers developed a shuttle vector expression system that enables protein expression in both *E. coli* and *Thermococcus*

kodakaraensis (Santangelo *et al.* 2008). The shuttle vector expression of a tagged enzyme was about 8-fold higher than with chromosome expression. Finally, the esterases or lipases from the *Thermococcales* consortium-library should be characterized, because they certainly possess interesting features concerning heat-stability and activity at high temperatures.

Only one clone from the metagenomic library of sediment from the river Elbe in Glückstadt was further investigated due to time constraints. But the identified esterase 143/F5 did not show thermophilic properties and was thus not further analyzed (3.5.4). However, for other applications this enzyme as well as the other over 80 lipolytic clones from the different libraries (Table 12) could possess suitable characteristics and thus it would be promising to do further research on them.

4.3 Classification of the lipolytic enzymes

Lipases and esterases were grouped into the eight major families I-VIII and eight subdivisions of family I according to sequence homologies and physiological functions (Arpigny and Jaeger 1999). With current alignment methods, it was not possible to group LipS and LipT into any of the eight existing families that were represented by 47 reference sequences (2.10; Chow *et al.* 2012). Hence, LipS and LipT were grouped into two new families that did not have distinctive similarity to any of the known families together with a set of homologous sequences found by a BLASTX-search (2.11.2; 3.6.3).

All seven sequences from the LipS group had four conserved motif blocks that consisted of at least five amino acids: H-G-F-T-G near the N-terminus, G-L-S-M-G-G containing the catalytic serine, P-I-N-A-A in the middle of the sequence and N-S-Y-H-V-A-T with the catalytic histidine. The catalytic aspartate was located in a D-H-V motif. From the LipS group, only one esterase was characterized until now. The esterase EstGtA2 from *Geobacillus thermodenitrificans* was expressed in *E. coli* and after purification, a specific activity of 2.58 U/mg was measured under optimal conditions on *p*NP octanoate (C_8) at 50°C and pH 8.0, which is lower than the activity of LipS (Charbonneau *et al.* 2010).

The five members of the LipT group had very high amino acid sequence identities to each other. Altogether, 18 conserved motif blocks consisting of five to 19 amino acids were found that were identical within all of the five sequences. The catalytic serine was located in a V-F-V-T-G-C-S-A-G-A-Y-G-A motif. To current knowledge, these annotated putative esterases have not been characterized.

Although Est5E5 showed a certain sequence similarity to members of family I.3, other physio-

logical criteria for these family members were not suitable (3.6.3). For the Est5E5 group, 21 conserved motif blocks of at least five amino acids were found and the serine was located in a T-G-Y-S-Q-G-G-H motif.

These results show that the diversity within the sequences of esterases and lipases is very high and many cannot be grouped into one of the existing eight families (Chow *et al.* 2012).

4.4 Heterologous overexpression of the lipolytic enzymes

It is estimated, that 60% of all heterologous genes are not expressed in *E. coli* (Gabor *et al.* 2004) and therefore, the large potential of interesting genes and proteins they encode cannot be explored. Still, *E. coli* is the most popular bacterial expression host, because of its inexpensive and simple cultivation that can reach high cell densities in fermentation and the large number of expression systems and tags for purification that can be applied.

4.4.1 Expression of Est5E5 in *E. coli*

The esterase Est5E5 had 84% identity to a conserved hypothetical protein from *Acidovorax radicis* N35. According to current knowledge, no enzymes of this wheat-root colonizing bacterium have been investigated for their potential as biocatalysts. The overexpression of Est5E5 was possible with yields of approx. 3.4 mg/g of cell pellet after His_6-tag purification (3.6.4). After concentrating the elution fractions (2.7.5), the samples were analyzed by SDS-PAGE (2.7.7) and revealed several bands, of which one distinct band at 50 kDa had the estimated size of Est5E5. This band could be verified as Est5E5 by subsequent Western Blot immunoassay detecting the His_6-tag (2.7.8).

4.4.2 Expression of LipT in *E. coli* and *P. antarctica*

LipT was only expressed with a low yield of approximately 1.6 to maximal 3.0 mg/g of cell pellet (3.6.4 and 3.8.1) after His_6-tag purification, but it showed relatively high activity. In order to reach this yield, the *E. coli* BL21 expression culture had to be induced with 1 mM IPTG and incubated at 17°C for 16 h instead of 4 h at 37°C. The reason for this probably lies in the lower activity of the lipase at this temperature. With a lower activity, it is less able to interfere with the host metabolism or cell wall components and it is thus less harmful.

Many attempts were made to find the reason for the low level of enzyme production and to increase protein yield. LipT contained a secretion signal sequence (3.6.2) that could have been recognized by *E. coli* for Sec-translocation, but no lipolytic activity could be determined in the

culture supernatant. An approach to express a truncated construct of LipT without the fist 30 nucleotides and thus without a possible signal sequence was also not successful concerning a better yield. Probably only a small amount of the enzyme was folded correctly into its active form and the misfolded fraction was degraded by proteases. As LipT could not be purified from inclusion bodies of the insoluble fraction of *E. coli*, the expression was probably prevented at an earlier stage. LipT had a 96% identity to a putative esterase from *Thermus scotoductus* SA-01. The codon usage of *E. coli* differs from *Thermus scotoductus* to 22.73% and to *Thermus thermophilus* HB27 even to 40.67% (http://www.gcua.de and http://www.kazusa.or.jp/codon). As an example, *E. coli* shows 100% relative adaptiveness to the codon GAT for the amino acid Asp and *Thermus thermophilus* HB27 only 5%. For this reason, the nucleotides of *lipT* were adapted to the codon usage of *E. coli* and the gene was synthesized [Mr. Gene (GeneArt), Regensburg, Germany]. This attempt as well as the use of other *E. coli* strains like Rosetta and Rosetta-gami 2 that provide rare codon tRNAs and enhanced disulfide bond formation unfortunately also did not yield a higher amount of recombinant LipT. Other lipases from *Thermus* species had to be expressed in yeasts like *Kluyveromyces lactis* and *Saccharomyces cerevisiae* (Lopez-Lopez *et al.* 2010; Rocha *et al.* 2011) with reasonably better results for unknown reasons. While the esterase EstTs1 (GenBank acc. no. ACS36170) from *Thermus scotoductus* SA-01 was successfully expressed in *E. coli* (du Plessis *et al.* 2010), an amino acid sequence comparison showed that it was not related with LipT as it only had a low amino acid identity of 27.5% according to an EMBOSS Needle alignment (http://www.ebi.ac.uk/Tools/psa/). Besides, it had a high max. identity of 99% to a lactonase from *Thermus scotoductus* SA-01 (NCBI acc. no ADW21534.1) according to a BLASTP-search (Altschul and Koonin 1998). Nevertheless, the reasons for expression problems with *Thermus*-lipases in *E. coli* still have to be further elucidated.

As a low temperature expression showed good results, an expression host should be found with an optimal growth temperature around 20°C. Thus, the strain *P. antarctica* Shivaji CMS35 was obtained from the DSMZ culture collection. It has not been used as an expression host before and it possessed suitable and valuable characteristics like a growth temperature between 4 and 30°C and an optimum at 22°C (Reddy *et al.* 2004), as well as sensitivity against most of the antibiotics commonly used in molecular biology (3.8). The expression of LipT in *P. antarctica* was compared to the expression in *E. coli*. Unfortunately, *P. antarctica´*s growth rate was decelerated because of the vectors used (IPTG-inducible pBR22b and pML5-T_7 have a size of 26.5 kb) and less of the enzyme was produced. By integration of the T_7-polymerase-gene carrying plasmid pML5-T_7 into the genome, a better growth and a high level production may be possible. By using the smaller, but not inducible broad-host-range vector pBBR1MCS-5, the

growth rate was already better and the yield was higher than with pBR22b (3.8.1).

After expression of LipT in *E. coli* BL21 and *P. antarctica*, the enzyme was purified by Ni-ion chromatography (2.7.3, 3.8.1) and the elution fractions were subsequently concentrated. After purification from *E. coli*, several bands were observed that could correspond with the size of LipT expressed as monomeric protein (38 kDa), dimer (76 kDa) or a trimer (114 kDa; 3.6.4, Figure 13). As the esterase was highly stable against heat-denaturation, detergents and solvents, it would have been possible, that the protein does not denature during the usual sample preparation (denaturing sample buffer, 5-10 min incubation at 95°C). However, the Western Blot analysis of LipT after an SDS-PAGE under denaturing conditions verified a molecular weight of 38 kDa (Figure 14).

In contrast, the protein band pattern after expression in *P. antarctica* looked differently. The concentrated elution fractions of LipT purified from *P. antarctica lipT*::pBBR1MCS-5 contained one protein fraction next to many others, that was consistent with the estimated protein size of LipT with approx. 38 kDa (3.8.1, Figure 29).

When LipT was purified from the crude cell extracts of *P. antarctica* containing the other construct *lipT*::pBR22b, 10 protein fractions with sizes between approx. 16 and 100 kDa could be observed after SDS-PAGE (3.8.1, Figure 29). None of the fractions corresponded with the estimated size of 38 kDa for LipT as monomer and only after a Western Blot immunoassay a double-band was clearly visible with approx. 38 and 38.5 kDa that corresponded with LipT (3.8.1, Figure 29). This double-band could be the result of a post-translational modification like e. g. glycosylation or the protein was processed in some other way. Surprisingly, a better activity could be measured for LipT expressed in *P. antarctica* (0.39 U/mg) than after expression in E. coli (0.12 U/mg). If it turns out that *P. antarctica* produces enzymes that are probably more active than their counterparts produced in *E. coli*, this would be an additional advantage. However, these first expression tests indicate that *P. antarctica* could be an ideal expression host after deletion of interfering genes responsible for e. g. recombination or proteases.

4.4.3 Expression of LipS in *E. coli*

The amino acid sequence of the enzyme LipS was 100% identical with a putative esterase from *Symbiobacterium thermophilum* IAM14863. Up to now, a gene encoding a β-tyrosinase (tyrosine phenol-lyase) from a *Symbiobacterium* species and a β-N-acetylhexosaminidase from *Symbiobacterium thermophilum* were expressed in *E. coli* and used as biocatalysts (Lee *et al.* 1997; Ogawa *et al.* 2006). Like for LipT, a higher yield of LipS could be reached at an expression temperature of 17°C with more than 15.0 mg of protein per gram of cell pellet after His_6-tag

purification (3.6.4). The yield of the protein was therefore even high enough for freeze-drying without significant losses. LipS was visible as one single band of approx. 31.7 kDa after denaturing SDS-PAGE and Western Blot analysis.

4.5 Enzymatic properties of Est5E5, LipS and LipT

Lipases have been defined as carboxylesterases that are able to act on long-chain acylglycerols with ≥10 carbon atoms in their acyl-chain (Jaeger *et al.* 1999). Additionally, the so-called "true lipases" are activated on interfaces between lipid and water and possess a surface loop structure called lid that permits interfacial activation. Considering the last two criteria, LipS is clearly a lipase, because its crystal structure revealed a lid and it was active even on *p*NP stearate (C_{18}; 3.6.5.1). Besides, of all three enzymes tested, only LipS showed hydrolytic activity on the substrates TBT, triolein and polyglycerol-3-laurate that were emulsified in the titrator and thus it probably was the only enzyme activated at an interface (3.6.5.10). The titration assay is much more sensitive than the TBT agar plate assay that is why the lipase showed much better activity on this substrate when measured in the titrator. LipT was able to hydrolyze long-chain substrates like *p*NP palmitate (C_{16}) and stearate, though with low activity (3.6.5.1), while Est5E5 was only able to act on *p*NP myristate (C_{14}) and no activity could be measured with *p*NP palmitate and stearate (3.6.5.1). Besides, Est5E5 was much more active on *p*NP butyrate (C_4) and hexanoate (C_6) than LipS and LipT. As it is unclear if the structures of both enzymes contain a lid, both could be classified equally as an esterase or a lipase. Just to emphasize the difference between LipT´s activity on longer *p*NP ester chain lengths, it was called a lipase in this work. It is noteworthy that clear classification of enzymes into lipases and esterases is sometimes not possible, as even *Candida antarctica* lipase B does not fulfill all criteria of a lipase with a missing lid-structure and without activation at interfaces (Martinelle *et al.* 1995; Trodler and Pleiss 2008).

The most important characteristics that the lipolytic enzymes in this study should have were thermostability, activity at elevated temperatures and on esters with long-chain acyl residues. Comparing the activities of the three enzymes, Est5E5 was not sufficiently stable against heat-denaturation, as it was inactivated after 60 min incubation at 50°C and after 30 min at 60°C (3.6.5.2). LipT was much more stable as it possessed over 20% residual activity after 54 h at 70°C and over 40% after 4 h at 90°C (Figure 17). Still, the highest stability was observed for LipS with over 35% activity after 66 h at 70°C and over 50% after 4 h at 90°C (Figure 17). Reasons for this stability, among others, could be the rather compact and rigid enzyme structure with flexible regions, a hydrophobic surface and the position of the N- and C-terminal ends close to

the core (3.7; Vieille and Zeikus 2001; Kamal *et al.* 2011; Radestock and Gohlke 2011; Kamal *et al.* 2012). Compared with the homologous esterase of *Rhodopseudomonas* sp., LipS contains more stabilizing arginine residues (6.8% instead of 2.8-4.0%) and less cysteine sensitive to oxidation (1.1% instead of 1.6-2%; Mrabet *et al.* 1992; Vieille and Zeikus 2001).

While the optimal temperature of Est5E5 lied with 50°C in a moderately thermophilic rage, LipS and LipT were truly thermophilic enzymes with optima at 70 and 75°C, respectively (3.6.5.2). There are only few lipolytic enzymes derived from metagenomes that show high temperature optima as well as high thermostability (Table 23). Most of the lipolytic enzymes discovered in metagenomic libraries made directly from soil DNA possess a temperature optimum in the mesophilic range between 25 and 50°C and many are cold-active, which means they are most active at temperatures around 30°C or lower. As examples, the metagenomic lipase LipCE has a temperature optimum at 30°C (Elend *et al.* 2007) and the metagenomic esterase CHA3 is active between 7 and 50°C (Heath *et al.* 2009). This shows again that many enzymes have habitat related properties and thermophilic enrichment cultures help to select enzymes with the desired characteristics. The carboxylesterase EstE1 was isolated from the metagenomic library of a hot spring (Rhee *et al.* 2005). Its maximum activity lied at 95°C, but it was only active on short-chained substrates and had a thermostability which is comparable to LipS and LipT. The lipase LipIAF5.2 from enriched biomass of a fed-batch reactor with temperatures between 50 and 70°C was very stable against thermal pressure as it retained 100% activity after 4h at 90°C (Meilleur *et al.* 2009). Still, its optimal temperature was more than 10°C lower than the optimum of LipS and LipT. Therefore, to current knowledge, LipS and LipT are the first metagenome-derived lipases revealing temperature optima at 70 and 75°C and also possessing high stabilities.

Table 23. Metagenome-derived esterases and lipases with temperature optima of at least 50°C.

Esterase/ lipase	Metagenomic library constructed with DNA from	T_{opt} (°C)	Thermal stability	Spec. activity U/mg (*p*NP substrate)	Reference
LipS	soil and water samples enrichment 65°C	70	50% activity after 48 h at 70°C and 4 h at 90°C.	12.03 (C_8) 6.04 (C_{10})	This study
LipT	enrichment of heating water samples 75°C	75	50% activity after 2 h at 70°C and 50 min at 90°C.	0.6 (C_{10}) 0.4 (C_{12})	This study
EstA3	biofilm growing within drinking water network	50	Inactivation when incubated for > 60 min at 45°C.	513.6 (C_4)	Elend *et al.* 2006
EstMa	hot spring soil, Indonesia	50	n. d.	4.45 (C_5)	Kim *et al.* 2006

Esterase/ lipase	Metagenomic library constructed with DNA from	T_{opt} (°C)	Thermal stability	Spec. activity U/mg (*p*NP substrate)	Reference
Est2k	fermented compost	50	68% activity after 15 min at 40°C.	17.1 (C_4)	Kim *et al.* 2010
JkP01	hot spring soil, Himachal Pradesh, India	50	80% activity after 75 min at 50°C; 50% after 5 min at 60°C.	2022.00 (C_{12})	Sharma *et al.* 2012
LipAAc	Brazilian Atlantic forest soil	50-60	100% activity after 1 h at 50°C; 53% after 1 h at 60°C; 33% after 1 h at 70°C.	9.0 (C_{10})	Faoro *et al.* 2011
LipIAF5.2	biomass of a fed-batch reactor	60	100% activity after 4h at 90°C.	160.0 (C_{14})	Meilleur *et al.* 2009
LipIAF1-6	biomass enrichment in a fed-batch bioreactor	60	100% activity after 30 min at 70°C; 30% after 30 min at 80°C.	4287.00 (C_4)	Cote and Shareck 2010
EstE1	hot springs and mud holes in solfataric fields, Indonesia	95	80% activity after 120 min at 85°C, 50% after 2 h at 90°C and after 2 min at 95°C.	n. d. (C_6)	Rhee *et al.* 2005

Obviously, large differences exist concerning the specific activity of the lipolytic enzymes. They vary between only few units per milligram (U/mg) and over 4,200 U/mg. Presumably not all values are comparable due to differences in measurement and calculation.

There are some lipases derived from cultivable thermophilic bacteria that have high temperature optima up to 96°C (Table 24). Interestingly, the optimal growth temperature of these organisms was sometimes up to 20°C lower (Est53) or higher (LipA, LipB) than their enzyme´s temperature optimum (Kakugawa *et al.* 2007; Salameh and Wiegel 2007). The activities of LipS and LipT were comparable to those enzymes and the stability was sometimes even better. While Est53 and LipTth could be overexpressed in *E. coli*, LipA and LipB had to be purified from the culture supernatant (Kakugawa *et al.* 2007; Salameh and Wiegel 2007; Royter *et al.* 2009). In order to use the purified enzymes in biotechnology, high amounts of the enzymes are requested that can most often only be achieved by heterologous overexpression.

Table 24. Enzymatic properties of LipS and LipT in comparison with esterases and lipases derived from thermophilic organisms. Only enzymes with temperature optima above 60°C and activity on *p*NP substrates with ≥8 carbon atoms as residue were considered.

Enzyme and organism (optimal growth temperature)	T_{opt} (°C)	Thermal stability	Spec. activity U/mg (*p*NP substrate)	Reference
Est53, *Thermotoga maritima* (80°C)	60	>90% activity after 90 min at 60°C, 70% after 90 min at 70°C and 50% after 30 min at 80°C.	13.0 (C_{12})	Kakugawa *et al.* 2007
LipA, *Thermosyntropha lipolytica* (60 - 66°C)	96	50% activity after incubation at 100°C for 6 h and at 74.1°C for 24 h with 0.5 to 2 M ammonium sulfate added.	12.4 (C_{12})	Salameh and Wiegel 2007
LipB, *Thermosyntropha lipolytica* (60 - 66°C)	96	50% activity after incubation at 100°C for 2 h and at 76.5°C for 24 h with 0.5 to 2 M ammonium sulfate added.	13.3 (C_{12})	Salameh and Wiegel 2007
LipTth, *Thermoanaerobacter thermohydrosulfuricus* (70°)	75	80-90% activity after 24 h at 70 and 75°C, 20% after 24 h at 80°C, 50% after 2 h at 85°C and 50 min at 90°C.	12.15 (C_{16})	Royter *et al.* 2009

In contrast to many other classes of enzymes, most lipases and carboxylesterases have the advantage that they do not require cofactors for their catalytic activity. Of the eight different metal ions tested, none had a significantly stimulating effect on the activity of LipS and LipT and some even lowered the enzyme activity (3.6.5.4). But surprisingly, Est5E5 showed a more than 3.5 times better activity when 10 mM Cu^{2+} was added to the hydrolysis reaction on *p*NP substrate (Figure 20). The activity was also significantly higher in the presence of Ca^{2+}, Fe^{3+}, Mg^{2+}, Mn^{2+} and Zn^{2+}. Until now, many oxidases and reductases are known as copper proteins, but for esterases, this strongly stimulating effect is unusual. Still, for *Candida rugosa* lipase, an enhanced activity and enantioselectivity under influence of a weakly acidic pH and Cu^{2+} ions could also be observed (Xu *et al.* 2006). In case of this lipase, this led to the assumption that the pH variation and Cu^{2+} addition effected a change in conformation and/or flexibility of the lipase structure which led to the activity enhancement. Structural analysis is necessary in order to find out how Cu^{2+} ions are able to enhance the hydrolysis reaction of Est5E5.

The optimal pH of the enzymes lied in an alkaline pH range. While LipS and LipT were most active at pH 8.0, Est5E5 had a pH optimum of 8.6 (3.6.5.3). Most bacterial lipolytic enzymes have their optimum in a neutral to alkaline pH range (Gupta *et al.* 2004). The pH optima for

esterification reactions can differ from the optimal pH for hydrolysis reactions (Buthe *et al.* 2005), but this was not further investigated in this study.

Like many other esterases and lipases, Est5E5, LipS and LipT showed relatively high stability against different inhibitors, solvents and detergents that were tested in different concentrations (3.6.5.5; 3.6.5.6). Concerning solvents, some general structural factors are considered as important for enzyme stability: monomeric proteins with molecular weights ranging from 20 kDa to 80 kDa, hydrophobic surfaces and the presence of disulphide bonds (Gupta and Khare 2009). For some proteases, these features have been shown to be crucial, but for many esterases and lipases, these structural reasons for solvent stability were not deeply investigated (Bornscheuer *et al.* 2002; Gupta and Khare 2009). For many enzymes, a correlation between enzyme thermostability and resistance to denaturation in organic solvent has been observed (Owusu and Cowan 1989; Burton *et al.* 2002). However, this stability is especially useful for industrial applications, because esterification reactions are taking place in non-aqueous media, i. e. organic solvents, or in ionic liquids (Reetz 2002). Furthermore, the enzymes can retain stability even when they are added to household cleaning products.

The enzymes Est5E5, LipT and LipS were tested on *p*NP esters that contained sterically more complex residues than the *p*NP substrates tested before (3.6.5.8). As pharmaceutically and chemically relevant substrates 2-phenylpropanoate (rac), 3-phenylbutanoate (rac), cyclohexanoate, 2-(3-benzoylphenyl) propanoate (=ketoprofen), 2-naphthoate, 1-naphthoate, adamantanoate and 2-(4-isobutylphenyl)-N-(4-nitrophenol) propanamide (=ibuprofenmide) were applied. While Est5E5 and LipS were active on most of these substrates, LipT only showed low activity. The naphtol and adamantane residues are especially complex substrates (Table 10) and not all lipolytic enzymes are active on them (Elend *et al.* 2006), but still Est5E5 was able to act on 1-naphtoate and adamantanoate while LipS was hydrolyzing 2-naphtoate (Table 19). All of the three enzymes were able to cleave the amide bond of ibuprofen amide and therefore showed promiscuous amidase activity.

The stereoselectivity of the enzymes was tested on the ester substrates (*S*)-/(*R*)-2-methyldecanoic acid ester, (*S*)-/rac-/(*R*)-2,3-dihydro-1*H*-indene-1-carboxylate (=indancarboxylic acid ester), (*S*)-/rac-ibuprofen ester and (*S*)-/rac-/(*R*)-naproxen ester in comparison with the commercially available fungal lipases from *Candida antarctica* (CalB) and *Rhizopus oryzae* (ROL; Table 11). The ester substrates contained *p*NP or methylumbelliferyl as chromogenic or fluorescent residues in order to investigate if there are differences concerning the reaction and to verify the respective results. The detection method for the fluorescence signal of the MU residue was more sensitive. As Table 22 shows (3.6.5.8), Est5E5, LipS and ROL

preferred the (*R*)-enantiomers of each substrate, while LipT mostly preferred the (*R*)-enantiomers except for naproxen, where it showed (*S*)-selectivity on both MU and *p*NP ester. CalB generally preferred the (*S*)-enantiomers of the substrates, but it showed (*R*)-selectivity for the MU ester of naproxen and (*S*)-selectivity for its *p*NP ester. The MU residue is bigger than *p*NP and obviously the (*R*)-enantiomer of naproxen MU ester fits better into the catalytic site of CalB.

LipS most often had the highest estimated *E* values up to *E*=10.3 for the (*R*)-enantiomer of *p*NP indancarboxylic acid ester, especially in comparison with LipT and CalB that generally reacted with lower selectivity. Interestingly, the selectivity seemed to be lower when the substrate contained the bigger MU molecule as residue. This could be due to the relatively narrow substrate pocket of LipS (3.7). The exceptionally high selectivity of LipS for the (*R*)-enantiomer of ibuprofen was measured separately by HPLC, where an enantiomeric excess (*ee*) of more than 99% and an enantioselectivity of E=200 could be determined for the phenyl ester (3.6.5.9). This feature is especially valuable for LipS´ applicability in the production of optically pure building blocks. Not many wild-type lipases are able to act with such a high enantioselectivity and often the enzymes have to be engineered to do so. With random mutagenesis by means of error-prone PCR, values like E=25.8 could be reached for *Pseudomonas aeruginosa* lipase acting on 2-methyldecanoic acid *p*NP ester. Five amino acid substitutions within the variant caused this higher enantioselectivity in contrast to the wild-type enzyme that only had E=1.1 (Liebeton *et al.* 2000). By directed evolution, the enantioselectivity of *Candida antarctica* lipase A was shifted from E=2−20 for the wild type to a much better enantioselectivity of E=45−276 for the variant acting on α-substituted *p*NP esters (Engstrom *et al.* 2010).

It is important to mention, that non-steroidal anti-inflammatory drugs (NSAIDs) like naproxen, ketoprofen and ibuprofen are physiologically much more active as (*S*)-enantiomers. Even so, the high (*R*)-selectivity of LipS could be used, in order to esterify racemic NSAIDs for example with 1-propanol. This ester can then be separated from the optically pure (*S*)-enantiomer (Carvalho *et al.* 2006).

The three enzymes Est5E5, LipT and LipS were tested for their activity on tri- and polyglycerides using the pH-stat method (3.6.5.10). Est5E5 and LipT, however, were not active on tributyrin (TBT), triolein and polyglycerol-3-laurate although at least on TBT activity could be observed for Est5E5 on agar plates. Probably the enzymes were not activated at the lipid-water interface like LipS, but the measurements should be repeated when higher yields of the enzymes are available.

Usually, esterases and lipases are able to catalyze both the hydrolysis and the esterification

reaction. Still, the esterification takes place at different conditions, as only a low amount of water should be present in order to favor this way of reaction. With lyophilized LipS, 1-propyl laurate and 1-tetradecyl myristate were synthesized in an experimental scale (3.6.5.11). By adjusting the reacting conditions and by applying the lipase immobilized on carrier-beads, the turnover rates could be improved. Immobilized enzymes are more stable and can be used repeatedly. Besides, they can easily be separated from the reaction and the product (Bornscheuer 2003). As LipS was able to catalyze the solvent-free synthesis reaction with long-chained lauric acid (C_{12}) and myristic acid (C_{14}), it seems to be a suitable lipase for the production of emollient esters that are desired ingredients for skin-care products. Still, further research has to be done concerning the synthesis of highly viscous cosmetic compounds like polyglycerol-3-laurate and myristyl-myristate (Muller *et al.* 2010) and the activity and reusability of LipS has to be further compared with the most often used mesophilic enzyme CalB which is also called Novozym434 (Novozymes, Bagsvaerd, Denmark).

Optically pure secondary alcohols are used as intermediates and building blocks for the production of pharmaceuticals. Regarding the kinetic resolution of secondary alcohols that was measured by gas chromatography (2.8.6), LipS showed rather low (*R*)-selectivity for 1-phenyl-1-propylacetate and 1-phenyl-1-ethylacetate (E=3-4). In contrast, it was highly (*R*)-selective for 1-phenyl-2-butylacetate and 1-phenyl-2-pentylacetate with an *ee* of more than 96% and approx. 50% conversion (3.6.5.12). Obviously, the selectivity of LipS was higher when the chiral center was one CH_2-group farther away from the aromatic ring (Chow *et al.* 2012).

4.6 Crystal structure of LipS

Two different variants of LipS, the wild-type (LipS-WT derived from *lipS::*pETM11+26) and LipS-His_6 (derived from *lipS*::pET-21a; 2.2), crystallized in two different space groups (SG; Fersini *et al*. 2012; Chow *et al.* 2012). LipS-WT crystallized with a higher resolution in SG P4 (3.7) and a high electron density around the catalytic Ser126 and H257 could be observed. This density was supposedly caused by spermidine which was added to this variant for improvement of the crystallization process and which probably fits into the catalytic pocket by coincidence as its structure mimics an acyl chain. The inhibiting effect of spermidine on LipS was subsequently shown in an enzyme assay (3.7).

The crystal structures of both variants did not provide information about the flexibility of the lid-domain as it was closed in both cases. Perhaps the lid was closed, because there was no interface that would have caused activation. Attempts to crystallize the enzyme together with a *p*NP substrate unfortunately failed. Another reason could be that the crystallization process

was carried out at room temperature and the lipase was thus not activated (Fersini *et al.* 2012). A comparison between the enzyme structure of LipS at room temperature and at 70°C would be interesting to get information about the flexibility and/or rigidity of the lipase.

An inserted domain constitutes the lid structure of LipS and is composed of two short anti-parallel β-strands (β6 and β7) and one α-helix ($\alpha D_{1'}$). A structural alignment (Chow *et al.* 2012) revealed a high similarity between the unusual lid-structure of LipS and the inserted domains of the lipolytic enzymes Est1E from *Butyrivibrio proteoclasticus* (PDB code 2WTM; Goldstone *et al.* 2010), the human monoglyceride lipase (MGL; 3PE6; Schalk-Hihi *et al.* 2011), EstD from *Lactobacillus rhamnosus* (3DKR; Bennett *et al.* to be published), the esterase LJ0536 from *Lactobacillus johnsonii* (3PF8; Lai *et al.* 2011) and Est30 from *Geobacillus stearothermophilus* (1TQH; Liu *et al.* 2004). The findings are illustrated in Figure 31.

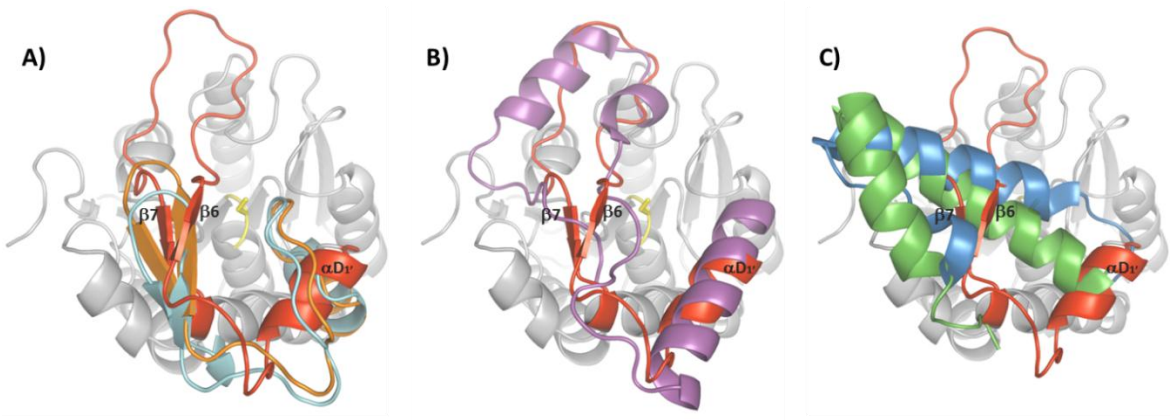

Figure 31. Cartoon representation of inserted domains of lipolytic enzymes. Superimposition of the inserted domain of LipS (red) with A) Est1E (2WTM, orange) and LJ0536 (3PF8, turquoise), B) human MGL (3PE6, purple) and C) EstD (3DKR, blue) and Est30 (1TQH, green). The core structure of LipS is shown in gray and the catalytic Ser126 in yellow. Core structures of LipS homologues are not shown.

Still, according to an EMBOSS Needle sequence alignment (http://www.ebi.ac.uk/Tools/psa/emboss_needle/) between LipS, Est1E and LJ0536, the identities were rather low. LipS and EstE1 had 38.7% nucleotide sequence identity and 17.2% amino acid sequence identity. The identities for LipS and LJ0536 were only slightly higher with 44.1% on nucleotide level and 19.4% on amino acid level.

As Est1E from the rumen bacterium *Butyrivibrio proteoclasticus* and LJ0536 from the gastrointestinal *Lactobacillus johnsonii* were structurally most similar to LipS, their activities should be compared to each other. The feruloyl esterase Est1E and the cinnamoyl esterase LJ0536 were mostly characterized on cinnamic acid esters and other compounds that were supposed to be

similar to their native substrates (Lai *et al.* 2009; Goldstone *et al.* 2010). Est1E was somehow active on *p*NP dodecanoate and *p*NP palmitate but the activity was not further quantified and the assay was performed at 37°C (Goldstone *et al.* 2010). The temperature optimum of LJ0536 only lied at 20°C (Lai *et al.* 2009). Accordingly, the enzymes´ structural similarities do not necessarily mean similar activities.

4.7 Physiological functions of Est5E5, LipS and LipT

Like in many other studies that focused on regarding the applicability of the enzymes in biotechnology, the three metagenomic enzymes were not further studied concerning the role they play for their native organism. The lipolytic enzymes characterized in this work were all derived from heterotrophic bacteria. LipS was most likely derived from *Symbiobacterium thermophilum*, a thermophilic bacterium that was first isolated from compost (Suzuki *et al.* 1988). Through the degradation of plant material, the temperature within a compost stack can reach over 63°C (Harper *et al.* 1992), and therefore *Symbiobacterium thermophilum* is adapted to this temperature. One can only speculate, that LipS could fulfill similar tasks like Est1E and LJ0536 (Lai *et al.* 2009; Goldstone *et al.* 2010) and that it could provide the host with carbon sources as it is able to cleave phenolic acids like ferulic, caffeic and *p*-coumaric acids that are esterified to the plant cell wall or occur esterified with aromatic organic acids within the plant cell. In further studies, LipS should be tested for its activity on these kinds of substrates.

The esterase Est5E5 had 84% identity to a hypothetical protein of *Acidovorax radicis* N35, a Gram-negative wheat-root colonizing bacterium (Li *et al.* 2011). Other members of this genus were isolated from activated sludge (Heylen *et al.* 2008). It could either be possible that Est5E5 provides access through the wax layer on the plant cells during infection or that it degrades carboxylic esters that are present in the surrounding area.

As LipT supposedly originated from a *Thermus* species, its function could also lie in providing the host bacterium with carbon sources that occur in the thermal environment. Nonetheless, an interesting issue would be to find out if LipT indeed exists in a glycosylated form and if this form is able to interact with the outer membrane of *Thermus* sp. and perhaps also of *E. coli.*

4.8 Concluding remarks and perspectives

In this study, over 100 lipolytic clones were found by function-based screening of different metagenomic libraries. Although it was not possible to examine every single clone, two interesting novel lipases and one carboxylesterase were characterized in detail. Among other useful

characteristics, the enzymes showed the desired thermostability and activity on long-chained ester substrates. Additionally, the lipase LipS acted with very high enantioselectivity and its crystal structure provides insights on a structural level.

Still, some favorable properties of the enzymes could be further improved as novel methods for rational and evolutive protein design have been developed within the past decade. With a rational approach, the catalytic pocket of LipS could be altered so that the enzyme is able to act on other substrates, e. g. (*S*)-enantiomers or esters with longer acyl-chain lengths. Probably for LipT and Est5E5 a better substrate specificity or respectively a higher temperature stability could be achieved with site-directed mutagenesis, error prone PCR or saturation mutagenesis. Furthermore, immobilization could be carried out with LipS for testing its activity in other synthesis reactions and perhaps for applying it later on in a reactor-scale.

The other metagenomic lipases and esterases remaining should be characterized and other ways should be found to improve the expression rates of recombinant enzymes in *E. coli* as well as in the psychrophilic bacterium *P. antarctica* which disclosed very suitable and useful characteristics as a heterologous host in this study. Therefore, recombinant expression can further be enhanced by improving the expression systems and its growth conditions for reaching high cell densities.

5 Abstract

Carboxylesterases (EC 3.1.1.1) and triacylglycerol lipases (EC 3.1.1.3) are lipolytic enzymes acting on ester bonds and catalyze both hydrolysis and synthesis reactions on a broad spectrum of substrates. Industrial production processes sometimes demand high working temperatures and thus customized biocatalysts showing high thermostability. Still, most lipases used today originate from mesophilic organisms and are susceptible to heat denaturation. Within this thesis, the identification and detailed characterization of two novel thermostable lipases and one carboxylesterase are described.

Two different long-term enrichment cultures that were either inoculated with heating water from the Biocenter Klein Flottbek (Hamburg, Germany) or soil and water samples from the nearby Botanical Garden were maintained at 75 and 65°C for 3 weeks. Microbial communities were characterized on a phylogenetic level and prevalently contained organisms related to *Thermus scotoductus* (up to 100% of the culture) and *Symbiobacterium thermophilum* (approx. 80% of the culture). From the genomic DNA, metagenomic libraries were constructed using *E. coli* Epi100 as host bacterium. Functional screening of these libraries using tributyrin and *p*NP-substrates (C_4 and C_{12}) between 50 and 70°C resulted in the identification of 10 lipolytic clones. Two of them that showed higher activity in previous tests have been studied in detail and the respective lipases were designated LipS and LipT. From six other metagenomes constructed within the working group, altogether over 100 clones with lipolytic activity were screened. The esterase Est5E5 was found by tributyrin-screening together with six other lipolytic clones within the metagenomic library of a biofilm growing on the valve of a fresh water pipeline, but only Est5E5 was further characterized.

LipS was identical in its amino acid sequence to an annotated esterase from *Symbiobacterium thermophilum* IAM14863 and LipT had 96% identity to a putative esterase from *Thermus scotoductus* SA-01, whereas Est5E5 showed 84% identity to a conserved hypothetical protein from *Acidovorax radicis* N35. None of these three enzymes could be grouped into any of the eight described lipase and esterase families with current alignment methods. Thus, they may constitute members of new families. After overexpression in *E. coli* BL21 (DE3) and subsequent His_6-tag purification, the recombinant LipS (32 kDa) revealed very high thermostability with 50% residual activity after 48 h incubation at 70°C while LipT (38 kDa) possessed 50% residual activity after 3 h at this temperature. Est5E5 (50 kDa) was less heat-stable and retained 50% activity after 40 min at 50°C.

With temperature optima at 70°C (LipS), 75°C (LipT) and 50°C (Est5E5), all three enzymes had thermophilic properties. Besides, they were stable against most solvents, detergents and inhibitors tested and were most active between pH 8.0 and 8.6.

LipS and Est5E5 showed the highest specific activity for *p*NP octanoate (C_8, 12.0 and 7.7 U/mg, respectively) and LipT for *p*NP decanoate (C_{10}, 0.6 U/mg). In contrast to Est5E5, LipS and LipT also showed activity on *p*NP palmitate (C_{16}) and stearate (C_{18}). Furthermore, the three enzymes acted on pharmaceutically relevant chiral substrates like naproxen and ibuprofen esters. LipS was highly (*R*)-specific for ibuprofen phenyl ester with an enantiomeric excess (*ee*) of over 99% as well as for acetates of secondary alcohols (1-phenyl-2-butylacetate and 1-phenyl-2-pentylacetate) with an *ee* of more than 96%. Interestingly, LipS was able to synthesize the esters 1-propyl laurate and 1-tetradecyl myristate at 70°C under non-aqueous conditions in comparable rates to the commercial *Candida antarctica* lipase B. The structure of LipS was solved by X-ray crystallographic analyses with a resolution of 1.99 Å and the crystal revealed an unusual and compact lid-structure in a closed conformation.

Furthermore, *Pseudomonas antarctica* Shivaji CMS35 was used to improve the low-temperature expression of the above mentioned lipase LipT. For this purpose, the genome was sequenced and analyzed. The psychrophilic bacterium exhibited characteristics suitable for serving as heterologous host (e. g. sensitivity against common antibiotics, secretion systems type I-III, Vb, VI, Sec and Tat) and showed promising results in comparison with IPTG-induced *E. coli* BL21 (DE3) concerning enzyme yield (*E. coli*: 3.01 mg/g of cell pellet, *P. antarctica*: 1.15 mg/g) and activity of LipT (*E. coli*: 0.12 U/mg, *P. antarctica*: 0.39 U/mg).

5.1 Zusammenfassung

Carboxylesterasen (EC 3.1.1.1) und Triacylglycerol-Lipasen (EC 3.1.1.3) sind lipolytische Enzyme, die sowohl Hydrolyse- als auch Synthese-Reaktionen an Esterbindungen von einer Vielzahl an Substraten katalysieren können. Industrielle Produktionsprozesse benötigen oft hohe Reaktionstemperaturen und daher passende Biokatalysatoren mit hoher Thermostabilität. Dennoch stammen die meisten der heute genutzten Lipasen aus mesophilen Organismen und sind anfällig für Hitzedenaturierung. In dieser Arbeit wurden zwei neuartige thermostabile Lipasen sowie eine Esterase identifiziert und im Detail charakterisiert.

Zwei verschiedene Anreicherungskulturen wurden zum einen mit einer Heizungswasserprobe aus dem Biozentrum Klein Flottbek (Hamburg, Deutschland) und zum anderen mit Boden- und Wasserproben aus dem benachbarten Botanischen Garten inokuliert und bei 75 bzw. 65°C für drei Wochen inkubiert. Die mikrobiellen Gemeinschaften wurden phylogenetisch charakterisiert und enthielten vornehmlich Organismen in enger Verwandtschaft zu *Thermus scotoductus* (bis zu 100% der Kultur) und *Symbiobacterium thermophilum* (ca. 80% der Kultur). Mit der genomischen DNA wurden anschließend Metagenom-Bibliotheken in *E. coli* Epi100 als Wirtsbakterium konstruiert. Durch deren funktionsbasierte Durchmusterung auf Tributyrin und mit *p*NP-Substraten (C_4 und C_{12}) bei 50 bis 70°C konnten zehn lipolytische Klone identifiziert werden. Zwei dieser Klone, die in vorangegangenen Tests höhere Aktivität zeigten, wurden weiter untersucht und die jeweiligen Lipasen als LipS und LipT bezeichnet. In sechs anderen Metagenomen, die innerhalb der Arbeitsgruppe konstruiert worden waren, wurden insgesamt über 100 Klone mit lipolytischer Aktivität gefunden. Die Esterase Est5E5 wurde zusammen mit sechs anderen lipolytisch-aktiven Klonen bei der Durchmusterung auf Tributyrin in der Metagenom-Bibliothek eines Biofilms gefunden, der sich auf dem Absperrschieber einer Trinkwasserleitung befand, es wurde jedoch nur Est5E5 genauer charakterisiert.

LipS war auf Aminosäure-Ebene identisch mit einer annotierten Esterase von *Symbiobacterium thermophilum* IAM14863 und LipT besaß 96% Identität zu einer putativen Esterase von *Thermus scotoductus* SA-01, wohingegen Est5E5 zu 84% identisch mit einem konservierten hypothetischen Protein von *Acidovorax radicis* N35 war. Keines dieser drei Enzyme konnte mit gängigen Abgleichungsmethoden einer der acht beschriebenen Lipase- und Esterase-Familien zugeordnet werden. Sie könnten daher Mitglieder neuer Familien darstellen. Nach Überexpression in *E. coli* BL21 (DE3) und anschließender His_6-tag Aufreinigung zeigte das rekombinante LipS (32 kDa) sehr hohe Thermostabilität mit 50% Restaktivität nach 48 Std. Inkubation bei 70°C,

während LipT (38 kDa) bei dieser Temperatur nach 3 Std. 50% Restaktivität beibehielt. Est5E5 (50 kDa) war weniger hitzestabil und besaß nach 40 Min. bei 50°C 50% Restaktivität.

Mit Temperaturoptima von 70°C (LipS), 75°C (LipT) und 50°C (Est5E5) zeigten alle drei Enzyme thermophile Eigenschaften. Zusätzlich waren sie gegen die meisten der getesteten Lösungsmittel, Detergentien und Inhibitoren stabil und waren im Bereich von pH 8.0 bis 8.6 am aktivsten.

LipS und Est5E5 zeigten die höchste spezifische Aktivität für *p*NP-Octanoat (C_8; 12,0 bzw. 7,7 U/mg) und LipT für *p*NP-Decanoat (C_{10}; 0,6 U/mg). Im Gegensatz zu Est5E5 konnten LipS und LipT auch *p*NP-Palmitat (C_{16}) und -Stearat (C_{18}) umsetzen. Die drei Enzyme waren auch auf pharmazeutisch relevanten chiralen Substraten wie Naproxen und Ibuprofen aktiv. LipS besaß hohe (*R*)-Spezifität auf Ibuprofen-Phenylester mit einem Enantiomerenüberschuss (*ee*) von über 99% und auf Acetaten sekundärer Alkohole (1-Pheny-2-butylacetat und 1-Phenyl-2-pentylacetat) mit einem *ee* von über 96%. Interessanterweise war LipS in der Lage, die Ester 1-Propyllaurat und 1-Tetradecylmyristat bei 70°C unter nichtwässrigen Bedingungen in vergleichbaren Raten wie die kommerzielle *Candida antarctica* Lipase B zu synthetisieren. Die Struktur von LipS wurde mit Röntgenkristall-Strukturanalysen zu einer Auflösung von 1,99 Å aufgeklärt und offenbarte eine ungewöhnliche und kompakte Lid-Struktur, die sich in einer geschlossenen Konformation befand.

Weiterhin wurde *Pseudomonas antarctica* Shivaji CMS35 verwendet, um die Expression der bereits erwähnten Lipase LipT bei niedriger Temperatur zu verbessern. Für diesen Zweck wurde das Genom sequenziert und analysiert. Das psychrophile Bakterium wies passende Charakteristika auf, um als heterologer Wirt zu dienen (u. a. Sensitivität gegenüber häufig genutzten Antibiotika, Sekretionssysteme Typ I-III, Vb, VI, Sec und Tat) und brachte vielversprechende Ergebnisse im Vergleich zu IPTG-induziertem *E. coli* BL21 (DE3) bezüglich Enzymausbeute (*E. coli*: 3,01 mg/g Zellpellet; *P. antarctica*: 1,15 mg/g) und Aktivität von LipT (*E. coli*: 0,12 U/mg; *P. antarctica*: 0,39 U/mg).

6 References

Altschul, S. F. and E. V. Koonin (1998). "Iterated profile searches with PSI-BLAST-a tool for discovery in protein databases." Trends Biochem. Sci. **23**(11): 444-447.

Amann, R. I., W. Ludwig, et al. (1995). "Phylogenetic Identification and in-Situ Detection of Individual Microbial-Cells without Cultivation." Microbiol Rev **59**(1): 143-169.

Antoine, E., J. L. Rolland, et al. (1999). "Cloning and over-expression in *Escherichia coli* of the gene encoding NADPH group III alcohol dehydrogenase from *Thermococcus hydrothermalis* - Characterization and comparison of the native and the recombinant enzymes." Eur J Biochem **264**(3): 880-889.

Arpigny, J. L. and K. E. Jaeger (1999). "Bacterial lipolytic enzymes: classification and properties." Biochem J **343 Pt 1**: 177-183.

Bachmann, B. J. (1983). "Linkage map of Escherichia coli K-12, edition 7." Microbiol Rev. **47**(2): 180–230.

Bayer, S., A. Kunert, et al. (2010). "Indication for a new lipolytic enzyme family: isolation and characterization of two esterases from a metagenomic library." J Mol Microbiol Biotechnol **18**(3): 181-187.

Beisson, F., A. Tiss, et al. (2000). "Methods for lipase detection and assay: a critical review." Eur J Lipid Sci Technol **102**(2): 133-153.

Beloqui, A., T. Y. Nechitaylo, et al. (2010). "Diversity of glycosyl hydrolases from cellulose-depleting communities enriched from casts of two earthworm species." Appl Environ Microbiol **76**(17): 5934-5946.

Bennett, M. D., M.-L. Delabre, et al. to be published.

Birnboim, H. C. and J. Doly (1979). "A rapid alkaline extraction procedure for screening recombinant plasmid DNA." Nucleic Acids Res **7**(6): 1513-1523.

Böhnke, S. (2010). Untersuchungen zur Struktur und Dynamik Ammoniak oxidierender Populationen in tidebeeinflussten Lebensräumen der Elbe. Diploma thesis, University of Hamburg, Germany.

Bornscheuer, U. T. (2003). "Immobilizing enzymes: how to create more suitable biocatalysts." Angew Chem Int Ed Engl **42**(29): 3336-3337.

Bornscheuer, U. T., C. Bessler, et al. (2002). "Optimizing lipases and related enzymes for efficient application." Trends Biotechnol **20**(10): 433-437.

Bradford, M. M. (1976). "A rapid and sensitive method for the quantitation of microgram quantities of protein utilizing the principle of protein-dye binding." Anal Biochem **72**: 248-254.

Brosius, J., A. Ullrich, et al. (1981). "Construction and fine mapping of recombinant plasmids containing the rrnB ribosomal RNA operon of *E. coli*." Plasmid **6**(1): 112-118.

Brummund, J., F. Meyer, et al. (2011). "Dissolving carbon dioxide in high viscous substrates to accelerate biocatalytic reactions." Biotechnol Bioeng **108**(11): 2765-2769.

Burton, S. G., D. A. Cowan, et al. (2002). "The search for the ideal biocatalyst." Nat Biotechnol **20**(1): 37-45.

Buthe, A., T. Recker, et al. (2005). "pH-optima in lipase-catalysed esterification." Biocatal Biotransformation **23**(5): 307-314.

Carvalho, P. d. O., F. J. Contesini, et al. (2006). "Optimization of enantioselective resolution of racemic ibuprofen by native lipase from *Aspergillus niger*." J Ind Microbiol Biotechnol **33**(8): 713-718.

Castenholz, R. W. (1969). "Thermophilic blue-green algae and the thermal environment." Bacteriol Rev **33**(4): 476-504.

Charbonneau, D. M., F. Meddeb-Mouelhi, et al. (2010). "A novel thermostable carboxylesterase from *Geobacillus thermodenitrificans*: evidence for a new carboxylesterase family." J Biochem **148**(3): 299-308.

Chen, C. S., Y. Fujimoto, et al. (1982). "Quantitative-Analyses of Biochemical Kinetic Resolutions of Enantiomers." J Am Chem Soc **104**(25): 7294-7299.

Chester, N. and D. R. Marshak (1993). "Dimethyl sulfoxide-mediated primer Tm reduction: a method for analyzing the role of renaturation temperature in the polymerase chain reaction." Anal Biochem **209**(2): 284-290.

Chow, J. (2008). Isolierung von neuartigen thermophilen Enzymen für die Biokatalyse. Diploma thesis, University of Hamburg, Germany.

Chow, J., F. Kovacic, et al. (2012). "The Metagenome-Derived Enzymes LipS and LipT Increase the Diversity of Known Lipases." PLoS One 7(10): e47665.

Chung, G. H., Y. P. Lee, et al. (1991). "Overexpression of a Thermostable Lipase Gene from *Pseudomonas fluorescens* in *Escherichia coli*." Appl Microbiol Biotechnol **35**(2): 237-241.

Cote, A. and F. Shareck (2010). "Expression and characterization of a novel heterologous moderately thermostable lipase derived from metagenomics in *Streptomyces lividans*." J Ind Microbiol Biotechnol **37**(9): 883-891.

Daniel, R. (2005). "The metagenomics of soil." Nat Rev Microbiol **3**(6): 470-478.

Dees, P. M. and W. C. Ghiorse (2001). "Microbial diversity in hot synthetic compost as revealed by PCR-amplified rRNA sequences from cultivated isolates and extracted DNA." FEMS Microbiol Ecol **35**(2): 207-216.

DeLano, W. L. (2002). The PyMOL Molecular Graphics System. New York, Schroedinger LLC.

Delmont, T. O., P. Robe, et al. (2011). "Accessing the soil metagenome for studies of microbial diversity." Appl Environ Microbiol **77**(4): 1315-1324.

DeLong, E. F. (1992). "Archaea in coastal marine environments." Proc Natl Acad Sci U S A **89**(12): 5685-5689.

Devescovi, G., J. Bigirimana, et al. (2007). "Involvement of a quorum-sensing-regulated lipase secreted by a clinical isolate of *Burkholderia glumae* in severe disease symptoms in rice." Appl Environ Microbiol **73**(15): 4950-4958.

Divakar, S. and B. Manohar (2007). Use of Lipases in The Industrial Production of Esters Industrial Enzymes. J. Polaina and A. P. MacCabe, Springer**:** 283-300.

Drepper, T., S. Arvani, et al. (2005). "High-level transcription of large gene regions: a novel T(7) RNA-polymerase-based system for expression of functional hydrogenases in the phototrophic bacterium *Rhodobacter capsulatus*." Biochem Soc Trans **33**(Pt 1): 56-58.

du Plessis, E. M., E. Berger, et al. (2010). "Characterization of a novel thermostable esterase from *Thermus scotoductus* SA-01: evidence of a new family of lipolytic esterases." Curr Microbiol **60**(4): 248-253.

Elend, C., C. Schmeisser, et al. (2007). "Isolation and characterization of a metagenome-derived and cold-active lipase with high stereospecificity for (*R*)-ibuprofen esters." J Biotechnol **130**(4): 370-377.

Elend, C., C. Schmeisser, et al. (2006). "Isolation and biochemical characterization of two novel metagenome-derived esterases." Appl Environ Microbiol **72**(5): 3637-3645.

Emsley, P., B. Lohkamp, et al. (2010). "Features and development of Coot." Acta Crystallogr D Biol Crystallogr **66**: 486-501.

Engstrom, K., J. Nyhlen, et al. (2010). "Directed evolution of an enantioselective lipase with broad substrate scope for hydrolysis of alpha-substituted esters." J Am Chem Soc **132**(20): 7038-7042.

Entcheva, P., W. Liebl, et al. (2001). "Direct cloning from enrichment cultures, a reliable strategy for isolation of complete operons and genes from microbial consortia." Appl Environ Microbiol **67**(1): 89-99.

Erra-Pujada, M., P. Debeire, et al. (1999). "The type II pullulanase of *Thermococcus hydrothermalis*: Molecular characterization of the gene and expression of the catalytic domain." J Bacteriol **181**(10): 3284-3287.

Fan, X., X. Niehus, et al. (2012). "Lipases as biocatalyst for biodiesel production." Methods Mol Biol **861**: 471-483.

Faoro, H., A. Glogauer, et al. (2011). "Identification of a new lipase family in the Brazilian Atlantic Forest soil metagenome." Environ Microbiol Rep **3**(6): 750-755.

Fazlena, H., A. H. Kamaruddin, et al. (2006). "Dynamic kinetic resolution: alternative approach in optimizing *S*-ibuprofen production." Bioprocess Biosyst Eng **28**(4): 227-233.

Fedeli, E. (1977). "Lipids of olives." Prog Chem Fats Other Lipids **15**(1): 57-74.

Feller, G. (2010). "Protein stability and enzyme activity at extreme biological temperatures." J Phys Condens Matter **22**(32).

Ferrer, P., J. L. Montesinos, et al. (2001). "Production of native and recombinant lipases by *Candida rugosa*: a review." Appl Biochem Biotechnol **95**(3): 221-255.

Fersini, F., Y. Dall´ Antonia, et al. (2012). "Cloning, expression, purification and preliminary X-ray analysis of a metagenome-derived lipase." Acta Crystallogr Sect F Struct Biol Cryst Commun **68**: 923–926.

Frazzetto, G. (2003). "White biotechnology." EMBO Rep **4**(9): 835-837.

Fucinos, P., A. Dominguez, et al. (2005). "Production of Thermostable Lipolytic Activity by *Thermus* Species." Biotechnol Prog **21**(4): 1198-1205.

Gabor, E. M., W. B. Alkema, et al. (2004). "Quantifying the accessibility of the metagenome by random expression cloning techniques." Environ Microbiol **6**(9): 879-886.

Goldstone, D. C., S. G. Villas-Boas, et al. (2010). "Structural and functional characterization of a promiscuous feruloyl esterase (Est1E) from the rumen bacterium *Butyrivibrio proteoclasticus*." Proteins **78**(6): 1457-1469.

Gouet, P., E. Courcelle, et al. (1999). "ESPript: analysis of multiple sequence alignments in PostScript." Bioinformatics **15**(4): 305-308.

Gupta, A. and S. K. Khare (2009). "Enzymes from solvent-tolerant microbes: useful biocatalysts for non-aqueous enzymology." Crit Rev Biotechnol **29**(1): 44-54.

Gupta, R., N. Gupta, et al. (2004). "Bacterial lipases: an overview of production, purification and biochemical properties." Appl Microbiol Biotechnol **64**(6): 763-781.

Hall, T. A. (1999). "BioEdit: a user-friendly biological sequence alignment editor and analysis program for Windows 95/98/NT." Nucl. Acids. Symp. **41**: 95-98.

Hamzic, M., J. Pietruszka, et al. (2011). "HPLC-CD selectivity assay for alcohol dehydrogenases." Chirality **23 Suppl 1**: E110-115.

Hanahan, D. (1983). "Studies on transformation of *Escherichia coli* with plasmids." J Mol Biol **166**(4): 557-580.

Handelsman, J., M. R. Rondon, et al. (1998). "Molecular biological access to the chemistry of unknown soil microbes: a new frontier for natural products." Chem Biol **5**(10): R245-249.

Hardeman, F. and S. Sjoling (2007). "Metagenomic approach for the isolation of a novel low-temperature-active lipase from uncultured bacteria of marine sediment." FEMS Microbiol Ecol **59**(2): 524-534.

Harper, E., F. C. Miller, et al. (1992). "Physical Management and Interpretation of an Environmentally Controlled Composting Ecosystem." Aust J Exp Agric **32**(5): 657-667.

Hausmann, S. and K. E. Jaeger (2010). Lipolytic Enzymes from Bacteria. Handbook of Hydrocarbon and Lipid Microbiology. T. KN. Berlin, Springer-Verlag**:** 2-28.

Heath, C., X. P. Hu, et al. (2009). "Identification of a Novel Alkaliphilic Esterase Active at Low Temperatures by Screening a Metagenomic Library from Antarctic Desert Soil." Appl Environ Microbiol **75**(13): 4657-4659.

Henderson, I. R., F. Navarro-Garcia, et al. (2004). "Type V protein secretion pathway: the autotransporter story." Microbiol Mol Biol Rev **68**(4): 692-+.

Henke, E., S. Schuster, et al. (2000). "Lipase-catalyzed resolution of ibuprofen." Monatshefte Fur Chemie **131**(6): 633-638.

Henne, A., R. A. Schmitz, et al. (2000). "Screening of environmental DNA libraries for the presence of genes conferring lipolytic activity on *Escherichia coli*." Appl Environ Microbiol **66**(7): 3113-3116.

Heylen, K., L. Lebbe, et al. (2008). "*Acidovorax caeni* sp nov., a denitrifying species with genetically diverse isolates from activated sludge." Int J Syst Evol Microbiol **58**: 73-77.

Hills, G. (2003). "Industrial use of lipases to produce fatty acid esters." Eur J Lipid Sci Technol **105**(10): 601-607.

Hilterhaus, L., O. Thum, et al. (2008). "Reactor concept for lipase-catalyzed solvent-free conversion of highly viscous reactants forming two-phase systems." Org Process Res Dev **12**(4): 618-625.

Hong, K. S., H. K. Lim, et al. (2007). "Selection and characterization of forest soil metagenome genes encoding lipolytic enzymes." J Microbiol Biotechnol **17**(10): 1655-1660.

Ikeda, M. and D. S. Clark (1998). "Molecular cloning of extremely thermostable esterase gene from hyperthermophilic archaeon *Pyrococcus furiosus* in *Escherichia coli*." Biotechnol Bioeng **57**(5): 624-629.

Imanaka, T. (2011). "Molecular bases of thermophily in hyperthermophiles." Proc Jpn Acad Ser B Phys Biol Sci **87**(9): 587-602.

Jaeger, K. E., B. W. Dijkstra, et al. (1999). "Bacterial biocatalysts: molecular biology, three-dimensional structures, and biotechnological applications of lipases." Annu Rev Microbiol **53**: 315-351.

Jaeger, K. E. and M. T. Reetz (1998). "Microbial lipases form versatile tools for biotechnology." Trends Biotechnol **16**(9): 396-403.

Jeon, J. H., J. T. Kim, et al. (2009). "Characterization and its potential application of two esterases derived from the arctic sediment metagenome." Mar Biotechnol **11**(3): 307-316.

Jeon, J. H., J. T. Kim, et al. (2009). "Cloning and characterization of a new cold-active lipase from a deep-sea sediment metagenome." Appl Microbiol Biotechnol **81**(5): 865-874.

Jiang, Z. (2008). "Lipase-catalyzed synthesis of aliphatic polyesters via copolymerization of lactone, dialkyl diester, and diol." Biomacromolecules **9**(11): 3246-3251.

Jiang, Z., H. Wang, et al. (2006). "Characterization of two novel lipase genes isolated directly from environmental sample." Appl Microbiol Biotechnol **70**(3): 327-332.

Kakugawa, S., S. Fushinobu, et al. (2007). "Characterization of a thermostable carboxylesterase from the hyperthermophilic bacterium *Thermotoga maritima*." Appl Microbiol Biotechnol **74**(3): 585-591.

Kamal, M. Z., S. Ahmad, et al. (2011). "In vitro evolved non-aggregating and thermostable lipase: structural and thermodynamic investigation." J Mol Biol **413**(3): 726-741.

Kamal, M. Z., T. A. Mohammad, et al. (2012). "Role of active site rigidity in activity: MD simulation and fluorescence study on a lipase mutant." PLoS One **7**(4): e35188.

Kane, M. D., L. K. Poulsen, et al. (1993). "Monitoring the Enrichment and Isolation of Sulfate-Reducing Bacteria by Using Oligonucleotide Hybridization Probes Designed from Environmentally Derived 16S Ribosomal-RNA Sequences." Appl Environ Microbiol **59**(3): 682-686.

Kazlauskas, R. J. (2006). Quantitative Assay of Hydrolases for Activity and Selectivity Using Color Changes. Enzyme-Assays: High-throughput Screening, Genetic Selection and Fingerprinting. J. L. Reymond. Weinheim, WILEY-VCH Verlag GmbH & Co. KGaA**:** 16-39.

Kim, Y. H., E. J. Kwon, et al. (2010). "Molecular cloning and characterization of a novel family VIII alkaline esterase from a compost metagenomic library." Biochem Biophys Res Commun **393**(1): 45-49.

Kim, Y. J., G. S. Choi, et al. (2006). "Screening and characterization of a novel esterase from a metagenomic library." Protein Expr Purif **45**(2): 315-323.

Kirk, O., T. V. Borchert, et al. (2002). "Industrial enzyme applications." Curr Opin Biotechnol **13**(4): 345-351.

Klibanov, A. M. (2001). "Improving enzymes by using them in organic solvents." Nature **409**(6817): 241-246.

Knietsch, A., T. Waschkowitz, et al. (2003). "Construction and screening of metagenomic libraries derived from enrichment cultures: generation of a gene bank for genes conferring alcohol oxidoreductase activity on *Escherichia coli*." Appl Environ Microbiol **69**(3): 1408-1416.

Kobayashi, S. (2010). "Lipase-catalyzed polyester synthesis-a green polymer chemistry." Proc Jpn Acad Ser B Phys Biol Sci **86**(4): 338-365.

Kobayashi, T. (2011). "Lipase-catalyzed syntheses of sugar esters in non-aqueous media." Biotechnol Lett **33**(10): 1911-1919.

Koeller, K. M. and C. H. Wong (2001). "Enzymes for chemical synthesis." Nature **409**(6817): 232-240.

Kourist, R. and U. T. Bornscheuer (2011). "Biocatalytic synthesis of optically active tertiary alcohols." Appl Microbiol Biotechnol **91**(3): 505-517.

Kovach, M. E., P. H. Elzer, et al. (1995). "Four new derivatives of the broad-host-range cloning vector pBBR1MCS, carrying different antibiotic-resistance cassettes." Gene **166**(1): 175-176.

Kragl, U., M. Eckstein, et al. (2002). "Enzyme catalysis in ionic liquids." Curr Opin Biotechnol **13**(6): 565-571.

Kroutil, W., A. Kleewein, et al. (1997). "A computer program for analysis, simulation and optimization of asymmetric catalytic processes proceeding through two consecutive steps. Type 2: sequential kinetic resolutions." Tetrahedron-Asymmetry **8**(19): 3263-3274.

Laemmli, U. K. (1970). "Cleavage of structural proteins during the assembly of the head of bacteriophage T4." Nature **227**(5259): 680-685.

Lai, K. K., G. L. Lorca, et al. (2009). "Biochemical properties of two cinnamoyl esterases purified from a *Lactobacillus johnsonii* strain isolated from stool samples of diabetes-resistant rats." Appl Environ Microbiol **75**(15): 5018-5024.

Lai, K. K., P. J. Stogios, et al. (2011). "An inserted alpha/beta subdomain shapes the catalytic pocket of *Lactobacillus johnsonii* cinnamoyl esterase." PLoS One **6**(8): e23269.

Lane, D. J., B. Pace, et al. (1985). "Rapid-Determination of 16S Ribosomal-RNA Sequences for Phylogenetic Analyses. " Proc Natl Acad Sci U S A **82**(20): 6955-6959.

Laumen, K., D. Breitgoff, et al. (1988). "Enzymic Preparation of Enantiomerically Pure Secondary Alcohols - Ester Synthesis by Irreversible Acyl Transfer Using a Highly Selective Ester Hydrolase from Pseudomonas Sp - an Attractive Alternative to Ester Hydrolysis." J Chem Soc Chem Commun (22): 1459-1461.

Lee, M. H., K. S. Hong, et al. (2010). "A new esterase EstD2 isolated from plant rhizosphere soil metagenome." Appl Microbiol Biotechnol **88**(5): 1125-1134.

Lee, M. H., C. H. Lee, et al. (2006). "Isolation and characterization of a novel lipase from a metagenomic library of tidal flat sediments: evidence for a new family of bacterial lipases." Appl Environ Microbiol **72**(11): 7406-7409.

Lee, S. G., S. P. Hong, et al. (1997). "Thermostable tyrosine phenol-lyase of *Symbiobacterium* sp. SC-1: gene cloning, sequence determination, and overproduction in *Escherichia coli*." Protein Expr Purif **11**(3): 263-270.

Lee, S. W., K. Won, et al. (2004). "Screening for novel lipolytic enzymes from uncultured soil microorganisms." Appl Microbiol Biotechnol **65**(6): 720-726.

Leveque, E., B. Haye, et al. (2000). "Cloning and expression of an alpha-amylase encoding gene from the hyperthermophilic archaebacterium *Thermococcus hydrothermalis* and biochemical characterisation of the recombinant enzyme." FEMS Microbiol Lett **186**(1): 67-71.

Levisson, M., J. van der Oost, et al. (2009). "Carboxylic ester hydrolases from hyperthermophiles." Extremophiles **13**(4): 567-581.

Li, D., M. Rothballer, et al. (2011). "*Acidovorax radicis* sp. nov., a wheat-root-colonizing bacterium." Int J Syst Evol Microbiol **61**(Pt 11): 2589-2594.

Liebeton, K., A. Zonta, et al. (2000). "Directed evolution of an enantioselective lipase." Chem Biol **7**(9): 709-718.

Liu, K., J. Wang, et al. (2009). "Isolation and biochemical characterization of two lipases from a metagenomic library of China Holstein cow rumen." Biochem Biophys Res Commun **385**(4): 605-611.

Liu, P., Y. F. Wang, et al. (2004). "Covalent reaction intermediate revealed in crystal structure of the *Geobacillus stearothermophilus* carboxylesterase Est30." J Mol Biol **342**(2): 551-561.

Lopez-Lopez, O., P. Fucinos, et al. (2010). "Heterologous expression of an esterase from *Thermus thermophilus* HB27 in *Saccharomyces cerevisiae*." J Biotechnol **145**(3): 226-232.

Manco, G., E. Giosue, et al. (2000). "Cloning, overexpression, and properties of a new thermophilic and thermostable esterase with sequence similarity to hormone-sensitive lipase subfamily from the archaeon *Archaeoglobus fulgidus*." Arch Biochem Biophys **373**(1): 182-192.

Marchant, R., I. M. Banat, et al. (2002). "The frequency and characteristics of highly thermophilic bacteria in cool soil environments." Environ Microbiol **4**(10): 595-602.

Marchant, R., A. Franzetti, et al. (2008). "Thermophilic bacteria in cool temperate soils: are they metabolically active or continually added by global atmospheric transport?"Appl Microbiol Biotechnol **78**(5): 841-852.

Martinelle, M., M. Holmquist, et al. (1995). "On the Interfacial Activation of *Candida antarctica* Lipase-A and Lipase-B as Compared with *Humicola lanuginosa* Lipase." Biochim Biophys Acta **1258**(3): 272-276.

Matthews, B. W. (1968). "Solvent Content of Protein Crystals." J Mol Biol **33**(2): 491-&.

McKenney, D., K. E. Brown, et al. (1995). "Influence of *Pseudomonas aeruginosa* exoproducts on virulence factor production in *Burkholderia cepacia*: evidence of interspecies communication." J Bacteriol **177**(23): 6989-6992.

Meier, T. (2009). Konstruktion von Metagenombanken aus ex-situ Kulturen von hydrothermalen Tiefseequellen. Diploma thesis, University of Hamburg, Germany.

Meilleur, C., J. F. Hupe, et al. (2009). "Isolation and characterization of a new alkali-thermostable lipase cloned from a metagenomic library." J Ind Microbiol Biotechnol **36**(6): 853-861.

Mitsuda, S., T. Umemura, et al. (1988). "Preparation of an Optically Pure Secondary Alcohol of Synthetic Pyrethroids Using Microbial Lipases." Appl Microbiol Biotechnol **29**(4): 310-315.

Mrabet, N. T., A. Vandenbroeck, et al. (1992). "Arginine Residues as Stabilizing Elements in Proteins." Biochemistry **31**(8): 2239-2253.

Muller, J. J., M. Neumann, et al. (2010). "Online Monitoring of Biotransformations in High Viscous Multiphase Systems by Means of FT-IR and Chemometrics." Anal Chem **82**(14): 6008-6014.

Murshudov, G. N., A. A. Vagin, et al. (1997). "Refinement of macromolecular structures by the maximum-likelihood method." Acta Crystallogr D Biol Crystallogr **53**(Pt 3): 240-255.

Musidlowska-Persson, A. and U. T. Bornscheuer (2002). "Substrate specificity of the γ-isoenzyme of recombinant pig liver esterase towards acetates of secondary alcohols." J Mol Catal B Enzym **19–20**(0): 129-133.

Musidlowska, A., S. Lange, et al. (2001). "By Overexpression in the Yeast *Pichia pastoris* to Enhanced Enantioselectivity: New Aspects in the Application of Pig Liver Esterase." Angew Chem Int Ed Engl **40**(15): 2851-2853.

Nacke, H., C. Will, et al. (2011). "Identification of novel lipolytic genes and gene families by screening of metagenomic libraries derived from soil samples of the German Biodiversity Exploratories." FEMS Microbiol Ecol **78**(1): 188-201.

Nardini, M., D. A. Lang, et al. (2000). "Crystal structure of *Pseudomonas aeruginosa* lipase in the open conformation. The prototype for family I.1 of bacterial lipases." J Biol Chem **275**(40): 31219-31225.

Nguyen, L. N., J. Bormann, et al. (2011). "Autophagy-related lipase FgATG15 of *Fusarium graminearum* is important for lipid turnover and plant infection." Fungal Genet Biol **48**(3): 217-224.

Nielsen, H., J. Engelbrecht, et al. (1997). "A neural network method for identification of prokaryotic and eukaryotic signal peptides and prediction of their cleavage sites." Int J Neural Syst **8**(5-6): 581-599.

Notredame, C., D. G. Higgins, et al. (2000). "T-Coffee: A novel method for fast and accurate multiple sequence alignment." J Mol Biol **302**(1): 205-217.

Ogawa, M., M. Kitagawa, et al. (2006). "A beta-N-acetylhexosaminidase from *Symbiobacterium thermophilum*; gene cloning, overexpression, purification and characterization." Enzyme Microb Technol **38**(3-4): 457-464.

Ogino, H., S. Inoue, et al. (2008). "Refolding of a recombinant organic solvent-stable lipase, which is overexpressed and forms an inclusion body, and activation with lipase-specific foldase." Biochem Eng J **40**(3): 507-511.

Ohno, M., H. Shiratori, et al. (2000). "*Symbiobacterium thermophilum* gen. nov., sp nov., a symbiotic thermophile that depends on co-culture with a *Bacillus* strain for growth." Int J Syst Evol Microbiol **50**: 1829-1832.

Ollis, D. L., E. Cheah, et al. (1992). "The alpha/beta hydrolase fold." Protein Eng **5**(3): 197-211.

Owusu, R. K. and D. A. Cowan (1989). "Correlation between Microbial Protein Thermostability and Resistance to Denaturation in Aqueous-Organic Solvent 2-Phase Systems." Enzyme Microb Technol **11**(9): 568-574.

Panda, T. and B. S. Gowrishankar (2005). "Production and applications of esterases." Appl Microbiol Biotechnol **67**(2): 160-169.

Peng, Q., X. Zhang, et al. (2011). "A novel esterase gene cloned from a metagenomic library from neritic sediments of the South China Sea." Microb Cell Fact **10**: 95.

Pfennig, N. and K. D. Lippert (1966). "Über das Vitamin B_{12}-Bedürfnis phototropher Schwefelbakterien." Arch Microbiol **55**(3): 245-256.

Pleiss, J., M. Fischer, et al. (2000). "Lipase engineering database - Understanding and exploiting sequence-structure-function relationships." J Mol Catal B Enzym **10**(5): 491-508.

Pleiss, J., M. Fischer, et al. (1998). "Anatomy of lipase binding sites: the scissile fatty acid binding site." Chem Phys Lipids **93**(1-2): 67-80.

Quyen, D. T., C. Schmidt-Dannert, et al. (2003). "High-level expression of a lipase from *Bacillus thermocatenulatus* BTL2 in *Pichia pastoris* and some properties of the recombinant lipase." Protein Expr Purif **28**(1): 102-110.

Radestock, S. and H. Gohlke (2011). "Protein rigidity and thermophilic adaptation." Proteins **79**(4): 1089-1108.

Reddy, G. S., G. I. Matsumoto, et al. (2004). "Psychrophilic pseudomonads from Antarctica: *Pseudomonas antarctica* sp. nov., *Pseudomonas meridiana* sp. nov. and *Pseudomonas proteolytica* sp. nov." Int J Syst Evol Microbiol **54**(Pt 3): 713-719.

Reetz, M. T. (2002). "Lipases as practical biocatalysts." Curr Opin Chem Biol **6**(2): 145-150.

Reetz, M. T., K. M. Kuhling, et al. (2000). "Circular dichroism as a detection method in the screening of enantioselective catalysts." Chirality **12**(5-6): 479-482.

Reyes-Duarte, D., M. Ferrer, et al. (2012). "Functional-based screening methods for lipases, esterases, and phospholipases in metagenomic libraries." Methods Mol Biol **861**: 101-113.

Rhee, J. K., D. G. Ahn, et al. (2005). "New thermophilic and thermostable esterase with sequence similarity to the hormone-sensitive lipase family, cloned from a metagenomic library." Appl Environ Microbiol **71**(2): 817-825.

Riesenfeld, C. S., P. D. Schloss, et al. (2004). "Metagenomics: genomic analysis of microbial communities." Annu Rev Genet **38**: 525-552.

Robles-Medina, A., P. A. Gonzalez-Moreno, et al. (2009). "Biocatalysis: towards ever greener biodiesel production." Biotechnol Adv **27**(4): 398-408.

Rocha, S. N., J. Abrahao-Neto, et al. (2011). "Heterologous expression of a thermophilic esterase in *Kluyveromyces* yeasts." Appl Microbiol Biotechnol **89**(2): 375-385.

Ronaghi, M., M. Uhlen, et al. (1998). "A sequencing method based on real-time pyrophosphate." Science **281**(5375): 363, 365.

Rosenau, F. and K. Jaeger (2000). "Bacterial lipases from *Pseudomonas*: regulation of gene expression and mechanisms of secretion." Biochimie **82**(11): 1023-1032.

Rosenau, F. and K. E. Jaeger (2004). Overexpression and secretion of biocatalysts in *Pseudomonas*. Enzyme functionality. A. Svendsen. New York, Basel, Marcel Dekker Inc.**:** 617-631.

Rosenau, F., J. Tommassen, et al. (2004). "Lipase-specific foldases." Chembiochem**5**(2): 152-161.

Royter, M., M. Schmidt, et al. (2009). "Thermostable lipases from the extreme thermophilic anaerobic bacteria *Thermoanaerobacter thermohydrosulfuricus* SOL1 and *Caldanaerobacter subterraneus* subsp. tengcongensis." Extremophiles**13**(5): 769-783.

Sako, Y., K. Takai, et al. (1996). "*Rhodothermus obamensis* sp. nov., a modern lineage of extremely thermophilic marine bacteria." Int J Syst Bacteriol **46**(4): 1099-1104.

Salameh, M. A. and J. Wiegel (2007). "Purification and characterization of two highly thermophilic alkaline lipases from *Thermosyntropha lipolytica*." Appl Environ Microbiol **73**(23): 7725-7731.

Salvadori, P., C. Bertucci, et al. (1991). "Circular-Dichroism Detection in HPLC." Chirality **3**(4): 376-385.

Sambrook, J., D.W. Russel, Ed. (2001). Molecular cloning, a laboratory manual. New York, USA, Cold Spring Harbor Laboratory Press.

Sanger, F., S. Nicklen, et al. (1977). "DNA sequencing with chain-terminating inhibitors." Proc Natl Acad Sci U S A **74**(12): 5463-5467.

Santangelo, T. J., L. Cubonova, et al. (2008). "Shuttle vector expression in *Thermococcus kodakaraensis*: Contributions of cis elements to protein synthesis in a hyperthermophilic archaeon." Appl Environ Microbiol **74**(10): 3099-3104.

Sarda, L. and P. Desnuelle (1958). "[Actions of pancreatic lipase on esters in emulsions]." Biochim Biophys Acta **30**(3): 513-521.

Schalk-Hihi, C., C. Schubert, et al. (2011). "Crystal structure of a soluble form of human monoglyceride lipase in complex with an inhibitor at 1.35 A resolution." Protein Sci **20**(4): 670-683.

Schmeisser, C. (2004). Metagenomanalyse eines Multispezies-Biofilms: Biochemische Charakterisierung und Kristallisierung der ersten multimeren Esterase aus einem bisher nicht kultivierten Mikroorganismus. Doctoral Thesis, Georg-August-University Goettingen, Germany.

Schmeisser, C., H. Steele, et al. (2007). "Metagenomics, biotechnology with non-culturable microbes." Appl Microbiol Biotechnol **75**(5): 955-962.

Schmeisser, C., C. Stockigt, et al. (2003). "Metagenome survey of biofilms in drinking-water networks." Appl Environ Microbiol **69**(12): 7298-7309.

Schmidt, O., H. L. Drake, et al. (2010). "Hitherto unknown [Fe-Fe]-hydrogenase gene diversity in anaerobes and anoxic enrichments from a moderately acidic fen." Appl Environ Microbiol **76**(6): 2027-2031.

Seed, B., Parker, R.C. and Davidson, N. (1982). "Representation of DNA sequences in recombinant DNA libraries prepared by restriction enzyme partial digestion". Gene **19**, 201-209.

Sharma, P. K., K. Singh, et al. (2012). "Characterization of a thermostable lipase showing loss of secondary structure at ambient temperature." Mol Biol Rep **39**(3): 2795-2804.

Sigurgisladottir, S., M. Konraosdottir, et al. (1993). "Lipase Activity of Thermophilic Bacteria from Icelandic Hot-Springs." Biotechnol Lett **15**(4): 361-366.

Simon, C. and R. Daniel (2011). "Metagenomic analyses: past and future trends." Appl Environ Microbiol **77**(4): 1153-1161.

Soetaert, W. and E. Vandamme (2006). "The impact of industrial biotechnology." Biotechnol J **1**(7-8): 756-769.

Staley, J. T. and A. Konopka (1985). "Measurement of in Situ Activities of Nonphotosynthetic Microorganisms in Aquatic and Terrestrial Habitats." Annu Rev Microbiol 39(1): 321-346.

Steele, H. L., K. E. Jaeger, et al. (2009). "Advances in recovery of novel biocatalysts from metagenomes." J Mol Microbiol Biotechnol **16**(1-2): 25-37.

Streit, W. R. and R. A. Schmitz (2004). "Metagenomics-the key to the uncultured microbes." Curr Opin Microbiol **7**(5): 492-498.

Suzuki, S., S. Horinouchi, et al. (1988). "Growth of a Tryptophanase-Producing Thermophile, *Symbiobacterium thermophilum* Gen-Nov, Sp-Nov, Is Dependent on Co-Culture with a *Bacillus* sp." J Gen Microbiol **134**: 2353-2362.

Tamir-Ariel, D., T. Rosenberg, et al. (2011). "The *Xanthomonas campestris* pv. vesicatoria citH gene is expressed early in the infection process of tomato and is positively regulated by the TctDE two-component regulatory system." Mol Plant Pathol **12**(1): 57-71.

Tatusov, R. L., N. D. Fedorova, et al. (2003). "The COG database: an updated version includes eukaryotes." BMC Bioinformatics **4**: 41.

Taylor, A. L. and C. D. Trotter (1972). "Linkage Map of *Escherichia coli* Strain K-12." Bacteriol Rev **36**(4): 504-524.

Tebbe, C. C. and W. Vahjen (1993). "Interference of humic acids and DNA extracted directly from soil in detection and transformation of recombinant DNA from bacteria and a yeast." Appl Environ Microbiol **59**(8): 2657-2665.

Tenreiro, S., M. F. Nobre, et al. (1995). "DNA:DNA hybridization and chemotaxonomic studies of *Thermus scotoductus*." Res Microbiol **146**(4): 315-324.

Terpe, K. (2006). "Overview of bacterial expression systems for heterologous protein production: from molecular and biochemical fundamentals to commercial systems." Appl Microbiol Biotechnol **72**(2): 211-222.

Thum, O. and K. M. Oxenbell (2008). "Biocatalysis – A Sustainable Method for the Production of Emollient Esters." SÖFW-Journal **134**(44-47).

Tirawongsaroj, P., R. Sriprang, et al. (2008). "Novel thermophilic and thermostable lipolytic enzymes from a Thailand hot spring metagenomic library." J Biotechnol **133**(1): 42-49.

Torres, P., D. Reyes-Duarte, et al. (2012). Lipase-Catalyzed Modifi cation of Phenolic Antioxidants. Lipases and Phospholipases: Methods and Protocols, Methods in Molecular Biology. G. Sandoval. New York, Springer Science+Business Media. **861:** 435-443.

Torsvik, V., J. Goksoyr, et al. (1990). "High diversity in DNA of soil bacteria." Appl Environ Microbiol **56**(3): 782-787.

Towbin, H., T. Staehelin, et al. (1979). "Electrophoretic transfer of proteins from polyacrylamide gels to nitrocellulose sheets: procedure and some applications." Proc Natl Acad Sci U S A **76**(9): 4350-4354.

Trodler, P. and J. Pleiss (2008). "Modeling structure and flexibility of *Candida antarctica* lipase B in organic solvents." BMC Struct Biol **8**: 9.

Tsai, S. W., J. J. Lin, et al. (1997). "Enzymatic synthesis of (*S*)-ibuprofen ester prodrug from racemic ibuprofen by lipase in organic solvents." Biotechnol Prog **13**(1): 82-88.

Ueda, K., A. Yamashita, et al. (2004). "Genome sequence of *Symbiobacterium thermophilum*, an uncultivable bacterium that depends on microbial commensalism." Nucleic Acids Res **32**(16): 4937-4944.

Vagin, A. and A. Teplyakov (1997). "MOLREP: an automated program for molecular replacement." J Appl Crystallogr **30**: 1022-1025.

Venter, J. C., K. Remington, et al. (2004). "Environmental genome shotgun sequencing of the Sargasso Sea." Science **304**(5667): 66-74.

Verger, R. (1997). "'Interfacial activation' of lipases: Facts and artifacts." Trends Biotechnol **15**(1): 32-38.

Vieille, C. and G. J. Zeikus (2001). "Hyperthermophilic enzymes: sources, uses, and molecular mechanisms for thermostability." Microbiol Mol Biol Rev **65**(1): 1-43.

Voget, S., C. Leggewie, et al. (2003). "Prospecting for novel biocatalysts in a soil metagenome." Appl Environ Microbiol **69**(10): 6235-6242.

Wilhelm, S., A. Gdynia, et al. (2007). "The autotransporter esterase EstA of *Pseudomonas aeruginosa* is required for rhamnolipid production, cell motility, and biofilm formation." J Bacteriol **189**(18): 6695-6703.

Xu, T. W., J. H. Xu, et al. (2006). "Investigating pH and Cu (II) effects on lipase activity and enantioselectivity via kinetic and spectroscopic methods." Biotechnol J **1**(11): 1293-1301.

Yu, E. Y., M. A. Kwon, et al. (2011). "Isolation and characterization of cold-active family VIII esterases from an arctic soil metagenome." Appl Microbiol Biotechnol **90**(2): 573-581.

Yun, S. H., C. W. Choi, et al. (2011). "Enrichment and proteome analysis of a hyperthermostable protein set of archaeon *Thermococcus onnurineus* NA1." Extremophiles **15**(4): 451-461.

Zhang, Y. Q., S. X. Ren, et al. (2003). "Genome-based analysis of virulence genes in a non-biofilm-forming *Staphylococcus epidermidis* strain (ATCC 12228)." Mol Microbiol **49**(6): 1577-1593.

7 Appendix

7.1 Sequences of esterase/lipase-coding ORFs and their respective primer sequences

7.1.1 pCos5E5 from a metagenomic library constructed with DNA from a biofilm growing on a valve of a water pipeline

>est1 (=*est5E5*)

ATGGTCGCTAGGGCGCAGGTGCGCGCAGATGCTGCGTTACATCCGCCGACATAGCCCACATGAGAGAGGATTGC
GACCATGAAGTACTTTCGCCTGACCTGTATCGCCGCCGTAGCGGCACTGCTCGCCGCTTGCGGAGGCTCCGACGA
CGCCGGACGCGGCGACCTGGTGGAGCTCCCCGTCACCCTGACCACTTTGACGGCCGACCAGATCGATGCGGGCA
CCACGTCCAGCGGCCTCAGGGCCCTTGCCGGCAAGGCACGGTGCGACGTGAAGGTCGTGGCGCTCAACTACTCA
CGGCAGGCGCCAAGGCCGGCGAACTCACCAACGCCTCGGGCGTGATGCTGGTGCCCGCAGGCAGCTGCAACGGC
GAGAAGGCTGCCCTGCTGGCCTATGCCAAGGGCACCGATGTGCAGAAGCCCCGCACCCTGGCCAACCCGCAGGA
CAGCGAGACCTTCCTGCTGGCCGCCATGTACGCCTCGCAGGGCTATGCCGTGGTCGCCACCGACTACCTCGGGTTT
GCCAAGTCGGGCTACAGCTACCACCCCTACCTGCACGCCGATTCGGAAGCCACCTCGGTGATCGATTCGGTGCGC
GCCGCACGCAAGGTCGCCGGCTCGGTAGGAGCCAACCTGTCGGGCAGGATCCTGTTCACCGGCTACTCGCAGGG
CGGACATGCCTCGATGGCCGCGCACCGTGCCGCCGAGCGCGACTACGGCAACGAATTTGACGTGGCGGCCGGC
GCCCACCTGGCAGGGCCCTACAACCTTTCGGGCTCGCTGCGCATTCCGGACGCGATCGCGGGCGTGCAGTTCTTC
GTGCCCTACCTCGTGACGGCCTGGCAGAAGGTCTACGGCAACATCTATTCCGATGTGAAGCAGGCCTTCAAGGCA
CCGTACTCCAACTATATCGAGACGCTGCTGCCCAACCCGACGATGAACTACACCACGCTGGTGACCTCGGGCACG
CTGCCGGGCGGCACGCCCAACCAGGCACGCGATGCGCTGTTCCAGCCGGCCTTCCTCGCCAGCAGCCAGACGAA
CGTGAACGACCCGCTCTACCTGGCCGCCCAGAAGAACGACCTCCTGGGCTGGACGCCCAAGTCGCGCGTGCTGCT
GTGCGGTGGCTCGGGCGACCCCACGGTGCCGCCTGCCGTGCACCAGCGCGTGATGGCCGCCGATTTCGCGGCCC
GCGGCGTGACCAACGTGATCTCGGTGGATGTGGACGGGCCCATCCAGGCCACCTTCGGCCCCGGCGGCGCAGCG
CCCACCGACCCGACTTCTGCAGCCTTTGCCACCTACTACGGCGCCTACCATGGCACCTATGAGCCACCGTTCTGCC
ATGCCCAGGCACGCGCCGCCTTCGACATCATCGTGAAGTAA

Primer *est1* for/rev see Table 5

>est2

ATGGCAGAACGGTGGCTCATAGGTGCCATGGTAGGCGCCGTAGTAGGTGGCAAAGGCTGCAGAAGTCGGGT CG
GTGGGCGCTGCGCCGCCGGGGCCGAAGGTGGCCTGGATGGGCCCGTCCACATCCACCGAGATCACGTTGGTC AC
GCCGCGGGCCGCGAAATCGGCGGCCATCACGCGCTGGTGCACGGCAGGCGGCACCGTGGGGTCGCCCGAGCCA
CCGCACAGCAGCACGCGCGACTTGGGCGTCCAGCCCAGGAGGTCGTTCTTCTGGGCGGCCAGGTAGAGCGGGTC
GTTCACGTTCGTCTGGCTGCTGGCGAGGAAGGCCGGCTGGAACAGCGCATCGCGTGCCTGGTTGGGCGTGCCGC
CCGGCAGCGTGCCCGAGGTCACCAGCGTGGTGTAGTTCATCGTCGGGTTGGGCAGCAGCGTCTCGATATAGTTG
GAGTACGGTGCCTTGAAGGCCTGCTTCACATCGGAATAGATGTTGCCGTAGACCTTCTGCCAGGCCGTCACGAGG
TAGGGCACGAAGAACTGCACGCCCGCGATCGCGTCCGGAATGCGCAGCGAGCCCGAAAGGTTGTAGGGCCCTGC
CAGGTGGGCGCCGGCCGCCACGTCAAATTCGTTGCCGTAGTCGCGCTCGGCGGCACGGTGCGCGGCCATCGAGG
CATGTCCGCCCTGCGAGTAGCCGGTGAACAGGATCCTGCCCGACAGGTTGGCTCCTACCGAGCCGGCGACCTTGC
GTGCGGCGCGCACCGAATCGATCACCGAGGTGGCTTCCGAATCGGCGTGCAGGTAGGGGTGGTAGCTGTAGCCC
GACTTGGCAAACCCGAGGTAGTCGGTGGCGACCACGGCATAGCCCTGCGAGGCGTACATGGCGGCCAGCAGGA
AGGTCTCGCTGTCCTGCGGGTTGGCCAGGGTGCGGGGCTTCTGCACATCGGTGCCCTTGGCATAGGCCAGCAGG
GCAGCCTTCTCGCCGTTGCAGCTGCCTGCGGGCACCAGCATCACGCCCGAGGCGTTGGTGAGTTCGCCGGCCTTG
GCGCCTGCCGTGTAGTAGTTGAGCGCCACGACCTTCACGTCGCACCGTGCCTTGCCGGCAAGGGCCCTGAGGCC
GCTGGACGTGGTGCCCGCATCGATCTGGTCGGCCGTCAAAGTGGTCAGGGTGACGGGGAGCTCCACCAGGTCGC
CGCGTCCGGCGTCGTCGGAGCCTCCGCAAGCGGCGAGCAGTGCCGCTACGGCGGCGATACAGGTCAGGCGAAA
GTACTTCATGGTCGCAATCCTCTCTCTATGTGGGCTATGTCGGCGGATGGTAACGCAGCATCGTGCGCGCACCTG
CGCCCTAGCGACCATTAG

Primer *est2* for CATATGGCAGAACGGTGGCTCATAG;
Primer *est2* rev AAGCTTATGGTCGCTAGGGCGCAGGTGC

>est3

ATGGTTGTTGCAAAAAAGCACGGTCGTGCTTTTTGTAATCTTCTTTCCTGGAGAACTCCCTTGAACACAAGACAAT
GCAAGACCGCCCTTTCGGTGCTGGCAACGGCCTGCCTGCTCGCAGCATGCGGTGGTGGCGGCTCGGACACCGCC
CCTGCGGCGCCCGTGGCCTCGGTGAAAGTGGCTGGCGACAGCCTGGCCGACAGCGGCACCTTCGGCTACAAATT
CACCGTGCAGGGCACGGCCGCCACCGGCGCCGGATCAACGCCGATCTGGCCCGAGCGCGTGGCCACCAGCTATG
GCCAGTCGCTGTGCGCACACTACGTCTTCAACGGCACGGCGTTTTCCGCCAATGCCGCCTGCTCGAACTATGCCGT
GGGCGGCGGGCGGATCAACAACTTCACGGCGCCCACCTCGCCCGTGTCCATCACCCAGCAGCTCAAGGACCTGG
GCAACGGCGGCTACACCGCCTCGGACCTGGTGCTGGTCGACGGGGGCGGCAACGATGCGGCGGACCTGGTAGG
CGCCTACCTCCGGGCGGCTACCGACAATGGCCAGGCCTATGCAGCCGTGCTGGGCTCGGTGCTGCCTGCGGCCA
CGGTCAACGCCGCCCTGGCGGGTGGTGCCGCAGGCCAGGCCCAGGTGGGTGGCGCCTACATGCAGGCGCTGGC
ACAGCAGTTCGCGGCCACCATCAAGGCCAACACGGTCGCCAAGGGCGCTCCCCGCGTGGCCGTGCTGAATGCCC
CCGGCATCACCCGCACTCCCCGCTTCCTGATGGTGCTGGCCTCGATCTCCGCCCAGCGCGGTGCCGAGGCCGCCA
AGCAGGCCGAGGCCCTGTTCGACGGCTGGGTCCAGGCCTTCAACGCGCAACTGGCCACAGCCTGGCCGGTGACG
AGCGCATCGTGGTGGTGGACTTCTACACATCTTTCAAGGACCAGTCGACCAACCCGGCCCAGTACCAGCTCACCA
ACGCCACCACGCCAGCCTGCCCGGCCACGGGCGTGGGCAGCGATGGCCTGCCGACCTACAGCTTCCCCACCTGC
ACGGCCGCAGCCCTCTCGGCCATGGCGCCACCTGCGGGTGCCCCCGGCGGTGCGGACTGGTGGAAGAGCTATGG
CTTCTCCGACAGCTTCCACCCCACGCCCTATGGCCACCAACTGGTCGGGCAGTTGGTGTCGCGTTCGCTGTCCCGG
GCGGGCTGGCTGTGA

Primer *est3* for CATATGGTTGTTGCAAAAAAGCACGGTCGTG

Primer *est3* rev AAGCTTCCAGCCCGCCCGGGACAGCGAAC

7.1.2 *Thermococcales* consortium

*>est71G8*_1 (1.5 kb)

ATGGACGTTAAGAGGGCCCTTGCAATAATAGTTGCACTTCTCGCCCTCGCGGCGGTTTTATCGGCTCCAGTTAGG
GCAGAGACCTCAGTGATACCGGGAGAGATAATACTGAGACCCCTCCCGGGTGTTCCGGCAATAGGTCTCCCCGG
GGACACAATAGAGGTGCAGCCGGCAGAAGGAGTCACGATCCAGGAGTTGCAGATAGTATCGATACTCCACGGTC
CGTACGACCTTAAGATACTGGGAACCGAAGACGGTGTCGTCAAGGCAAAGATACCCGAGGAGGCGGCTCCGGAC
GTTTATTTCCTAATCGTGAAGAGCGACAAGGGAGAAGTGACAATTCCAAACGGCGTCTGGGTAATGAAAGAGGC
ACCAAAGGTTCTCAAGATCGCCCATGGAAGCGATTTCCACGTGACGAGCGGCTCGAAGATGGGCTTCGTCTGTGG
GGAGTACTTCCAGAAGAGCATCCCCGAGATACTCAAGTACTGCGACGACCCGATACCAATGCACAGCTACACCGC
CACTGACAGCTTCATGACGTACTACGCGATGGTCGACAGCGGTGAGGTAAACCTGATGGTAAGCACCGGCGACG
ACGTTGACACCAACGGTGACAAGAAGGGTTACCAGCTCTTCGATCTGGCAATCCTCCATGGAACCGCCGCCGGAA
TGCCCTTCATAGGCATCAAGGGCAACCACGACCACCCGCCGACCTACTACTCGAAGTACGTTGGCCCCAGGTACTT
CTACGAGGTCATCGGGAACTTCCTCATCATCGGTCTTGACAGCCGCGGTGAGGAGAGGCATCCCGAGATGGAGC
AGCTCCAATGGATGGAGGATGTCCTTAAATCCCACCCGAACAAGACGGTCATAGTCCTGGTTCACCACCCCTTCT
GGTACAAAACCGACGAGGGGAAGTACGGCACCATAAAGGGCTACACTGCCTTTGACGACAACGACTGGAGCGCC
CTCATGAAGTATGTAAGCTGGGACTGGGCCGGCAGAGATGGCCAGTACCAGGACATAGCCAGGTACTTCCTCCAG
CTCGTCGAGAAGTACAACGTCAGGCTCATCCTGGCGGGCCACATACACCACGACAAGCCGATACTGTACATCGA
CAAGGACGGGAACGAGCACTGGTTCTACACTCTAACCACCACGGGAGCGCCGGACAAGACCAGCAACCCTCCG
AGTAAGGCGGATATCCAAAAGGGCTACAAGATCCCAAGCTGGTACGGTTCCCAAGTCATATACGTCTACCCAAA
CGGGACTGTAAGCTTCCCTGAGATAGACGATGTCCTCCGCCCGGGAATAAGCTCCCTGCCGGTTCCACAGAAGT
TCGTCGTCCTCAGGCAGAACGGTGAGGATGGAACCGCCGTTCACTTCTTCAACAACCTCGGCAAGGCCGTCAGCG
GCCCTCTCGTGGTTCGGATACCCGAAGGCGCCAAGGTGGACCCCGACGCGACCACCATAA

Primer *est71G8*_1 (1.5 kb) for CATATGGACGTTAAGAGGGCCCTTGCA

Primer *est71G8*_1 (1.5 kb) rev GGATCCGTGGT CGCGTCGGGGTCCACC

*>est71G8*_1 (0.6 kb)

ATGCCGTTTAAACTGCCTATCTTTCGGAAAAGGGTCCTTGAAGTGCTCGCTTCCTCCGATGAGACCAAGGTCATGC
ACGTAAGCGACACTCCCGAGAGTGTCTACCGCTTCATCGATGAGCTCATAGAAAAAACCCGACCCGATTACGTTA
TCCATACCGGCGACCTGGCCGACAACGTAAAGCTGGAGAGACGGCCCGAACTAAGACCCCGCTACCAGGGCGC
AATAAGGAGGCTCGCCCACGTCCTCAAGGGCTACGGGGTGAAACTCTACGTCGTTCCGGGAAACGAGGACGACC
CGGAGCTGGTCAGGGAGTTCTTTAGGAAGGCCGTTGTCGATCCCGGGACAGTCGTGGAGATAGAGGGGAAGA
GGTTCGCCCTCGGTCACACCTGGAGGGACGTCCTTGAACTCGATGCGGATTTTAAGCTCTATGGCCATAACTTCAA
GCTCATCGAAAAGGGCCTGAACGGCGTTCTCGGCGTAAACTTTGTGCTCCTTCCGAGCGGGAGGACGTACAAGG
TAAAGTATCCCGGAGGGACGGATTTCGACAGGGGATATAAGATGTGGAGGGGTATGTGA

Primer *est71G8*_2 (0.6 kb) for CATATGCCGTTTAAACTGCCTATCTTTCGG

Primer *est71G8*_2 (0.6 kb) rev CTCGAGCATACCCCTCCACATCTTATATC

>est73E12

ATGCTGATAGGTATAATGAGCGATACCCATGACAACCTGCCGGCCATCTCCAAGGCGGTTGAGCTGTTCAACGGG
AGGAACGTTGAGCTTGTAATCCACGCGGGTGACTACGTTGCCCCCTTCGTTGCCAGGGAACTCAAGAAGCTCAAG
GCACCGCTCAAGGGTGTCTTCGGCAACAACGACGGCGAAAGGAAGGGTCTCTACGAGGCACTGGGGATATACGA
TGAGATACTGGAAATCGAGGCCGATGGCATGAAGATAGCGGTAACCCACGGCACCGATGAGCGCATAGTCCGTG
CACTGGCCAGAAGCAGGCTCTACGACGTTGTCATAGTCGGCCACACCCACCGCTACGAGATACGCGAGGAGGGA
AGGACCATACTCGTCAACCCCGGCGAGGTCTGCGGCTACGTCACAGGAGTGAAGAGCGTCGCCCTGCTCGACAC
TCGGAAGAGGGAGGTGCAGATAGTCAACCTCGACACCGGGGAGCTCCTGGGGGCAATGAGTCTCTAA

Primer *est73E12* for CATATGCTGATAGGTATAATGAGCGATACCC

Primer *est73E12* rev CTCGAGGAGACTCATTGCCCCCAGGAG

>est79/C1

ATGGAACTCTACAAGGCCAAATTCGGTGAACTAAAGCTCGGCTGGGTCGTTCTCGTCCACGGCTTAGGGGAACA
CAGCGGGAGGTATGGAAGGCTCATTTCGATGCTCACAGATGCCGGCTTTGCCGTCTATGCCTTCGACTGGCCCGG
CCACGGTAAGAGCCCCGGCAAGAGGGGGCACACGAGCGTCGAGGAGGCAATGGAAATAATCGACTCGATAATC
GAGGAGATCGGGGAGAAGCCATTCCTCTTCGGCCACAGCCTCGGCGGTTTAACCGTCATCAGATACGCAGAAAC
GAGGCCCGATAAAATACGGGGCGTAATCGCTTCCTCGCCGGCCCTCGCCAAAAGTCCGGAAACGCCGGGCTTCAT
GGTGGCATTGGCTAAGTTCCTCGGAAAAATCGCACCAGGAGTTGTTCTCTCCAACGGACTGAAGCCGGAGCTACT
CTCCCGGAATCCCGAGGCCGTGAAGCGCTACGTCGAAGACCCGCTCGTTCACGACAGGATTTCGGCCAAGCTGGG
GAGGAGCATTTTCGTGAACATGGAGCTTGCCCACAGGGACGCAGGGAAAATAAAGGTTCCCGTGCTGCTAATCG
TCGGCACGGGCGACGTGATAACACCGCCCGAGGGCTCAAGGAAGCTCCTGGAGGAGCTTGAAGTTGAGGACAAG
ATGCTAAAGGAGTTCGAGGGAGCGTACCACGAGATATTTGAAGATCTGGAATGGGCAGATGAACTCCATAGAGC
TATAGTGGAGTGGCTGGTCGAAATGGCAAAAAGGAAAAGCGTCAGATAA

Primer *est79/C1* for CATATGGAACTCTACAAGGCCAAATTC

Primer *est79/C1* rev CTCGAGGACGCTTTTCCTTTTTGCCATTTCG

7.1.3 Elbe sediment "Glückstadt"

>est143/F5

ATGTGGGCGAGGACTACTTCTTCTACGACATCGGCGCGACGGCGTCGTGGGGCATCATCTCCGTCGATCTGCGCT
GGGTCAGCACCGACATCGACAACATCGACTGCTCGCTCGCCGACAACTGCGAAGGCGGCGTCGTACTCTCGGTC
TCGGCCGACCTGCCCGGCTAACGCCGGCGTCAAAGCGAACATGCAAAACCCCCGCGCCAAACGCGGGGGTTTTC
GTTTGTCAGGCCTCGCCCAAGAACGCGAGCGCAGCCGCCTTGAACGCCTTGTCGCCGACGCTCGACATGTGATC

GCGCCCGGGAACCATCACGACACGCGCATGCGGCAACGCGTCGGCCAGCAGACCCGG CGGCCCCGTGATGTTGT
CCTTCTCGCCCACAACCAGCAGCACGGGAACGGAAAGCCCCGCAAACTCTTCCGCCGTGAACGAGTGCCGCCGT
CGCGTCATGCACAGCGCCAGCGCCTCAAGGTCATTGCTGCTCTGCTCCGCGAATACGCGAAACGTGCGTGGCACG
ACACCCACGATTTCCGACGCATCGCGTGCGCGCAGACCGGCCGCGATCGCATCCGTCTCCAACCGCCCGCGGCC
GTAGTAATTCTCGCCGACGCCGGCCACGATCGCCCGCCGGACCCGATGCGGCGCATCGTGCAGCACGCGCAGCG
TTATGAACCCGCCCATCGAGTACCCCATCAGATCCGCTTGCGCGTATCCCAGATGATCGAGCAAGCGAACGACAT
CCGTAGCAAGCTCGCTCTCGTCATAAGCCTCGAGCCGATGCGGCTTGTCGCTCTGACCGTGCCCACGCACGTCAA
GCGCGATCACCTGCCTGCCGGCCTTGGTCAGCGCGTCGTACCAATTCGGCGCGCGCCAGTTTATGCCCCGGTTCG
ACGCGAACCCGTGAACCAGAACGATAGGCGGCCCCTCACCCAAAACCTCATAGGCAAGGTTCAACGGCCCGGGA
ACGGTCAGGAACGGCATTTGGCCTCTTGA

Primer *est143/F5* for CATATGTGGGCGAGGACTACTTCTTCTAC

Primer *est143/F5* rev AAGCTTGGCCAAATGCCGTTCCTGAC

7.2 Acknowledgements

First of all, I would like to thank my doctoral advisor Prof. Wolfgang Streit for providing me with this interesting topic, for having confidence and giving me the chance to accomplish research in his working group. I appreciate the support throughout the years very much.

Thanks to Prof. Wilhelm Schäfer for kindly accepting the role as a second assessor of this thesis.

Many thanks go out to my cooperation partners Filip Kovacic, Prof. Karl-Erich Jäger, Ulrich Krauss, Benjamin Lauinger, Patrick Bongen and Prof. Jörg Pietruszka from the Research Center Jülich, Jochen Müller-Dieckmann, Yuliya Dall Antonia and Francesco Fersini from the EMBL c/o DESY, Marlen Schmidt, Ina Menyes and Prof. Uwe Bornscheuer from Greifswald University as well as Marrit Eckstein and Oliver Thum from Evonik Industries.

Thanks to Andreas Pommerening-Röser and Eva Spieck for their support and for arousing my interest in microbiology during the first years of my studies at this university. I also have to thank my bachelor students that contributed dedicatedly to this work.

Furthermore, I am truly thankful to Christel Vollstedt and Nele Ilmberger, not only for proofreading of this thesis, but also for supervising me during my diploma and PhD times and for always having a laugh together.

I could always rely on the help of Angela Jordan, Regina Liebram, Uschi Reinitz, Christiane Debus and Martina Schmidt. Thank you very much, also for the pleasant conversations.

There is not enough space on this page to thank all my colleagues in appropriate manner. Nevertheless, in random order: Thank you Mirjam for giving me valuable scientific advice and also for always having great fun together. Arek, Nine, Steffi, Daggi and Claudia from the girl´s office and the once in a while visitor Ulrich: it was a great pleasure to work with you and thank you for the support and the extremely entertaining years we spent together. Thanks to Ebrahim, Sabine, Katja, Nico, Moritz, Mariita, Christian, Julia, Andreas as well as the former colleagues Patrick and Sascha and of course all the others for creating an enjoyable atmosphere.

Finally, I am much obliged that my family, all my close friends and my dear boyfriend supported me unconditionally throughout the years. Without you, this work would not have been possible.

7.3 Declaration on oath

I hereby declare, on oath, that I have written the present dissertation by my own and have not used other than the acknowledged resources and aids.

Hamburg, 26.07.2012

7.4 Publications

At the time of print, the results of this research have been submitted as follows:

- **"The metagenome-derived enzymes LipS and LipT increase the diversity of known lipases"**. Jennifer Chow, Filip Kovacic, Yuliya Dall Antonia, Ulrich Krauss, Francesco Fersini, Christel Schmeisser, Benjamin Lauinger, Patrick Bongen, Joerg Pietruszka, Marlen Schmidt, Ina Menyes, Uwe T. Bornscheuer , Marrit Eckstein, Oliver Thum, Andreas Liese, Jochen Mueller-Dieckmann, Karl-Erich Jaeger and Wolfgang R. Streit. PLoS ONE (2012). 7(10): e47665. doi:10.1371/journal.pone.0047665
- **"Cloning, expression, purification and preliminary X-ray analysis of a metagenome-derived lipase"**. Francesco Fersini, Yuliya Dall'Antonia, Jennifer Chow, Wolfgang R. Streit & Jochen Mueller-Dieckmann. *Acta Crystallographica section F* (2012). F68, 923-926. doi:10.1107/S1744309112025651

OPEN ACCESS Freely available online

PLOS ONE

The Metagenome-Derived Enzymes LipS and LipT Increase the Diversity of Known Lipases

Jennifer Chow[1], Filip Kovacic[2], Yuliya Dall Antonia[3], Ulrich Krauss[2], Francesco Fersini[3], Christel Schmeisser[1], Benjamin Lauinger[4], Patrick Bongen[4], Joerg Pietruszka[4], Marlen Schmidt[6], Ina Menyes[6], Uwe T. Bornscheuer[6], Marrit Eckstein[5], Oliver Thum[5], Andreas Liese[7], Jochen Mueller-Dieckmann[3], Karl-Erich Jaeger[2], Wolfgang R. Streit[1]*

1 Department of Microbiology and Biotechnology, Biocenter Klein Flottbek, University of Hamburg, Hamburg, Germany, **2** Institute of Molecular Enzyme Technology, Heinrich Heine University Duesseldorf, Research Center Juelich, Juelich, Germany, **3** European Molecular Biology Laboratory (EMBL) Hamburg Outstation, c/o Deutsches Elektronen-Synchrotron (DESY), Hamburg, Germany, **4** Institute of Bioorganic Chemistry, Heinrich Heine University Duesseldorf, Research Center Juelich, Juelich, Germany, **5** Bioprocess Development Consumer Specialties and Biocatalysis Biotechnology, Evonik Industries AG, Essen, Germany, **6** Department of Biotechnology & Enzyme Catalysis, Institute of Biochemistry, Greifswald University, Greifswald, Germany, **7** Institute of Technical Biocatalysis, Hamburg University of Technology, Hamburg, Germany

Abstract

Triacylglycerol lipases (EC 3.1.1.3) catalyze both hydrolysis and synthesis reactions with a broad spectrum of substrates rendering them especially suitable for many biotechnological applications. Most lipases used today originate from mesophilic organisms and are susceptible to thermal denaturation whereas only few possess high thermotolerance. Here, we report on the identification and characterization of two novel thermostable bacterial lipases identified by functional metagenomic screenings. Metagenomic libraries were constructed from enrichment cultures maintained at 65 to 75°C and screened resulting in the identification of initially 10 clones with lipolytic activities. Subsequently, two ORFs were identified encoding lipases, LipS and LipT. Comparative sequence analyses suggested that both enzymes are members of novel lipase families. LipS is a 30.2 kDa protein and revealed a half-life of 48 h at 70°C. The *lipT* gene encoded for a multimeric enzyme with a half-life of 3 h at 70°C. LipS had an optimum temperature at 70°C and LipT at 75°C. Both enzymes catalyzed hydrolysis of long-chain (C_{12} and C_{14}) fatty acid esters and additionally hydrolyzed a number of industry-relevant substrates. LipS was highly specific for (*R*)-ibuprofen-phenyl ester with an enantiomeric excess (*ee*) of 99%. Furthermore, LipS was able to synthesize 1-propyl laurate and 1-tetradecyl myristate at 70°C with rates similar to those of the lipase CalB from *Candida antarctica*. LipS represents the first example of a thermostable metagenome-derived lipase with significant synthesis activities. Its X-ray structure was solved with a resolution of 1.99 Å revealing an unusually compact lid structure.

Citation: Chow J, Kovacic F, Dall Antonia Y, Krauss U, Fersini F, et al. (2012) The Metagenome-Derived Enzymes LipS and LipT Increase the Diversity of Known Lipases. PLoS ONE 7(10): e47665. doi:10.1371/journal.pone.0047665

Editor: Mark R. Liles, Auburn University, United States of America

Received June 21, 2012; **Accepted** September 13, 2012; **Published** October 24, 2012

Funding: This work was kindly funded by the German Federal Ministry of Education and Research (BMBF) cluster Biokatalyse2021 (http://www.biokatalyse2021.de). The research leading to the crystallization results has received funding from the European Community's Seventh Framework Programme (FP7/2007–2013) under grant agreement n° 227764 (P-CUBE; www.p-cube.eu/). K.-E. Jaeger and U. Krauss acknowledge support by the "Deutsche Forschungsgemeinschaft" (DFG) in frame of the research training group GK1166 "Biocatalysis in non-conventional media:" (BioNoCo; www.bionoco.rwth-aachen.de). J. Pietruszka thanks the BMBF for funding the project "ExpreSys:" in the framework of the funding measure GenoMik (http://genomik-transfer.de/en/index_en.php?section=home). The funders had no role in study design, data collection and analysis, decision to publish, or preparation of the manuscript.

Competing Interests: M. Eckstein and O. Thum are employed by Evonik Industries. This does not alter the authors' adherence to all the PLOS ONE policies on sharing data and materials.

* E-mail: wolfgang.streit@uni-hamburg.de

Introduction

Lipolytic enzymes including lipases (EC 3.1.1.3) and carboxylesterases (EC 3.1.1.1) are important biocatalysts employed for a large number of biotechnological applications [1–3]. Many lipases exhibit high chemo-, regio- and enantioselectivity and are tolerant against organic solvents which makes them even more attractive for organic synthesis reactions [4,5].

A variety of biotechnologically interesting reactions require elevated temperatures and thermostable rather than mesophilc enzymes [6–8]. While the general prediction of thermostabilty of an enzyme entirely based on the deduced amino acid sequence of a protein is perhaps not reliable [9], several traits appear to be associated with thermostable proteins. Mainly disulfide bonds and intrahelical salt bridges are more frequently observed in thermostable enzymes. Furthermore, the overall composition of amino acids appears to be of importance for the thermostability and especially polar residues that form additional hydrogen bonds appear to be of importance. Further the use of charged residues to form additional ionic interactions is yet another key trait of thermostable enzymes [10,11]. Recently it was also suggested that the frequency of Asn-Glu could be a factor to distinguish between mesophilic and thermophilic proteins [12]. Esterification at higher temperatures offers the advantages that the reactions can take place at higher rates and the use of organic solvents can be avoided. The respective biocatalysts thus need to be thermotolerant showing high activity at elevated temperatures above 70°C. Ideal resources for such enzymes are microbes living under

extreme conditions [13,14]. While in the last decade many thermostable enzymes - including a significant number of esterases - have been uncovered, the number of truly thermophilic and bacterial lipases is still limited with less than ten thermostable bacterial lipases being characterized to date. Among them is a remarkably stable enzyme from *Thermoanaerobacter thermohydrosulfuricus* (LipTth) and a lipase from *Caldanaerobacter subterraneus* (LipCst) [15]. Further, several thermoactive lipases have been reported in the genus *Geobacillus* [16–18]. Although these enzymes are active at high temperatures, they appear to be less stable over time when incubated at elevated temperatures. Furthermore, thermostable lipases have been reported in different *Thermus* isolates [19,20] and were recently expressed in thermophilic yeasts [21,22]. A thermostable esterase from *Thermus scotoductus* has been reported that was partially biochemically characterized [23]. Finally, two thermostable lipases have been reported from *Thermosyntropha lipolytica*, an anaerobic, thermophilic, alkali-tolerant bacterium that grows syntrophically with methanogens on lipids [24]. Both enzymes from this microbe were active at temperatures of >90°C and showed remarkable half-life times at 100°C.

Furthermore, a number of moderately thermostable lipases that originated from fungi have been described and some of them have been analyzed or optimized through evolutive strategies [25–28]. Of those, the most frequently used and best characterized moderately thermostable lipase is CalB, which originates from the mesophilic yeast *Candida antarctica* [25]. By applying several rounds of protein engineering methods, the thermal stability of CalB was improved greatly [29–31]. While these enzymes were all derived from cultivable bacteria or fungi, surprisingly, no truly thermostable lipases acting on long-chain *p*NP-esters with temperature optima of 70°C or higher have been reported using a metagenome-based approach since the first discovery of lipolytic enzymes from metagenomes over ten years ago [32,33].

Metagenome-based technologies for the identification of novel biocatalysts have been applied very successfully within the last decade and have resulted in the identification of numerous novel biocatalysts [34,35]. However, the basic steps of accessing non-cultivated microorganisms have been outlined earlier and include the isolation of environmental DNAs, cloning into small or large insert vectors and amplification of these libraries in a suitable host [36,37]. The libraries are then screened using a wide array of different methods. With respect to the screening and detection of lipases and esterases in metagenomes [38], more than 100 metagenomic enzymes have been reported and in part characterized [33]. Some of these enzymes reveal remarkable traits that are potentially useful for biotechnological applications and have broadened our knowledge on the diversity of lipases. Perhaps the first true lipase reported from a metagenome source was described by Henne and colleagues [32]. Unfortunately, only a fraction of the metagenome-derived lipolytic enzymes has been characterized in more detail concerning their structural features [39–43].

Here, we have used metagenome-based technologies to identify and characterize novel bacterial lipolytic enzymes which catalyze both hydrolysis and esterification reactions at temperatures above 70°C. Metagenomic libraries from enriched soil and water samples were constructed and screening revealed two novel lipases designated LipS and LipT which showed a high temperature optimum and also a high stability against thermal denaturation. These lipases were biochemically characterized and the X-ray structure of LipS was solved at a resolution of 1.99 Å in its apo form and together with spermidine. Thus, LipS belongs to the first metagenomic lipases that have been analyzed by crystallographic methods so far.

Materials and Methods

Environmental Samples and Enrichment Cultures

Ten soil and water samples were collected from different sites at the Botanical Garden (Klein Flottbek, Hamburg, Germany, 53°33′44.56′N, 9°51′40.11′E). The sample sites included topsoil that consisted mainly of sand as well as humus-rich soil. Water samples were taken from sweet water brooks and ponds. Approximately 0.5 g of each soil sample and 0.5 ml of each liquid sample were then mixed in a 100 ml Erlenmeyer flask containing 50 ml of mineral salt medium (MSM) and incubated overnight at room-temperature and 150 rpm in order to detach bacterial cells from soil and plant particles. After sedimentation of these particles by gravity, the samples were used to inoculate mineral salt medium (MSM) in a 2 l glass bottle composed of 0.8 l H_2O, 0.1 l solution 1 and 0.1 l solution 2 [solution 1 (1 l, 10×): 70 g Na_2HPO_4×2 H_2O, 20 g KH_2PO_4. Solution 2 (1 l, 10×): 10 g $(NH_4)_2SO_4$, 2 g $MgCl_2$×6 H_2O, 1 g $Ca(NO_3)_2$×4 H_2O]. The medium was supplemented with pyruvate (0.1% w/v), olive oil (1% v/v), vitamins [100 ml, 1000×: 1 mg biotin, 10 mg nicotinic acid, 10 mg thiamin-HCl (vitamin B1), 1 mg *p*-aminobenzoic acid, 10 mg Ca-D-(+)-pantothenic acid, 10 mg vitamin B6 hydrochloride, 10 mg vitamin B12, 10 mg riboflavin, 1 mg folic acid] and trace elements [44]. The enrichment culture was maintained at 65°C and aerated with 120 rpm on a magnetic stirrer.

For the second enrichment, water samples were taken from a heating system in the Biocenter Klein Flottbek (Hamburg, Germany). The temperature of the water at the time of sampling was above 50°C. The medium [modified medium D [45]] contained tryptone and yeast extract (0.1% w/v each) as well as trace elements [46]. This *Thermus*-enrichment culture was inoculated with 20% of water sample (v/v) and incubated at 75°C in a 2 l glass bottle on a magnetic stirrer with 200 rpm for several weeks. Both enrichment media were refilled with autoclaved H_2O_{dest} on a regular basis to maintain the initial volume.

No specific permits were required for the described field studies as the Botanical Garden and the Biocenter Klein Flottbek are non-protected areas concerning soil and water samples and owned by the University of Hamburg. The samples did not involve endangered or protected species.

E. coli Culture Conditions

E. coli strains were grown aerobically at 37°C on Luria-Bertani (LB) medium supplemented with appropriate antibiotics [47]. *E. coli* clones and constructs are listed in TABLE S1.

DNA Isolation, 16S rRNA Analysis and Library Construction

After three weeks of incubation, cells from the enrichment cultures were harvested by centrifugation. Genomic DNA was isolated by using a phenol/chloroform method with TE-buffer containing sucrose [10 mM Tris-HCl, 1 mM EDTA and 20% sucrose (w/v)], lysozyme solution (1 mg/ml in TE-buffer) and proteinase K solution [1 mg/ml, 20% SDS (w/v), 1 mg/ml RNase].

For phylogenetic characterization of the enrichments, bacterial 16S rRNA genes were amplified using the standard primers 616V (5′-AGAGTTTGATYMTGGCTCAG-3′) and 1492R (5-CGGY-TACCTTGTTACGAC-3′). The amplified genes were ligated into pDrive cloning vector and transformed in competent *E. coli* DH5α cells by heat shock. 16S rDNA was sequenced with automated sequencing ABI377 technology following the manufacturer's instructions.

Libraries were constructed with the cosmid vector pSuperCos which carries ampicillin and neomycin resistance genes and phage packaging mixes which were both supplied within the Gigapack® III Gold Packaging Extract kit (Stratagene, La Jolla, CA, USA). Construction was carried out according to the manufacturers instructions. Genomic DNA fragments with a size of 20–40 kb obtained after partial *Bsp*143I digestion were ligated into the *Bam*HI restriction site of the cosmid vector before phage-infection of *E. coli* Epi100 cells was performed. Cosmid clones were grown on LB agar supplemented with 100 µg/ml ampicillin.

Screening of Lipolytic Clones

E. coli clones were tested for lipolytic activity by transferring them on LB agar plates containing tributyrin (TBT, 1% vol/vol) as indicator substrate [48]. In order to detect active clones, the cosmid clones were grown at 37°C overnight; then a further incubation for 1–3 days at 56°C followed. The second incubation step was introduced to slowly lyse the *E. coli* cells and to release those enzymes that are active on TBT at elevated temperatures and produce a clear halo. In a microtiter plate scale, clones were grown in a 96 deep-well plate containing 1.2 ml of LB with ampicillin. After incubation for 16 to 24 h at 37°C and 250 rpm, cells were harvested by centrifugation and the supernatant was discarded. Cells were lysed by 1 h incubation with 125 µl/well 0.1 M potassium phosphate buffer (PB) pH 8.0 containing lysozyme (10 mg/ml) at 37°C. Cell debris was collected by centrifugation for 10 min at 3,600 rpm. In a 96 well microtiter plate, 10 µl of the crude cell extract were incubated with 190 µl of PB (0.1 M, pH 8.0) that contained either 1 mM 4-nitrophenyl (*p*NP) butyrate or dodecanoate. The samples were incubated for 30 min at 56°C and subsequently, the extinction of 4-nitrophenol released from the substrate was measured spectrophotometrically in a microtiter plate reader (Benchmark, Bio-Rad, Hercules, CA, USA) at 405 nm against an enzyme free blank.

Cosmid DNA was isolated from the positive clones obtained in the initial screening, retransformed in *E. coli* DH5α and the resulting clones examined with the same type of assay for esterase/lipase activity in order to avoid false positive clones.

Subcloning and in vitro Transposon Mutagenesis

For the identification of ORFs encoding lipolytic activity, the positive cosmid clones were subcloned with *Eco*RI, *Hind*III or *Sac*I, ligated into pTZ19R, which carries a chloramphenicol resistance gene, and transformed into *E. coli* DH5α. The subclones were streaked onto LB agar plates with TBT and screened for hydrolytic activity. On positive subclones, *in vitro* transposon mutagenesis using the EZ::TN™ <KAN-2> transposon kit (Epicentre, Madison, Wisconsin, USA) was carried out following the manufacturer's instructions. Clones harboring a transposon in the responsible gene were screened negative on TBT containing agar plates. With the inserted priming sites of the transposon, the corresponding gene was sequenced by automated sequencing ABI377 technology following the manufacturer's instructions. Alternatively, the inserts of the subclones were sequenced with the vector specific primers M13 for (5-GTAAAACGACGGCCAGT-3′) and M13 rev (5′-CAGGAAACAGCTATGACC-3′).

Cloning and Expression of lipS and lipT

Gene sequences were amplified from cosmid DNAs by PCR in 35 cycles with the primer pairs pCos9D12_for (5′-CATATGAGCCGGAAAAGCAGG-3′) and pCos9D12_rev (5′-AAGCTTGCTGTGCTTCCGGATGAAC-3′) for the amplification of *lipS* and pCos6B1_for (5′-CATATGCGGCGGTTACTAGCCTTGC-3′) and pCos6B1_rev (5′-AAGCTTCCGCACCCTAGGCGCCGCC TTC-3′) for *lipT*. Primers were designed to introduce a 5′-*Nde*I and a 3′-*Hind*III restriction site into the cloned fragments. The PCR fragments were ligated into pDrive cloning vector (Qiagen, Hilden, Germany), cut with *Nde*I and *Hind*III and ligated into pET21a (Novagen, Merck, Darmstadt, Germany), which has an ampicillin resistance gene and a His-tag coding sequence for the C-terminus of the corresponding protein. Plasmids containing *lipS* and *lipT* gene sequences were designated *lipS*::pET21a and *lipT*::pET21a, respectively. To confirm that the correct genes had been amplified from the original cosmid DNA, the PCR fragments cloned into pET21a were sequenced. Competent *E. coli* BL21 (DE3) cells were transformed by heat shock with *lipS*::pET21a and *lipT*::pET21a for the overproduction of the corresponding proteins. Cultures were grown at 17°C and 250 rpm for 6–8 h until an optical density at 600 nm of 0.8 was reached. The production of the recombinant proteins was then induced by the addition of 1 mM isopropyl-β-D-thiogalactopyranoside (IPTG). After 16 h, the cells were harvested by centrifugation and disrupted by French pressure cell and ultrasonication in order to purify LipS and LipT from soluble fractions. Cell extracts were incubated with Ni-NTA Agarose (Qiagen, Hilden, Germany), loaded on columns and affinity chromatography was carried out according to the manufacturers protocol. Protein containing elution fractions were then dialyzed overnight against 0.1 M PB (pH 8.0). The proteins were analyzed by SDS polyacrylamide gel electrophoresis using 12 or 15% (w/v) gels and Western-immunoblotting using 6-His-specific antibodies.

Catalytic Activity Toward 4-nitrophenyl (pNP) Substrates

Enzyme activity studies were performed by incubating the enzymes with 1 mM *p*NP-substrate in 0.1 M PB (pH 8.0) at assay temperatures of 70°C (LipS) or 75°C (LipT), unless otherwise indicated. The reaction was measured against an enzyme-free blank to subtract auto-hydrolysis by spectro-photometrical quantification of the released 4-nitrophenol at 405 nm [molar extinction coefficient ε (0.1 M PB pH 8.0) = 19,454 M^{-1} cm^{-1}, ε (0.1 M PB pH 7.0) = 10,400 M^{-1} cm^{-1}]. One unit is defined as the amount of enzyme that catalyzes the formation of 1 µmol 4-nitrophenol per minute. Enzyme activity was tested against different *p*NP-acyl esters [butyrate (C4), hexanoate, octanoate, decanoate, dodecanoate, myristate (C14), palmitate (C16) and stearate (C18), Sigma]. Above 70°C, even long-chained *p*NP esters (C16–C18) were sufficiently soluble, so that no detergents were added. The temperature optima of LipS and LipT were determined with *p*NP-dodecanoate as substrate at temperatures ranging from 20 to 90°C for 10 min. To study the thermal stability of the enzymes, LipS and LipT were incubated at 70 and 90°C, respectively, for up to 72 hours and their residual activity was measured using *p*NP-dodecanoate (1 mM final concentration) by incubation for 20 min at 70°C for LipS and 75°C for LipT.

The pH optimum of LipS and LipT was investigated with buffers of different pH values, that were adjusted at 70°C [pH 5–5.6, citrate buffer (0.05 M); pH 5.6–8, PB (0.1 M); pH 8–9, Tris-HCl (0.1 M); pH 9–10.6, glycine/NaOH (0.1 M)]. Enzyme activity was measured with *p*NP-decanoate as substrate.

LipS and LipT were tested for their stability and activity in the presence of metal ions, inhibitors, detergents and solvents. After 1 h incubation with these substances at room temperature, residual enzyme activities were determined at 70°C or 75°C and at pH 8.0 in 0.1 M PB by using *p*NP-decanoate or -dodecanoate as substrates.

As metal ions, Ca^{2+}, Co^{2+}, Cu^{2+}, Fe^{3+}, Mg^{2+}, Mn^{2+}, Rb^{2+} and Zn^{2+} were used with a concentration of 1 or 10 mM in 0.1 M PB.

EDTA (ethylenediaminetetraacetic acid), DTT (dithiothreitol) and PMSF (phenylmethyl-sulfonyl fluoride) were used as enzyme inhibitors with 1 or 10 mM concentration in PB. In order to examine the stability against detergents, SDS (sodium dodecyl sulfate), Triton X-100 and Tween 80 were applied with 1 or 5% concentration (w/v, v/v) in 0.1 M PB pH 8.0.

The stability of LipS and LipT in various organic solvents was studied using dimethyl sulfoxide (DMSO), isopropanol, methanol, dimethylformamide (DMF), acetone, acetonitrile and ethanol at final concentrations of 10% or 30% (v/v) in 0.1 M PB pH 8.0.

The substrate range of the two enzymes was tested with the following achiral or racemic *p*NP-esters at a final concentration of 0.5 mM in 0.1 M PB pH 8.0:2-phenylpropanoate, 3-phenylbutanoate, cyclohexanoate, 2-(3-benzoylphenyl) propanoate, 2-naphthoate, 1-naphthoate, adamantanoate and 2-(4-isobutylphenyl)-N-propanamide ester. Activity was measured at 405 nm after 10, 20 and 30 minutes incubation at 70°C.

Activity on chiral *p*NP-esters was analyzed with (*S*)-/(*R*)-2-methyldecanoic acid ester [49,50], (*S*)-/rac-/(*R*)-2,3-dihydro-1*H*-indene-1-carboxylate ["Indancarboxylic acid ester", [51]], (*S*)-/rac-ibuprofen-ester and (*S*)-/rac-/(*R*)-naproxen-ester [52,53].

Enzyme activity on these *p*NP-esters with 0.33 mM final concentration was measured at 410 nm after incubation for up to 40 min at 60 and 65°C in 0.05 M Soerensen buffer pH 8.0 containing 0.1% (w/v) gum arabic, 5 mM sodium deoxycholate and 10% DMSO. Controls concerning these additives did not reveal a significant effect on enzyme activity.

HPLC-MS Analysis of LipS on pNP and Phenyl Esters of Ibuprofen

To determine enantioselectivity referring to the *p*NP and the phenyl ester of ibuprofen, kinetic resolution has been carried out in analytical scale: 17.32 ml potassium buffer (0.1 mM, pH 8.0) were mixed with 2 ml DMSO and 0.66 ml of a substrate stock solution (10 mM in DMSO). 652 µg LipS were added and the reaction was shaken at 60°C for 30 min. The reaction was stopped by adding 8 ml 2 M HCl and followed by immediate extraction with methyl *tert*-butyl ether (MTBE, 2×20 ml). The solvent was removed under reduced pressure. The extracted ibuprofen was converted to the corresponding methyl ester by adding a 0.5 M diazomethane solution in diethyl ether. The solvent was removed under reduced pressure. The *ee* was determined by HPLC (Dionex) using a chiral stationary phase: Chiralpak IA (Daicel), 99.8:0.2 (*n*-heptane:isopropanol), 0.5 ml/min, 225 nm, $t_R(S) = 10.23$ min, $t_R(R) = 11.17$ min. The *ee* of the phenyl ester was determined using the same conditions as the methyl ester [$t_R(S) = 16.32$ min, $t_R(R) = 18.07$ min]. Because the enantiomers of the *p*NP ester could not be separated by chiral HPLC, the *ee* was determined by measuring the g factor (dissymmetry factor) with achiral HPLC with CD detector [54–56]. Column: Hyperclone ODS C18, conditions: 90:10, $CH_3CN:H_2O$, 0.5 ml/min, 220 nm, t_R(ibuprofen) = 2.7 min, t_R(*p*NP ester) = 4.5 min. Calculation of the enantioselectivity (*E*) value was performed by the method of *Faber et al.* [57].

Catalytic Activity Measured using Titration Assays

Tributyrin, triolein and polyglycerol-3-laurate were chosen as substrates for LipS and LipT to study activity on triglycerides using an automated titrator (Titrando 842 with Dosino 800, Metrohm, Filderstadt, Germany) and the pH-stat method. The substrate concentrations of the triglycerides ranged from 5 to 50 mM and of polyglycerol-3-laurate from 0.5 to 7.5% (w/v) in 2 mM Tris-HCl buffer pH 7.0. The substrate was emulsified with an automated stirrer (stirrer 802, Metrohm, Filderstadt, Germany) in the reaction vessel. The reaction was performed at 60°C, below the optimal temperature of the enzymes, in order to avoid autohydrolysis of the substrates. In order to have a control rate and for determination of autohydrolsis, the pH of the substrate solution was measured at 60°C for 5 min before the enzyme was added. The consumption rate of 20 mM KOH which was used to keep the pH at 7.0 indicated enzyme activity and was used to calculate the specific activity expressed in units per milligram of enzyme (U/mg). One unit was the amount that produced 1 µmol of fatty acid per minute under the specified assay conditions.

Esterification (Propyl Laurate) Assay

The propyl laurate assay was applied with 1-propanol and lauric acid as well as 1-tetradecanol and myristic acid as substrates for LipS. Both reactants were incubated in equimolar conditions (20 mmol) at 70°C together with 15 mg of lyophilized enzyme in a closed bottle under slow rotation. After 0, 24 and 48 h, the acid values of the reaction mixtures were determined by titration of a 0.5 g sample solved in 20 ml of toluene against 0.5 M $KOH_{ethanol}$ with phenolphthalein as pH indicator. The resulting acid values were used for the calculation of propyl laurate/tetradecyl myristate units per mg of enzyme. One unit was defined as 1 µmol of propyl laurate or tetradecyl myristate formed per minute by the enzyme under above mentioned assay conditions.

Enzyme-catalyzed Kinetic Resolution of Four Acetates of Secondary Alcohols

Three racemic acetates, i. e. 1-phenyl-1-propyl acetate, 1-phenyl-2-butyl acetate and 1-phenyl-2-pentyl acetate, were synthesized from the corresponding racemic alcohols as already described [58,59] except for 1-phenyl-1-ethyl acetate, which was commercially available. For the kinetic resolution, 10 mM acetate were added to a 1 ml solution containing 0.25 mg pure enzyme dissolved in PB (0.1 M, pH 7.0) and were mixed in a thermoshaker (Eppendorf, Hamburg, Germany) with 13,000 rpm at 70°C. Samples (100 µl) were taken at different time intervals and extracted twice with 100 µl dichloromethane. The combined organic layers were dried over anhydrous sodium sulfate and the organic solvent was removed in a nitrogen stream. The enantiomeric excess (%*ee*) of substrate and product were determined by gas chromatography as described earlier [58,59] [GC, Shimadzu GC-14A gas chromatograph, column: heptakis(2,6-*O*-methyl-3-*O*-pentyl)-β-cyclodextrin (Machery-Nagel, Düren, Germany); carrier gas H_2; flame ionization detector]. The retention times were as follows: 1-phenyl-1-propyl acetate $t_R(S) = 5.7$ min, $t_R(R) = 6.9$ min; 1-phenyl-1-propanol $t_R(S) = 11.8$ min, $t_R(R) = 12.7$ min; 1-phenyl-1-ethyl acetate $t_R(S) = 3.9$ min, $t_R(R) = 5.3$ min; 1-phenyl-1-ethanol $t_R(S) = 6.2$ min, $t_R(R) = 6.8$ min; 1-phenyl-2-butyl acetate $t_R(S) = 17.5$ min, $t_R(R) = 19.3$ min; 1-phenyl-2-butanol $t_R(S) = 21.9$ min, $t_R(R) = 23.6$ min; 1-phenyl-2-pentyl acetate $t_R(S) = 31.5$ min, $t_R(R) = 31.9$ min; 1-phenyl-2-pentanol $t_R(S) = 37.5$ min, $t_R(R) = 37.5$ min. *E*-value and conversion were calculated from the *ee* of substrate and product according to Chen *et al.* [60].

Classification of LipS and LipT

Amino acid sequences of the eight major bacterial lipase/esterase families [61] were obtained from the NCBI GenBank database (see supplementary TABLE S2). Independent alignments for all families were constructed using T-coffee [62]. All metagenome derived lipase/esterase sequences were sorted into the eight families based on alignment scores (see supplementary TABLE S3) and visual inspection of the respective alignments.

Sequences homologous to LipS and LipT were retrieved from the NCBI GenBank database. The LipS and LipT groups of sequences as well as 11 other metagenome sequences could not unequivocally be assigned to any of the known lipase families. Therefore, all of those sequences were compared to each other and when feasible sorted into a subgroup. In conclusion, those sequences constitute the LipS and LipT family as well as five additional unknown metagenome lipase/esterase sequence families (UF1-5).

Due to low sequence conservation between the different bacterial lipase/esterase sequence families, the independently constructed alignments had to be combined into a final dataset using Genedoc [63]. Tree reconstruction was carried out using the RaxML webserver [http://phylobench.vital-it.ch/raxml-bb/, [64]]. Tree viewing and editing was carried out using ATV [65] or TreeIllustrator v0.52 [66].

Crystallographic Analyses

LipS was crystallized and crystallographic data sets were collected and reduced as described previously [67]. The structure of wild-type LipS (LipS-WT) was solved by molecular replacement (MR) using the structure of carboxylesterase Est30 from *Geobacillus stearothermophilus* (PDB code 1TQH) as a model. The search was carried out with Molrep [68], which identified 4 molecules per asymmetric unit (a.u.), as expected from a Matthews parameter of 2.6 [69]. Iterative cycles of manual rebuilding in COOT [70] with crystallographic refinement in Refmac5 [71] converged at a final model at 1.99 Å resolution of good quality. The last rounds of refinement were done without non-crystallographic symmetry (NCS) restraints and with individual, isotropic B-factors.

A second construct of LipS with His_6-tag at the C-terminus (LipS-H6) crystallized in SG $P4_22_12$ and diffracted X-ray radiation to 2.80 Å resolution. Those data were phased by MR using the refined structure of LipS-WT solved in SG P4. Crystals in this SG contained only 2 molecules per a.u. Refinement and quality statistics of both models are given in TABLE S4. The PyMOL software was used for structural alignment, analysis, secondary structure assignment and visualization of protein structures [72].

Data Submission to Public Databases

The DNA sequences of *lipT* and *lipS* were deposited at GenBank under the accession numbers JQ028671 and JQ028672, respectively. The crystallographic data were submitted with the PDB database under the accession codes 4FBL and 4FBM.

Results

Enrichment Strategies and Construction of Metagenomic Libraries

From two different habitats, altogether 11 samples were taken and used to inoculate two different enrichment cultures. Bacteria from a water sample of a heating water system were grown at 75°C on medium D, while bacteria from the ten different soil and water samples of the Botanical Garden were enriched at 65°C on MSM supplemented with pyruvate and olive oil. After one and two weeks, respectively, visible turbidity appeared in the culture media. After three weeks of incubation, the cell density was high enough so that cells were harvested and sufficient genomic DNA could be isolated for library construction. The growth of the organisms appeared to be rather slow, probably because of the relatively low cell density of the inoculum that was used. The microbial communities were characterized on a phylogenetic level by amplification and sequencing of 16S rRNA genes. The gene sequences were aligned with nucleotide sequences deposited in the NCBI database via BLAST-search [http://blast.ncbi.nlm.nih.gov/Blast.cgi, [73]]. An examination of five highly similar 16S rRNA sequences from the enrichment of heating water samples showed, that it mostly contained bacteria closely related to *Thermus scotoductus* [NCBI acc. no. EU330195.1; max. identity 97%, Expect (E)-value 0.0]. Twenty analyzed sequences revealed that the enrichment of soil and water samples from the Botanical Garden contained 70% bacteria belonging to the *Symbiobacterium* group with the highest similarity to *Symbiobacterium thermophilum* IAM 14863 (NCBI acc. no. NC_006177; 99% max. identity, E-value 0.0). The phylum *Bacillales* was represented by *Geobacillus*-species and uncultivated *Bacilli* to 25% (e. g. NCBI acc. no. AB548612.1; *Geobacillus debilis* gene for 16S rRNA, partial sequence, 99% max. identity, E-value 0.0), whereas 5% of the community comprised members of Clostridia (e. g. NCBI acc. no. FN667168.1; uncultured compost bacterium partial 16S rRNA gene, clone FS1689, 95% max. identity, E-value 0.0).

With the extracted DNA, large insert metagenomic libraries were constructed by using the cosmid vector pSuperCos and *E. coli* Epi100 as heterologous host. The library of the heating water enrichment culture comprised 576 clones, of which 28 analyzed clones had an average insert rate of 70%. The library of the soil and water samples enrichment consisted of 6,500 clones. The analysis of 87 clones showed an insert rate of 96%. Both libraries had an average insert size of 27.5 kb.

Identification of the Lipolytic Genes lipS and lipT from Metagenomic DNAs

Screening of both libraries using a microtiter plate assay and *p*NP-dodecanoate as substrate identified four clones from the heating water enrichment library and six putative clones from the soil and water enrichment library that showed significant activities in these tests. The two most promising clones, one from each library, were characterized in detail. The positive clone from the heating water enrichment library was designated pCos6B1 and encoded a 27 kb insert. The clone from the soil and water samples enrichment library was designated pCos9D12 and encoded for a 26.5 kb insert. The cosmid clones pCos6B1 and pCos9D12 were subcloned in pTZ19R plasmids and transformed into *E. coli* DH5α. Sequencing of these subclones in combination with activity screening was pursued to identify the corresponding lipolytic genes. For pCos6B1, one subclone showed activity on TBT agar plates after incubation at 56°C and subsequently, a transposon mutagenesis was carried out and resulted in the identification of the corresponding ORF. The corresponding lipase gene on pCos9D12 was identified by sequencing in combination with primer walking. The ORFs linked to the lipolytic activities were designated *lipS* and *lipT* for the clones pCos9D12 and pCos6B1, respectively. The genes *lipS* and *lipT* encode putative proteins that consist of 280 and 331 amino acids, respectively. The translated gene sequences of *lipS* and *lipT* were compared with protein sequences deposited in the NCBI database by a BLASTX-search [73]. The BLASTX-search revealed their high similarities with genes annotated as putative esterases in known thermophilic microbes. The amino acid sequence of LipS shows 100% identity to a predicted *Symbiobacterium thermophilum* esterase (YP_075874) and LipT shows 97% identity to a predicted esterase from *Thermus scotoductus* (YP_004201971.1). LipT only showed low amino acid similarity to a previously described esterase EstTs1 of *Thermus scotoductus* [GenBank acc. no. ACS36170; 27.5% similarity according to a Needle (EMBOSS) alignment (http://www.ebi.ac.uk/Tools/psa/) [23]]. A common GXSXG motif that occurs in carboxylesterases and lipases was found in both enzymes. In LipS,

the catalytic serine is embedded in a GLSMG motif, while LipT contained a GCSAG motif. Furthermore, sequence analyses with SignalP 4.0 [http://www.cbs.dtu.dk/services/SignalP/[74]] indicated that *lipT* presumably encodes a secretion signal sequence with a cleavage site between Ala21 and Val22. For *lipS*, only a very low probability for a possible signal sequence was found with a hypothetical cleavage site between Ala17 and Gln18.

Overexpression, Purification and Molecular Weight of LipS and LipT

Both genes *lipS* and *lipT* were cloned and overexpressed in order to verify the hydrolytic function of the corresponding enzymes and allow a biochemical characterization. Therefore, the genes were ligated into pET21a and transformed into *E. coli* BL21 (DE3). The recombinant enzymes contained a C-terminal His_6-tag and were purified by Ni-NTA affinity chromatography under native conditions. LipS could be purified with 15.0 mg/g of cell pellet (wet weight). The maximum yield of LipT was 1.6 mg/g of pellet (data not shown). Thus, the protein yield after purification was overall better for LipS than for LipT (supplementary TABLE S5). The molecular weights of the proteins were verified by SDS-PAGE analysis under denaturing conditions. After Coomassie-staining, LipS was visible as a single band with a size of 31.7 kDa including the His_6-tag (supplementary FIGURE S1A). LipT appeared to be at least a dimer, revealing a molecular weight of at least 78 kDa after incomplete denaturation (supplementary FIGURE S1B).However, a monomeric form of approx. 36 kDa corresponding with the calculated molecular weight was observed by a Western blot analysis using His_6-tag specific antibodies (data not shown) and after extended heat denaturation of 30 min at 70°C (supplementary FIGURE S1A).

Activity of LipS and LipT on Commercial pNP-ester Compounds

To characterize both enzymes, a substrate spectrum was recorded with *p*NP-esters which had an acyl chain length of 4 to 18 C-atoms. The highest activities were observed with *p*NP-octanoate in case of LipS and with *p*NP-decanoate in case of LipT (FIGURE 1). Both enzymes were most active between acyl-chain lengths of 6 to 14 C (25–58% of the maximum activity). Significantly lower activities were measured with short (C4) and long (C16 and C18) acyl chain lengths (FIGURE 1). Kinetic studies with the preferred substrates *p*NP-octanoate (LipS) and *p*NP-decanoate (LipT) disclosed significant differences between both enzymes (TABLE 1). LipS revealed a 20-fold higher specific activity compared to LipT and both enzymes differed in their K_m and k_{cat} values significantly.

Temperature Optima, Thermostability and pH Dependent Activities of Recombinant LipS and LipT

Using 1 mM *p*NP-dodecanoate as substrate, the recombinant enzymes LipS and LipT revealed temperature optima of 70°C and 75°C, respectively. Interestingly, LipS was only weakly active at temperatures lower than 40°C, whereas LipT showed 50% of its activity at 40°C. Intriguingly, at 90°C, LipT still retained 91% of its maximum activity, LipS, however, only 23.5% (FIGURE 2A). To assess thermostability, both enzymes were incubated at elevated temperatures over extended time periods. After 48 h of incubation at 70°C, LipS revealed 50% residual activity; after 72 h, 13.6% of the activity could be measured (FIGURE 2B); incubated at 90°C, LipS still possessed 52% of its initial activity after 4 h of incubation. However, after 24 h, less than 1% of residual activity was measured at 90°C. LipT showed 43% residual activity after 24 h at 70°C and 23% after 52 h (FIGURE 2B). Incubation at 90°C for 24 h resulted in a residual activity of 22%. Altogether, these data suggest that both enzymes were thermostable.

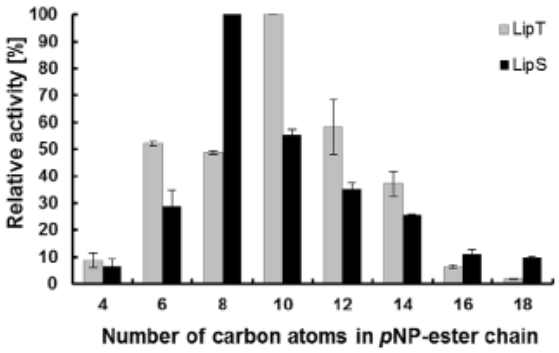

Figure 1. Substrate spectrum of LipS and LipT shown as relative activity on 4-nitrophenyl (*p*NP) esters with fatty acid chains of 4 to 18 C-atoms. Reactions were incubated at 70°C (LipS) or 75°C (LipT) with final substrate concentrations of 1 mM in potassium phosphate buffer (PB, 0.1 M, pH 8.0). Extinction was measured at 405 nm against an enzyme-free blank. Data are mean values of at least three independent measurements and bars indicate the standard deviation.
doi:10.1371/journal.pone.0047665.g001

LipS and LipT were most active at pH 8.0 when tested in 0.1 M PB and with 1 mM *p*NP-decanoate as substrate at their temperature optima. Below pH 8.0, activity was rapidly decreasing and at pH 6.0, only 11.4% (LipS) and 6.8% (LipT) residual activity was observed. Above pH 9.0, no significant activities were measured (data not shown).

Activity of LipS and LipT in the Presence of Metal Ions, Inhibitors, Detergents and Solvents

To characterize the effects of metal ions, different ions (Ca^{2+}, Co^{2+}, Cu^{2+}, Fe^{3+}, Mg^{2+}, Mn^{2+}, Rb^{2+} and Zn^{2+}) were added to the assays at 1 and 10 mM final concentrations. Activity was measured with *p*NP-dodecanoate and compared with a metal ion-free control. The activity of LipS as well as LipT's activity decreased in the presence of most of these ions and no significantly stimulating effects indicating a cofactor-dependent activation were observed (supplementary FIGURE S2).

Furthermore, EDTA, DTT and PMSF were applied in final concentrations of 1 and 10 mM (FIGURE S3). EDTA decreased LipSs activities at 1 mM to 74.1% and at 10 mM to 46.0% residual activity. The effects on LipT were less pronounced as it still revealed 98.0% residual activity at 1 mM EDTA and 65.7% at 10 mM EDTA. Incubation with 1 and 10 mM DTT resulted in a residual activity of LipS of 76.3% and 71.5%, respectively. LipT was not affected by the presence of 1 mM DTT and 85.4% of its activity remained in the presence of 10 mM DTT. PMSF did not show an effect on the activity of LipS in both concentrations of the inhibitor. LipT was inhibited by 10 mM PMSF to a residual activity of 49.0%, while lower concentrations of PMSF had no effect. SDS, Triton X-100 and Tween 80 were applied with 1 and 5% concentration (w/v, v/v) as detergents. With a final concentration of 1%, the substances lowered the activity of LipS only insignificantly. A concentration of 5% strongly decreased the activity to 0% (SDS), 14.3% (Triton X-100) and 20.1% (Tween 80). LipT was not even active in the presence of 1% SDS and was

Table 1. Biochemical parameters of recombinant LipT and LipS determined using 4-nitrophenol-decanoate (C10) for LipT and –octanoate (C8) for LipS.

Enzyme	U/mg	v_{max} (mol min^{-1})	K_m (mol l^{-1})	k_{cat} (min^{-1})	k_{cat}/K_m (M^{-1} sec^{-1})
LipT	0.6	$5.4 \cdot 10^{-8}$	$1.1 \cdot 10^{-3}$	0.1	0.8
LipS	12.0	$2.0 \cdot 10^{-7}$	$2.2 \cdot 10^{-3}$	1.3	10.3

The measurements were performed at 75 and 70°C, respectively, in 0.1 M PB pH 8.0.
Data are mean values of three independent measurements.
doi:10.1371/journal.pone.0047665.t001

strongly affected by 1% Triton X-100. It revealed only 13.0% residual activity; and in the presence of 1% Tween 80, only 18.4% residual activity was observed. After incubation with 5% solutions of the two detergents Triton X-100 and Tween 80, LipT was almost completely inactivated (3.3% residual activity with Triton X-100; 0.3% residual activity with Tween 80).

The solvent stability of LipS and LipT was investigated in the presence of DMSO, isopropanol, methanol, DMF, acetone, acetonitrile and ethanol at concentrations of 10 and 30% (v/v) in 0.1 M PB pH 8.0 (TABLE S6). The presence of all solvents affected LipS. With 10% of solvent, residual activities between 67.9 and 27.7% were detected when compared to a solvent-free control, while 30% of solvent decreased the activities of LipS to 45.9–8.5%. The only exception was 30% of DMSO, where at least 92.9% of activities of both enzymes remained. Interestingly, LipT was much more stable in the presence of various solvents.

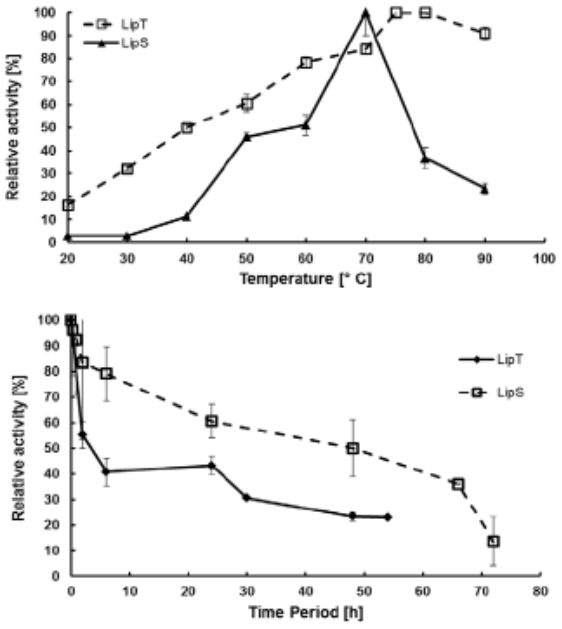

Figure 2. Temperature optimum (A) and thermal stability (B) of LipS and LipT. Data are mean values of at least three independent measurements and bars indicate the standard deviation. Temperature range and optimum of LipS and LipT were measured with *p*NP-dodecanoate at temperatures ranging from 20°C to 90°C for 10 min. Assays were performed by incubation of the enzymes at 70°C for up to 72 hours and by measuring residual activities with *p*NP-dodecanoate at 70°C (LipS) and 75°C (LipT).
doi:10.1371/journal.pone.0047665.g002

Substrate Range and Enantioselectivity of LipS and LipT

LipS and LipT were tested for their hydrolytic activity on a wide range of substrates; among them achiral or racemic *p*NP-esters in a final concentration of 0.5 mM at 70°C (TABLE 2). LipS hydrolyzed 2-phenylpropanoate (0.42 U/mg), 3-phenylbutanoate (0.09 U/mg), cyclohexanoate (1.26 U/mg), 2-(3-benzoylphenyl) propanoate (0.62 U/mg), 2-naphthoate (0.06 U/mg), and 2-(4-isobutylphenyl)-N-propanamide ester (0.07 U/mg). The substrates 1-naphthoate and adamantanoate were, however, not converted by LipS. The substrate range of LipT was narrower in comparison, as it hydrolyzed 3-phenylbutanoate (0.03 U/mg), 2-(3-benzoylphenyl) propanoate (0.06 U/mg), 2-naphthoate (0.02 U/mg) and 2-(4-isobutylphenyl)-N-propanamide ester (0.08 U/mg). Interestingly, LipT hydrolyzed 1-naphtoate, even though with weak activity (0.01 U/mg). LipT did not cleave the ester bonds of 2-phenylpropanoate, cyclohexanoate and adamantanoate.

The stereoselectivity of LipS and LipT were assayed on chiral *p*NP-esters namely (*S*)-/(*R*)-2-methyldecanoic acid ester, (*S*)-/rac-/(*R*)-2,3-dihydro-1*H*-indene-1-carboxylate ("indancarboxylic acid ester"), (*S*)-/rac-ibuprofen-ester and (*S*)-/rac-/(*R*)-naproxen-ester (TABLE 2). Reactions with *p*NP-esters as substrates were measured after incubation at 60°C and 65°C. These relatively mild temperatures were chosen to avoid autohydrolysis that readily occurs at higher temperatures. In comparison, the commercial enzymes CalB and ROL (*Rhizopus oryzae* lipase) were tested at the same temperatures. CalB and LipT did not show stereoselectivity. ROL showed a preference for the (*R*)-enantiomer of indancarboxylic acid ester and ibuprofen ester. The highest activity of all enzymes at this temperature was observed with LipS and it also revealed the most distinct enantioselectivity, as it was more active on the (*R*)-enantiomers of the different substrates. LipS favored the (*R*)-enantiomers of 2-methyldecanoic acid ester ($E = 8$), indancarboxylic acid ester ($E = 12$) and naproxen-ester ($E = 9$) [75]. It, however, revealed only very poor activities on the (*S*)-ibuprofen ester (TABLE 2). This result was verified by HPLC analysis. LipS preferred the (*R*)-enantiomer of ibuprofen *p*NP-ester with an *ee* of >>59% for the product and ~90% for the remaining substrate ($E = 11$, conversion 60%). The stereoselectivity of LipS was even higher on ibuprofen phenyl ester, where an *ee* of 99% was detected for the product and 81% for the substrate at 45% conversion for the phenyl ester which leads to an *E*-value >>100 (FIGURE 3).

Activity of LipS on Tri- and Polyglycerides

Furthermore, we assayed the activities of LipS and LipT on tri- and polyglycerides. LipT did not reveal significant activities in the titration assays using tributyrin, triolein and polyglycerol-3-laurate as substrates. However, LipS had a specific activity of 0.14 U/mg at 60°C using 50 mM tributyrin. The activity was higher with

Table 2. Specific activity* (U/mg) of LipT and LipS on *p*NP esters.

*p*NP-Substrate		LipT	LipS	CalB	ROL
Octanoate[1)]	/	+	+ +	+	+
2-Phenylpropanoate[2)]	rac	−	+ +	n. d.	n. d.
3-Phenylbutanoate[2)]	rac	+	+	n. d.	n. d.
Cyclohexanoate[2)]	/	−	+ + + +	n. d.	n. d.
2-(3-Benzoylphenyl) propanoate[2)]	rac	+	+ +	n. d.	n. d.
2-Naphtoate[2)]	/	+	+	n. d.	n. d.
1-Naphtoate[2)]	/	+	−	n. d.	n. d.
Adamantanoate[2)]	/	−	−	n. d.	n. d.
Methyldecanoate[1)]	(*S*)	+	+	+	+
	(*R*)	+	+ +	+	+
2,3-Dihydro-1H-indene-1-carboxylate (indan acid ester)[1)]	(*S*)	+	+	+	−
	rac	+	+	+	+
	(*R*)	+	+ +	+	+
Ibuprofen ester[1)]	(*S*)	+	−	+	−
	rac	+	+ +	+	+
2-(4-isobutylphenyl)-N-(4-nitrophenyl) propanamide (Ibuprofen amide ester)[2)]	rac	+	+	n. d.	n. d.
Naproxen ester[1)]	(*S*)	+	+	+	+
	rac	+	+	+	+
	(*R*)	+	+ +	+	+

CalB (purchased from Sigma-Aldrich, Buchs, Switzerland) and ROL (purchased from Fluka/Sigma-Aldrich, Buchs, Switzerland) were used as references.
The extinction was measured spectrophotometrically against an enzyme-free blank with
[1)]0.33 mM substrate solution (final concentration in 0.05 M Soerensen buffer pH 8.0 containing 0.1% gum arabic, 5 mM sodium deoxycholate and 10% DMSO) after incubation at 60°C (CalB) or 65°C (LipT, LipS, ROL) at 410 nm ($\varepsilon = 7{,}392\ M^{-1}\ cm^{-1}$).
[2)]0.5 mM substrate solution (final concentration in 0.1 M PB pH 8.0) after incubation at 70°C at 405 nm ($\varepsilon = 19{,}454\ M^{-1}\ cm^{-1}$).
*Specific activity: n. d., not determined; −, no detectable activity or <0.01 U/mg; +, 0.01–0.30 U/mg; + +, 0.31–0.60 U/mg; + + +, 0.61–0.90 U/mg; + + + +, 0.91–1.26 U/mg. Specific activities of CalB and ROL refer to the dry-weight of the lyophilisate. Data are mean values of three independent measurements.
doi:10.1371/journal.pone.0047665.t002

50 mM triolein (0.20 U/mg); and LipS revealed 0.61 U/mg on a 7.5% emulsion of polyglycerol-3-laurate.

Kinetic Resolution of Acetates of Secondary Alcohols

In addition, the enantioselective hydrolysis of four acetates of secondary alcohols was investigated using LipS. Whereas the hydrolysis of 1-phenyl-1-propyl acetate and 1-phenyl-1-ethyl acetate proceeded with low enantioselectivity ($E = 3$–4), excellent selectivity of LipS was observed for 1-phenyl-2-butyl acetate and 1-phenyl-2-pentyl acetate. In both cases, the corresponding chiral (*R*)-alcohols were obtained with >96% *ee* at approx. 50% conversion. This suggests that selectivity of LipS towards secondary alcohols is higher if the chiral center is not adjacent to the aromatic ring, but a further CH_2-group away to enable high discrimination of the two enantiomers.

Esterification by LipS

To further study the esterification of LipS, the enzyme activity was assayed in the propyl laurate assay and benchmarked with CalB as a control. At 70°C, the esterification reactions between 1-propanol and decanoic acid as well as 1-tetradecanol and myristic acid were catalyzed by 15 mg of lyophilized LipS and CalB. After 48 h, the formation of 1-propyl laurate was catalyzed by LipS (0.12 U/mg) and CalB (0.35 U/mg). The synthesis of 1-tetradecyl myristate also took place with LipS (0.09 U/mg) and CalB (0.28 U/mg) (FIGURE 4).

Crystallographic Analysis of LipS

A variety of constructs were expressed and purified for crystallization experiments as described earlier [67]. The initial construct LipS-H6 in SG $P4_22_12$ diffracted X-ray radiation to 2.80 Å resolution, while a second construct, LipS-WT, diffracted X-ray radiation to 1.99 Å resolution. Both constructs contain the native N-termini which are disordered until about residue 35.

LipS displayed a dimeric character during purification by size exclusion chromatography. Consistent with this observation, the asymmetric units of LipS in SG P4 and $P4_22_12$ contain one and two identical dimers, respectively. Analysis of the LipS-WT and LipS-H6 interfaces with Protein Interfaces, Surfaces and Assemblies (PISA) server [76] calculates the buried area between two protein molecules and based on solvatation energy (ΔG) gained upon assembly formation, it calculates a complexation significance score (CSS). The analysis confirms that the observed interactions are of biological significance (CSS = 0.69; ΔG = −20.5), because the CSS is expressed on a scale from 0, for non-significant interface, to 1, for significant interface. The dimer interface covers 1245 $Å^2$ (12.2% of the total surface of a monomer) of accessible surface area per monomer. It is primarily formed by the short helical segment αD_1, at the N-terminal part of the insertion and the long helix αD (FIGURE 5A). Several hydrogen bonds and salt bridges involving Q138, R154, A162, T203 and E209, in addition to numerous hydrophobic contacts, stabilize the dimer interface.

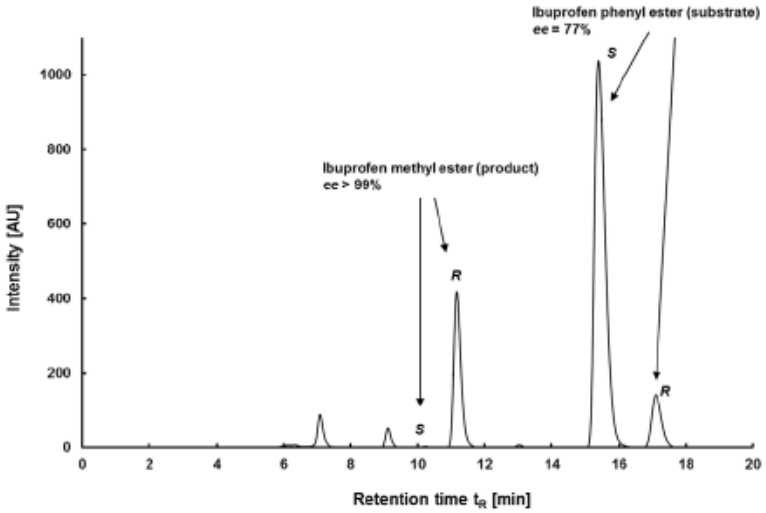

Figure 3. HPLC-MS measurement of LipS catalyzing (*R*)-selectively the hydrolysis of ibuprofen phenyl ester. The products of the reaction were converted to the corresponding methyl esters for measurement.
doi:10.1371/journal.pone.0047665.g003

LipS assumes the fold of a classical α/β hydrolase [77]. Members of this fold family accommodate a wide variety of enzymatic activities, including lipases, esterases, peroxidases, dehalogenases and epoxide hydrolases [78]. It consists of a central β-sheet made of six parallel β-strands (β2, β3, β4, β5, β8, β9) and one antiparallel β-strand (β1). Hence, the central β-sheet is missing the first β-strand of the canonical α/β hydrolase architecture so that it consists of 7 instead of 8 strands. The central β-sheet is sandwiched by helices αA and αG on one side and helices αB through αF on the opposite side (FIGURE 5A). The active site of LipS is formed by the catalytic triad S126, D227 and H257 with the catalytic serine located at the sharp γ-turn between β4 and αD (FIGURE 5C). The position of the catalytic triad and the oxyanion hole (F58 and M127) at conserved topological sites clearly designates this newly characterized enzyme as a hydrolase.

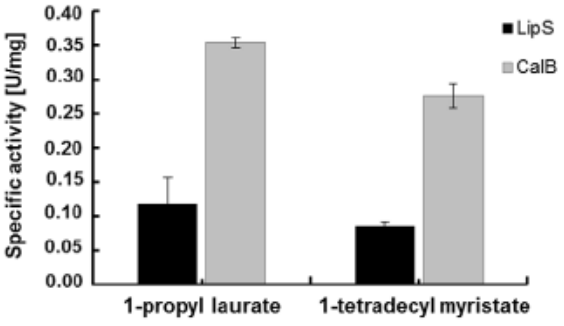

Figure 4. Esterification reactions between 1-propanol and lauric acid (20 mmol each) as well as 1-tetradecanol and myristic acid (15 mmol each). Synthesis reactions were catalyzed by LipS and CalB (purchased from Sigma-Aldrich, Buchs, Switzerland) under solvent-free conditions at 70°C. Specific activities of LipS and CalB refer to the dry-weights of the lyophilisates. Data are mean values of at least three independent measurements and bars indicate the standard deviation.
doi:10.1371/journal.pone.0047665.g004

After refinement, the active site of LipS-WT in SG P4 contained strong residual density immediately adjacent to S126 and H257. This density was interpreted with spermidine (FIGURE S4A, B). Spermidine was used as an additive to improve crystal quality and was subsequently shown to inhibit the activity of LipS with its substrate *p*NP-decanoate in concentration dependent manner (FIGURE S4C). The terminal amino-group of spermidine comes remarkably close to both S126 and H257 when the secondary amid group interacts with D187, which lines the end of the active site cavity. Thus, it is likely that spermidine mimics substrate bound in the active site (FIGURE S4D).

We reasoned that comparing 3D structures may reveal biologically interesting similarities that were not detectable by comparing amino acid sequences. Therefore, the comparison of LipS with related 3D structures was performed using DALI server [79]. The structurally most closely related enzymes were esterases, Est30 from *Bacillus stearothermophilus* [1TQH, *Z*-score 30.7, RMSD 1.8, [80]], EstD from *Lactobacillus rhamnosus* [3DKR, *Z*-score 28.7, RMSD 1.8 [81]], Est1E from *Butyrivibrio proteoclasticus* [2WTM, *Z*-score 24.0, RMSD 2.4 [82]] and human mono-glyceride lipase [3PE6, *Z*-score 28.1, RMSD 2.2 [83], FIGURE S5]. Structural superimposition of LipS with these four enzymes revealed notable similarity of their overall structures which all resemble the α/β-hydrolase fold (FIGURE 6). The core of the α/β-hydrolase fold, the central β-sheet and flanking α-helices, was highly similar between them (RMSD 1.2 Å to 1.8 Å) contrary to the 40 amino acid large subdomain (E156 to V195) inserted between β5 and αE of LipS. This subdomain of LipS is surface exposed and folds into a short helix $\alpha D_1'$ and two short antiparallel β-strands, β6 and β7. Among above listed structural homologues, only Est1E has a mixed α/β secondary structure topology similar to LipS. The inserted subdomains of Est30, EstD and human MGL all have a α-helical topology which differs from the topology of LipS (FIGURE 6B, C). Recently, the topology of an inserted subdomain similar to the one from Est1E was recognised in the cinnamoyl esterase LJ0536 from *Lactobacillus johnsonii* [84], which is apparently not deposited in the DALI database and thus, it was not detected as a structural homologue of LipS. The core structure of the α/β-fold of LJ0536

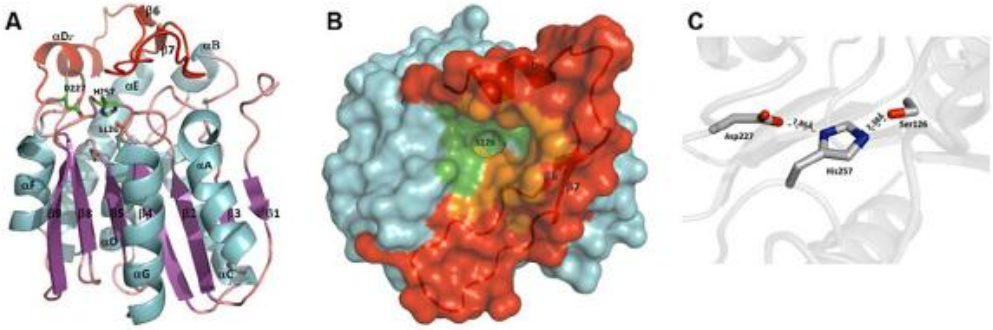

Figure 5. Protein structure of LipS. A) Ribbon representation of the LipS monomer colored according to secondary structure elements. The inserted lid-domain is indicated in red. The catalytic triad residues Ser126, His257 and Asp227 are shown as stick representation. **B)** Surface representation of the LipS monomer with the lid-domain (β6, β7, αD$_1$′) shown as a cartoon representation in red. The active site S126 (in yellow) is completely occluded from the bulk solvent and only accessible through a narrow tunnel. The active site pocket identified by CASTp server is colored in green. Amino acids building a pocket as part of the inserted domain are shown in orange. **C)** The catalytic triad residues of LipS are properly placed to establish hydrogen bonds.
doi:10.1371/journal.pone.0047665.g005

resembles the structure of LipS like the other above mentioned cores of the LipS homologues.

Superimposition of LipS with its homologues and inspection of inserted domains revealed similarity of LipS with Est1E, LJ0536 but also with evolutionarily distant human MGL. Based on the presence of β-strands (β6, β7) in the inserted domain of LipS, which are indeed structurally equivalent with β9, β10 of LJ0536 and β9, β10 of Est1E (FIGURE 6A), it seems that the inserted domains of these three enzymes are structurally related. It is noteworthy, that shifting of this β9/β10 hairpin of Est1E was proposed to lead to the formation of a substrate binding hydrophobic pocket [84]. However, notable differences between inserted domains of these three enzymes were observed. Thus, the loop connecting β6 and β7 in LipS is 17 amino acids long compared to 3 and 4 in Est1E and LJ0536, respectively. Furthermore, the short helix αD$_1$′ of LipS did not superimpose with any of the α-helices in Est1E and LJ0536. Additionally, the second short β-hairpins of Est1E (β7/β8) and LJ0536 (β7/β8) are absent in LipS. Although the secondary structure topology of the inserted domain of human MGL (α/α/α-fold) is diverse to the one of LipS (β/β/α-fold), it resembles its eukaryotic counterpart in MGL more closely than in Est1E and LJ0536 (FIGURE 6B). The αD$_1$′ of LipS superimposed well with α4 of human MGL, although α4 is 10 residues longer than αD$_1$′. Interestingly, an important biological function of the hydrophobic α4 for docking of human MGL onto membranes in order to gain access to the lipid substrates was suggested [85]. The part of LipSs inserted domain containing two β-strands β6 and β7 and a loop connecting them superimposed well with the region in human MGL ranging from 174 to 206, made by loops and the α5 and 3/10-helix, which is identical in its size to the LipS motif. Our results indicate that biologically important structural features of both prokaryotic and eukaryotic lipases are unified in the inserted subdomain of LipS and thus, LipS might represent an enzyme which is on evolutionary scale placed between eukaryotic and prokaryotic lipases.

Insertions of different lengths and conformations in other α/β-hydrolases at that location [86] suggest their evolutionarily importance for distinct biological functions of the enzymes. These inserted subdomains have dual biological function, a) as a lid which, in dynamic process, opens and closes the active site for exposure to the solvents and substrates and b) as a motif that

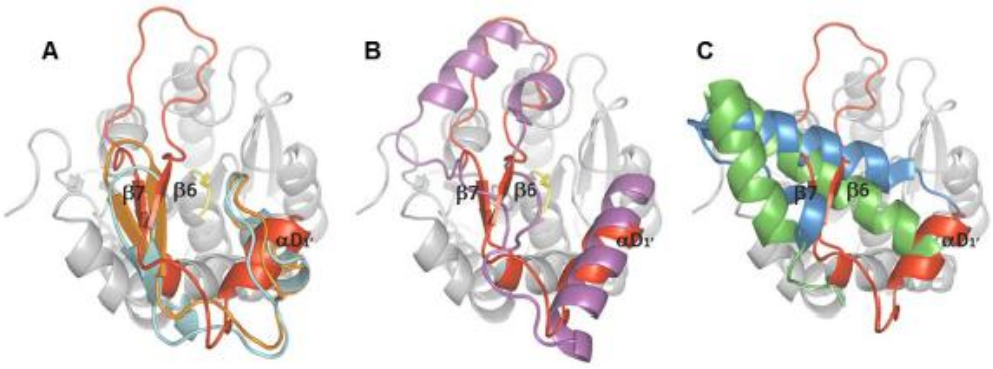

Figure 6. Topology of the inserted domains of α/β-hydrolases. Superimposition of the inserted domain of LipS (in red) with **A)** Est1E (2WTM, orange) and LJ0536 (3PF8, turquoise), **B)** human MGL (3PE6, purple) and **C)** EstD (3DKR, blue) and Est30 (1TQH, green). The core structure of LipS is indicated in grey and catalytic S126 in yellow. The core structures of LipS homologues are not shown for simplicity.
doi:10.1371/journal.pone.0047665.g006

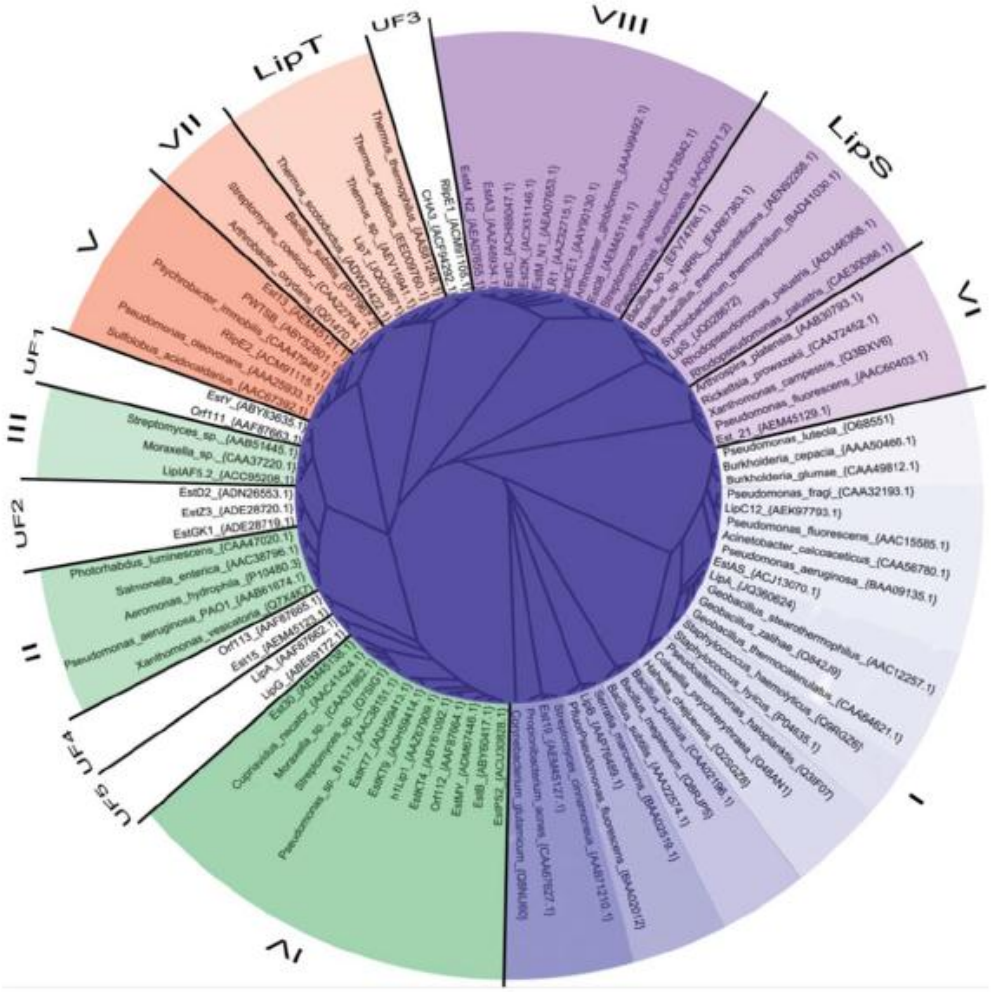

Figure 7. Phylogenetic tree illustrating the sorting of 40 metagenome derived lipase/esterase sequences into the eight known lipase/esterase families [61]. The eight families are color coded and labeled with the respective family name (LipS, LipT) or number (I-VIII). The five subfamilies containing the 11 unassignable metagenome lipase/esterase sequences are shown in white and are labeled with the respective family name (UF1-UF5). For the reference sequences, the full organism name as well as the accession number is given at the respective clade. Metagenome sequences are labeled with their protein name and accession number, respectively.
doi:10.1371/journal.pone.0047665.g007

shapes the active site for accommodation of appropriate substrates. Indeed, the flexible inserted domains serving as a lid were suggested for Est1E and human MGL but not for LJ0536, which adopts the same conformation in absence and presence of a ligand bound in the active site. The conformations of the inserted domains in all four LipS molecules found in one asymmetric unit were identical. Furthermore, data that the inserted domain assumes the same conformation with and without bound spermidine in structures of LipS suggests that this is rather a rigid structure.

Analysis of the cavities on LipSs surface using the Computed Atlas of Surface Topography of proteins (CASTp) server [87] revealed only one pocket in vicinity of the catalytic S126 (FIGURE 5B). This pocket with an area of 546.1 $Å^2$ was defined as an active site pocket. 30 amino acids, 20 hydrophobic and 10 hydrophilic (TABLE S7), contribute in formation of the active site pocket, thus providing amphipathic environment for substrate binding. Similarly to human MGL, the binding pocket of LipS is occluded with only narrow and restricted opening to the bulk solvent (FIGURE 5B). Human MGL, Est1E and LJ0536, although similar to LipS, have their active site much more exposed to the solvent compared with LipS. Thirteen amino acids of the inserted domain (TABLE S7) contribute at the same time in formation of the active site pocket of LipS (FIGURE 5B). Similar with other LipS homologues, the inserted domain of LipS shapes the catalytic pocket of LipS. Not surprisingly, mutations of inserted domain of Est1E have affected its substrate specificity [82]. Therefore, we would like to propose that the novel fold of the inserted domain of LipS, at the frontier between eukaryotic and prokaryotic lipases, could be essential for its selectivity in hydrolysis of a range of complex substrates listed in TABLE 2.

Table 3. Activities of LipS and LipT in comparison with other characterized and published bacterial thermostable lipases.

Source	T_{opt} [°C]	*p*NP-substrate	Specific activity [U/mg]	Reference
LipS (metagenomic)	70	C8	12.03	This study
		C10	6.04	
LipT (metagenomic)	75	C10	0.6	This study
Est53, *T. maritima*	60	C12	13.0	[107]
LipA, *T. lipolytica*	96	C12	12.4	[24]
LipB, *T. lipolytica*	96	C12	13.3	[24]
LipTth, *T. thermohydrosulfuricus*	75	C16	12.15	[15]

Only lipases with temperature optima of ≥60°C and activity on *p*NP-substrates with ≥8 C atoms as acyl residue were considered.
doi:10.1371/journal.pone.0047665.t003

Classification of LipS and LipT

Using modern alignment methods, we tried to sort 40 metagenome derived lipase/esterase sequences into the 8 known bacterial lipase/esterase families [61]. The sequences were grouped by aligning them manually to a subset of sequences representing the respective family. The quality of the independently calculated alignments is reasonably good, as judged from visual inspection, conservation of key amino acids [61] and T-coffee alignment scores. Nevertheless, the low sequence conservation between the eight families did not directly allow the construction of a meaningful alignment for the full dataset. Therefore, the seed alignment had to be constructed by assembling the sub-alignments in into a full dataset. Thus, the presented tree (FIGURE 7) serves solely as an illustration for the assignment of the metagenome derived sequences to the eight known bacterial lipase/esterase families, but does not allow any conclusions with respect to the relationship between the respective families. Using this alignment strategy, 11 out of 40 metagenome derived sequences could not be assigned to any of the eight known and established families. Likewise, LipS and LipT together with a set of homologous sequences could not be assigned unequivocally based on sequence similarity (FIGURE 7). This sequence comparison thus suggests that they are both part of novel lipase families without distinctive similarity to any of the known eight bacterial lipase/esterase families [61].

Discussion

We have isolated two novel lipase genes from metagenomic samples by a combined enrichment and direct cloning approach. Two different enrichment cultures were set up and 65 as well as 75°C were chosen as incubation temperatures in order to cover a broader spectrum of thermophilic organisms. Although the combined enrichment and metagenome technology applied significantly reduces the overall biodiversity in the environmental sample, it has been successfully applied by our lab and others to identify numerous useful biocatalyst genes from metagenomic samples [88–91]. In one such study, even a moderately thermostable metagenomic lipase was identified [92].

The two lipase genes identified in this work shared high similarities with already known genes in the databases. LipS was similar to a predicted but not characterized esterase from the compost bacterium *Symbiobacterium thermophilum* and LipT was similar to a predicted esterase from *Thermus scotoductus*. Interestingly, *Symbiobacterium thermophilum* is supposed to have the highest content of horizontally acquired genes among all bacteria known so far [93]. Of its protein coding genes, 17.7% originate from Bacilli and 36.9% from Clostridia. *S. thermophilum* can be isolated from enrichment cultures using compost or soil as inoculum [94]. It grows at an optimum temperature ranging from 45 to 65°C. However, it is uncultivable as a single species and it relies on commensalism [94]. Up to date only a single genome has been published having a size of 3.6 Mb [95].

While more than 100 strains of *Thermus* have been reported [96] only very few *T. scotoductus* isolates are known. *T. scotoductus* has been isolated from thermal springs but it can also be found in man-made sources such as gold mines [97,98]. Only recently, the first genome of a *T. scotoductus* strain, i.e. SA-01, was established and revealed a genome size of 2.4 Mb [99]. *T. scotoductus* usually grows at temperatures between 65 and 70°C [100,101], while other *Thermus* species have their optimal growth temperature between 62°C and 75°C [96]. Interestingly, the isolation of *T. thermophilus* from heating water systems has been reported [102]. Within this context it is notable that heating water systems harbor obviously rather diverse microbial communities [103,104].

The classification of LipS and LipT into one of the lipase and carboxylesterase families according to Arpigny and Jaeger [61] was not possible. Both enzymes are thus most likely members of novel lipase families (FIGURE 7) which presumably contain other lipase-members derived from cultivated thermophilic microbes as well.

It is noteworthy, that LipS and LipT represent the first metagenome-derived lipases that reveal a temperature optimum of ≥70°C. Since both enzymes, however, were derived from metagenomes, we can only speculate about their native substrates and functions within the cells.

We have characterized the substrate spectra of both enzymes in great detail using a range of industry-relevant substrates. Both LipT and LipS showed a clear preference for *p*NP-esters with long chained fatty acid residues (>C8), their temperature optima were at 70 and 75°C and both enzymes showed a high thermal stability at 70 as well as at 90°C. Both LipS and LipT do not require cofactors and are stable against most detergents, solvents and even enzyme inhibitors. Especially the substrate range of LipS is not limited to *p*NP-esters with simple fatty acid residues. It is also able to hydrolyze sterically more complex substrates with phenolic or cyclohexanoic residues. LipS showed a high (*R*)-selectivity for ibuprofen, naproxen, methyl decanoic acid and indancarboxylic acid ester, which can be useful for the production of chiral pharmaceuticals. Ibuprofen, for example, is physiologically active as (*S*)-enantiomer [105]. LipS could be applied in the dynamic kinetic resolution of the racemate by hydrolyzing remaining (*R*)-enantiomers in order to obtain an enantiopure product [106]. With respect to the catalytic activities of both enzymes, they showed comparable or better activities than activities published for other thermostable bacterial lipases [[15,24,107], TABLE 3].

Further, in small-scale experiments, esterification reactions were catalyzed by LipS with the result that 1-propyl laurate as well as 1-tetradecyl myristate were produced with non-immobilized enzyme. The observed activities were comparable to those observed for *Candida antarctica* lipase CalB. Altogether, these data suggest that LipS and LipT are very promising enzyme candidates for biotechnological applications at elevated temperatures.

The structure of LipS was solved for two different constructs which crystallized in two different space groups. In the higher resolution SG P4, there is clear additional electron density immediately adjacent to the catalytic S126 and H257 (FIGURE S4A, B). In LipS in SG $P4_22_12$, however, there is no such electron density. This excludes the possibility that the observed density results from expression in *E. coli*. We interpreted this residual density with spermidine, which was added during crystallization of LipS in SG P4 but not in SG $P4_22_12$. At this point, there is no indication that spermidine is part of any native substrate of LipS. Identical conformations of the lid-domain, which covers the active site, in the absence and presence of a ligand, indicate that this domain may not undergo conformational rearrangements during the catalytic cycle. Concerning Est1E and LJ0536, it was shown that the lid is flexible [82,84]. The closed lid-conformation resulted in an occluded binding pocket, which most likely only leaves a narrow and restricted opening to the bulk solvent. Occlusion of the binding pocket in human monoglyceride lipase MGL, together with structural rearrangements of the hydrophobic lid in MGL, are thought to support the extraction of its substrate 2-arachidonoyl glycerol from the membrane by providing an accommodating environment [83]. While the precise cellular substrate of LipS is unknown, its surface does not indicate increased hydrophobicity around the binding pocket. A closed, water secluded active site may therefore provide a protective environment to prevent spurious hydrolysis of its substrate at the elevated level of its optimal temperature range.

In summary, LipS and LipT are both very interesting and promising enzymes with a high potential for downstream biotechnological applications. This was confirmed by their extensive biochemical characterization and in the case of LipS this was supported by the structural data. The sequence and structural characterization clearly suggests that both enzymes increase the diversity of known esterase and lipase families.

Supporting Information

Figure S1 15% SDS-PAGE of recombinant and purified LipS and LipT. Asterisks indicate the corresponding protein bands after His6-tag affinity chromatography. 15 µg of protein from the crude cell extracts or from the purified proteins were loaded and electrophoresed. **A)** 1, 4: crude cell extract; 2, 3 purified protein after extended heat treatment (30 min at 70°C and 5 min 95°C). **B)** Purified LipT after incomplete heat-denaturation (5 min 95°C).
(TIF)

Figure S2 Effect of metal ions applied in 1 and 10 mM concentration on LipT and LipS. Residual activity of the enzymes was measured with *p*NP- dodecanoate at 75°C (LipT) and 70°C (LipS). Compared with the control without metal ions, none of the cations showed positive effects significant enough for being considered as cofactor. Data are mean values of at least three independent measurements and bars indicate the standard deviation.
(TIF)

Figure S3 Effects of 1 and 10 mM EDTA, DTT and PMSF on the activity of LipS and LipT. The residual activity was measured at 70°C (LipS) and 75°C (LipT) using *p*NP-substrates.
(TIF)

Figure S4 Effect of spermidine on the active site of LipS. **A)** Electron density maps (blue) around S126, H257 and spermidine. The additional density linking both residues and extending further towards the active site cavity was interpreted as spermidine. **B)** The spermidine moiety, shown as a space model colored in grey, is located in the active site cavity of LipS in vicinity of catalytic S126 and H257 indicated as sticks model. **C)** Spermidine inhibits LipS activity at concentrations of 3 and 5 mM compared to a control without added spermidine. Enzyme activity was determined after 5 min preincubation with spermidine using *p*NP-decanoate as substrate and incubation at 70°C for 10 min. **D)** Spermidine displays similarity with LipSs substrate *p*NP-decanoate.
(TIF)

Figure S5 Structure based sequence alignment of LipS with its homologues. It revealed very low structural similarity in the region of the inserted domain, which is indicated by bold letters in LipS. 2WTM, Est1E form *Butyrivibrio proteoclasticus* [82]; 3PF8, LJ0536 from *Lactobacillus johnsonii* [84]; 3PE6, monoglyceride lipase (MGL) from *Homo sapiens* [83]; 1TQH, Est30 from *Geobacillus stearothermophilus* [80]; 3DKR, esterase D from *Lactobacillus rhamnosus* [81]. In the top line, secondary structure elements of LipS are shown with the inserted domain ($\alpha D_{1'}$, β6 and β7) colored in gray. Identical and similar amino acids conserved in at least four structures were shaded in black and gray respectively. Catalytic triad residues of LipS are indicated in bold and yellow. Residues which are not seen in the structures are shown as small letters.
(TIF)

Table S1 Bacterial strains and plasmids used in this work.
(DOCX)

Table S2 Amino acid sequences of members from the eight major lipase and esterase families [61] received from GenBank together with members of the new LipS and LipT groups.
(DOCX)

Table S3 Metagenomic esterases and lipases from uncultured organisms grouped into existing families [61]. The classification is based on alignment scores with members of family I-VIII or unknown families (UF). **UF1-5: Unknown Families of metagenomic esterases/lipases:** Sequences were grouped together into one family if at least two unclassified sequences shared significant similarity and sufficiently high T-COFFEE alignment scores. All sequences considered here as unclassified cannot be unequivocally grouped into any of the known other eight lipase/esterase families. ***:I/S/G:** Identical/Similar/Gapped amino acid positions in the respective alignment. Sequence identity/similarity is given with respect to one of the sequences of a known organism. Identity/similarity can be higher to metagenomic sequences in the subfamily.
(DOCX)

Table S4 Refinement and quality statistics of the crystallized constructs LipS-H6 and LipS-WT.
(DOCX)

Table S5 Purification table of the proteins LipS and LipT. (1) Crude cell extract; (2) heat denaturation at 70°C for 30 min; (3) immobilized metal ion affinity chromatography with Ni-ions. In case of LipT, the elution fractions have been combined and concentrated to a residual volume of 0.4 ml in a centrifuge (Vivaspin20, MWCO 10,000; Sartorius Stedim Biotech GmbH, Göttingen, Germany; Centrifuge 5804R, rotor A-4-44, Eppendorf, Hamburg, Germany). Activity was measured using 0.5 mM *p*NP-octanoate at 70°C (LipS) or 0.5 mM *p*NP-decanoate at 75°C (LipT).
(DOCX)

Table S6 Residual activities of LipS and LipT in the presence of organic solvents. The enzymes were incubated for 1 h at room temperature with the solvents diluted in 0.1 M PB pH 8.0 before *p*NP-dodecanoate was added as substrate. After incubation for 10 min at 70°C (LipS) and 75°C (LipT), the reaction was measured in a photometer at 405 nm against an enzyme-free blank containing the respective solvent and concentration. Data are mean values of at least three independent measurements; ± indicates the standard deviation.
(DOCX)

Table S7 Amino acids and atoms building the active site pocket of LipS. Amino acids belonging to the inserted domain are indicated in bold.
(DOCX)

Acknowledgments

J. Pietruszka thanks Melanie Schölzel, Vera Ophoven, TrucPham as well as Christoph Lorenz for supporting experiments.

Author Contributions

Conceived and designed the experiments: JC CS WRS. Performed the experiments: JC YDA FF BL PB MS IM. Analyzed the data: JC FK YDA UK FF BL PB MS IM UTB ME OT AL JMD KEJ WRS. Contributed reagents/materials/analysis tools: FK UK JP UTB ME OT AL JMD KEJ. Wrote the paper: JC WRS.

References

1. Jaeger KE, Reetz MT (1998) Microbial lipases form versatile tools for biotechnology. Trends Biotechnol 16: 396–403.
2. Jaeger KE, Dijkstra BW, Reetz MT (1999) Bacterial biocatalysts: molecular biology, three-dimensional structures, and biotechnological applications of lipases. Annu Rev Microbiol 53: 315–351.
3. Jaeger KE, Eggert T (2002) Lipases for biotechnology. Curr Opin Biotechnol 13: 390–397.
4. Reetz MT (2002) Lipases as practical biocatalysts. Curr Opin Chem Biol 6: 145–150.
5. Liese A, Seelbach K, Wandrey C (2006) Industrial Biotransformations; Liese A, Seelbach K, Wandrey C, editors. Weinheim: WILEY-VCH Verlag GmbH & Co. KGaA.
6. Turner P, Mamo G, Karlsson EN (2007) Potential and utilization of thermophiles and thermostable enzymes in biorefining. Microb Cell Fact 6: 9.
7. Yeoman CJ, Han Y, Dodd D, Schroeder CM, Mackie RI, et al. (2010) Thermostable enzymes as biocatalysts in the biofuel industry. Adv Appl Microbiol 70: 1–55.
8. Bruins ME, Janssen AE, Boom RM (2001) Thermozymes and their applications: a review of recent literature and patents. Appl Biochem Biotechnol 90: 155–186.
9. Vieille C, Burdette DS, Zeikus JG (1996) Thermozymes. Biotechnol Annu Rev 2: 1–83.
10. Li WF, Zhou XX, Lu P (2005) Structural features of thermozymes. Biotechnol Adv 23: 271–281.
11. Dalhus B, Saarinen M, Sauer UH, Eklund P, Johansson K, et al. (2002) Structural basis for thermophilic protein stability: structures of thermophilic and mesophilic malate dehydrogenases. J Mol Biol 318: 707–721.
12. Ebrahimi M, Lakizadeh A, Agha-Golzadeh P, Ebrahimie E, Ebrahimi M (2011) Prediction of thermostability from amino acid attributes by combination of clustering with attribute weighting: a new vista in engineering enzymes. PloS one 6: e23146.
13. Hough DW, Danson MJ (1999) Extremozymes. Curr Opin Chem Biol 3: 39–46.
14. Schiraldi C, De Rosa M (2002) The production of biocatalysts and biomolecules from extremophiles. Trends Biotechnol 20: 515–521.
15. Royter M, Schmidt M, Elend C, Hobenreich H, Schafer T, et al. (2009) Thermostable lipases from the extreme thermophilic anaerobic bacteria *Thermosediminibacter thermohydrosulfuricus* SOL1 and *Caldanaerobacter subterraneus* subsp. tengcongensis. Extremophiles : life under extreme conditions 13: 769–783.
16. Kim HK, Park SY, Lee JK, Oh TK (1998) Gene cloning and characterization of thermostable lipase from *Bacillus stearothermophilus* L1. Biosci Biotechnol Biochem 62: 66–71.
17. Li H, Zhang X (2005) Characterization of thermostable lipase from thermophilic *Geobacillus* sp. TW1. Protein Expr Purif 42: 153–159.
18. Leow TC, Rahman RN, Basri M, Salleh AB (2007) A thermoalkaliphilic lipase of *Geobacillus* sp. T1. Extremophiles : life under extreme conditions 11: 527–535.
19. Dominguez A, Sanroman A, Fucinos P, Rua ML, Pastrana L, et al. (2004) Quantification of intra- and extra-cellular thermophilic lipase/esterase production by *Thermus* sp. Biotechnol Lett 26: 705–708.
20. Fucinos P, Dominguez A, Sanroman MA, Longo MA, Rua ML, et al. (2005) Production of thermostable lipolytic activity by *Thermus* species. Biotechnol Prog 21: 1198–1205.
21. Lopez-Lopez O, Fucinos P, Pastrana L, Rua ML, Cerdan ME, et al. (2010) Heterologous expression of an esterase from *Thermus thermophilus* HB27 in *Saccharomyces cerevisiae*. J Biotechnol 145: 226–232.
22. Fucinos P, Atanes E, Lopez-Lopez O, Esperanza Cerdan M, Isabel Gonzalez-Siso M, et al. (2011) Production and characterization of two N-terminal truncated esterases from *Thermus thermophilus* HB27 in a mesophilic yeast: effect of N-terminus in thermal activity and stability. Protein Expr Purif 78: 120–130.
23. du Plessis EM, Berger E, Stark T, Louw ME, Visser D (2010) Characterization of a novel thermostable esterase from *Thermus scotoductus* SA-01: evidence of a new family of lipolytic esterases. Curr Microbiol 60: 248–253.
24. Salameh MA, Wiegel J (2007) Purification and characterization of two highly thermophilic alkaline lipases from *Thermosyntropha lipolytica*. Appl Environ Microbiol 73: 7725–7731.
25. Uppenberg J, Hansen MT, Patkar S, Jones TA (1994) The sequence, crystal structure determination and refinement of two crystal forms of lipase B from *Candida antarctica*. Structure 2: 293–308.
26. Gutarra ML, de Godoy MG, Silva Jdo N, Guedes IA, Lins U, et al. (2009) Lipase production and *Penicillium simplicissimum* morphology in solid-state and submerged fermentations. Biotechnol J 4: 1450–1459.
27. Bordes F, Tarquis L, Nicaud JM, Marty A (2011) Isolation of a thermostable variant of Lip2 lipase from *Yarrowia lipolytica* by directed evolution and deeper insight into the denaturation mechanisms involved. J Biotechnol 156: 117–124.
28. Romdhane IB, Frikha F, Maalej-Achouri I, Gargouri A, Belghith H (2012) Gene cloning and molecular characterization of the *Talaromyces thermophilus* lipase catalyzed efficient hydrolysis and synthesis of esters. Gene 494: 112–118.
29. Siddiqui KS, Cavicchioli R (2005) Improved thermal stability and activity in the cold-adapted lipase B from *Candida antarctica* following chemical modification with oxidized polysaccharides. Extremophiles 9: 471–476.
30. Tufvesson P, Annerling A, Hatti-Kaul R, Adlercreutz D (2007) Solvent-free enzymatic synthesis of fatty alkanolamides. Biotechnol Bioeng 97: 447–453.
31. Le QA, Joo JC, Yoo YJ, Kim YH (2012) Development of thermostable *Candida antarctica* lipase B through novel in-silico design of disulfide bridge. Biotechnol Bioeng.
32. Henne A, Schmitz RA, Bomeke M, Gottschalk G, Daniel R (2000) Screening of environmental DNA libraries for the presence of genes conferring lipolytic activity on *Escherichia coli*. Appl Environ Microbiol 66: 3113–3116.
33. Chow J, Krauss U, Jaeger K-E, Streit WR (2011) Carboxylesterases and Lipases from Metagenomes. In: Bruijn FJd, editor. Handbook of Molecular Microbial Ecology II : Metagenomics in Different Habitats. Hoboken, New Jersey: John Wiley & Sons Inc. 499–506.
34. Schmeisser C, Steele H, Streit WR (2007) Metagenomics, biotechnology with non-culturable microbes. Appl Microbiol Biotechnol75: 955–962.
35. Perner M, Ilmberger N, Köhler HU, Chow J, Streit WR (2011) Emerging Fields in Functional Metagenomics and Its Industrial Relevance: Overcoming Limitations and Redirecting the Search for Novel Biocatalysts. In: Bruijn FJd, editor. Handbook of Molecular Microbial Ecology II: John Wiley & Sons, Inc. 481–498.
36. Handelsman J (2004) Metagenomics: application of genomics to uncultured microorganisms. Microbiol Mol Biol Rev 68: 669–685.
37. Liles MR, Williamson LL, Rodbumrer J, Torsvik V, Parsley LC, et al. (2009) Isolation and cloning of high-molecular-weight metagenomic DNA from soil microorganisms. Cold Spring Harbor protocols 2009: pdb prot5271.
38. Reymond J-L (2006) Enzyme Assays: High-throughput Screening, Genetic Selection and Fingerprinting. Weinheim: WILEY-VCH Verlag GmbH & Co. KGaA.

39. Nam KH, Kim SJ, Priyadarshi A, Kim HS, Hwang KY (2009) The crystal structure of an HSL-homolog EstE5 complex with PMSF reveals a unique configuration that inhibits the nucleophile Ser144 in catalytic triads. Biochem Biophys Res Commun 389: 247–250.
40. Nam KH, Kim MY, Kim SJ, Priyadarshi A, Kwon ST, et al. (2009) Structural and functional analysis of a novel hormone-sensitive lipase from a metagenome library. Proteins 74: 1036–1040.
41. Fu J, Leiros HK, de Pascale D, Johnson KA, Blencke HM, et al. (2012) Functional and structural studies of a novel cold-adapted esterase from an Arctic intertidal metagenomic library. Appl Microbiol Biotechnol.
42. Byun JS, Rhee JK, Kim ND, Yoon J, Kim DU, et al. (2007) Crystal structure of hyperthermophilic esterase EstE1 and the relationship between its dimerization and thermostability properties. BMC Struct Biol 7: 47.
43. Kim S, Joo S, Yoon HC, Ryu Y, Kim KK, et al. (2007) Purification, crystallization and preliminary crystallographic analysis of Est25: a ketoprofen-specific hormone-sensitive lipase. Acta Crystallogr Sect F Struct Biol Cryst Commun 63: 579–581.
44. Sako Y, Takai K, Ishida Y, Uchida A, Katayama Y (1996) *Rhodothermus obamensis* sp. nov., a modern lineage of extremely thermophilic marine bacteria. Int J Syst Bacteriol 46: 1099–1104.
45. Castenholz RW (1969) Thermophilic blue-green algae and the thermal environment. Bacteriol Rev 33: 476–504.
46. Brock TD, Freeze H (1969) *Thermus aquaticus* gen. n. and sp. n., a nonsporulating extreme thermophile. J Bacteriol 98: 289–297.
47. Sambrook J, Russel DW, editor (2001) Molecular cloning, a laboratory manual. New York, USA: Cold Spring Harbor Laboratory Press.
48. Lawrence RC, Fryer TF, Reiter B (1967) Rapid method for the quantitative estimation of microbial lipases. Nature (London) 213: 1264–1265.
49. Reetz MT, Zonta A, Schimossek K, Liebeton K, Jaeger KE (1997) Creation of enantioselective biocatalysts for organic chemistry by in vitro evolution. Angew Chem Int Ed Engl 36: 2830–2832.
50. Franken BJ, Pietruszka J (2009) Protocols to screen for enantioselective lipases. In: Timmes KN, editor. Handbook of Microbiology of Hydrocarbons, Oils, Lipids, and Derived Compounds. Berlin-Heidelberg: Springer. 2860–2876.
51. Pietruszka J, Simon RC, Kruska F, Braun M (2009) Dynamic Enzymatic Kinetic Resolution of Methyl 2,3-Dihydro-1H-indene-1-carboxylate. European J Org Chem: 6217–6224.
52. Reetz MT, Prasad S, Carballeira JD, Gumulya Y, Bocola M (2010) Iterative Saturation Mutagenesis Accelerates Laboratory Evolution of Enzyme Stereoselectivity: Rigorous Comparison with Traditional Methods. J Am Chem Soc 132: 9144–9152.
53. Sandstrom AG, Wikmark Y, Engstrom K, Nyhlen J, Backvall JE (2012) Combinatorial reshaping of the *Candida antarctica* lipase A substrate pocket for enantioselectivity using an extremely condensed library. Proc Natl Acad Sci U S A 109: 78–83.
54. Salvadori P, Bertucci C, Rosini C (1991) Circular-Dichroism Detection in HPLC. Chirality 3: 376–385.
55. Reetz MT, Kuhling KM, Hinrichs H, Deege A (2000) Circular dichroism as a detection method in the screening of enantioselective catalysts. Chirality 12: 479–482.
56. Hamzic M, Pietruszka J, Sandkuhl D (2011) HPLC-CD selectivity assay for alcohol dehydrogenases. Chirality 23 Suppl 1: E110–115.
57. Kroutil W, Kleewein A, Faber K (1997) A computer program for analysis, simulation and optimization of asymmetric catalytic processes proceeding through two consecutive steps. Type 2: sequential kinetic resolutions. Tetrahedron-Asymmetry 8: 3263–3274.
58. Musidlowska A, Lange S, Bornscheuer UT (2001) By Overexpression in the Yeast *Pichia pastoris* to Enhanced Enantioselectivity: New Aspects in the Application of Pig Liver Esterase. Angew Chem Int Ed Engl 40: 2851–2853.
59. Musidlowska-Persson A, Bornscheuer UT (2002) Substrate specificity of the γ-isoenzyme of recombinant pig liver esterase towards acetates of secondary alcohols. J Mol Catal B Enzym 19–20: 129–133.
60. Chen CS, Fujimoto Y, Girdaukas G, Sih CJ (1982) Quantitative-Analyses of Biochemical Kinetic Resolutions of Enantiomers. J Am Chem Soc 104: 7294–7299.
61. Arpigny JL, Jaeger KE (1999) Bacterial lipolytic enzymes: classification and properties. Biochem J 343 Pt 1: 177–183.
62. Notredame C, Higgins DG, Heringa J (2000) T-Coffee: A novel method for fast and accurate multiple sequence alignment. J Mol Biol 302: 205–217.
63. Nicholas K, Nicholas HJ, Deerfield D (1997) GeneDoc: Analysis and Visualization of Genetic Variation. EMBNEWS 4: 14.
64. Stamatakis A, Hoover P, Rougemont J (2008) A rapid bootstrap algorithm for the RAxML Web servers. Syst Biol 57: 758–771.
65. Zmasek CM, Eddy SR (2001) ATV: display and manipulation of annotated phylogenetic trees. Bioinformatics 17: 383–384.
66. Trooskens G, De Beule D, Decouttere F, Van Criekinge W (2005) Phylogenetic trees: visualizing, customizing and detecting incongruence. Bioinformatics 21: 3801–3802.
67. Fersini F, Dall'antonia Y, Chow J, Streit WR, Mueller-Dieckmann J (2012) Cloning, expression, purification and preliminary X-ray analysis of a putative metagenome-derived lipase. Acta Crystallogr Sect F Struct Biol Cryst Commun 68: 923–926.
68. Vagin A, Teplyakov A (1997) MOLREP: an automated program for molecular replacement. J Appl Crystallogr 30: 1022–1025.
69. Matthews BW (1968) Solvent Content of Protein Crystals. J Mol Biol 33: 491–497.
70. Emsley P, Lohkamp B, Scott WG, Cowtan K (2010) Features and development of Coot. Acta Crystallogr D Biol Crystallogr 66: 486–501.
71. Murshudov GN, Vagin AA, Dodson EJ (1997) Refinement of macromolecular structures by the maximum-likelihood method. Acta Crystallogr D Biol Crystallogr 53: 240–255.
72. DeLano WL (2002) The PyMOL Molecular Graphics System. 1.5.0.1 ed. New York: Schroedinger LLC.
73. Altschul SF, Madden TL, Schaffer AA, Zhang J, Zhang Z, et al. (1997) Gapped BLAST and PSI-BLAST: a new generation of protein database search programs. Nucleic Acids Res 25: 3389–3402.
74. Nielsen H, Engelbrecht J, Brunak S, von Heijne G (1997) Identification of prokaryotic and eukaryotic signal peptides and prediction of their cleavage sites. Protein Eng 10: 1–6.
75. Kazlauskas RJ (2006) Quantitative Assay of Hydrolases for Activity and Selectivity Using Color Changes. In: Reymond JL, editor. Enzyme-Assays: High-throughput Screening, Genetic Selection and Fingerprinting. Weinheim: WILEY-VCH Verlag GmbH & Co. KGaA. 16–39.
76. Krissinel E, Henrick K (2007) Inference of macromolecular assemblies from crystalline state. J Mol Biol 372: 774–797.
77. Ollis DL, Cheah E, Cygler M, Dijkstra B, Frolow F, et al. (1992) The alpha/beta hydrolase fold. Protein Eng 5: 197–211.
78. Holmquist M (2000) Alpha/Beta-hydrolase fold enzymes: structures, functions and mechanisms. Curr Protein Pept Sci 1: 209–235.
79. Holm L, Rosenstrom P (2010) Dali server: conservation mapping in 3D. Nucleic Acids Res 38: W545–549.
80. Liu P, Wang YF, Ewis HE, Abdelal AT, Lu CD, et al. (2004) Covalent reaction intermediate revealed in crystal structure of the *Geobacillus stearothermophilus* carboxylesterase Est30. J Mol Biol 342: 551–561.
81. Bennett MD, Delabre M-L, Holland R, Norris GE to be published.
82. Goldstone DC, Villas-Boas SG, Till M, Kelly WJ, Attwood GT, et al. (2010) Structural and functional characterization of a promiscuous feruloyl esterase (Est1E) from the rumen bacterium *Butyrivibrio proteoclasticus*. Proteins 78: 1457–1469.
83. Schalk-Hihi C, Schubert C, Alexander R, Bayoumy S, Clemente JC, et al. (2011) Crystal structure of a soluble form of human monoglyceride lipase in complex with an inhibitor at 1.35 A resolution. Protein Sci 20: 670–683.
84. Lai KK, Stogios PJ, Vu C, Xu X, Cui H, et al. (2011) An inserted alpha/beta subdomain shapes the catalytic pocket of *Lactobacillus johnsonii* cinnamoyl esterase. PLoS One 6: e23269.
85. Labar G, Bauvois C, Borel F, Ferrer JL, Wouters J, et al. (2010) Crystal structure of the human monoacylglycerol lipase, a key actor in endocannabinoid signaling. Chembiochem 11: 218–227.
86. Heikinheimo P, Goldman A, Jeffries C, Ollis DL (1999) Of barn owls and bankers: a lush variety of alpha/beta hydrolases. Structure 7: R141–146.
87. Dundas J, Ouyang Z, Tseng J, Binkowski A, Turpaz Y, et al. (2006) CASTp: computed atlas of surface topography of proteins with structural and topographical mapping of functionally annotated residues. Nucleic Acids Res 34: W116–118.
88. Voget S, Leggewie C, Uesbeck A, Raasch C, Jaeger KE, et al. (2003) Prospecting for novel biocatalysts in a soil metagenome. Appl Environ Microbiol 69: 6235–6242.
89. Daniel R (2005) The metagenomics of soil. Nat Rev Microbiol 3: 470–478.
90. Beloqui A, Nechitaylo TY, Lopez-Cortes N, Ghazi A, Guazzaroni ME, et al. (2010) Diversity of glycosyl hydrolases from cellulose-depleting communities enriched from casts of two earthworm species. Appl Environ Microbiol 76: 5934–5946.
91. Schmidt O, Drake HL, Horn MA (2010) Hitherto unknown [Fe-Fe]-hydrogenase gene diversity in anaerobes and anoxic enrichments from a moderately acidic fen. Appl Environ Microbiol 76: 2027–2031.
92. Meilleur C, Hupe JF, Juteau P, Shareck F (2009) Isolation and characterization of a new alkali-thermostable lipase cloned from a metagenomic library. J Ind Microbiol Biotechnol 36: 853–861.
93. Nishida H, Yun CS (2011) Phylogenetic and Guanine-Cytosine Content Analysis of *Symbiobacterium thermophilum* Genes. Int J Evol Biol 2011: 634505.
94. Ohno M, Shiratori H, Park MJ, Saitoh Y, Kumon Y, et al. (2000) *Symbiobacterium thermophilum* gen. nov., sp. nov., a symbiotic thermophile that depends on co-culture with a *Bacillus* strain for growth. Int J Syst Evol Microbiol 50: 1829–1832.
95. Ueda K, Yamashita A, Ishikawa J, Shimada M, Watsuji T-o, et al. (2004) Genome sequence of *Symbiobacterium thermophilum*, an uncultivable bacterium that depends on microbial commensalism. Nucleic Acids Res 32: 4937–4944.
96. Cava F, Hidalgo A, Berenguer J (2009) *Thermus thermophilus* as biological model. Extremophiles 13: 213–231.
97. Balkwill DL, Kieft TL, Tsukuda T, Kostandarithes HM, Onstott TC, et al. (2004) Identification of iron-reducing *Thermus* strains as *Thermus scotoductus*. Extremophiles 8: 37–44.
98. Kieft TL, Fredrickson JK, Onstott TC, Gorby YA, Kostandarithes HM, et al. (1999) Dissimilatory Reduction of Fe(III) and Other Electron Acceptors by a *Thermus* Isolate. Appl Environ Microbiol 65: 1214–1221.
99. Gounder K, Brzuszkiewicz E, Liesegang H, Wollherr A, Daniel R, et al. (2011) Sequence of the hyperplastic genome of the naturally competent *Thermus scotoductus* SA-01. BMC Genomics 12: 577.

100. Kristjansson JK, Hjorleifsdottir S, Marteinsson VT, Alfredsson GA (1994) *Thermus scotoductus*, sp. nov, a Pigment-Producing Thermophilic Bacterium from Hot Tap Water in Iceland and Including *Thermus* sp. X-1. Syst Appl Microbiol 17: 44–50.
101. Skirnisdottir S, Hreggvidsson GO, Holst O, Kristjansson JK (2001) Isolation and characterization of a mixotrophic sulfur-oxidizing *Thermus scotoductus*. Extremophiles 5: 45–51.
102. Brock TD, Boylen KL (1973) Presence of thermophilic bacteria in laundry and domestic hot-water heaters. Appl Microbiol 25: 72–76.
103. Kjeldsen KU, Kjellerup BV, Egli K, Frolund B, Nielsen PH, et al. (2007) Phylogenetic and functional diversity of bacteria in biofilms from metal surfaces of an alkaline district heating system. FEMS Microbiol Ecol 61: 384–397.
104. Kjellerup BV, Thomsen TR, Nielsen JL, Olesen BH, Frolund B, et al. (2005) Microbial diversity in biofilms from corroding heating systems. Biofouling 21: 19–29.
105. Hutt AJ, Caldwell J (1984) The importance of stereochemistry in the clinical pharmacokinetics of the 2-arylpropionic acid non-steroidal anti-inflammatory drugs. Clin Pharmacokinet 9: 371–373.
106. Gihani MT, Williams JM (1999) Dynamic kinetic resolution. Curr Opin Chem Biol 3: 11–15.
107. Kakugawa S, Fushinobu S, Wakagi T, Shoun H (2007) Characterization of a thermostable carboxylesterase from the hyperthermophilic bacterium *Thermotoga maritima*. Appl Microbiol Biotechnol74: 585–591.